Comparison of 1-D and 2-D Modeling Approaches for Simulating Runoff and Sediment Transport in Overland Areas

by

Seonggu Hong

Dissertation submitted to the Faculty of the
Virginia Polytechnic Institute and State University
in partial fulfillment of the requirement for the degree of
Doctor of Philosophy
in
Biological Systems Engineering

APPROVED :

Saied Mostaghimi, Chairman

Theo A. Dillaha

Daniel L. Gallagher

Conrad D. Heatwole

Blake B. Ross

John V. Perumpral, Dept. Chairman

October 26, 1995
Blacksburg, Virginia

Key words : Finite element method, Simulation models, Overland runoff, Soil erosion

Comparison of 1-D and 2-D modeling approaches in simulating overland runoff and sediment transport in overland areas

by

Seonggu Hong

Saied Mostaghimi, Chairman

Biological Systems Engineering

(ABSTRACT)

One-dimensional and two-dimensional modeling approaches were compared for their abilities in predicting overland runoff and sediment transport. Both the 1-D and 2-D models were developed to test the hypothesis that the 2-D modeling approach could improve the model predictions over the 1-D approach, based on the same mathematical representations of physical processes for runoff and sediment transport.

Runoff processes were described based on the St. Venant equations and the sediment transport was based on the continuity relationship. The finite element method was employed to solve the governing equations. The nonlinear, time-dependent system of equations obtained by the finite element formulation was solved by the substitution method and the implicit method.

The models were verified by comparing the analytical solutions presented by Singh and Regl (1983) and the solution by the Izzard method (Chow, 1959). The comparison showed that both the 1-D and 2-D models provided reasonable estimations of runoff and sediment loadings. Evaluation of the models was based on four different hypothetical case studies and two experimental studies. The hypothetical case studies investigated the effects of the discretization level, cross slopes, and the size of the field area on the model predictions. The two experimental studies provided a comparison of model predictions with observed data.

The results of the hypothetical case studies indicated that the maximum differences in the model predictions at the outlet were about 30% between the two modeling approaches. When the discretization level was sufficient to reasonably describe the shape of the surface, the 1-D model prediction were almost the same as the 2-D model predictions. Even though cross slopes existed in the field, the differences in the model predictions at the outlet were not significant between the 1-D and 2-D models. The differences in the model predictions of runoff and sediment loading were not affected by the changes in the size of the field. Since the 2-D model resulted in 10 to 20% differences in model predictions when different boundary conditions were used and the 1-D model

predictions were also affected by the choice of element length, the differences in model predictions at the outlet, shown in model application results, which were less than 30% in most cases, could not be considered significant.

The model applications to the experimental studies also showed that no substantial differences existed in the model predictions between the 1-D and 2-D models. Even though the spatial distributions of the flow depth and sediment concentration were significantly different, runoff volumes and sediment yields at the outlet showed less than 10% differences.

Compared with the 1-D model, the 2-D model required much more computational time and effort to simulate the same problems. In addition, convergence problems due to negative flow depths limited the 2-D model applications. The 2-D simulations required more than twice the computational time needed for the 1-D simulations. As long as the model predictions at the outlet are concerned, the much greater computational costs and efforts could not justify the use of the 2-D approach.

Based on the simulation results from the selected hypothetical case and experimental studies, the 2-D model provided better representations of spatial distribution of flow depths and sediment concentrations than the 1-D model. However, no substantial differences in predictions of total runoff volume and sediment yield at the outlet area were found between the 1-D and 2-D models.

Acknowledgments

I wish to express most sincere appreciation to Dr. Saied Mostaghimi, committee chairman, for his total guidance, invaluable comment, and encouragement throughout this study.

I would like to express my appreciation to the members of my advisory committee : Drs. Theo Dillaha, Dan Gallagher, Conrad Heatwole, and Blake Ross. I also thank Dr. Storm at Oklahoma State University for sharing his experimental data.

Deep gratitude is expressed to my parents, Doopyo Hong and Jungja Koh and father and mother in law in Atlanta for their encouragement and support.

I wish to thank Korean Government for providing me the financial support for three years. I believe I could not continue my study without the scholarship. I thank Dr. S. K. Kwon at Seoul National University for his encouragement. In addition, I would like express my gratitude to Dr. S. W. Park at Seoul National University.

Finally, true appreciation is extended to my wife, Jinsook Hwang for her constant love and support.

Table of Contents

1. INTRODUCTION **1**

1.1 GOAL AND OBJECTIVES 4

2. LITERATURE REVIEW **6**

2.1 INTRODUCTION 6

2.2 REVIEW OF SELECTED NPS MODELS 6

2.2.1 AGNPS *7*

2.2.2 ANSWERS *8*

2.2.3 CREAMS *9*

2.2.4 FESHM *9*

2.2.5 Summary *10*

2.3 RUNOFF ROUTING MODELS 11

2.3.1 SCS curve number method *11*

2.3.2 Dynamic equations *12*

2.3.3 Diffusion wave approximation *15*

2.3.4 Kinematic wave approximation *16*

2.3.5 Summary *20*

2.4 NUMERICAL METHODS FOR SOLVING DYNAMIC EQUATIONS 20

2.4.1 Finite difference method *20*

2.4.2 Finite element methods *22*

2.4.3 Summary *22*

2.5 INFILTRATION MODELS 23

2.5.1 Holtan's infiltration model *23*

2.5.2 Green-Ampt model *24*

2.5.3 Smith and Parlange's equation *25*

2.5.4 Parlange et al.'s equation *25*

2.5.5 Summary *26*

2.6 SOIL EROSION AND SEDIMENT TRANSPORT 27

2.6.1 Conceptualization of soil erosion processes *27*

2.6.2 Summary and discussion *39*

2.7 SUMMARY AND CONCLUSION 40

3. METHODOLOGY 42

3.1 INTRODUCTION 42

3.2 RUNOFF SIMULATION 42

3.2.1 Governing equations 43

3.2.2 Interpolation functions 43

3.2.3 Finite element formulations 45

3.2.4 Solution techniques 49

3.3 RAINFALL EXCESS 52

3.4 SEDIMENT TRANSPORT SIMULATION 53

3.4.1 Governing equations 54

3.4.2 Finite element formulations 54

3.4.3 Solution techniques 56

3.5 ESTIMATION OF SOURCE AND SINK TERMS 57

3.5.1 Splash erosion process 58

3.5.2 Hydraulic erosion process 59

3.6 SUMMARY 59

4. MODEL VALIDATION AND SENSITIVITY ANALYSIS 61

4.1 INTRODUCTION 61

4.2 MODEL TESTING 61

4.2.1 Verification of Runoff Simulation Models 62

4.2.2 Verification of Sediment Transport Models 75

4.2.3 Summary of sediment transport model testing 79

4.3 SENSITIVITY ANALYSIS FOR THE 1-D MODELS 80

4.3.1 Model parameters for the sensitivity analysis 81

4.3.2 Sensitivity of runoff model parameters 82

4.3.3 Summary of Sensitivity Analysis 88

4.4 SUMMARY AND CONCLUSION 88

5. MODEL APPLICATIONS 90

5.1 INTRODUCTION 90

5.2 CRITERIA FOR COMPARING MODEL PREDICTIONS 91

5.3 HYPOTHETICAL CASES 93

5.3.1 Hypothetical Case Study #1 :Effects of Discretization Level on Model Predictions 93
5.3.2 Hypothetical Case Study #2 : Cross Slope Effects on Model Predictions 101
5.3.3 Hypothetical Case Study #3 : Channelized Flow 110
5.3.4 Hypothetical Case Study #4 : Effects of field size 122
5.3.5 Summary and Discussion of Hypothetical Case Studies 126
5.4 FIELD APPLICATIONS 127
5.4.1 Storm's Experimental Study 128
5.4.2 Vegetative Filter Strip Experimental Study 138
5.4.3 Summary and Discussions of Field Applications 143
5.5 SUMMARY AND CONCLUSIONS 145
6. SUMMARY AND CONCLUSIONS **147**
7. RECOMMENDATIONS FOR FUTURE STUDIES **153**
REFERENCES **155**
APPENDIX I **161**
APPENDIX II **164**
APPENDIX III **215**
VITA **232**

List of Figures

Figure 2-1. Froude numbers for different sets of Chezy's C and flow depth. 18
Figure 2-2. Kinematic wave numbers for different sets of slope and flow rate 19
Figure 2-3. Sediment transport capacity by Meyer and Wischmeier's equation for different set of flow depths and velocities 32
Figure 2-4. Sediment transport capacity by Yalin's equation for different set of velocity and depth 33
Figure 2-5. Sediment transport capacity by Yang's equation for different set of velocity and depth 35
Figure 2-6. Sediment transport capacity by Engelund and Hansen's equation for different set of velocity and depth 35
Figure 3-1. Schematic diagram for runoff simulation model. 51
Figure 3-2. Schematic diagram for sediment transport model. 57
Figure 4-1. 1-D and 2-D discretization for model verification 63
Figure 4-2. Comparison of flow rates by 1-D simulations and Izzard method 65
Figure 4-3. Comparison of flow rates by 2-D simulations and Izzard method 65
Figure 4-4. Comparison of flow rates by 1-D and 2-D simulations 66
Figure 4-5. Six different discretization schemes for analyzing triangular oscillation. 68
Figure 4-6. Comparison of flow rates between Singh's analytical solution and 1-D simulation. 78
Figure 4-7. Comparison of sediment concentrations between Singh's analytical solution and 1-D simulations by different source and sink terms. 79
Figure 4-8. Comparison of sediment load between Singh's analytical solution and 1-D simulations. 79
Figure 4-9. Percent changes of total runoff volume 82
Figure 4-10. Percent changes of peak flow rate 83
Figure 4-11. Percent changes of total sediment load 83
Figure 4-12. Percent changes in flow depth. 85
Figure 4-13. Percent changes in velocity 85
Figure 4-14. Percent changes in model predictions due to mesh size changes 87
Figure 4-15. Percent changes in velocity due to time step changes 87
Figure 5-1. Example of meshes for the first hypothetical overland area for both 1-D and 2-D simulations. 94
Figure 5-2. Effect of different discretization level on peak flow rate simulations by the 1-D model. 95

Figure 5-3. Effect of different discretization level on sediment concentration simulations by the 1-D model. 95
Figure 5-4. Effect of different discretization level on sediment load simulations by the 1-D model. 96
Figure 5-5. Effects of different flow lengths on peak flow rate simulation by 1-D model. 97
Figure 5-6. Effects of different flow lengths on sediment concentration simulation by 1-D model. 97
Figure 5-7. Effects of different flow lengths on sediment load simulation by 1-D model. 98
Figure 5-8. Effects of different flow lengths on peak flow rate simulation by the 2-D model. 100
Figure 5-9. Effects of different flow lengths on sediment concentration simulation by the 2-D model. 100
Figure 5-10. Effects of different flow lengths on sediment load simulation by the 2-D model. 101
Figure 5-11. Comparison of hydrograph for different slope conditions 103
Figure 5-12. Comparison of sediment concentrations for different slope conditions 104
Figure 5-13. Comparison of sediment loads for different slope conditions 104
Figure 5-14. Comparison of hydrograph for different boundary conditions 106
Figure 5-15. Comparison of sediment concentrations for different boundary conditions 107
Figure 5-16. Comparison of sediment loads for different boundary conditions 107
Figure 5-17. Comparison of model predictions for different boundary conditions 109
Figure 5-18. Elevation contours for the hypothetical case study # 3. 111
Figure 5-19. Spatial distribution of model predictions for the 1% main slope with 0.2% cross slope 113
Figure 5-20. Spatial distribution of model predictions for the 1% main slope with 0.2% cross slope 114
Figure 5-21. Spatial distributions of 1-D estimations for the 5% main slope with 0.5% cross slope 116
Figure 5-22. Spatial distributions of 2-D estimations for the 5% main slope with 0.5% cross slope 116
Figure 5-23. Spatial distribution of 1-D estimations for the 5% main slope with 1% cross slope 117
Figure 5-24. Spatial distribution of 2-D estimations for the 5% main slope with 1% cross slope 117
Figure 5-25. A comparison of runoff hydrograph predicted by the 1-D and 2-D models for H505 118
Figure 5-26. A comparison of sediment loading rate predicted by the 1-D and 2-D models for H505 119
Figure 5-27. A comparison of runoff hydrograph predicted by the 1-D and 2-D models for H510 119
Figure 5-28. A comparison of sediment loading rate predicted by the 1-D and 2-D models for H505 120
Figure 5-29. Contours of elevations for the hypothetical case study #4. 122
Figure 5-30. Contours for flow depths for the small field in the hypothetical case #4. 123
Figure 5-31. Comparison of flow rate and sediment loading for the small field. 124
Figure 5-32. Estimated flow rate and sediment loading for the large field. 125
Figure 5-33. Elevation contour for T1R2 at 30th minute 130
Figure 5-34. Flow depth distribution for T1R2 131
Figure 5-35. Runoff hydrograph for T1R2 132

Figure 5-36. Time distribution of sediment loadings for T1R2 133
Figure 5-37. Runoff hydrograph for T1V2 134
Figure 5-38. Sediment concentration changes for T1V2 134
Figure 5-39. Runoff hydrographs for T2V2 135
Figure 5-40. Sediment concentration changes for T2V2 135
Figure 5-41. Comparison of hydrographs for QF3. 140
Figure 5-42. Comparison of sediment loading rates for QF3. 141
Figure 5-43. Comparison of hydrographs for QF2. 141
Figure 5-44. Comparison of sediment loading rate for QF2. 142
Figure 5-45. Sediment concentration changes between filter and no-filter fields. 142

List of Tables

Table 4-1. Surface conditions of hypothetical overland area used for model testing. 62
Table 4-2. Simulation results for different type of meshes. 69
Table 4-3. Simulation conditions for analytical solutions 75
Table 4-4. Parameters for simulation models. 76
Table 4-5. Base values for sensitivity analysis of runoff simulation models. 81
Table 4-6. Basis values for sensitivity analysis of sediment transport models. 81
Table 5-1. Description of hypothetical overland area 93
Table 5-2. Comparison of 1-D and 2-D model predictions for different level of discretization 99
Table 5-3. Comparison of 1-D and 2-D model predictions for different cross slopes. 105
Table 5-4. Input conditions for hypothetical case study #3. 110
Table 5-5. Comparison of 1-D and 2-D estimations for different slope conditions in the hypothetical study #3. 120
Table 5-6. Comparison of model predictions for different field size 125
Table 5-7. Input parameters for Storm's experimental field plots 129
Table 5-8 Comparison model estimations and observations for different slope conditions in the field application # 1. 137
Table 5-9. Plot characteristics for filter strip simulations. 139
Table 5-10. Input parameters used in simulation of filter strips. 139
Table 5-11. Comparison of model predictions of the impact of filter strips on runoff and sediment losses. 143

1. INTRODUCTION

A National Water Agenda for the 21st century recommended the development of a unified national water resources policy for the United States (Woodruff, 1993). It also pointed out that control of water pollution from agriculture is a key aspect for solving water quality problems in the United States. Despite nearly achieving the goals of Clean Water Act, water quality problems persist, and one of the primary causes of the problems is nonpoint sources (NPS) of pollution. Nonpoint sources of pollution are diffuse in nature and is usually associated with land use activities. They are directly affected by the occurrence of meteorological events such as rainfall. NPS pollution is difficult to monitor, and its control measures are site-specific. Agricultural NPS pollutants originate from tillage operation and application of fertilizers, animal waste, and pesticides. Control of NPS pollution could be effectively achieved through implementation of Best Management Practices (BMPs). The treatment methods used for point source pollution control are not appropriate for NPS pollution control since pollution processes occur over wide areas for the latter.

Major agricultural NPS pollutant transport processes are influenced by rainfall and runoff processes in particular. Thus, it is important to appropriately characterize rainfall and runoff processes when predicting pollutant transport and investigating its control methods. Innumerable studies have been conducted to understand NPS pollutant transport processes and to evaluate methods for controlling them. One of the earliest studies on NPS pollution led the development of the Universal Soil Loss Equation (USLE) (Schwab et al., 1981). This empirical and statistical relationship provided a tool for understanding soil erosion processes and enabled us to devise management tools for reducing soil erosion. Based on this experience, more sophisticated tools have been developed for different purposes.

Along with the development of computational tools, simulation models have become popular and useful for studying and investigating effective management methods for reducing NPS pollution. Simulation models could reasonably predict hydrologic and pollutant transport processes on a watershed and help determine the suitable management practices for specific conditions. NPS pollution models generally consist of two submodels: the hydrologic simulation model and the transport simulation model. The hydrologic model simulates infiltration, evapotranspiration, and runoff processes, and the transport model incorporate soil erosion,

sediment-bounded chemical transport, and solute transport processes. Some of these components are simplified or ignored according to the purpose and field characteristics. The results of the hydrologic model are used in simulating pollutant transport processes.

NPS models can be categorized as either event-based or continuous models. An event-based model is one that simulates hydrologic and pollutant transport processes for a single runoff event occurring over a specific period of time. This type of simulation is based on numerical techniques for solving differential equations. Therefore, boundary condition and initial condition such as soil moisture content are important. Continuous models, on the other hand, perform simulations over a longer period of time between storm events as well as during the storm events. Most continuous watershed models simulate not only direct runoff, but also interflow, groundwater flow, and evapotranspiration. These components, while not significant in event-based simulation, cannot be ignored in the continuous simulations.

Models could also be classified as either distributed or lumped models. In distributed models, processes such as infiltration or runoff are simulated using spatially-variable input data in the watershed. Distributed models perform simulations by breaking the watershed into a number of smaller homogeneous subareas. This type of models represent each sub-area with different characteristics, and it is possible to efficiently apply numerical methods for solving the systems of equations. A shortcoming of this type of models is their large input data requirement. This problem becomes serious when the watershed needs to be divided into a large number of subareas. Meanwhile, lumped models simulate runoff and pollutant transport processes by assuming uniformity in watershed characteristics. They simulate the processes as a single unit rather than a combined one composed of several different sub-units. The lumped models are more empirical and simpler to use as compared with the distributed models. In reality, however, it is difficult to precisely distinguish the lumped from the distributed models. Every deterministic model also assumes that a sub-unit is of uniform characteristics.

With regard to model accuracy, it is worthwhile to investigate whether both runoff and pollutant transport processes are appropriately described. Most NPS models employ simplified methods to simulate runoff processes, ranging from empirical to physically-based methods. Most of these models employ one-dimensional approach. Even though some of grid based models may be considered to be two-dimensional or quasi-two-dimensional approaches, in reality, they should be classified as one-dimensional models. The reason is that flow directions should be provided as an input data before running the models. The models cannot simulate secondary directional flow, therefore, flow partition should be provided as input when flow divides or converges. Flow

directions may be easily specified based on elevation data, but it can hardly be defined when flow division or convergence exists .

Pollutant transport processes in most NPS simulation models are described as a function of flow characteristics such as flow depth and velocity. For example, sediment transport capacity is frequently represented in the form of flow depth and/or velocity as well as soil and soil surface conditions. Therefore, when the estimation of flow characteristics is not accurate, the prediction of pollutant transport can not be expected to be accurate either. In order to obtain accurate estimations of pollutant transport, runoff processes should be appropriately simulated. More accurate simulations of runoff flow are required particularly when flow characteristics change significantly, such as in areas where topography is complex or structural management practices are installed.

A large selection of BMPs exist for control of NPS pollution. Many of these practices are used to control or retard runoff losses from the land surface. For example, some structural management practices, such as terraces, reduce slope length and divert runoff flows. They provide more opportunities for the pollutants to settle down, and thereby reduce the total pollutant losses to downstream water bodies. The application of existing NPS pollution models seems to be limited to topographically simple areas. They cannot be applied to such areas over which flow characteristics change due to complex topography. Their basic assumptions for the model may not hold when topography is not simple. The only way to apply such models to those areas is either simplification or change of input parameter to represent the net effects. This approach does not simulate actual runoff flow changes and the resulting pollutant transport processes. Moreover, input parameters can be changed only if we know the net effects. This approach cannot be considered as a simulation or modeling process but a procedure to fit the computational results to expected solutions. A more detailed approach is, therefore, required to simulate various topographic conditions where flow convergence or division are frequently observed.

In order to improve model predictions of NPS pollutant transport, more efforts should be concentrated on either developing better procedures for runoff simulation or developing improved relationships for describing pollutant transport processes. In reality, most relationships for pollutant transport process are represented by runoff and pollutant characteristics. Since the primary media for pollutant transport is runoff water, simulation of pollutant transport could be improved by better representation of runoff characteristics. Therefore, it is important to investigate the significance of appropriate representation of runoff characteristics in NPS pollution modeling. In this study, a fundamental approach to sediment transport modeling is investigated based on the hypothesis that improved representation of local hydrologic/hydraulic characteristics can enhance

the predicting capability of NPS models. In other words, it is hypothesized that detailed simulation of surface runoff processes can provide improved description of source and sink terms, thus resulting improved sediment transport predictions.

There are many factors which affect runoff characteristics, such as roughness coefficient, initial moisture condition and topography. Parameters such as roughness coefficient or initial moisture conditions are often provided as input data. They are determined by model users based on field conditions and their experiences. Unlike these parameters, topographic information could affect simulation of runoff processes according to model dimension in different ways. In the one-dimensional (1-D) modeling approach, field topography is represented by average slope in one direction assuming that secondary directional slope is insignificant and does not affect overall runoff processes. Flow path in 1-D modeling, therefore, is exactly the same as the length of the field or element. However, it is evident that flow path could be significantly different when considering variations in elevation in the field. Runoff flow converges along cross slope before flowing down along the dominant major slope. A two-dimensional (2-D) model allows the simulation of these processes. However, it is uncertain whether the 2-D approach can really improve the prediction of runoff characteristics and pollutant transport such as soil erosion and sediment transport, over the 1-D approach.

1.1 Goal and Objectives

The goal of this study is to test the hypothesis that the 2-D modeling approach can improve the simulation of sediment transport processes as compared with the 1-D simulation, where the only difference between 1-D and 2-D approaches is the incorporation of secondary directional slope. The specific objectives are:

1) Develop both 1-D and 2-D surface runoff models based on the full dynamic equations using the same mathematical basis and solution techniques.

2) Develop both 1-D and 2-D sediment transport models. The governing equations are essentially the same for the 1-D and 2-D approaches, except for the secondary directional term in 2-D. Runoff results are used as input in sediment transport models.

3) Investigate the differences in model predictions between the 1-D and 2-D models. Based on model applications to hypothetical case studies and field experimental studies, predictions are compared to investigate whether any significant improvements are achieved by using the 2-D approach compared to 1-D approach in simulating runoff and sediment transport processes.

2. LITERATURE REVIEW

2.1 Introduction

Nonpoint source (NPS) pollution is strongly related to hydrologic processes occurring on a watershed. As raindrops hit the soil surface, soil particles are disintegrated and detached from the surface due to the kinetic energy of rain drops. At the initial stage of rain, most of rain water passes through the surface and into deep soil. Rainfall excess causes runoff on the soil surface as infiltration rate becomes less than rainfall rate. The surface runoff also detaches and transports soil particle and other materials or pollutants. Since runoff is the medium for NPS pollutants transport, appropriate simulation of runoff and infiltration processes are required for reasonable estimation of sediment and solute transport. Thus, many NPS models include runoff simulation as well as pollutant transport simulation components.

During the last two decades, many NPS models have been developed for specific purposes and applied to different situations. Some of well-known NPS models are ANSWERS (Beasley et al., 1980), FESHM (Ross, 1978), CREAMS (Knisel, 1980), and AGNPS (Young et al., 1987). However, most of the existing NPS models employ simplified or approximation methods to simulate runoff processes such as the USDA-SCS curve number method in AGNPS.

In this chapter, selected NPS models are briefly reviewed, and different relationships for rainfall-runoff, infiltration, soil erosion, and solute transport process are discussed. Selected approaches for runoff simulation associated with numerical technique to solve the governing equations are also reviewed. In addition, the models' strength and weakness are also discussed in this chapter.

2.2 Review of selected NPS models

In this section, the models to be reviewed are AGNPS and ANSWERS as grid-based models, CREAMS as a field scale model, and FESHM as a one-dimensional finite element model. ANSWERS is based on the continuity equation and Manning's relation for runoff simulation, while AGNPS uses the SCS curve number method. FESHM employs the kinematic wave model which is a simplified form of St. Venant equations. These models are major NPS models which are

currently being used for various purposes. Each has its own strength in a certain component but shows limitations in other applications or simulations. The models are reviewed with respect to the procedures they employ for runoff estimation and sediment transport simulations.

2.2.1 AGNPS

The AGricultural NonPoint Source pollution (AGNPS) (Young et al., 1987) is a distributed, event-based model. AGNPS simulates runoff processes, soil erosion and transport, nitrogen, phosphorus, and chemical oxygen demand concentration. Runoff processes are simulated by the SCS curve number method. Peak runoff is estimated with an empirical relationship which uses parameters such as channel slope, runoff volume, and watershed length-width ratio. Soil erosion is estimated by a modified USLE. Sediment transport processes are estimated by considering the particle fall velocity, and average channel flow velocity is determined using the Manning's equation. Nutrient concentrations are estimated using the equations used in CREAMS (Young et al., 1987). The model uses square cells for its watershed subdivision.

The AGNPS model was tested for runoff estimations with observations from 20 different watershed in the north central United States (Young et al., 1989). The authors reported that peak runoff rates were estimated adequately with the coefficient of determination of 0.81, between the observed and estimated values. Reasonably good agreements were shown between model predictions and measured sediment yield from two watershed in Iowa and Nebraska (Young et al, 1989). Total nitrogen and total phosphorus estimations were compared realistically with measured data from 20 different points in the seven watersheds, even though these results were for small runoff events only.

Meanwhile, Wu et al. (1993) applied AGNPS to experimental watersheds and compared its predictions with CREAMS and ANSWERS. Their results indicated that AGNPS underestimated sediment yield for the storm events that produces large sediment yields while the estimated and measured runoff showed reasonable agreements. Since AGNPS simulates infiltration and runoff using the USDA-SCS curve number method, which has limited physical significance, it is difficult to use AGNPS to properly simulate sediment and solute transport processes in areas that structural management practices are established. Furthermore, the modified USLE is a statistical model that does not consider hydraulic characteristics. Using this type of relationship, appropriate prediction of soil erosion and transport can not be achieved, especially when the input parameters for the model are not known.

2.2.2 ANSWERS

The Areal Nonpoint Source Watershed Environmental Response Simulation (ANSWERS) (Beasley et al., 1980) is categorized as a distributed, event-based watershed scale model. ANSWERS simulates runoff process using an explicit, backward difference scheme of the continuity equation. Infiltration is estimated by Holtan's empirical equation. The model was updated to simulate sediment detachment and transport for different particle sizes (Dillaha and Beasley, 1983). Like AGNPS, ANSWERS employs square grid system for watershed sub-division.

The continuity equation is solved by combining it with the Manning's equation in which the hydraulic radius is assumed to be the same as the depth of water in surface detention. The depth is described as an empirical function of the height of maximum micro-relief and surface roughness parameter (Beasley et al., 1980). This relation was developed by using several field parameters to describe the surface storage potential of a surface. Since the flow relationship used in runoff routing is Manning's equation, flow is assumed to be uniform. Even though the uniform flow rarely exists in natural conditions, the equation is extensively used to approximate the flow velocity. However, the application of the equation may be questionable when flow velocity and depth vary spatially, because Manning's equation is based upon the assumption of uniform flow, which means no changes in flow depth or flow characteristics. Since flow depth is determined by the height of maximum micro-relief and surface characteristic parameter, it may not be easy to represent actual flow characteristics such as velocity and flow depth. When the flow depth and velocity are very important factors used in estimating pollutant transport processes, this approach may not be valid any more.

ANSWERS can simulate the impacts of best management practices for NPS pollution control through modification of input parameter values (Thomas et al. 1989). Some structural management practices such as ponds and parallel tile-outlet can be simulated by assuming a removal efficiency of a certain percentage for both sediment and surface runoff. However, most management practices for controlling NPS pollutant transport are based on flow retardation in order to reduce transport capacity of the flow. Flow characteristics around these structures change more significantly than other regions. Evaluation of management practices accompanying such changes in flow characteristics may not be achieved by this approach. We can not expect reasonable simulation of pollutant transport process with the uniform flow assumption since flow characteristics changes due to the installation of management practices.

Wu et al. (1993) reported that ANSWERS underestimated sediment yield for large storm events while it provided more consistent results for estimating runoff than AGNPS or CREAMS. They remarked that errors in estimating sediment yield could partly be explained by inadequacy of the method used in estimating runoff, soil moisture, and surface conditions. However, they noted that it is difficult to explain the large difference between the observed and prediction values of sediment yield for large storm events.

2.2.3 CREAMS

The field-scale model, Chemical, Runoff, and Erosion from Agricultural Management Systems (CREAMS) was developed to simulate the effects of management systems on NPS pollution (Knisel et al., 1980). The model consists of three major components; hydrology, erosion and sedimentation, and chemistry. The hydrologic sub-model estimates runoff volume and peak rate using either SCS curve number method or runoff routing using Green-Ampt infiltration model. Peak runoff and total runoff volume are mainly estimated for soil erosion simulation. Soil erosion is estimated using the USLE. Soil erosion and deposition processes are simulated based on the concepts of sediment transport capacity of runoff water. Both rainfall and runoff flow are considered as the media for the soil erosion and deposition processes. In the simulation of solute transport, the mixing of solute between soil water and runoff is assumed to occur uniformly in the top 1 cm layer of the soil.

In CREAMS, runoff can be estimated for a limited range of management practices. Since the model was developed for fields with relatively homogeneous soil and under a single management practice, model application can be made by lumping field characteristics or separate simulations could be made when field characteristics are not uniform.

2.2.4 FESHM

The Finite Element Storm Hydrograph Model (Ross, 1978) is a 1-D, distributed, event-based, finite element model. Runoff routing is performed using the kinematic wave model. Infiltration is estimated using Holtan's model. Soil erosion and sediment transport are simulated by an upgraded version of USLE (Wolfe, 1982). It does not simulate chemical or nutrient transport processes. Runoff routing for both overland and channel flow is performed by the kinematic wave approximation. Even though the kinematic wave model is good for simulating overland flow processes (Woolhiser, 1990), it can be applied only when the kinematic assumption does not fail. The assumption is that the friction slope is the same as the topographic slope. Since FESHM is a

1-D model, each sub-shed is divided into appropriate number of strips. The flow length of the strip should be determined by the user as a representative flow path through the strip. When overland area is not a rectangle, as usually is the case, the length of flow path and the width of the strip are different from the actual length of each element.

The kinematic wave model is more physically based than any of the runoff routing methods used in the models discussed above. Even though FESHM can be reasonably applied to simulate overland flow processes, the model has the limitation that inertia and convective terms should be negligible. Around the area where structural management practices are installed, flow depth and velocity change significantly so that the ignored terms become important. Moreover, the 1-D approach also becomes questionable since the flow division and convergence occur around the region. FESHM is valid only when discretization is made such that flow directions are properly represented.

2.2.5 Summary

As discussed, most existing NPS models seem to perform pollutant transport simulation without appropriate runoff simulation, particularly for structural management practices. They employ simplified and approximate approaches in simulating runoff processes. These approaches may not provide enough information about runoff characteristics for reasonable predictions of pollutant transport.

When evaluating three NPS models, AGNPS, ANSWERS, and CREAMS for three different experimental watersheds, Wu et al. (1993) reported that estimations of sediment yield showed large difference from the observed values. Meanwhile, runoff estimations were reasonably good such that the ratio of the estimation to the measured ranged between 0.3 and 1.2. These results suggest that runoff estimations seem to be performed reasonably well both by physically-based or empirical relationships. However, sediment transport processes were not accurately predicted. All three models showed consistent underestimation of sediment yield for large storms. On the other hand, the estimations of sediment yield were consistently greater than the measured values for small storms. In summary, total runoff volume could be reasonably estimated by these methods, however, when simulating the NPS pollutant transport processes, accurate representation of local runoff characteristics such as depth and flow velocity are more important than total runoff amount. In the following sections, various relationships for runoff, infiltration, and pollutant transport are discussed.

2.3 Runoff routing models

The simulation of storm runoff processes should incorporate interception, evaporation, infiltration, and routing of surface runoff. Interception and evaporation are usually ignored by the event-based models because their amount are negligible, compared to runoff amount. Thus, the main processes in the event based model are infiltration process and runoff routing. Runoff routing methods can be categorized into empirical and physically-based methods. The SCS curve number method is an example of the empirical and the kinematic wave model is an example of the latter. The runoff routing scheme employed in ANSWERS may lie in between the two since it consists of the continuity equation based on the principle of mass conservation and empirical relationship for estimating flow depth. In the following sections, some of runoff routing methods frequently used in the NPS models are reviewed.

2.3.1 SCS curve number method

The Soil Conservation Service (SCS) runoff equation which was introduced in 1950's is an empirical rainfall-runoff relationship for estimating runoff amount under various land use and soil types (Soil Conservation Service, 1972). Because of its simplicity, it has been widely used throughout the nation. The method is based on the analysis of storm event rainfall and runoff records and it states that rainfall amount should be sufficient to satisfy the initial abstractions, including interception, depression storage, and infiltration quantity. After runoff begins, runoff amount increases as the rainfall continues and detention increases up to a certain maximum retention. With the assumptions that the ratio of the actual retention to the maximum retention is equal to the ratio of the actual runoff to the amount of rainfall, and the initial abstraction is equal to two tenths of the maximum storage, the runoff relationship becomes (SCS, 1972) :

$$Q = \frac{(P - 0.2S)^2}{(P + 0.8S)} \qquad \text{for } P > 0.2\ S \qquad (2\text{-}1)$$

where Q = runoff
P = rainfall
S = maximum retention

The maximum retention, S, is related to a runoff curve number defined by :

$$CN = \frac{1000}{S+10} \tag{2-2}$$

where CN is the curve number. The maximum retention is limited by soil water characteristics such as infiltration rate and initial water content of the soil.

Even though this method has been used for more than 40 years, it does not provide enough information about runoff characteristics for physically-based NPS models. Rallison and Miller (1981) described some of the limitations of this method. One limitation is that the method does not provide transient expression. For example, the equation usually uses daily rainfall amount without considering the intensity of rainfall. The rainfall intensity is an important factor in both runoff routing and pollutant transport simulation. The CN method does not adequately represent infiltration and runoff processes which change over time, especially when pollutant transports are affected by flow depth and velocity.

2.3.2 Dynamic equations

Mathematical description for surface runoff can be obtained by applying the principles of the conservation of mass and the conservation of momentum. The so-called St. Venant equations are developed with the assumptions that : i) flow velocity is uniform over the water depth , ii) pressure change is hydrostatic, iii) friction on the boundaries can be represented by the relations for steady state flow, and iv) the average slope is small such that the cosine of its angle is near one (Cunge et al., 1980). When flow depth and velocity are chosen to be dependent variables, the 1-D continuity equation can be written as : (Cunge et al., 1980) :

$$\frac{\partial h}{\partial t} + \frac{A}{b}\frac{\partial u}{\partial x} + u\frac{\partial h}{\partial x} + \frac{u}{b}\left(\frac{\partial A}{\partial x}\right)_{h=const} = R_e \tag{2-3}$$

where h = flow depth
t = time
u = velocity
x = distance
A = area, a function of depth, h
b = width, a function of depth, h
R_e = rainfall excess

The momentum equation with an additional assumption that the momentum influx by rainfall is negligible is :

$$\frac{\partial u}{\partial t} + u\frac{\partial u}{\partial x} + g\frac{\partial h}{\partial x} + g(S_f - S_o) = 0 \qquad (2\text{-}4)$$

where g = acceleration by gravity
S_f = friction slope
S_o = bottom slope

In many cases, it is assumed that A/b in Equation 2-3 can be represented by flow depth and the change in cross sectional area along x direction is negligible or zero so that the continuity equation takes the form :

$$\frac{\partial h}{\partial t} + h\frac{\partial u}{\partial x} + u\frac{\partial h}{\partial x} = R_e \qquad (2\text{-}5)$$

The two unknown variables, flow depth and velocity, can be solved by these equations when the friction slope in the momentum equation is described by the steady flow equation :

$$u = \frac{1}{n} S_f^{1/2} R^{2/3} \quad \text{or} \quad S_f = \left(\frac{u \cdot n}{R^{2/3}}\right)^2 \qquad (2\text{-}6)$$

where n = Manning's coefficient
S_f = bottom slope
R = hydraulic radius

It can be seen that the system of equations is non-linear. The dynamic equations can be solved using a numerical method such as the method of characteristics, finite difference, or finite element method. However, due to the non-linearity of this system, iteration or a linearization technique is required for solving them and, therefore, the cost of finding the solution become expensive.

A comprehensive study on the finite difference solution of the dynamic equations was made by Liggett and Woolhiser (1967). They provided guidelines for solving the equations by the finite difference scheme. They investigated the characteristic method, explicit methods including Leap-Frog scheme and Lax-Wendroff scheme, and implicit method with respect to stability and their characteristics. The error analysis they provided can also be used in the finite element method, since the time integration in the method is one of finite difference methods.

Cooley and Moin (1976) and Szymkiewicz (1991) used the finite element method to simulate open channel flow. Cooley and Moin employed a predictor-corrector scheme, while Szymkiewicz used Newton's method for solving non-linear systems. The 2-D simulations on the

watershed flow were also performed by Chow and Ben-Zvi (1973), and Taylor et al. (1974). The 2-D dynamic equations are also derived in the similar fashion. Unlike 1-D modeling, the 2-D representation has three unknown variables of flow depth, and velocities in x and y directions. The 2-D continuity equation can be written as :

$$\frac{\partial h}{\partial t} + \frac{\partial (uh)}{\partial x} + \frac{\partial (vh)}{\partial y} = R_e \tag{2-7}$$

where u and v are velocities in x and y direction, respectively. By applying the principle of the conservation of momentum to the water body in x and y directions, two momentum equations are derived (Taylor et al., 1974) :

$$\frac{\partial u}{\partial t} + u\frac{\partial u}{\partial x} + v\frac{\partial u}{\partial y} + g\frac{\partial h}{\partial x} + g(S_{fx} - S_{ox}) = 0 \tag{2-8}$$

$$\frac{\partial v}{\partial t} + u\frac{\partial v}{\partial x} + v\frac{\partial v}{\partial y} + g\frac{\partial h}{\partial y} + g(S_{fy} - S_{oy}) = 0 \tag{2-9}$$

where S_{fx} and S_{fy} are friction slope in x and y direction and S_{ox} and S_{oy} are bottom slope in each direction. The momentum influx by rainfall is ignored as in 1-D equation.

Chow and Ben-Zvi (1973) used the finite difference scheme to solve the equations and compared the results with the experimental observations which showed reasonable agreements. In their study, infiltration was not included. Kawahara and Yokoyama (1980) also presented the finite element simulation of 2-D runoff flow using three-node triangular element. They pointed out that appropriate description of friction on the bed was important in simulating runoff and obtaining the computational stability. Zhang and Cundy (1989) also applied the finite difference method for overland flow based on the explicit predictor-corrector scheme which was originally developed for simulating aerodynamic problems. The time steps they used ranged from 0.012 to 0.006 seconds. Cuhadaroglu and Maidment (1992) also presented a 2-D finite element model based on triangular element, where they introduced the usefulness of GIS integration with runoff simulations. Most recently, Tayfur et al. (1993) investigated the applicability of 2-D dynamic equations to simulating overland flows. They employed a centered implicit finite difference method and Newton-Raphson iterative technique. In their concluding remark, they pointed out the importance of local hydraulic characteristics such as flow depth and velocity in solute transport and sediment transport studies and stressed the necessity of 2-D modeling in simulating pollutant transport.

In general, direct application of the dynamic equations to simulate surface runoff processes is costly. Due to their non-linearity, iteration techniques or linearization are required to find solution. Thus, simplified forms of the dynamic equations were introduced and investigated. When the local and convective terms in Equation 2-4 are assumed to be negligible, the momentum equation becomes (Cunge et al., 1980):

$$\frac{\partial h}{\partial x} = S_o - S_f \tag{2-10}$$

This simplification of the momentum equation is combined with the continuity equation to define the diffusion wave model. Instead of using Equation 2-10, the momentum equation can be further simplified as :

$$S_o = S_f \tag{2-11}$$

Equation 2-11 is combined with the continuity equation, resulting in the so-called kinematic wave model. This method approximates the full dynamic equations based on the assumptions that the inertia terms in the momentum equation are negligible and flow is a function of depth (Cunge et al., 1980)

2.3.3 Diffusion wave approximation

Diffusion wave model, or diffusion analogy using Equation 2-10 instead of using the momentum equation (2-4) can be written by combining Equation 2-10 and Equation 2-3 (Stephenson and Meadows,1986) :

$$\frac{\partial q}{\partial t} + C\frac{\partial q}{\partial x} = D\frac{\partial^2 q}{\partial x^2} \tag{2-12}$$

where C = wave celerity
D = dispersion coefficient
q = flow rate

Since Equation 2-12 is a form of the classical parabolic type partial differential equation, it is commonly called the diffusion wave model. The diffusion wave approximation has the advantage of being able to simulate wave propagation or attenuation since it has a diffusion term. Ponce et al. (1978) stated that the diffusion wave approximation is appropriate for simulating most flood wave propagation in stream channels. However, in some cases like the presence of backwater, a dam-break flood, or flow reversals, the full dynamic equation would have to be used.

Computational algorithms for diffusion wave model in channel routing can be found in the literature (Blandford and Ormsbee, 1993, Akan and Yen, 1981). An interesting example of the diffusion wave model application to channel routing is presented by Chung et al. (1993). They employed Laplace transform method to obtain the solution of the diffusion wave model in which the transform was numerically inversed.

2.3.4 Kinematic wave approximation

The kinematic wave approximation assumes that the longitudinal change in depth, and velocity change in space and time, are all negligible. Equation 2-11 indicates that the equation of motion can be approximated by a uniform flow formula of the general form :

$$q = a \cdot h^b \tag{2-13}$$

where a, b = constant
q = discharge per unit width
h = water depth

In other words, the kinematic wave approximation simply states that the friction slope is equal to the bed slope. The friction slope can be evaluated using any suitable friction equation such as Manning's equation or Chezy's equation. Substituting Equation 2-13 into the continuity equation gives :

$$\frac{\partial h}{\partial t} + a \cdot b \cdot h^{b-1} \frac{\partial h}{\partial x} = R_e \tag{2-14}$$

One of the advantages of the kinematic wave assumption is that analytical solutions for the model can be obtained for simple cases so that the solutions obtained from numerical schemes for the kinematic model can be easily compared. However, the kinematic wave approximation has the limitation that it can not fully explain flow behavior since both the inertia and pressure terms are omitted from the momentum equation.

Vieira (1983) investigated various flow conditions to which the kinematic wave model can be reasonably applied. He used the dimensionless analysis technique to provide criteria for appropriate use of different approximations. He used two independent dimensionless parameters, Froude number and kinematic wave number. Froude number is defined as :

$$F = C\sqrt{\tan\theta / g} \quad \text{or} \quad \frac{V_o}{\sqrt{gH_o}} \tag{2-15}$$

where F = Froude number
θ = slope
V_o= normal velocity
H_o= normal depth

and the kinematic wave number is :

$$k = (g^3 L \tan\theta / C^4 q^2)^{1/3} \tag{2-16}$$

where k = kinematic wave number
L = length of the reach
C = Chezy's constant
q = lateral inflow

For $k > 5$, Vieira (1983) found that the diffusion and kinematic wave models are very similar. When $k < 3$, the diffusion approximation can be used if $F < 0.25$, and kinematic wave model can be used if $F > 1$. Meanwhile, Vieira recommended that full dynamic equations should be used for $k < 5$. In most overland conditions, k values are much larger than 50. Thus, kinematic wave approximation can be reasonably used.

It may be worthwhile to investigate the ranges of k and F for average overland flow conditions. When the depths of overland flow are considered to range between 0.001 and 0.1 m and velocity between 0.01 and 0.5 m/sec, values of k and F can be calculated to evaluate which method is more appropriate for different surface conditions. Figure 2-1 shows the variations in the Froude number for various flow depths and velocities. The maximum value of F is obtained when flow depth is small with high velocity.

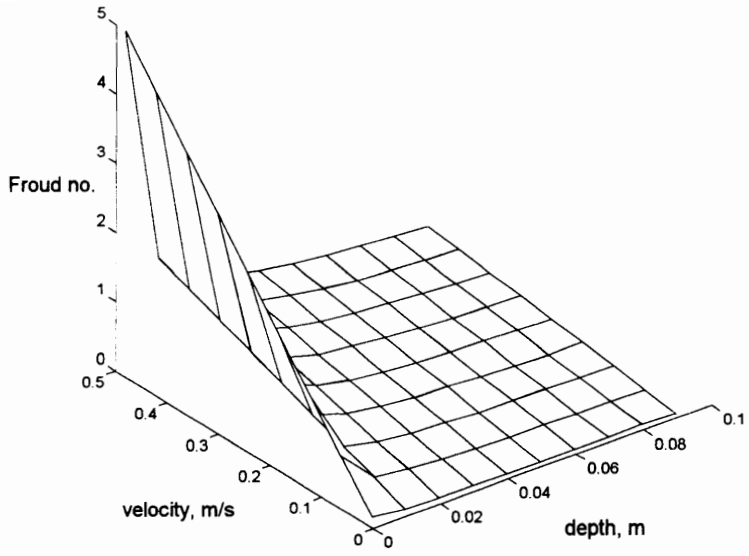

Figure 2-1. Froude numbers for different sets of Chezy's C and flow depth.

The kinematic wave number is another factor to consider in determining which approximation method can be used. As Equation 2-16 indicates, k increases as the lateral inflow decreases. In simulating overland flow processes, the lateral inflow can be considered as rainfall excess. For the range of rainfall excess from 1 to 20 cm/hr, the kinematics wave numbers are plotted in Figure 2-2 for different slope conditions. Chezy's constant is taken as 100 and total reach of the flow as 100 m for representative values. Under this condition, the kinematic wave number would be greater than 10. Therefore, either diffusion or kinematic wave model can be used for most overland conditions. Vieira (1983) suggested that the kinematic wave model could be used for most natural slopes for which the kinematic wave number is much larger than 50. Also he mentioned that the full St. Venant equation should be used for lower values of kinematic wave number, particularly for $F > 1$.

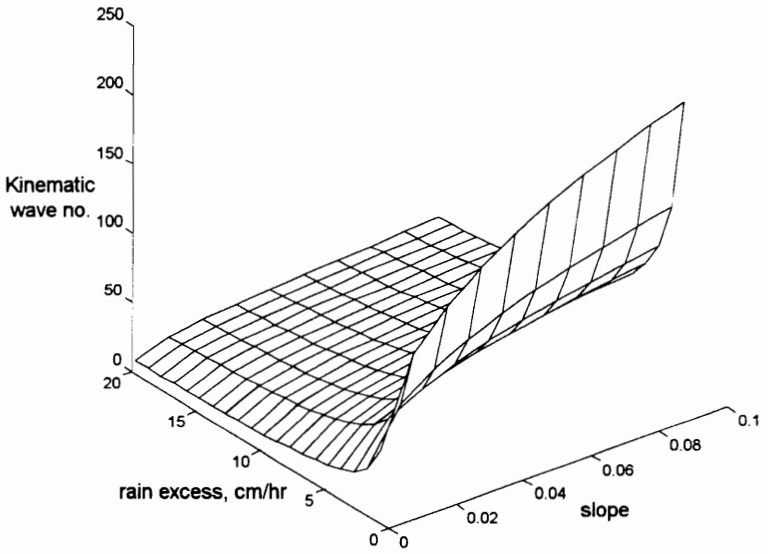

Figure 2-2. Kinematic wave numbers for different sets of slope and flow rate

The kinematic wave model has been most extensively used in overland flow simulations and soil erosion studies, mainly because of its simplicity, compared to the other methods. The applications of the kinematic wave model have been made to river flow simulations since the 1950's (Ross and Shanholtz, 1979; Henderson,1966). The finite element method was used to solve the kinematic wave model for simulating runoff processes by Judah et al. (1975), Jayawardena and White (1977), and Ross (1978). Many soil erosion and sediment transport studies were coupled with the kinematic wave model for simulating runoff processes (Sharda et al., 1994; Laguna and Giraldez, 1993; Woolhiser et al., 1990; Wolfe, 1982). More discussions on the criteria for using the kinematic wave model can be found in the literature (Ponce, 1978; Henderson, 1966).

Goodrich et al. (1991) applied the finite element method to a 2-D kinematic runoff routing based on a triangular irregular network (TIN), which is a digital elevation model in a vector-based geographic information system (GIS). They compared the simulation results with those from 1-D kinematic wave model and reported that the 2-D model took much more CPU time for runoff estimation for the same overland area compared to the 1-D model. However, they stated that the computational difficulties in 2-D runoff routing may be surmounted by the integration of digital elevation model with GIS.

2.3.5 Summary

The dynamic equations can be simplified into the kinematic wave or diffusion wave model without losing much accuracy in simulating runoff processes for simple overland flow processes. However, they are limited in their applications to certain cases where the changes in hydraulic characteristics are significant since the simplified models do not include spatial changes in flow depth and velocity. The approximate methods may be used for most overland flow conditions without losing much accuracy unless flow characteristics change significantly. When flow characteristics change significantly, the full dynamic equations are recommended for more reliable estimations.

2.4 Numerical methods for solving dynamic equations

There are no known exact analytical solutions for the dynamic equations. The equations can be solved analytically only when they are simplified. Otherwise, they should be solved using numerical integration methods such as finite difference method, finite element method, or method of characteristics. The method of characteristics is a semi-graphical technique in which the dynamic equations are transformed into a set of the ordinary differential equations (Overton and Meadow, 1976). Another numerical technique, numerical inversion of Laplace transform, can be used when the dynamic equations are simplified into the diffusion wave model (Chung et al., 1993). In the following sections, the finite difference and finite element methods are discussed based on their applications to the dynamic equations.

2.4.1 Finite difference method

The finite difference method is an approximate technique using Taylor's series expansions which replaces the continuous derivative terms with approximate finite difference equations. This method transforms a set of differential equations into a set of algebraic equations which can be easily solved by digital computers. The finite difference method can be classified into implicit scheme and explicit scheme, based on time integration scheme.

Since the dynamic equations are hyperbolic type partial differential equations, von Neumann condition and Courant-Friedrich-Lewy (CFL) condition are satisfied for the stability of the finite difference method (Sod, 1989). The Von Neuman condition requires that the

amplification factor, which is derived by taking discrete Fourier transform, should meet the following condition :

$$\rho(\varepsilon) \leq 1 + Ck \tag{2-17}$$

where $\rho(\varepsilon)$ = amplification factor, $0 < \varepsilon < 2\pi$
C = constant
k = time step

The CFL condition or Courant condition can be written as (Zhang and Cundy, 1989) :

$$C = \Delta t\left(\frac{u_{max}}{\Delta x} + \frac{v_{max}}{\Delta y} + c\left(\frac{1}{\Delta x^2} + \frac{1}{\Delta y^2}\right)^{1/2}\right) \leq 1 \tag{2-18}$$

where C = Courant number
c = celerity, $\sqrt{gh}$
Δx, Δy = grid size dimensions in x and y directions
u_{max}, v_{max} = maximum velocities in x and y directions

The finite difference method generally uses square grids for discretizing 2-D problem domains in order not to lose the accuracy. When problem domains are complex in their shape, it is not easy to discretize them using square grid systems. The problem domain in hydrologic simulations is a watershed or its subsheds. Particularly, when a small part of whole domain need to be re-discretized, the entire problem domain should be re-discretized in order not to lose the accuracy of the solutions. Use of the finite difference scheme may not be convenient in applications to hydrologic modeling with respect to watershed discretization. Meanwhile, it is most useful when watershed is discretized by square grid system such as in ANSWERS or AGNPS.

The finite difference method seems to be one of the popular techniques for solving differential equations in engineering applications because of its easy derivation of algebraic equations from difference equations. Tayfur et al. (1993) presented a finite difference scheme for solving the 2-D St. Venant equations and described some limitations in applying the equations in the field. They adopted the centered implicit scheme and the Newton-Raphson iterative technique in their applications (Tayfur et al., 1993).

2.4.2 Finite element methods

The finite element method is another numerical approximation method based on the calculus of variations. The method uses polynomials as the basis functions. The finite element method can be virtually applied to systems with any type of geometric problem domain or boundary conditions. Unlike the finite difference method, the finite element method can represent problem domains in more detail at the same level of discretization as the finite difference, since the method can adopt triangular or quadrilateral elements for discretization.

In this method, the governing differential equations are multiplied by a weighting function to obtain one or two order less system of differential equations. The weighting functions are interpolation functions determined by the characteristics of the element. Finally, the differential equations become the algebraic equations with unknowns at each nodes in the elements. With respect to the accuracy of the solutions, the finite element method is not different from the finite difference method. In fact, finite difference equations can be derived analogously to the finite element method and they are utilized to investigate the stability analysis of the finite element system. Major advantages of the finite element method over the finite difference method include the representation of complex geometry of problem domain and their portable structure. Either triangular or quadrilateral element can be used in 2-D problems and partial re-discretization is possible without losing accuracy.

In hydrologic modeling, the finite element scheme has been used for solving the full dynamic equations by Cooley and Moin (1976) and Taylor et al. (1974). Jayawardena and White (1977), Ross (1978), and Vieux (1989) used the method to solve the equations using the kinematic wave approximation. In addition, the method is extensively being used in both surface and sub-surface flow problems.

2.4.3 Summary

Both the finite element and finite difference methods can be used in solving the dynamic equations. The finite element method is more advantageous than the finite difference method in terms of representation of watershed boundaries since the finite element methods allow the use of more flexible shapes of the element. Overland area elements in hydrologic or NPS simulations are determined mostly based on soil type and land use. They have quite complex geometry so that it is difficult to represent them in a square grid network as used in finite element methods.

2.5 Infiltration models

Infiltration is defined as the water movement from the surface into the soil profile. In simulating hydrologic or NPS pollutant transport processes, infiltration models are used for estimating infiltration amount as well as rainfall excess which is considered as lateral inflow. In this section, the widely-used Holtan's model, Green-Ampt model, and Smith and Parlange's model (1978) are briefly described. Parlange et al.'s model (1982) and Smith et al.'s model (1993) are included in this review because of their sophisticated physical representation of infiltration process. Holtan's equation is an empirical model which is used in such models as FESHM and ANSWERS. The Green-Ampt model is based on Darcy's law, and Smith and Parlange's (1978) model and Smith et al.'s model (1993) are based on Richards equation.

2.5.1 Holtan's infiltration model

Holtan (1961) described an empirical equations based on a water storage concept :

$$f_p = a \cdot F_p^{\,n} + f_c \qquad (2\text{-}19)$$

where f_p = infiltration capacity
F_p = available storage in the surface area
n = experimental coefficient (1.4)
a = index of surface connected porosity
f_c = constant or steady state infiltration

Holtan's equation is based on field experiments and the principle that infiltration rate decreases as the pores in the soil fill up with water. The main advantages of this empirical equation are that the use of this equation is not difficult and the input parameters can be obtained from general description of soil type and crop conditions. This seems to be the reason why some of NPS model such as ANSWERS and FESHM adopted this equation for estimating rainfall excess. However, this model is very sensitive to the parameter 'a' which varies widely with antecedent moisture. Since F_p is determined by the depth of effective control zone, which is arbitrarily determined, the application of the model may be limited.

2.5.2 Green-Ampt model

Green and Ampt (1911) proposed an approximate infiltration model using Darcy's law. They derived the equation by assuming that ponding depth is time variant and surface water flows into a deep homogeneous soil with a uniform initial water content.

$$f_p = K_S (H_O + S_f + L_F) / L_F \quad (2\text{-}20)$$

where K_s = hydraulic conductivity of transition zone
H_o = ponding depth
S_f = effective suction at the wetting front
L_F = distance from the surface to the wetting front

Since its development, the Green-Ampt equation has been modified by Morel-Seytoux and Khanji (1974), Mein and Larson (1973), and others. This method has the advantages that it can describe the infiltration under various initial and boundary conditions and parameters in the model can be obtained from soil properties.

The modified Green-Ampt model by Mein and Larson (1973), using cumulative infiltration, takes the form :

$$f_p = K_s + K_s \cdot M \cdot S_{av}/F_p \quad (2\text{-}21)$$

where f_p = infiltration
$M = (\theta_S - \theta_i)$
S_{av} = suction at the wetting front
F_p = cumulative infiltration
θ_s = soil water content at saturation
θ_i = initial soil water content

The volume of infiltration up to the ponding time (t_p) is :

$$F_S = S_{av}\, M/(R/K_S - 1) \quad (2\text{-}22)$$

where R = rainfall. For $t > t_p$:

$$K_S (t - t_p + t_p') = F - M\, S_{av} \ln(1+F/M\, S_{av}) \quad (2\text{-}23)$$

where t_p' = time required to infiltrate a volume equivalent to F_S under ponded surface condition.

Moor (1981) presented a solution for the Green-Ampt model modified by Mein and Larson (1973) for a two-layer soil profile. By comparing four infiltration models (SCS curve number

method, Holtan's method, Modified Green-Ampt method by Mein and Larson (1973), and Richards equation), Wells et al. (1986) stated that the modified Green-Ampt model by Mein and Larson gave as good an estimation of infiltration as Richards' equation.

2.5.3 Smith and Parlange's equation

Smith and Parlange (1978) introduced a new infiltration model based on two parameters, saturated hydraulic conductivity and a parameter that is related to soil sorptivity. The model was developed based on the assumption that hydraulic conductivity varies slowly and soil water diffusivity varies rapidly near the saturation. The model can be written as following :

$$f = \frac{K_s \exp(FK_s / C)}{\exp(FK_s / C) - 1} \tag{2-24}$$

where f = infiltration rate
K_S = saturated hydraulic conductivity
F = cumulative infiltration
C = parameter related to initial water deficit

The two parameter used in this model, the saturated soil hydraulic conductivity and a parameter related to sorptivity and initial saturation, can be measured by infiltrometer test. The parameter C is directly proportional to the initial water deficit. Woolhiser et al. (1990) adopted this model to calculate rainfall excess in a simulation model for simulating runoff and sediment transport. The parameters for this model is estimated using the data sets presented by Rawls et al. (1982). Although they did not compare the estimated values with measured infiltration data, the runoff estimation seemed to be reasonable (Woolhiser et al., 1990).

2.5.4 Parlange et al.'s equation

Smith and Parlange (1978) compared Green-Ampt model and their model with solutions by a numerical method of Richards equation and found that the numerical solutions fell between the estimations by Green-Ampt model and their model. Based on these results, Parlange et al. (1982) introduced an infiltration model by introducing a new parameter in addition to the usual sorptivity and saturated hydraulic conductivity. This relationship was used in simulating infiltration processes by Smith et al. (1993) for multistorm events in which rainfall rate is less than infiltration rate. Smith and his colleagues included soil water redistribution based on the principle

of mass conservation in the wetted profile. The basic infiltration model proposed by Paralnge et al. (1982) was :

$$f_c = K_s[1+\frac{\alpha}{\exp[I'\alpha / (\Delta\theta G)]-1}] \quad (2\text{-}25)$$

where α = interpolating coefficient
$I' = G\Delta\theta\ln[f_c/(f_c-K_S)$
$\Delta\theta = \theta_S-\theta_i$
G = integral capillary drive across the wetting front
f_c = infiltration rate

Parlange et al. (1982) compared the model estimation with other methods' such as Green-Ampt's, Smith and Parlange's, and Haverkamp et al.'s (1977). The procedure by Haverkamp et al (1977) is based on Philip's time expansion and infiltration relationship. Parlange et al.'s model (1982) estimations were close to the numerical solutions obtained by Richards' equation. However, the method uses many parameters which are difficult to measure in the field. The result also showed that Paralnge et al.'s model was quite accurate for both clay and sandy soils when α was near 0.8. The Green-Ampt model slightly overestimated cumulative infiltration but Smith Parlange's model underestimated it for both clay and sandy soils. Smith et al. (1993) reported that complex infiltration processes could be most accurately simulated by Parlange et al.' model (1982) with the consideration of soil water redistribution during the period when rainfall rate is less that infiltration rate.

2.5.5 Summary

Four different infiltration models were described in this section. Holtan's equation is a more empirically-based relationship than others, and its predictions are very sensitive to the value of empirical parameters. Compared with the solutions obtained by Richards' equation, which is considered the closest to the exact solutions, Parlange et al's model (1982) seems to be a more reliable method than Green-Ampt or Smith and Parlange's model. When the interpolating parameter, α, is taken as a constant, the input requirement of the model is the same as Green-Ampt or Smith and Parlange's model (1978).

2.6 Soil erosion and sediment transport

Soil erosion is a complex process of removing surface soils and organics by rainfall, surface runoff, or wind. Soil particle transported by surface runoff become sediment. Sediment problems include reducing water storage capacity of reservoirs, lakes, stream channels, etc. Sediment causes high turbidity which affects aquatic habitat. Moreover, sediment carries chemicals which are adsorbed to soil particles. A general approach in studying soil erosion processes is through the formulation of the fundamental equations of water and sediment transport (Laguna and Giraldez,1993).

2.6.1 Conceptualization of soil erosion processes

There are two main approaches in the conceptualization of soil erosion and deposition studies (Rose, 1985): one is based on Foster's approach (Foster et al., 1981; Foster, 1982), and the other is by Rose and his associates (Rose et al., 1983a, 1983b; Rose, 1985). The first approach is based on the explicit description of rill and interrill processes. The interrill process involves cross slope runoff flow and its supply of sediment into rills. The rill process explains down-slope process along with the slope. Meanwhile, the second conceptualization proposed by Rose et al. (1983a) does not have explicit conceptualization of rill/interrill processes. An independent approach for soil erosion and sediment transport modeling presented by Borah (1989) can be considered as similar to Rose's approach. Borah' method also does not make a distinction between rill and interrill processes.

In the following sections, three methods of Foster, Rose, and Borah are discussed for sediment routing and source and sink estimation. Different conceptualizations result in different relationships in determining source and sink terms in the continuity equations for pollutant transport.

2.6.1.1 Sediment routing

Sediment transport can be described based on the principle of the conservation of mass. By assuming that sediment movement is the same as the velocity of runoff water, the governing equation for sediment transport in one dimension can be written as (Bennett, 1974; Borah, 1989; Rose et al., 1983a) :

$$\frac{\partial Q_s}{\partial x} + \frac{\partial (CA)}{\partial t} = SS \qquad (2\text{-}26)$$

where Q_s = sediment discharge
C = sediment concentration
A = cross sectional area of flow
SS = source and sink term
x, t = space and time, respectively

For two dimensional cases, the governing equation can be written by including y directional concentration change in a similar way. The source and sink term, SS, can be determined in different ways according to different conceptualizations. Equation 2-26 does not include elevation changes over time due to the sediment deposition or erosion, which may affect both runoff and sediment transport for long term simulations.

2.6.1.2 Foster's approach and its derivatives

Soil erosion and transport processes in overland areas are explained by rill and interrill processes (Foster et al., 1981; Foster, 1982). The interrill erosion process includes both detachment and transport of soil particles by either rainfall impact or sheet flow. Runoff water and soil particles feed to rill flow and rill process. The amount of soil particle entering from lateral cross-slope into rill is estimated by a modified USLE equation. The lateral inflow of sediment is combined with sediment entrained within the rill to give potential load of sediment. The potential load is compared with a sediment transport capacity which is determined by surface and flow conditions. The potential load is compared with the capacity to determine whether deposition or erosion has occurred. Foster employed the Yalin's bed-load transport equation for estimating the sediment transport capacity. Again, Foster's conceptualization of soil erosion and transport processes can be summarized in a sequence of processes: soil particle detachment and transport by rainfall, soil erosion and transport by sheet flow, lateral inflow of sediment into rill, and erosion or deposition by sediment transport capacity determined by flow conditions. This approach is similar to that presented by Meyer and Wischmeier (1969).

2.6.1.2.1 Interrill process

Interrill erosion processes are mainly due to rainfall and sheet flow. Foster (1982) explained interrill process by erosivity due to rainfall energy and intensity, soil erodibility, slope, cover and management factors. These factors are based on parameter of USLE equation. After Foster's conceptualization of soil erosion, many similar approaches were presented and applied to estimate the amount of soil erosion from soil surface (Singh and Prasad, 1982; Shirley and Lane,

1978; Laguna and Giraldez, 1993). The WEPP (Water Erosion Prediction Project) technology also uses similar relationship to Foster's concept of interrill erosion (Nearing et al., 1989). The differences between WEPP and other existing approaches lies in introducing rill parameters into interrill relationship, such as rill spacing or rill width. However, this approach is fundamentally the same in that different relationships just introduce new parameters to explain several factors which determine erosion and transport processes.

By lumping several factors, simpler interrill erosion relationships can be introduced. Laguna and Giraldez (1993) used a relationship for interrill erosion based on other investigations, which was represented as a function of rainfall rate. They used two parameters; an exponent for rainfall rate and a lumped parameter determined by soil erodibility and C factor in USLE equation. The exponent in the relationship is usually taken as 1 or 2 (Singh and Regl, 1983; Blau et al., 1988; Croley, 1982; Woolhiser et al., 1990).

Unlike these relationships, Woolhiser et al. (1990) incorporate the influence of flow depth to represent reduction in splash erosion due to increased flow depth. In fact, they did not explicitly use interrill erosion concept but employed splash erosion along with hydraulic erosion comparable to rill erosion. However, the basic approaches in determining source and sink terms for soil erosion prediction are identical to Foster's concept.

2.6.1.2.2 Rill processes

Rill erosion or deposition processes is determined by sediment transport capacity. Foster pointed out that rill erosion is more critical in serious erosion problem than interrill erosion (Foster, 1982). Factors affecting rill erosion include cover and management and shear stress on soil surface which is determined by flow conditions. Rill erosion and flow are assumed to be uniformly distributed across the slope even though actual erosion processes are conceptualized to be concentrated in small channels or rills. With the assumption that erosion in a single rill is a function of shear stress, gross rill erosion can be written as :

$$E_R = a(\tau - \tau_{cr})^b \qquad (2\text{-}27)$$

where E_R = rill erosion detachment capacity rate
τ = flow's shear stress
τ_{cr} = critical shear stress
a , b = empirical parameters

E_R is in mass per unit total surface area per unit time. Since there is no explicit expression of deposition and erosion, the erosion estimated by Equation 2-27 can be considered as net amount (Rose, 1985). The empirical parameters explain soil erodibility and other factors related with soil cover.

In a different form, rill erosion is frequently represented by runoff characteristics (Shirley and Lane, 1978; Laguna and Giraldez, 1993) :

$$E_R = \gamma(k \cdot h^b - c \cdot q) \tag{2-28}$$

where γ = empirical parameter
b = an exponent
q = flow rate per unit width
h = flow depth
k = rill erosion coefficient
c = sediment concentration

In Equation 2-28, there are two parameters, γ and k. k is related to soil erodibility, and γ is in the range of 3 to 33 m^{-1} as a proportional coefficient. Equation 2-28 indicates that rill erosion amount is proportional to the difference between sediment load and sediment transport capacity since the first term in the parenthesis of Equation 2-28 indicates sediment transport capacity.

Another expression was presented by Croley and Foster (1984), which is similar to Equations 2-27 and 2-28 :

$$E_R = \xi(1 - \frac{q \cdot c}{T_c}) \tag{2-29}$$

where ξ = a coefficient which is $K_r(\tau_f - \tau_c)$ for $T_c > q \cdot c$ and $(v_c \cdot T_c)/q$ for $T_c > q \cdot c$
T_c = transport capacity

K_r is a coefficient related to soil erodibility, and τ_f and τ_c is shear stress of flow and critical shear stress, respectively. v_c indicates settling velocity of soil particles. Equation 2-29 was later used in the WEPP by Nearing et al. (1989).

Woolhiser et al. (1990) presented an equation similar to the above equations, but they termed it as hydraulic erosion since they did not distinguish between rill and interrill erosion processes. The amount of erosion or deposition is represented by sediment transport capacity and current local sediment concentration :

$$E_h = c_g(C_{mx} - C_s)A \tag{2-30}$$

where E_h = hydraulic erosion

c_g = transfer rate coefficient
C_{mx} = sediment transport capacity
C_S = current sediment concentration
A = cross sectional area of flow

E_h is practically the same as the rill erosion, E_R. In erosion cases, c_g is determined by soil erodibility factor, K, in USLE equation while it is determined by settling velocity of soil particle. In their model, Woolhiser et al. (1990) provided six different equations for estimating sediment transport capacity. Selected equations for estimating sediment transport capacity are discussed in the following section.

Rill erosion is a process to describe soil erosion or deposition by runoff flow. The amount is determined by comparing the current sediment concentration and sediment transport capacity. Unlike the equations for interrill erosion, rill erosion process is directly determined by flow characteristics since sediment transport capacity is determined by runoff characteristics. Thus, appropriate estimation of sediment transport capacity is very important in evaluating source and sink terms in simulating sediment transport.

2.6.1.2.3 Sediment transport capacity

Many sediment transport capacity equations can be found in the literature. Some of them are empirically-based and simple to use, others are more physically-based and complex. In this section, Meyer and Wischmeier's (1969) equation based on tractive force concept, Yalin's (1963) equation, Yang's(1973) equation, and Engelund and Hansen's (1967) equation are briefly described and discussed with respect to runoff characteristics.

2.6.1.2.3.1 Meyer and Wischmeier's equation

In order to estimate sediment transport capacity, Meyer and Wischmeier assumed that the flow velocity is proportional to $S^{1/3}Q^{1/3}$ (Meyer and Wischmeier, 1969). With this assumption, sediment transport capacity of runoff was estimated using the findings by Laursen (1956) that the capacity of flowing water is approximately proportional to the fifth power of flow velocity :

$$C_{mx} = S_{tf}S^{5/3}Q^{5/3} \tag{2-31}$$

where C_{mx} = sediment transport capacity
S_{tf} = parameter related to soil particle size and density
S = slope
Q = flow rate

Equation 2-31 can be re-written as the function of flow depth and velocity with a constant, c_1:

$$C_{mx} = c_1 u^4/h \quad (2\text{-}32)$$

where c_1 = a coefficient
u = flow velocity
h = flow depth

As shown in Figure 2-3, the sediment transport capacity increases rapidly when flow depth is very small and velocity is large. Meanwhile, the sediment transport capacity at larger flow depth does not increase so much as in small depth. Since overland flow has a shallow flow depth compared to stream flow, sediment load estimation becomes very sensitive to flow conditions when Meyer and Wischmeier's equation (Equation 2-32) is used.

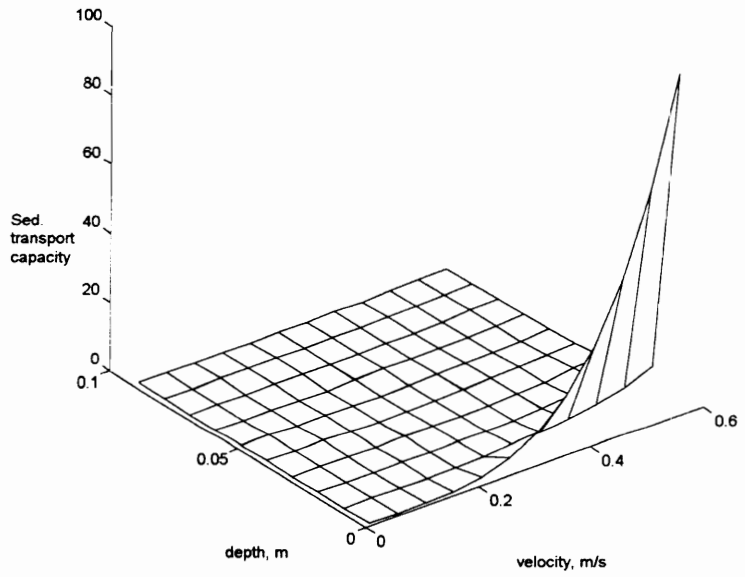

Figure 2-3. Sediment transport capacity by Meyer and Wischmeier's equation for different set of flow depths and velocities

2.6.1.2.3.2 Yalin's equation

Based on dimensionless analyses for seven independent quantities related to soil erosion processes, Yalin (1963) presented an expression for bed-load transport capacity for steady, uniform flow. The relationship is a function of kinematic viscosity, density of fluid, soil particle density, typical size of the particle, flow depth, and surface slope :

$$C_{mx} = 0.635 d u_* S_s \frac{\alpha}{uh}\left(1 - \frac{1}{\alpha\beta}\ln(1+\alpha\beta)\right) \quad (2\text{-}33)$$

where C_{mx} = sediment transport capacity
d = typical size of soil particle
h = flow depth
u_* = shear velocity, $(ghS)^{1/2}$ where g is gravitational acceleration and S is slope
S_s = specific weight of soil particle
$\alpha = Y/Y_{cr}-1$ for $Y > Y_c$ and zero otherwise
$\beta = 2.45/(S_s^{0.4})\cdot\sqrt{Y_c}$
$Y = u_*^2/((S_s-1)gd)$
Y_c = critical value of Y

When slope is 5% and Y_c is assumed to be Y at about 1mm of depth, the value of C_{mx} can be plotted as in Figure 2-4. For the 0.05 mm medium size of soil particle, the sediment transport capacity represented by Equation 2-33 increases as flow depth increases. This is similar to Meyer and Wischmeier's equation (Equation 2-32). Meanwhile, Yalin's equation shows an increase in sediment transport capacity with the reduced velocity, which is the reverse of Meyer and Wischmeier's equation.

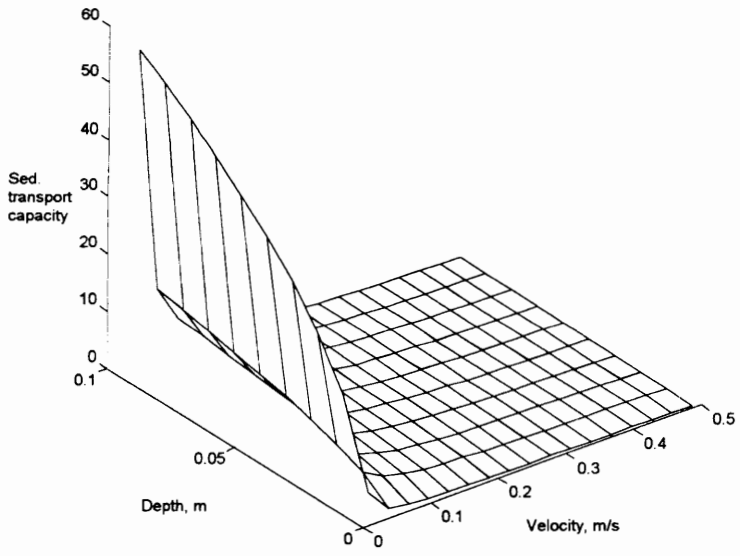

Figure 2-4. Sediment transport capacity by Yalin's equation for different set of velocity and depth

2.6.1.2.3.3 Yang's equation

Based on the unit stream power, which is defined as the time rate of potential energy expenditure per unit weight of water in an alluvial channel, Yang presented a relationship for sediment transport capacity for sediment particle sizes, ranging from 0.062 to 2 mm (Yang, 1973). The sediment transport capacity in part per million in weight can be estimated by :

$$\log(C_{mx}) = 5.435 - 0.286\log(\frac{\omega d}{\nu}) - 0.457\log(\frac{U_*}{\omega}) + (1.799 - 0.409\log(\frac{\omega d}{\nu}) - 0.314\log(\frac{U_*}{\omega}))\log(\frac{VS}{\omega} - \frac{V_{cr}S}{\omega}) \quad (2\text{-}34)$$

where C_{mx} = sediment transport capacity
ω = terminal fall velocity
d = mean sieve diameter
ν = kinematic viscosity
U_* = shear velocity
V = average flow velocity
S = slope
V_{cr} = critical water velocity at incipient motion
VS = unit stream power
$V_{cr}S$ = critical unit stream power at incipient motion

The dimensionless critical velocity, V_{cr}/ω, is taken as 2.05 when the shear velocity Reynolds number U_*d/ν is greater than 70. When the shear velocity Reynolds number is less than 70 :

$$\frac{V_{cr}}{\omega} = \frac{2.5}{\log(\frac{U_*d}{\nu}) - 0.06} + 0.66 \quad (2\text{-}35)$$

The critical unit stream power $V_{cr}S$, is not related to sediment or flow characteristics, but it is determined by the regression analysis between the calculated results and the measurements.

Figure 2-5 indicates that sediment transport capacity increases as flow velocity increases. The sediment transport capacity has a very large value when flow depth is small, which is similar to Meyer and Wischmeier's equation. It is notable that large values of sediment transport capacity is estimated at lower flow depth conditions by Yang's equation.

2.6.1.2.3.4 Engelund and Hansen's equation

Engelund and Hansen (1967) presented relationships for sediment transport in alluvial streams based on the similarity principle. In their equation, sediment transport capacity is determined by flow characteristics and soil particle size (Equation 2-36).

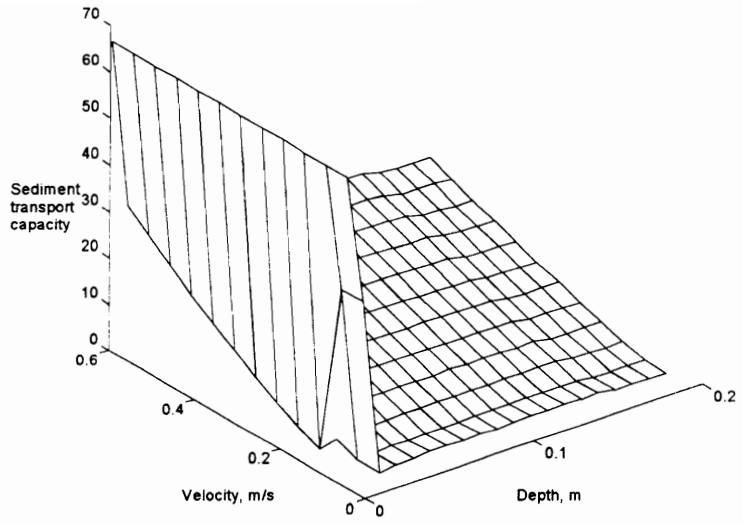

Figure 2-5. Sediment transport capacity by Yang's equation for different set of velocity and depth

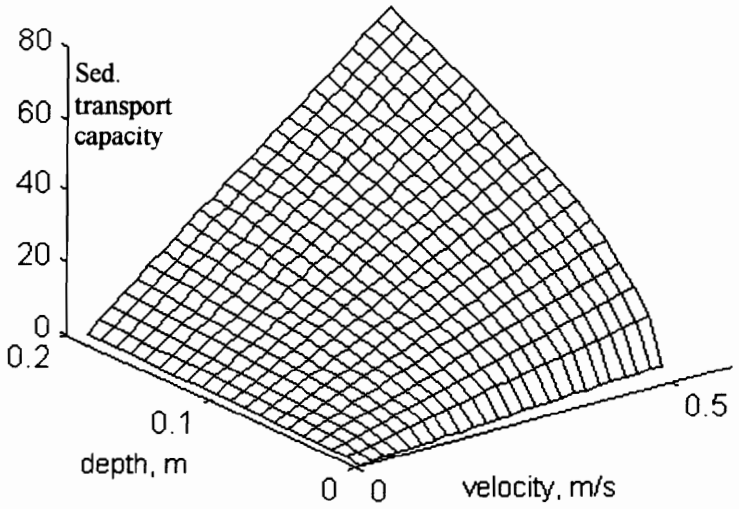

Figure 2-6. Sediment transport capacity by Engelund and Hansen's equation for different set of velocity and depth

$$C_{mx} = \frac{0.05uu_*^3}{g^2 dh(S_s - 1)^2} \quad (2\text{-}36)$$

Equation 2-36 is simple and it can be easily used without providing many parameters. Moreover, this relationship can be applied to overland flow conditions without serious limitations such as Yang's (Julien and Simons, 1985). In their reviewing several sediment transport capacity relationships, Julien and Simons (1985) pointed out the limitations in applying the equations used for turbulent flow in streams to the simulation of rainfall erosion in laminar sheet flows.

With the similar flow conditions to the previous illustrations, Equation 2-36 show the variations as shown in Figure 2-5. Sediment transport capacity increases as flow depth or velocity increase. Engelund and Hansen's relationship is closer to Yalin's equation than the other two equations in that the capacity increases with an increase in flow depth, while Yalin's equation does not show much variations in the capacity with respect to the changes in velocity.

2.6.1.2.4 Summary and discussion

The Foster's approach and its derivatives describe rill and interrill processes separately. In estimating sediment transport, their approaches are based on Meyer and Wischmeier's (1969) concept which consists of four sub-processes of detachment and transport by rainfall and runoff. Total amount of detached soil and total transport capacity are compared to the estimated sediment amount carried downslope.

Recent efforts on soil erosion predictions such as WEPP, are also based on the Foster's concept. The major differences from the original Foster's approach include incorporation of additional parameters to describe more factors which affect erosion processes and the use of a different equation for transport capacity. However, incorporation of additional parameters can not always guarantee better predictions of soil erosion and sediment transport since appropriate values for the new parameters are usually difficult to obtain. In fact, we may achieve better model prediction by using fewer number of parameters which are lumped to explain several factors. In this context, the number of parameters used in an equation may not be a good criterion for selecting soil erosion and transport equations.

By comparing different equations for sediment transport capacity, it could be seen that there are some contradictions among them. Some equations predict an increase while the other equations predict a decrease in sediment transport capacity with an increase in flow depth. A common trend with the equations is that the sediment transport capacity increases with an increase

in flow velocity except for Yalin's equation. This may be explained by the differences in the conditions under which the equations were derived. Especially, an equation derived for relatively deep flow conditions is quite difficult to apply for estimating the transport capacity at shallow flow conditions. In the meantime, these contradiction seems to suggest the difficulties which exist in estimating sediment transport capacity and simulating soil erosion processes.

2.6.1.3 Rose's approach

An approximate analytical model for soil erosion and deposition processes was developed by Rose et al. (1983a, 1985). Unlike Foster's approach, it does not consider rill or interrill processes, separately. The model, which assumes kinematic flow, describes rainfall detachment, sediment deposition, and soil entrainment by overland flow. These processes are considered as continuous and simultaneous processes. That is, soil detachment by rainfall and runoff is described, and deposition due to the gravity is assumed to occur during the processes.

Rainfall detachment rate is defined as the mass of soil detached by rainfall per unit area and time. It is assumed that the rate is proportional to the fraction of soil exposed to raindrops :

$$e=aC_eP^p \tag{2-37}$$

where e_i = detachment rate by rainfall
a = measure of the detachability of soil by rainfall
C_e = friction of soil not protected by surface cover
P = rainfall rate
p = constant, $1.3 < p < 2$

This relationship may be comparable to the equation for estimating interrill erosion amount of Foster's and its derivatives since it is basically a function of rainfall rate. In Equation 2-37, sediment is sorted conceptually into a number (I) of particle-size or aggregate-size ranges. The mass fraction of soil aggregates in the i-th class size range is 1/I. Thus, the detachment rate, e_i, of sediment in the size range, i, will be given by :

$$e_i = e / I \tag{2-38}$$

Due to the gravity, some of detached soil particles get deposited. This is described by estimating the rate of sediment deposition which depends on the terminal velocity :

$$d_i = v_i c_i \tag{2-39}$$

where d_i = deposition rate of i range
v_i = terminal velocity of i range
c_i = sediment concentration in size range class i

Total sediment deposition is computed as the sum of each d_i, for each sediment size i, so that each size class is defined by its settling velocity. The third process, sediment entrainment, includes concentration changes over time. The sediment entrainment, r, is explained using the concept of stream power :

$$r_i = (\rho g S K R_i / I)(\gamma_i - \frac{v_i}{R_i}\frac{x_*}{x})C_r + \frac{\partial(hc_i)}{\partial t} \quad \text{for} \quad x > x_* \tag{2-40}$$

where r_i = rate of sediment entrainment
$\gamma_i = 1 + v_i/R_1$
R_1 = Runoff
ρ = density of water
g = gravity acceleration
S = slope of the plane
$K = 0.276\eta$, η= efficiency of bed load transport
$x_* = \Omega_o/(\rho g S R_1)$, Ω_o is threshold stream power
C_r = fraction of bed exposed to entrainment
h = overland flow depth

By applying the principle of mass conservation of sediment, Equation 2-26 for size range i is :

$$\frac{\partial(qc_i)}{\partial x} + \frac{\partial(hc_i)}{\partial t} = e_i - d_i + r_i \tag{2-41}$$

Since r_i includes $\partial(hc_i)/\partial t$, Equation 2-41 becomes an ordinary differential equation. Thus, Equation 2-41 can be solved analytically to give :

$$c(x,t) = (aC_e P^2 / R_1 I)\sum_{i=1}^{I}(1/\gamma_i) + rgSKC_r(1 - x_*/L) \quad \text{for} \quad (x < x_*) \tag{2-42}$$

This model was applied to a small arid watershed in Arizona and showed good agreement between the measured data and the model results (Rose et al., 1983b).

2.6.1.4 Borah's approach

Borah (1989) presented a sediment routing procedure for small watersheds which accounts for soil erosion, sediment transport, deposition and discharges. Soil detachment by raindrop impact is considered to occur only when raindrop penetrate the water depth on the surface. The sediment routing equation he presented is based on mass conservation of sediment. The model uses a sediment transport formula based on the flow conditions, representative sediment size group, and

transport capacity of sediment in the group. The model simulates deposition when potential sediment exchange rate is less than zero, and estimates erosion when the rate is greater than zero. The volumetric potential sediment exchange rate is estimated by :

$$g^p = [AC^p - (A_s)_{i-1,j-1}] / \Delta t_j - q_s \quad (2\text{-}43)$$

where g^p = volumetric potential sediment exchange rate
i,j = discrete point along x axis and time
A_s = sediment load
A = cross sectional area of flow
q_s = volumetric rate of lateral sediment inflow per unit length
t = time
p = superscript representing potential
C^p = volumetric sediment concentration at the potential rate

When g^p is less than zero, the transport capacity is less than the sediment load or concentration present in the flow and deposition may occur. Thus, g^p is considered to indicate the potential rate of sediment deposition. When g^p is greater than zero, the transport capacity is greater than the sediment amount in the flow and erosion may occur. By considering that additional energy is required to detach soils from the solid layer beneath the soil surface, two different erosion processes are assumed. One is erosion from normal surface soil and the other is from the parent rock or solid materials.

2.6.2 Summary and discussion

In the previous sections, Foster's and its derivatives, Rose's, and Borah's approaches in simulating soil erosion and sediment transport processes were reviewed. Foster's approach is different from the other two in that it makes distinction between rill and interrill processes. Except for the recent efforts in WEPP, most rill geometry and their related factors are not included in the models. Although the concepts of rill and interrill processes are distinct and useful in simulating soil erosion processes, their description or parameterization are not easy. Meanwhile, Foster's and its derivatives have been applied widely and much information is available on their input parameter.

Rose's approach shows some similarities to Foster's. Both approaches have a common consideration of erosion process by raindrops. Meanwhile, Rose's approach includes soil deposition process, explicitly, while Foster's approach does not. It is notable that the continuity

equation of sediment becomes an ordinary differential equation from a hyperbolic type partial differential equation in the course of conceptualization. However, determination of parameters required in model applications seems to be difficult since there is not enough information available.

Based on the sediment exchange rate, Borah's approach made an effort to simulate soil erosion and sediment transport processes without using USLE parameters which he considered inadequate to simulate complex dynamic processes of soil erosion and its transport processes. Even though Borah reported that the model had showed reasonable prediction results (Borah, 1989), model applications to real field would require more information on input parameters.

2.7 Summary and conclusions

Based on the literature review presented in this Chapter, it is evident that most existing NPS models can not be accurately applied to predict complex runoff flow, which may accompany flow division and convergence. These flow regions often occur near structural management practices which are constructed to control flow and pollutant transport. Field conditions are inclined to give more complex flow phenomena so that runoff characteristics may change in an unexpected manner. The range of the kinematic wave number also indicates that the use of full dynamic equations are sometimes required even in normal overland flow situations. Thus, runoff simulation models based on the full dynamic equations are desirable to deal with various flow conditions.

As a numerical technique to solve the governing differential equations, either the finite element method or the finite difference technique could be used. The finite element method is more advantageous in discretization of watershed or overland area. The finite element method is more flexible than the finite difference method which is restricted to square grid for discretization. Another strength in the finite element method is its portability in its program structure where different system of equations can be easily applied using a common skeleton of program only if such matrices as stiffness and capacitance are changed. Thus, in this study, both 1-D and 2-D models can be easily developed with the same matrix solver.

Several infiltration equations were reviewed including Holtan's, Green-Ampt's, Smith and Parlange's, and Parlange's methods. A compromised relationship, Parlange et al's (1982) method which lies in between Green-Ampt's and Smith and Parlange's, is more comprehensive over wide range of soil characteristics. Parlange's equation can be used to estimate infiltration amount and rainfall excess for a wider range of soils than any other infiltration models.

In simulating sediment transport, source and sink terms can be estimated by many different methods. Foster's concept or its derivative have been extensively used for a long time so that input parameters can be easily obtained. However, Foster's concept include explicit representation of rill and interrill processes. Although the rill process is dominant and important in estimating soil erosion and sediment transport, sufficient information about the rill characteristics are not available. Thus, it is not necessary to distinguish rill and interrill processes in simulation of soil erosion and sediment transport. In this context, an approach presented by Woolhiser et al. (1990) could be used without much difficulty.

Sediment transport capacity could be reasonably simulated by Engelund and Hansen's (1967) equation. Sediment transport capacity estimated by Engelund and Hansen's equation is directly proportional to both flow depth and velocity. Julien and Simons (1985) also reported that Engelund and Hansen's equation is more reliable for overland flow condition than any other equation for estimating sediment transport capacity. Moreover, it has a compact form represented by flow depth, velocity, and soil particle properties.

3. METHODOLOGY

3.1 Introduction

The main difference between the 1-D and 2-D models is the representation of secondary directional flow in the 2-D approach. The 1-D approach is based on the assumption that the flow is one dimensional and secondary directional flows can be negligible, whereas, the 2-D approach takes into account the secondary flow in simulating flow processes. However, neither of these approaches consider the effects of vertical flow or differences in hydro-pressure. There are numerous 1-D or 2-D simulation models for simulating runoff and sediment transport processes. As reviewed in the previous chapter, their mathematical description of runoff flow and transport processes, as well as their background assumptions, may be different. Thus, direct comparison of these models' predictions are difficult without their modification, since both their mathematical equations and their assumptions should be the same to compare the simulation results. If differences exist in mathematical formulations between 1-D and 2-D models, then one can not accept them as the differences due to the model dimension. They may be interpreted as the differences introduced by the mathematical descriptions. For these reason, the 1-D and 2-D models are developed in this study for comparing their simulation of runoff and sediment transport processes.

Runoff simulation models are based on the St. Venant equation and sediment transport models are based on the principle of conservation of mass in both 1-D and 2-D approaches. In this chapter, model formulations are described and the characteristics and algorithms of each components are discussed.

3.2 Runoff Simulation

Runoff simulation models are based on the St. Venant equations so that various overland flow conditions could be simulated. When an approximation method is used, the model applications

may be limited to simple cases. These equations are solved by the finite element method in which linear interpolation functions are used in both 1-D and 2-D.

3.2.1 Governing equations

In this study, Equations (2-4) and (2-5) were used for 1-D and Equations (2-7), (2-8), and (2-9) were employed for 2-D runoff simulations. As described in the previous chapter, both the 1-D and 2-D equations are identical except that the 2-D equation includes an additional term in y-direction for secondary directional flows.

Variables used in this study are flow depth (h) and velocities in x and y direction (u, v). Instead of using these, other variables such as flow rate and elevation of water surface could be used. Use of any combinations of these variables are advantageous for certain conditions. Cunge et al. (1980), for example, suggested that flow depth, rather than elevation is recommended when cross-sectional changes are small. Certain numerical techniques could be easier to integrate without significant errors than others for a certain particular combination (Cunge et al., 1980).

3.2.2 Interpolation functions

Interpolation or shape functions in the finite element method are used to approximate the dependent variables and transformation of coordinates. When the number of nodal points are N, the solution, u, in 1-D can be approximated by a polynomial of N-th order. The interpolation functions are represented as a function of geometry of element. In this study, linear functions are used in both 1-D and in 2-D. The triangular element system was selected so that the meshes can be easily generated from digital information systems such as geographic information systems. Moreover, triangular system can be used efficiently to represent irregular boundaries and refine meshes in some regions where the solution varies rapidly (Pinder and Gray, 1977).

In some cases, the interpolation functions can be expressed by a function of time as well as coordinates in time-dependent problems (Pinder and Gray, 1977). In this case, not only initial conditions but the end conditions of the problem should be provided. That is, flow conditions at both $t = 0$ and $t = \infty$ should be specified. In this study, however, the interpolation functions are determined by the geometry of elements only.

3.2.2.1 1-D linear interpolation function

A linear polynomial function, u(x), is represented by the general linear polynomial :

$$u(x) = a + bx \tag{3-1}$$

where a and b are constants and x is coordinate. The following interpolation functions N(x), are used for linear line element :

$$N_i(x) = \frac{(x_{i+1} - x)}{(x_{i+1} - x_i)}$$
$$N_{i+1}(x) = \frac{(x - x_i)}{(x_{i+1} - x_i)} \tag{3-2}$$

where subscript i and i+1 represent the sequence of nodal points. Using these interpolation functions, dependent variables can be approximated through the following equations :

$$u \cong u'(x) = \sum N_i u_i = [N]\{u\}, \quad \text{and}$$
$$h \cong h'(x) = \sum N_i h_i = [N]\{h\} \tag{3-3}$$

where u_i and h_i indicate flow velocity and depth, respectively, at node i. In matrix expressions, {u} denotes a unit column vector, and u'(x) and h'(x) represent approximate functions of u(x) and h(x), respectively. These functions can be rewritten in a local coordinate system where a new coordinate ξ, is used instead of x. Thus, the interpolation functions are redefined in terms of ξ which ranges between -1 and 1 as :

$$N_i(\xi) = \frac{(1 - \xi)}{2}$$
$$N_{i+1}(\xi) = \frac{(1 + \xi)}{2} \tag{3-4}$$

These linear interpolation functions are used in integrating the governing equations. In 1-D case, integration of the equations obtained by the finite element formulation can easily be done in either local or natural coordinate systems. Whereas, the local coordinate system is much more efficient to perform the integration in 2-D quadrilateral elements.

3.2.2.2 2-D linear interpolation functions for triangular element

Interpolation functions in 2-D are represented in x and y coordinate system. Similar to 1-D, the general expression of interpolation functions (N_i) for a triangular plane in 2-D can be written as :

$$N_i = a_i + b_i x + c_i y \tag{3-5}$$

where a_i, b_i, and c_i are constants, and x and y are coordinates. Using the information for the three nodal points in the element, the constants can easily be obtained. Thus, the interpolation functions are derived as following :

$$\begin{aligned} N_i &= [(x_j y_k - x_k y_j) + x(y_j - y_k) + y(x_k - x_j)] / 2A, \\ N_j &= [(x_k y_j - x_i y_k) + x(y_k - y_i) + y(x_i - x_k)] / 2A, \quad \text{and} \\ N_k &= [(x_i y_j - x_j y_i) + x(y_i - y_j) + y(x_j - x_i)] / 2A \end{aligned} \tag{3-6}$$

where i, j, and k indicate nodes, and A is the area of the element. The interpolation functions have the property that :

$$N_i + N_j + N_k = 1 \tag{3-7}$$

A triangular coordinate is also defined in a similar way to the local coordinate system. When sub triangles are represented by A_i, A_j, and A_k such that $A = A_i + A_j + A_k$, the area coordinates are defined as $L_i = A_i/A$, $L_j = A_j/A$, and $L_k = A_k/A$. It can be demonstrated, from algebraic manipulation, that the interpolation functions of Equation (3-7) are exactly identical to the area coordinates, L_i, L_j, and L_k. When the differential equations are represented in terms of the area coordinates, the integration is easily performed by integral formulas.

3.2.3 Finite element formulations

The governing equations for runoff simulation are formulated and solved based on the variational principles (Connor and Brebbia, 1976). Since the equations are the first order partial differential equations, the finite element formulation can easily be made compared with higher order partial differential equations. The dependent variables in the governing equations are substituted by polynomials such as Equation (3-3), and then they are represented in a matrix system. The matrices obtained for each element are combined in a global matrix, namely stiffness matrix, capacitance matrix, forcing vector, and solution vector.

3.2.3.1 1-D formulations

The continuity relationship gives a partial differential equation for runoff simulation. For an element, an interpolation function as a weighting function is multiplied by the continuity

Equation (2-5) after substituting the dependent variables given by approximations in Equation (3-3):

$$\int([N]\frac{\partial([N]\{h\})}{\partial t}+[N]\{h\}\frac{\partial([N]\{u\})}{\partial x}+[N]\{u\}\frac{\partial([N]\{h\})}{\partial x}-R_e)dx=0 \qquad (3\text{-}8)$$

where R_e represents rainfall excess in the element. In a similar way, the momentum equation can also be represented by the following equation :

$$\int([N]\frac{\partial([N]\{u\}}{\partial t}+[N]\{u\}\frac{\partial[N]\{u\}}{\partial x}+g\frac{\partial[N]\{h\}}{\partial x}+g(S_f-S_o))=0 \qquad (3\text{-}9)$$

where S_o and S_f are surface slope and friction slope, respectively. In this study, the friction slope is reasonably represented by Manning's equation. This is a most common approach in representing the surface slope when assuming uniform flow :

$$S_f=\frac{n^2u|u|}{R^{4/3}} \qquad (3\text{-}10)$$

where n = Manning's coefficient
u = flow velocity
R = hydraulic radius

Hydraulic radius is a function of flow depth. Thus, the friction slope contribute higher non-linearity to the momentum equation. In this study, the friction slope is considered to have the only flow velocity as its unknown. Absolute value of velocity and hydraulic radius are assigned by the values at the previous time step. When solution vector is represented by {U}, Equations (3-8), (3-9), and (3-10) are combined to give the following system of equations :

$$[C]\{\dot{U}\}+[K]\{U\}=\{F\} \qquad (3\text{-}11)$$

where [C] = capacitance matrix
[K] = stiffness matrix
{U} = solution vector, $[u_1, h_1, u_2, h_2]^T$
{Ú} = the first order derivative of {U} with respect to time
{F} = forcing vector

The capacitance matrix is symmetric :

$$[C] = \frac{L}{6}\begin{bmatrix} 2/g & 0 & 1/g & 0 \\ 0 & 2 & 0 & 1 \\ 1/g & 0 & 2/g & 0 \\ 0 & 1 & 0 & 2 \end{bmatrix} \tag{3-12}$$

Meanwhile, the stiffness matrix is not symmetric and contains dependent variables :

$$[K] = \frac{1}{6}\begin{bmatrix} -2u_1 - u_2 + 2g\alpha L & -3g & 2u_1 + u_2 + g\alpha L & 3g \\ -2h_1 - h_2 & -2u_1 - u_2 & 2h_1 + h_2 & 2u_1 + u_2 \\ -u_1 - 2u_2 + g\alpha L & -3g & u_1 + 2u_2 + 2g\alpha L & 3g \\ -h_1 - 2h_2 & -u_1 - 2u_2 & h_1 + 2h_2 & u_1 + 2u_2 \end{bmatrix} \tag{3-13}$$

where α indicates $n^2|u|/h^{4/3}$ in metric unit system. Dependent variables in this matrix are evaluated by their values at the previous time step. The forcing vector determined by rainfall excess in each element is evaluated by :

$$\{F\} = \frac{L}{2}\begin{Bmatrix} S_o \\ R_e \\ S_o \\ R_e \end{Bmatrix} \tag{3-14}$$

where the rainfall excess, R_e, is evaluated by a separate module for simulating infiltration process. The solution techniques for solving this system are discussed later in this chapter.

3.2.3.2 2-D formulations

The finite element formulation for 2-D governing equations is also performed in a similar way as 1-D. In 2-D formulation, the number of dependent variables or degree of freedom is three (u, v, and h) while 1-D has only two unknowns (u and h). Thus, system matrices such as stiffness and capacitance matrices have a 9 x 9 dimension. Through the same procedure as in the 1-D formulation, the same system as Equation (3-11) can be obtained. Meanwhile, when the solution vector, [U] is $[h_1, u_1, v_1, h_2, u_2, v_2, h_3, u_3, v_3]^T$, the capacitance matrix becomes :

$$[C] = \begin{bmatrix} 2 & 0 & 0 & 1 & 0 & 0 & 1 & 0 & 0 \\ 0 & 2 & 0 & 0 & 1 & 0 & 0 & 1 & 0 \\ 0 & 0 & 2 & 0 & 0 & 1 & 0 & 0 & 1 \\ 1 & 0 & 0 & 2 & 0 & 0 & 1 & 0 & 0 \\ 0 & 1 & 0 & 0 & 2 & 0 & 0 & 1 & 0 \\ 0 & 0 & 1 & 0 & 0 & 2 & 0 & 0 & 1 \\ 1 & 0 & 0 & 1 & 0 & 0 & 2 & 0 & 0 \\ 0 & 1 & 0 & 0 & 1 & 0 & 0 & 2 & 0 \\ 0 & 0 & 1 & 0 & 0 & 1 & 0 & 0 & 2 \end{bmatrix} \qquad (3\text{-}15)$$

The stiffness matrix in 2-D is :

$$[K] = \frac{1}{24}\begin{pmatrix} u1y1 + v1x1 & h1y1 & h1x1 & u2y1 + v2x1 \\ 4gy1 & u1y1 + v1x1 + 4g\alpha A & 0 & 4gy1 \\ 4gx1 & 0 & u1y1 + v1x1 + 4g\beta A & 4gx1 \\ u1y2 + v1x2 & h1y2 & h1x2 & u2y2 + v2x2 \\ 4gy2 & u1y2 + v1x2 + 2g\alpha A & 0 & 4gy2 \\ 4gx2 & 0 & u1y2 + v1x2 + 2g\beta A & 4gx2 \\ u1y3 + v1x3 & h1y3 & h1x3 & u2y3 + v2x3 \\ 4gy3 & u1y3 + v1x3 + 2g\alpha A & 0 & 4gy3 \\ 4gx3 & 0 & u1y3 + v1x3 + 2g\beta A & 4gx3 \end{pmatrix}$$

$$\begin{pmatrix} h2y1 & h2x1 & u3y1 + v3x1 & h3y1 & h3x1 \\ u2y1 + v2x1 + 2g\alpha A & 0 & 4gy1 & u3y1 + v3x1 + 2g\alpha A & 0 \\ 0 & u2y1 + v2x1 + 2g\beta A & 4gx1 & 0 & u3y1 + v3x1 + 2g\beta A \\ h2y1 & h2x2 & u3y2 + v3x2 & h3y2 & h3x2 \\ u2y2 + v2x2 + 4g\alpha A & 0 & 4gy2 & u3y2 + v3x2 + 2g\alpha A & 0 \\ 0 & u2y2 + v2x2 + 4g\beta A & 4gx2 & 0 & u3y2 + v3x2 + 2g\beta A \\ h2y3 & h2x3 & u3y3 + v3x3 & h3y3 & h3x3 \\ u2y3 + v2x3 + 2g\alpha A & 0 & 4gy3 & u3y2 + v3x2 + 4g\alpha A & 0 \\ 0 & u2y3 + v2x3 + 2g\beta A & 4gx3 & 0 & u3y3 + v3x3 + 4g\beta A \end{pmatrix} \qquad (3\text{-}16)$$

where the abbreviations are :

$$\begin{pmatrix} u1 \\ u2 \\ u3 \end{pmatrix} = \begin{pmatrix} 2u_1 + u_2 + u_3 \\ u_1 + 2u_2 + u_3 \\ u_1 + u_2 + 2u_3 \end{pmatrix}, \begin{pmatrix} y1 \\ y2 \\ y3 \end{pmatrix} = \begin{pmatrix} y_2 - y_3 \\ y_3 - y_1 \\ y_1 - y_2 \end{pmatrix}, \text{and} \begin{pmatrix} x1 \\ x2 \\ x3 \end{pmatrix} = \begin{pmatrix} x_3 - x_2 \\ x_1 - x_3 \\ x_2 - x_1 \end{pmatrix} \qquad (3\text{-}17)$$

and,

$$\alpha = \frac{n^2|u|}{h^{4/3}} \quad \text{and} \quad \beta = \frac{n^2|v|}{h^{4/3}} \tag{3-18}$$

The forcing vector, {F} has a 1 x 9 dimension.

$$\{F\} = \frac{A}{3}[R_e, gS_{ox}, gS_{oy}, R_e, gS_{ox}, gS_{oy}, R_e, gS_{ox}, gS_{oy}]^T \tag{3-19}$$

where S_{ox} and S_{oy} indicate the bottom slopes in x and y directions.

3.2.4 Solution techniques

The system of equations derived by the finite element formulation is a nonlinear time dependent problem. As described in the formulations, the nonlinear stiffness matrix is evaluated by the solutions at the previous time step. This method is more convenient and easier to program than other methods, such as Newton's method, which requires the derivation of tangent stiffness matrix. The tangent stiffness matrix can be obtained by taking the first derivative with respect to the solution {U}. Time integration is performed based on the finite difference technique for this problem. Since the interpolation functions are only functions of space coordinates, the finite difference schemes should be used. The implicit method was selected by considering its stability characteristics. Detailed description of the methods used in this study are presented in the next sections.

3.2.4.1 Implicit Euler method for time integration

In implicit Euler method, or fully implicit method, time derivative is written for time t+Δt. Thus, Equation (3-11) becomes :

$$[C]\frac{1}{\Delta t}(\{U^{i+1}\} - \{U^{i}\}) + [K]\{U^{i+1}\} = \{F^{i+1}\} \tag{3-20}$$

where i and i+1 indicate time step. The procedure for evaluating the nonlinear stiffness matrix is discussed in the next section. In a compact form, Equation (3-20) becomes :

$$[K']\{U^{i+1}\} = \{F'\} \tag{3-21}$$

where $[K'] = [C] + \Delta t[K]$

$\{F'\} = \Delta t\{F^{i+1}\} + [C]\{U^{i}\}$

Or using the difference of solutions between time steps i and I+1:

$$[K']\{\Delta U\} = \{F\} \tag{3-22}$$

where $\{\Delta U\} = \{U^{i+1}\} - \{U^i\}$

$\{F'\} = \Delta t(\{F^{i+1}\} - [K]\{U^i\})$

These equations can be easily solved when matrices, [K'] and {F'} are provided. Meanwhile, matrix [K] is determined by the solution {U}, therefore, we have to resort to another technique for the nonlinear problem.

3.2.4.2 Substitution method for nonlinear problems

The substitution method is the method in which unknown dependent variables in the stiffness matrix are evaluated by those at the previous time step. Equation (3-11) can be re-written:

$$[\bar{K}]\{\Delta U\} = \{\bar{F}\} \tag{3-23}$$

where $[\bar{K}] = [C] + \Delta t[K(U_{n-1}^{i+1})]$

$\{\bar{F}\} = \Delta t(\{F^{i+1}\} - [K(U_{n-1}^{i+1})]\{U_{n-1}^{i+1}\}) + [C](\{U^i\} - \{U_{n-1}^{i+1}\})$

and n-1 indicates the previous iteration. The initial conditions are used in solving this equation at the first iteration. With any matrix solver, Equation (3-23) can easily be solved at this moment.

In the substitution method, an over-relaxation factor ω, is used to improve the convergence rate. After finding the magnitude of change in solution, $\{\Delta U\}$, the solution vector at the next time step is upgraded using the over-relaxation factor in the following way :

$$\{U^{i+1}\} = \{U^i\} + \omega\{\Delta U\} \tag{3-24}$$

The over-relaxation factor is determined by numerical experiments and is dependent upon the type of the problem. Dhatt and Touzot (1984) suggested that the factor has a value between 1.7 and 1.9 for plasticity problems.

In solving nonlinear equations, the solution should be found through the iterations. In this case, we need a certain criterion to evaluate the convergence of solution. For this purpose, vector norms are usually used. The norm used in this study is the Euclidean norm (Dhatt and Touzot, 1984) :

$$\|n\| = \frac{\sqrt{\{\Delta U\}^T \{\Delta U\}}}{\sqrt{\{U\}^T \{U\}}} \tag{3-25}$$

The iteration is terminated when the norm $\|n\|$ is less than a certain value provided externally. The value is chosen arbitrarily, for example, 0.005 or 1.0 E-5 (Dhatt and Touzot, 1984).

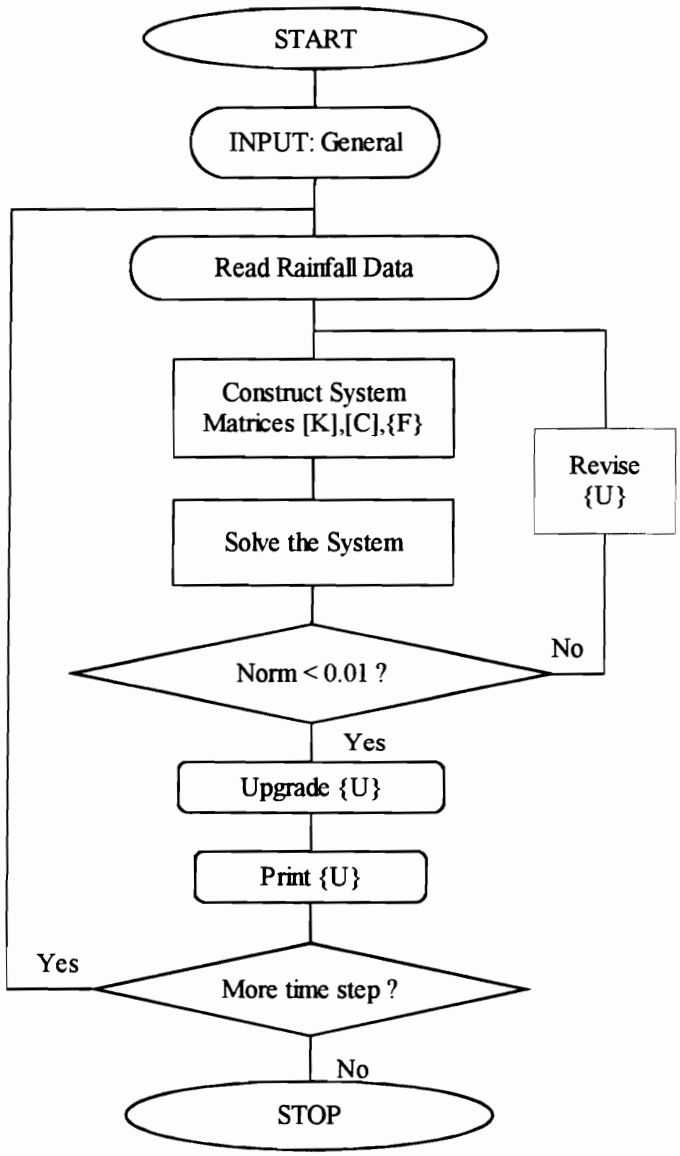

Figure 3-1. Schematic diagram for runoff simulation model.

Cathers and O'Connor (1993) compared four different schemes in terms of their convergence characteristics in solving the shallow water equations. Even though they used linear form of the equations, they found that the convergence rate of each equation was affected by the time step and grid size. These results can be easily interpreted based on the Von Neumann's stability condition which can be found by the discrete Fourier analysis (Sod, 1989). Even though these discussions are for the linear systems, some characteristics of the stability conditions can be applied to solving the dynamic equations. In nonlinear cases, the stability criteria would be more restricted which can be determined by numerical experiments.

Simulation of runoff processes are performed by solving the system equation (Equation 3-23). Incorporating a sub-routine, runoff simulation model can be represented as shown in Figure 3-1.

3.3 Rainfall excess

To evaluate forcing vector {F} in Equation (3-11), rainfall excess should be estimated. For this purpose, Parlange's infiltration equation (Parlange et al., 1982) is used. As described in the literature review, the equation requires three parameters; saturated hydraulic conductivity, integral capillary drive across the wetting front, and interpolation parameter. Since a value of 0.8 is recommneded for the interpolation parameter (Parlange et al., 1982), only two parameters are required for model applications. These parameters are identical with the parameters used in Green-Ampt or Smith and Parlange's equations.

Newton's method is used to solve the equation. From Equation (2-25),

$$\frac{\Delta F}{\Delta t} = f = K_s\left(1 + \frac{\alpha}{\exp(F\alpha / B) - 1}\right) \tag{3-26}$$

where F indicates the cumulative infiltration and the others are the same as in Equation (2-25). Based on an integral in the following form :

$$\int dt = \int \frac{1}{f} dF \tag{3-27}$$

that is,

$$\Delta t \cdot K_s = \int \frac{\exp(F\alpha / B) - 1}{\exp(F\alpha / B) + \alpha - 1} dF \tag{3-28}$$

a function is introduced :

$$\Gamma(F) = \int \frac{\exp(F\alpha / B) - 1}{\exp(F\alpha / B) + \alpha - 1} dF - \Delta t \cdot K_s \tag{3-29}$$

Thus, the first derivative of $\Gamma(F)$ is :

$$\Gamma'(F) = 1 - \frac{\alpha}{(\alpha - 1) + \exp(F\alpha / B)} \tag{3-30}$$

According to

$$F_1 = F_0 - \frac{\Gamma(F)}{\Gamma'(F)} \tag{3-31}$$

and

$$\int \Gamma dF = -\Delta t \cdot K_s + (F_1 - F_0) - \alpha \{ \frac{F_1 - F_0}{\alpha - 1} + \frac{B}{\alpha(\alpha - 1)} (\Phi(F_1) - \Phi(F_0)) \} \tag{3-32}$$

where $\Phi(F) = \log(\alpha - 1 + \exp(\frac{F\alpha}{B}))$, the cumulative infiltration at the next time step can be determined. In most cases, the solution can be obtained with less than ten iterations. For the model's application, the two parameters required in this equation can be obtained by the procedures presented in the literature such as Rawls et al.(1982) and Woolhiser et al. (1990).

3.4 Sediment Transport Simulation

Sediment transport processes are simulated by the continuity relationship. Both 1-D and 2-D continuity equations are solved by the finite element method with the same interpolation functions as in the runoff simulations. Since flow velocity and depth are provided by runoff simulation models, sediment transport equations can be solved without nonlinear iterations. Meanwhile, they require estimation of the source and sink terms which are determined by both runoff characteristics and surface conditions. The following sections describe the finite element formulations for 1-D and 2-D continuity equations and its solution technique.

3.4.1 Governing equations

The governing equation for sediment transport in 2-D is similar to Equation (2-26) :

$$\frac{\partial(hC)}{\partial t} + \frac{\partial(huC)}{\partial x} + \frac{\partial(hvC)}{\partial y} = SS \qquad (3\text{-}33)$$

Since flow characteristics such as flow velocity and depth are given by runoff simulations, only sediment concentration, C, is considered a dependent variable. The continuity equation can be used for simulating both sediment and solute transport processes provided that the corresponding source and sink terms for either solute or sediment are properly evaluated. Thus, once a sediment transport simulation model is formulated, it can be used for both sediment and solute transport simulations coupled with a corresponding module for source and sink terms.

In most cases, evaluation of the source and sink terms requires flow characteristics as input. For example, the relationships for rill erosion in simulating sediment transport are represented by flow depth and velocity as well as soil characteristics. Thus, when simulating sediment transport, one needs to appropriately estimate flow characteristics using a runoff simulation model.

3.4.2 Finite element formulations

Similar to runoff simulations, sediment transport is simulated using the finite element method for the continuity Equations (2-26, 3-33). The interpolation functions are also the same as those used in the runoff simulations. Thus, the concentration is approximated by the interpolation functions in 2-D :

$$C(x,y) = \sum N_i C_i \qquad (3\text{-}34)$$

where C = sediment concentration
N = interpolation function and i indicates nodal point.

The interpolation functions, N_i are also functions of space coordinates. Even though flow velocity and depth are not dependent variables, they are evaluated by the interpolation functions since flow rate, q, and depth, h, are not constant over an element. That is, the Equation (3-33) can be rewritten as :

$$[N]\{h\}\frac{\partial([N]\{U\})}{\partial t}+[N]\{h\}[N]\{u\}\frac{\partial([N]\{U\})}{\partial x}+R_e[N]\{U\}=SS \tag{3-35}$$

for 1-D and :

$$[N]\{h\}\frac{\partial([N]\{U\})}{\partial t}+[N]\{h\}[N]\{u\}\frac{\partial([N]\{U\})}{\partial x}+[N]\{h\}[N]\{v\}\frac{\partial([N]\{U\})}{\partial y}+R_e[N]\{U\}=SS \tag{3-36}$$

for 2-D. The matrices are the same as those introduced in Equation (3-3) except for the solution vector. The solution vector, {U} is $\{C_1, C_2\}$ for 1-D and $\{C_1, C_2, C_3\}$ for 2-D. {h}, {u}, and {u} indicate flow depth, x-, and y-directional velocity, respectively. Multiplying a weighting function to the continuity equation, we have the system of equations similar to Equation (3-11) in runoff simulations :

$$[C]\{\dot{U}\}+[K]\{U\}=\{F\} \tag{3-37}$$

where [C] is the capacitance matrix, [K] is stiffness matrix, and {F} is forcing vector.

However, the stiffness matrix in Equation (3-37) is not related with the solution vector, {U}, so that Equation (3-37) is a linear time-dependent problem. The forcing vector, {F}, includes both the source and sink terms.

For 1-D, the capacitance matrix is :

$$[C]=\frac{L}{12}\begin{bmatrix}3h_1+h_2 & h_1+h_2\\ h_1+h_2 & h_1+3h_2\end{bmatrix} \tag{3-38}$$

and the stiffness matrix is :

$$[K]=\frac{1}{6}\begin{bmatrix}-3hu+2R_eL & 3hu+R_eL\\ -3hu+R_eL & 3hu+2R_eL\end{bmatrix} \tag{3-39}$$

where R_e, L, and hu are rainfall excess, element length, and average flow rate per unit width, respectively, and subscript numbers in Equation (3-38) indicate nodal numbers. For 2-D, the capacitance matrix is :

$$[C]=\frac{A}{60}\begin{bmatrix}6h_1+2h_2+2h_3 & 2h_1+2h_2+h_3 & 2h_1+h_2+2h_3\\ 2h_1+2h_2+h_3 & 2h_1+6h_2+2h_3 & h_1+2h_2+2h_3\\ 2h_1+h_2+2h_3 & h_1+2h_2+2h_3 & 2h_1+2h_2+6h_3\end{bmatrix} \tag{3-40}$$

where A indicates the area of the element. The stiffness matrix is :

$$[K]=\frac{1}{24}\begin{bmatrix} Q_{x1}Y1+Q_{y1}X1+4R_eA & Q_{x1}Y2+Q_{y1}X2+2R_eA & Q_{x1}Y3+Q_{y1}X3+2R_eA \\ Q_{x2}Y1+Q_{y2}X1+2R_eA & Q_{x2}Y2+Q_{y2}X2+4R_eA & Q_{x2}Y3+Q_{y2}X3+2R_eA \\ Q_{x3}Y1+Q_{y3}X1+2R_eA & Q_{x3}Y2+Q_{y3}X2+2R_eA & Q_{x3}Y3+Q_{y3}X3+4R_eA \end{bmatrix} \quad (3\text{-}41)$$

where :

$$\begin{pmatrix} Q_{x1} \\ Q_{x2} \\ Q_{x3} \end{pmatrix} = \begin{pmatrix} 2h_1u_1+h_2u_2+h_3u_3 \\ h_1u_1+2h_2u_2+h_3u_3 \\ h_1u_1+h_2u_2+2h_3u_3 \end{pmatrix}, \quad \begin{pmatrix} Q_{y1} \\ Q_{y2} \\ Q_{y3} \end{pmatrix} = \begin{pmatrix} 2h_1v_1+h_2v_2+h_3v_3 \\ h_1v_1+2h_2v_2+h_3v_3 \\ h_1v_1+h_2v_2+2h_3v_3 \end{pmatrix}, \quad \begin{pmatrix} X1 \\ X2 \\ X3 \end{pmatrix} = \begin{pmatrix} x_3-x_2 \\ x_1-x_3 \\ x_2-x_1 \end{pmatrix}, \text{ and}$$

$$\begin{pmatrix} Y1 \\ Y2 \\ Y3 \end{pmatrix} = \begin{pmatrix} y_2-y_3 \\ y_3-y_1 \\ y_1-y_2 \end{pmatrix}.$$

u, v, and h indicate x and y directional velocity and flow depth at each nodal point, respectively, and x_i and y_i indicate coordinate at nodes. Similarly, the forcing vectors are defined with L/2[SS, SS]^T and A/3[SS, SS, SS]^T for 1-D and 2-D, respectively.

3.4.3 Solution techniques

Equation (3-37) used for both 1-D and 2-D approaches is a linear and time-dependent problem since the stiffness matrix is not a function of concentration vector {U}. The system is solved by the implicit Euler method using the same matrix solver used in the runoff simulations. Thus, Equation (3-37) also becomes :

$$[\overline{K}]\{\Delta U\} = \{\overline{F}\} \quad (3\text{-}42)$$

where $[\overline{K}] = [C] + \Delta t[K]$

$\{\overline{F}\} = \Delta t(\{F^{i+1}\} - [K]\{U^i\})$

$\{\Delta U\} = \{U^{i+1}\} - \{U^i\}$

Since the system of Equation (3-42) is linear, the solution is obtained much faster than in runoff simulation.

Simulation of sediment transport processes is performed by evaluating the amount of source and sink. Sediment transport model is represented in Figure 3-2.

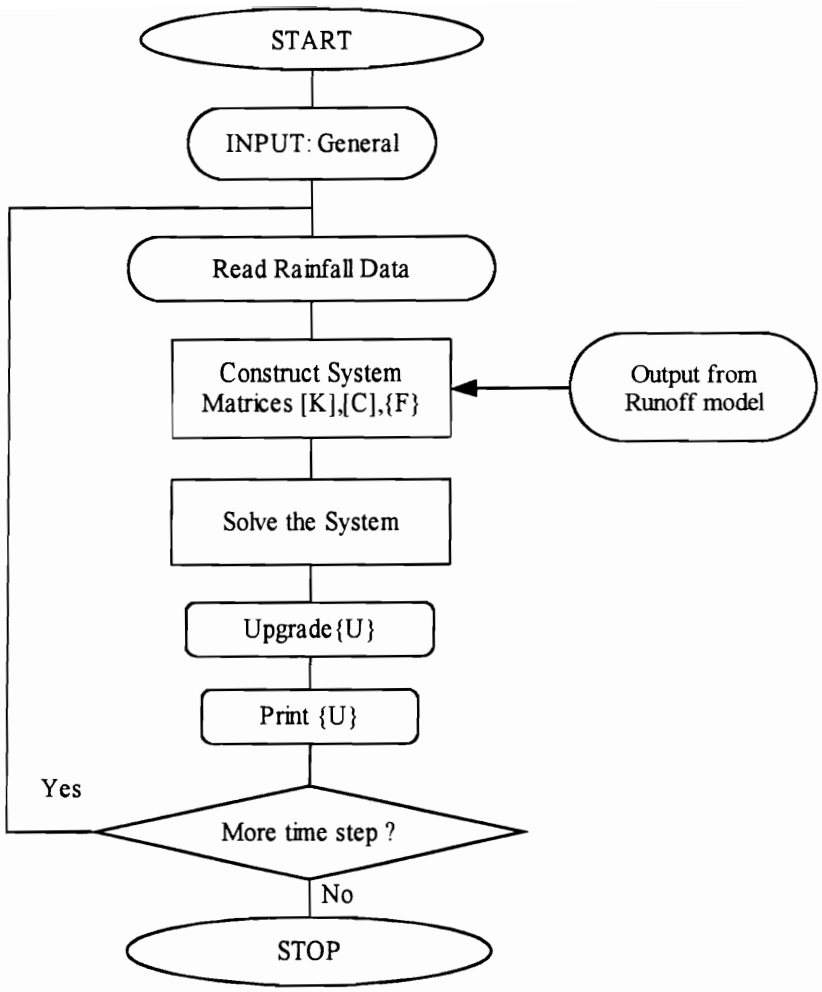

Figure 3-2. Schematic diagram for sediment transport model.

3.5 Estimation of Source and Sink Terms

In simulating sediment transport processes, the amount of soil erosion and deposition should be properly defined. As described in the second chapter, some methods do not express deposition process explicitly while other procedures describe each processes including deposition in detail. The procedure presented by Woolhiser et al. (1990) is employed in this study.

Soil erosion processes are simulated by two components: the soil erosion by rainfall splash and the hydraulic erosion by shear force of runoff water on the surface. Most approaches in simulating soil erosion processes by rainfall splash are determined by rainfall rate and surface

conditions. However, Woolhiser et al.s' (1990) relationship for soil erosion by rainfall splash includes flow depth. Soil erosion and deposition processes by runoff flow are described in a relationship similar to Foster's (1982) method and its derivatives (Foster et al., 1981; Laguna and Giraldez, 1993). Splash erosion and hydraulic erosion are analogous to interrill erosion and rill erosion, respectively.

3.5.1 Splash erosion process

Soil erosion induced by rainfall is represented by (Woolheiser, et al., 1990) :

$$E_s = c_f k(h) r q \quad \text{for} \quad q > 0$$
$$= 0 \quad \text{for} \quad q < 0 \tag{3-43}$$

where c_f = constant related to soil surface
$k(h)$ = reduction factor accounting for the reduction in splash erosion by flow depth
r = rainfall rate
q = rainfall excess

This equation is different from other relationships presented for interrill erosion in that it uses both rainfall excess and rainfall intensity and considers reduction effects by flow depth. However, it is not much different from other relationships for interrill erosion in that the exponent for the rainfall intensity ranges from 1.5 to 2 (Laguna and Giraldez, 1993). A notable parameter in this equation is a reduction factor, k(h). This parameter represents the reduction in splash erosion caused by increasing depth of runoff water. It has a maximum value of 1.0 before runoff occurs and a minimum value of zero for very large flow depth. Woolhiser et al. (1990) suggested that it can be estimated by :

$$k(h) = \exp(-c_h h) \tag{3-44}$$

The parameter c_h determines the effect of surface water depth (h) on raindrop detachment. Surface water reduces splash erosion by absorbing the raindrop energy after runoff flow forms. Since the reduction rate is also related with the size of raindrop, c_h is determined by considering both the size of raindrop and flow depth.

3.5.2 Hydraulic erosion process

Hydraulic erosion or deposition process represents the sediment exchange rate between the runoff water and the soil surface. This process is simulated similar to other approaches for rill erosion process by using the sediment transport capacity or equilibrium concentration of sediment. Woolhiser et al. (1990) described hydraulic erosion/deposition processes using :

$$E_h = c_g(C_{mx} - C_s)A \tag{3-45}$$

where E_h = hydraulic erosion/deposition rate
c_g = transfer rate coefficient
C_{mx} = equilibrium transport capacity
C_s = current sediment concentration
A = cross sectional area of flow

The transfer rate coefficient is related to soil characteristics. It has low values for cohesive soils and high values for fine, non cohesive soils. Woolhiser et al. (1990) employed a method which estimate the coefficient based on the USLE soil erodibility factor.

The equilibrium sediment concentration or sediment transport capacity can be estimated by various transport capacity relationships found in the literature. Woolhiser et al. (1990) provided six different options to use in their model, KINEROS. In fact, most soil erosion or NPS models adopt one of these models for overland processes. The present study employs an equation presented by Engelund and Hansen (Woolhiser et al., 1990) as described in the last chapter (Equation 2-36). The equation include both depth and velocity of runoff flow which are major output from runoff simulation models in both 1-D and 2-D approaches.

Source and sink terms now can be calculated and the forcing vector can be made using the computed source and sink term in Equations (2-26) and (3-33). The source and sink terms are based on element-wise calculations as shown in Equations (3-14) and (3-19).

3.6 Summary

Both 1-D and 2-D simulation models for runoff and sediment transport were developed using the finite element method. Linear interpolation functions were used for both 1-D and 2-D.

Two node line element and three node linear triangle element were used for 1-D and 2-D, respectively. System matrices such as capacitance and stiffness for the element were constructed from the finite element formulation. Major modules developed by Dhatt and Touzot (1984) were used for solving the systems in this study.

Once the runoff simulation is performed for a certain overland area, runoff characteristics such as flow depth and velocity and the amount of rainfall excess are estimated. Sediment transport models can then be applied to the area for sediment transport if the source and sink terms used in forcing vector are properly estimated using the results from the runoff model. In simulating sediment transport, erosion processes were represented by those presented by Woolhiser et al. (1990). Sediment transport capacity was estimated by Engelund and Hansen's equation (1967).

For actual field or watershed applications, the sediment transport model requires extremely large amount of input data on soil surface and chemical characteristics. More detailed simulation may have to be performed for various groups of soil particle size. However, in this study, soil erosion and sediment transport are simulated for the medium size soil particle.

4. MODEL VALIDATION AND SENSITIVITY ANALYSIS

4.1 Introduction

In the previous chapter, two models were presented for simulating runoff and pollutant transport processes. In this chapter, the models are tested to determine if they were properly constructed and whether they appropriately simulate various processes. Models may have errors either in their mathematical formulation or encoding the programs. The mathematical errors include incorrect derivation of equations or errors in mathematical formulations. A linear stability analysis was also performed for investigating convergence and stability criteria. Even though this study is based on the nonlinear cases, the stability analysis for the linearized system may be useful for the application of the model to various field conditions. For the runoff models, Izzard method (Chow, 1959) was used to compare model predictions. The method is based on the analysis of dimensionless hydrograph. In the 2-D runoff model, there were some oscillations in prediction results even though they were negligible in terms of their magnitude. A numerical experiment presented by Chow and Ben-zvi (1973) were used to verify the 2-D runoff model. The sediment transport models were tested using the analytical solutions provided by Singh and Regl (1983) and Singh (1983) which estimated both runoff and sediment concentration. In the last section, the sensitivity analysis is presented to help understand how various parameters affect the simulation of runoff and sediment transport processes.

4.2 Model Testing

Model testing or model validation was performed to confirm that models were constructed appropriately. Runoff simulation models were tested using the results obtained by the Izzard method (Chow, 1959). The method was based on the analyses of the dimensionless hydrographs obtained from experiments for simulated rainfall events with a constant rate. For the verification

of the 2-D runoff model, a numerical experiment based on the finite difference method (Chow and Ben-Zvi, 1973) was used.

The sediment transport models were tested using the analytical solutions presented by Singh (1983). Singh and Regl (1983) and Singh (1983) presented analytical procedures for estimating runoff and sediment concentration from overland areas. Their analytical solution was based on the kinematic wave approximation. Since the solution includes runoff, the model prediction of runoff was also compared.

4.2.1 Verification of Runoff Simulation Models

4.2.1.1 Model verification using the Izzard method

Runoff simulation models were tested for a hypothetical impermeable overland area. Runoff rates were estimated by the models and then compared with those calculated by the Izzard method. The Izzard method is based on the analysis of the hydrographs resulting from simulated rainfall (Chow, 1959). The method presented by Izzard assumes that the form of the rising hydrograph can be represented by a single dimensionless curve. This method was known to provide accurate runoff estimations for laminar flow conditions under a uniform rainfall intensity (Chow, 1959).

4.2.1.1.1 Discretization and input conditions

The surface was assumed to be a smooth asphalt pavement and an arbitrary rainfall event of 4.8 cm/hr is applied for 10 minutes (Chow, 1959). The surface conditions for the model applications are summarized in Table 4-1.

Table 4-1. Surface conditions of hypothetical overland area used for model testing.

Manning's n	Slope, %	Length, m	Rainfall, cm/hr	Duration, min
0.013	0.5	21.95	4.8	10

This overland area has only one directional slope so that there is no side directional flow. In other words, it is a one-dimensional flow. Therefore, no differences in runoff estimations between the 1-D and 2-D models were expected.

For the 1-D and 2-D models, the overland flow length of 21.95 m was discretized into 7 and 13 node and 14 and 26 node meshes, respectively. Since the 2-D discretization requires both x and y coordinates, the width of elements were chosen arbitrarily. The model predictions are not affected by the choice of width since flow rate per unit width was used. Sample meshes for the discretization are illustrated in Figure 4-1. The time step of one minute was used for both 1-D and 2-D models and the maximum number of iteration was 120.

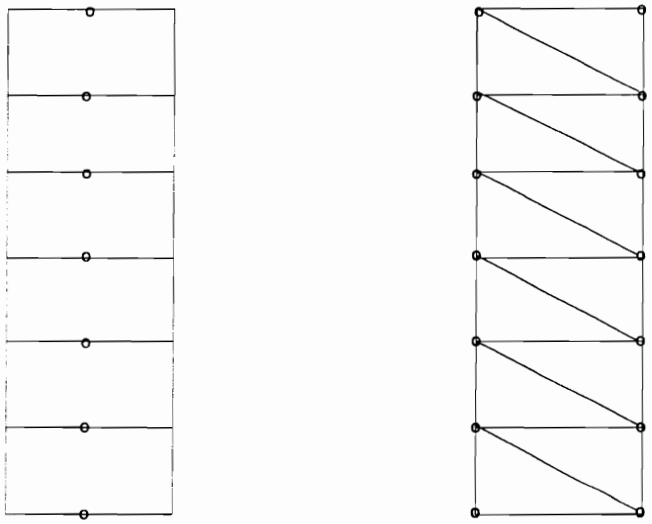

a) 1-D mesh with 7 nodes b) 2-D mesh with 14 nodes

Figure 4-1. 1-D and 2-D discretization for model verification

4.2.1.1.2 Model applications and results

The convergence of both 1-D and 2-D models were achieved within about 30 iterations when the over-relaxation factor of 0.5 was used, which is much smaller than the those used in plasticity problems such as structural analyses (Dhatt and Touzot, 1984). When a value of 1.0 or larger was used for the over-relaxation factor, the number of iteration needed to achieve convergence increased. The total computational time for a 2-D simulation run was about twice

more than that required for the 1-D simulation. The 2-D simulation requires additional nodal points to make areal element. In this study, the 2-D model simulation required 3 nodes while the 1-D needed only two nodal points per element. In addition, the 2-D model has one more degree of freedom per each node than the 1-D model, which is the y-directional velocity. Thus, the total number of unknowns in the 2-D model is much greater than those for the 1-D.

4.2.1.1.2.1 Runoff calculation by the Izzard method

For spatially-varied unsteady surface flow, Chow (1959) suggested two approximation solutions, one for laminar and the other for turbulent flow. The Izzard method is for laminar flow (Chow, 1959). The method assumes that the form of the rising hydrograph can be represented by a single dimensionless curve. Runoff rate was calculated by the Izzard method using :

$$q_e = \frac{iL}{518.4} \tag{4-1}$$

where q_e = equilibrium flow rate in m^2/sec
i = rainfall intensity in mm/hr
L = length of surface flow in m

The equilibrium flow rate can be estimated from the dimensionless curve. The flow rate after rain stops can also be calculated using Equation (4-2) :

$$t_r = \frac{D_o F(r)}{60 q_e} \tag{4-2}$$

where F(r) = a function of dimensionless flow rate : $0.5(r^{-2/3} - 1)$
D_o = detention at i = 0
$r^{1/3} = D/D_o$
D = detention at the time t after the rainfall began

More detailed procedure on the dimensionless hydrograph are given in Chow (1959). The method was reported to be suitable for laminar flow and limited to cases where rainfall intensity is in inches per hour (Chow, 1959)

4.2.1.1.2.2 Results and analysis

Runoff estimations by the method were compared with the simulation results of both 1-D and 2-D models as shown in Figures 4-2, 3, and 4. The 1-D predictions of peak flow rate at the 10th minute for both 7 node and 13 node meshes were very close to those computed by the Izzard

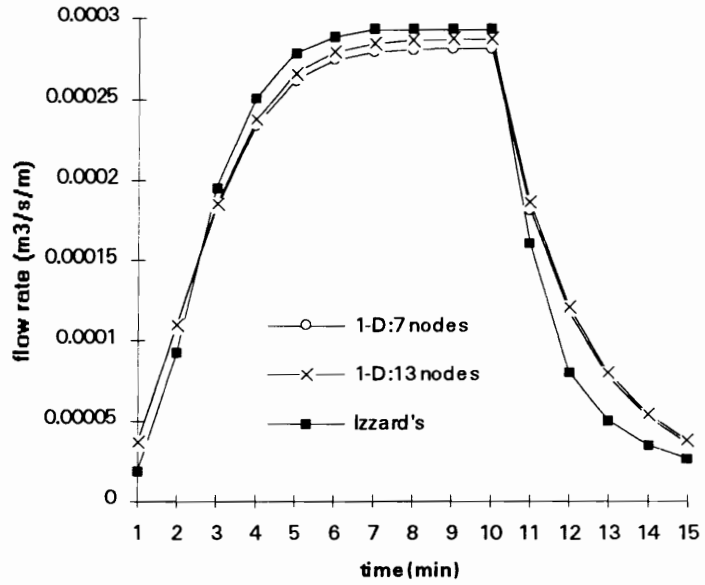

Figure 4-2. Comparison of flow rates by 1-D simulations and Izzard method

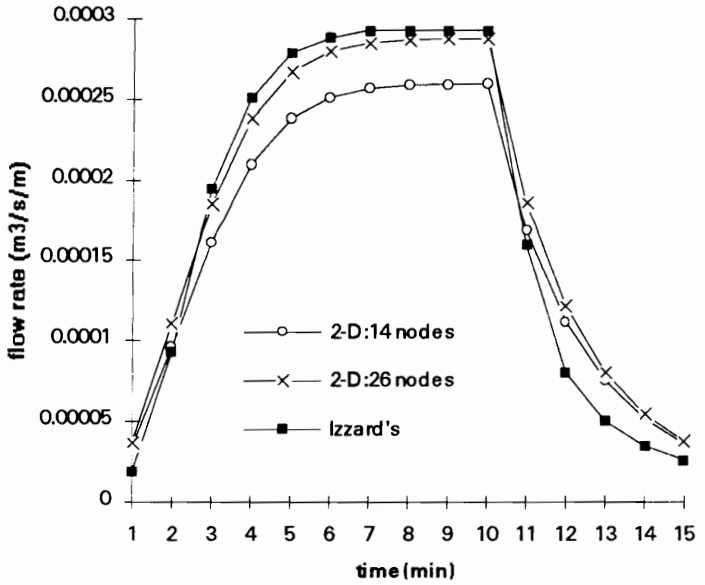

Figure 4-3. Comparison of flow rates by 2-D simulations and Izzard method

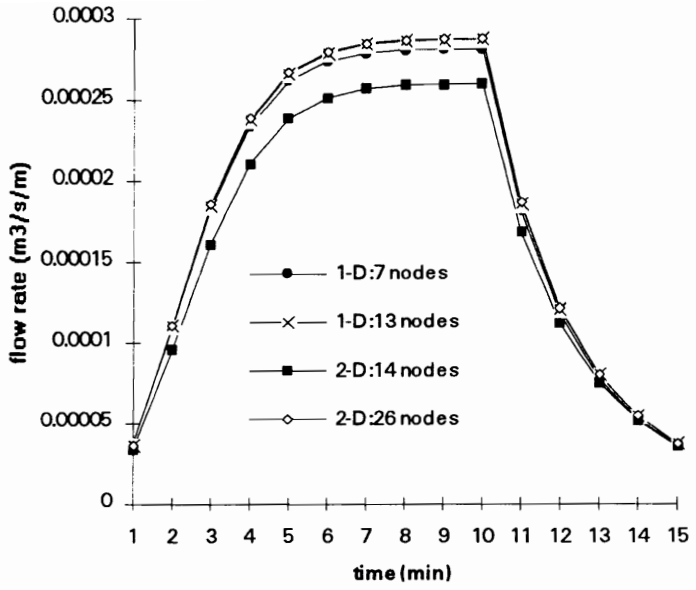

Figure 4-4. Comparison of flow rates by 1-D and 2-D simulations

method. For the 1-D estimation, the peak runoff rate simulated by 7 node mesh was about 4.2% less than that calculated by the Izzard method and 2.1% less by 13 node mesh (Figure 4-2). Overall, the 1-D model predictions agreed with the solution obtained by the Izzard method reasonably well. Meanwhile, flow rates at the recession limb of the hydrograph did not match closely with the Izzard method's results, compared to other time periods. Flow rates calculated by the Izzard method were consistently less than the simulated values during the recession limb of hydrograph. It appears that the runoff process predicted by the Izzard method responded more quickly to rainfall. The peak flow rate by the Izzard method occurred at 7th through 10th minute, while the model predictions showed continued increase until the cessation of rainfall.

The 2-D simulations also showed similar forms of hydrographs. The hydrographs predicted by the 2-D model (Figure 4-3) were plotted using the average value of flow rate at two outlet nodes since there are two outlet nodes in 2-D simulations. Figure 4-3 shows a comparison of the hydrographs estimated by the Izzard method and the 2-D runoff model. With 14 node meshes, the peak flow rate predicted by the 2-D model was 12.3% less while the peak for the 26 node predictions was just 1.7% less than that calculated by the Izzard method. When the discretization level of 14 node mesh in 2-D is considered to be the same as 7 node mesh in 1-D (Figure 4-1), the

2-D estimation of peak flow is relatively low as compared to 1-D estimation at the same level of discretization.

Secondary directional velocities exist in 2-D predictions, even though the magnitude is negligibly small. Since the overland has only one directional slope, velocities in the cross slope direction should be zero. The magnitude of the velocities in the cross slope direction ranged from 0.1 to 3% of main directional velocity. In this study, this phenomenon is called triangular oscillation. To find out whether this phenomenon was unique to the triangular element model or not, a quadrilateral element-based model was also developed. The peak flow rates estimated by the quadrilateral element model did not show such oscillations and were exactly the same as those predicted by 1-D.

When the 1-D and 2-D predictions were compared, the results were not significantly different while flow rates produced by the 14 node 2-D was relatively lower than the others (Figure 4-4). Differences in flow rates between the 1-D and 2-D were about 0.3% throughout the simulation. For peak flow rate at the 10th minute, the difference between the models' estimations and calculation by the Izzard method was about 2% for both 1-D and 2-D models. Additional description of computational problems are discussed in the following sections.

Based on the comparison with the computation by the Izzard method, both 1-D and 2-D runoff models performed reasonably well. It could be seen that both 1-D and 2-D runoff models were appropriately developed to simulate overland runoff processes.

4.2.1.1.3 Computational aspects in model applications

4.2.1.1.3.1 Triangular oscillations in 2-D

Runoff simulation results by the 2-D triangular model showed that velocities and flow depths were different at the two outlet nodes. Since the overland flow in these simulations was one-dimensional and y-directional slope did not exist, the estimations should be the same at both nodes. In order to investigate this phenomenon, a set of numerical experiments was performed for six different discretization schemes (Figure 4-5).

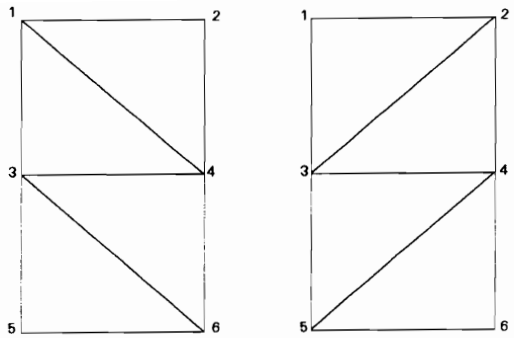

a)

b)

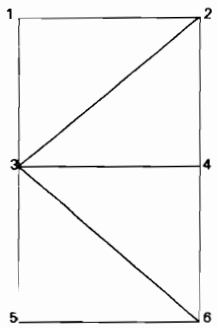

c)

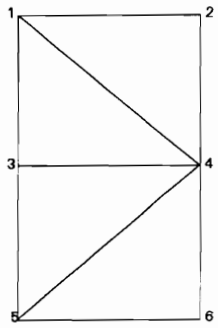

d)

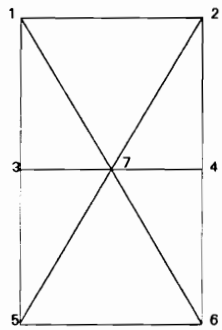

e)

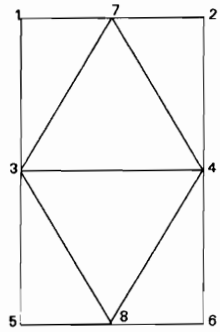

f)

Figure 4-5. Six different discretization schemes for analyzing triangular oscillation.

The six discretization schemes included two sets with diagonals in one direction (Figure 4-5, a and b), two with diagonals with alternate directions (Figure 4-5, c and d), and symmetric cases in which diagonals were connected with centered nodal points (Figure 4-5,e and f). Rainfall and surface conditions were the same as in the model testing (Table 4-1) while the total flow length was assumed to be 10 m in order to simplify the meshes. The boundary conditions were also assumed to be zero depth and zero velocities in both x and y directions at the upstream boundary nodes.

The simulation results at the outlet nodes are shown in Table 4-2. The magnitude of cross sectional velocities (x) was between 0 to 0.2% of velocities in the main slope. Among the meshes, differences in flow depths are less than 3% and those of velocities are less than 2%.

Table 4-2. Simulation results for different type of meshes.

Mesh	Outlet node number	depth mm	Velocity (x) m/sec	Velocity(y) m/sec	Flow rate m^2/sec
a)	5	0.758	0.147	0.000109	0.000112
	6	0.872	0.1435	0.000319	0.000125
b)	5	0.872	0.1435	0.000319	0.000125
	6	0.758	0.147	0.000109	0.000112
c)	5	0.865	0.1476	0.00029	0.000128
	6	0.819	0.1342	3.54E-05	0.00011
d)	5	0.819	0.1342	3.54E-05	0.00011
	6	0.865	0.1476	0.00029	0.000128
e)	5	0.839	0.1395	0.000132	0.000117
	6	0.839	0.1395	-0.000132	0.000117
f)	5	0.797	0.1445	0.000152	0.000115
	6	0.797	0.1445	-0.000152	0.000115
	8	0.865	0.13889	0	0.00012

The simulation results were different between the symmetric element sets (e and f) and non-symmetric sets (a) through (d). Symmetric sets did not show any differences in flow or velocity values at the two end outlet nodes while the non-symmetric sets had about 11 to 15% differences in flow rate between the nodes. In fact, there were no y-directional velocities at the

nodes 5 and 6 from the symmetric set. Meanwhile, the non-symmetric sets gave non-zero y-directional velocities the magnitude of which seemed to affect the differences in x-directional velocities and depth.

When comparing the sets (a) and (b) with sets (c) and (d), it could be seen that the simulation results were identical between set (a) and (b). The computation results at node 3 of set (a) were exactly the same as those at node 4 of (b). Sets (c) and (d) also showed similar results. This analysis indicates that the shape of the triangular element may affect the results. However, these differences, due to transverse shape, seem to be negligible since the overall average value of differences in flow rate, calculated by using flow rates from sets (a), (c), (e), and (f), was about 1%. Sets (c) and (d) showed larger relative values of y-velocities compared to x-velocities and greater differences in flow rates between the outlet nodes than sets (a) and (b). This suggest that the larger differences in y-directional velocity could result in greater differences in the estimations.

One main reason for this type of oscillation seems to be due to the use of triangular elements in discretization. Therefore, a four node quadrilateral model was also applied to this case to evaluate the effect of element shape on the results. The simulation results by the quadrilateral model did not show this type of oscillations.

Even though there were computational oscillations due to the use of triangular elements, the errors could be considered negligible in terms of the accuracy of results since the differences from the total average value was just about 1%.

4.2.1.1.3.2 Stability criteria for the linear case

In applying a numerical technique to find solutions for any type of problem, the stability should be investigated and proper conditions for the stability criteria should be satisfied. Otherwise, solutions cannot be accepted. The Fourier method is a method for analyzing convergence of the solution in linear cases. In this study, however, the governing equations used in runoff routing are nonlinear and time dependent. The Fourier method was applied to investigate the stability of the system after the 1-D equations were assumed to be linear such that :

$$\frac{\partial u}{\partial t} + u_o \frac{\partial u}{\partial x} + g\frac{\partial h}{\partial x} + g(S_f - S_o) = 0 \qquad (4\text{-}3)$$

and

$$\frac{\partial h}{\partial t} + h_o \frac{\partial u}{\partial x} + u_o \frac{\partial h}{\partial x} = R_e \tag{4-4}$$

where u_o = linearized velocity
h_o = linearized flow depth
u = velocity
h = flow depth
g = gravitational acceleration
R_e = Rainfall excess
S_f and S_o = friction and bottom slopes, respectively.

Linearized velocity and flow depth are used and the friction slope is also assumed to be a linear function. Based on this linearized equations, the system of equations is written as :

$$[C]\{\dot{U}\} + [K]\{U\} = \{F\} \tag{4-5}$$

where $[C]$ = capacitance matrix
$[K]$ = stiffness matrix
$\{F\}$ = Forcing vector
$\{U\}$ = solution vector
$\{\dot{U}\}$ = the first order difference vector of solution in time

The stiffness matrix is no longer a function of unknowns such as depth and velocity. By applying the implicit method for time integration, equation (4-5) is :

$$[C]\{U\}_{i+1}^{t+1} = [C]\{U\}^{t} - \Delta t[K]_i^{t+1}\{U\}_i^{t+1} + \Delta t\{F\}^{t+1} \tag{4-6}$$

again,

$$\{U\}_{i+1}^{t+1} = [A]\{U\}_i^{t+1} + \{B\} \tag{4-7}$$

where t and i are time step and iteration level, respectively. Matrix [A] is the iteration amplification matrix and $\{B\}$ is a vector that remains constant during iteration. In a linear system, [A] is constant at all iterations and time levels. When the exact solution vector is described by $\{U\}_e^{t+1}$, equation (4-7) becomes :

$$\{U\}_e^{t+1} = [A]\{U\}_e^{t+1} + \{B\} \tag{4-8}$$

Thus, the error vector, $\{e\}_i$ in the i-th approximation is :

$$\{e\}_{i+1} = \{U\}_i^{t+1} - \{U\}_e^{t+1} \tag{4-9}$$

The vector $\{U\}_e^{t+1}$ converges as the error vectors become close to the zero vector with iterations. For the time stability :

$$\left\| \frac{[C]}{[C]+\Delta t[K]^{t+1}} \right\| \leq 1 \tag{4-10}$$

and for iteration convergence :

$$\left\| \frac{\Delta t[K]^{t+1}}{[C]} \right\| \leq 1 \tag{4-11}$$

where $\|\cdot\|$ indicates any vector norm.

With the implicit method, the linear finite element equations for equations (4-3) and (4-4) are analogous to the following finite difference equations :

$$\begin{aligned} &\frac{1}{6\Delta t}[(u_{j-1}+4u_j+u_{i+1})^{t+1}-(u_{j-1}+4u_j+u_{i+1})^{t}]+\frac{u_o}{2\Delta x}(u_{j+1}-u_{j-1})^{t+1} \\ &+\frac{g}{2\Delta x}(h_{j+1}-h_{j-1})^{t+1}+\frac{g\alpha}{6}(u_{j-1}+4u_j+u_{i+1})^{t+1}=gS_o, \end{aligned} \tag{4-12}$$

and

$$\begin{aligned} &\frac{1}{6\Delta t}[(h_{j-1}+4h_j+h_{i+1})^{t+1}-(h_{j-1}+4h_j+h_{i+1})^{t}]+\frac{h_o}{2\Delta x}(u_{j+1}-u_{j-1})^{t+1} \\ &+\frac{u_o}{2\Delta x}(h_{j+1}-h_{j-1})^{t+1}=R_e \end{aligned} \tag{4-13}$$

The variables u and h can be represented by discrete amplitudes :

$$\begin{Bmatrix} u \\ h \end{Bmatrix} = \begin{Bmatrix} u' \\ h' \end{Bmatrix} e^{i(wt-\sigma x)} = \begin{Bmatrix} u' \\ h' \end{Bmatrix}^n e^{-i\sigma x} \tag{4-14}$$

where $i=\sqrt{-1}$,

w, σ = angular frequency and wave number of the Fourier component in the discrete system, and

u', h' = constant amplitudes of u and h.

Since u_{j-1} can be written as D_+u_j and u_{j+1} as D_-u_j, where D_+ and D_- are difference operators, equations (4-12) and (4-13) can be written by only u_j^{t+1} and u_j^{t+1}. The operators are in fact represented as :

$$\begin{aligned} D_+u' &= \sum_j u_{j+1}e^{ij\Delta x} = \sum_j u_j e^{i(j-1)\Delta x} \\ &= e^{-i\Delta x}u' \end{aligned} \tag{4-15}$$

Similarly, D_-u' becomes $e^{i\Delta x}u'$. Thus, equations (4-12) and (4-13) can be written as :

$$\frac{1}{6\Delta t}(4+2\cos\sigma\Delta x)u_j^{t+1}-\frac{u_o}{2\Delta x}(2i\sin\sigma\Delta x)u_j^{t+1}+\frac{g\alpha}{6}(4+2\cos\sigma\Delta x)u_j^{t+1}$$
$$-\frac{g}{2\Delta x}(2i\sin\sigma\Delta x)h_j^{t+1}=\frac{1}{6\Delta t}(4+2\cos\sigma\Delta x)u_j^{t}+gS_o \tag{4-16}$$

$$\frac{1}{6\Delta t}(4+2\cos\sigma\Delta x)h_j^{t+1}-\frac{h_o}{2\Delta x}(2i\sin\sigma\Delta x)u_j^{t+1}-\frac{u_o}{2\Delta x}(2i\sin\sigma\Delta x)h_j^{t+1}$$
$$=\frac{1}{6\Delta t}(4+2\cos\sigma\Delta x)h_j^{t}+gS_o \tag{4-17}$$

since $\cos\sigma x = (e^{-i\sigma\Delta x} + e^{-i\sigma\Delta x})/2$ and $i\cdot\sin\sigma x = (e^{-i\sigma\Delta x} - e^{-i\sigma\Delta x})/2$. In a matrix form, these can be written in the form like equation (4-7) where [A] and {B} are :

$$[A]=\begin{bmatrix}\frac{1}{3\Delta t}(2+\cos\sigma\Delta x)-\frac{u_o}{\Delta x}i\sin\sigma\Delta x+\frac{g\alpha}{3}(2+\cos\sigma\Delta x) & -\frac{g}{\Delta x}i\sin\sigma\Delta x\\ -\frac{u_o}{\Delta x}i\sin\sigma\Delta x & \frac{1}{3\Delta t}(2+\cos\sigma\Delta x)-\frac{h_o}{\Delta x}i\sin\sigma\Delta x\end{bmatrix}^{-1}$$
$$\begin{bmatrix}\frac{1}{3\Delta t}(2+\cos\sigma\Delta x) & 0\\ 0 & \frac{1}{3\Delta t}(2+\cos\sigma\Delta x)\end{bmatrix} \tag{4-18}$$

and

$$\{B\}=\begin{Bmatrix}gS_o\\ R_e\end{Bmatrix} \tag{4-19}$$

where $\{U\} = [u', h']^T$.

Von Neumann's necessary condition for stability is that the complex eigenvalue, λ, which is the ratio of the amplitude of the numerical solution at successive time levels, should be :

$$|\lambda|=\left|\frac{u'^{t+1}}{u'^{t}}\right|=\left|\frac{h'^{t+1}}{h'^{t}}\right|\le 1 \tag{4-20}$$

Substituting the equation (4-20) into (4-7) with (4-18) and (4-19), we can evaluate λ without much difficulties. For all cases, the computed values of $|\lambda|$ were less than unity indicating that the Von Neumann's necessary condition was satisfied.

However, as mentioned previously, these characteristics are based on the linearized equations. Flow depth and velocity were linearized instead of being considered unknowns in the

analysis. In model applications, therefore, time step and mesh size need to be less than those values calculated by the stability criteria. Particularly, complex topography will restrict the stability criteria obtained from the linearized condition.

4.2.1.1.3.3 Over-relaxation factor

The over-relaxation factor was used to partition the contribution of the results from the previous iteration step. This factor was chosen to be 0.5 for the optimum value of iterations from numerical experiments. When the factor increased to near 1.0 or decreased to near 0.1, the number of iteration for obtaining a convergence increased. This value looks much different from those used in elasticity problems such as structural analyses (Dhatt and Touzot, 1984). Dhatt and Touzot (1984) suggest 1.7 to 1.9 for the value of the factor. However, the factor is determined based on numerical experiments and it varies depending on the characteristics of the problem.

4.2.1.2 Summary of runoff model testing

Runoff simulation models were tested using the approximate solution obtained by the Izzard method. Both the 1-D and 2-D models simulated runoff processes reasonably. When the discretization level is the same, the models' predictions were not different from each other. The flow rate estimations were just about 0.3% different between the 1-D and 2-D models. Differences in peak flow rates between calculation by the Izzard method and model predictions were less than 2%.

For the 2-D model, there was a computational noise. Even though there was no cross directional slope, the 2-D model produced non-zero velocities in that direction. When the model used quadrilateral elements, this type of oscillation did not appear. The analysis of triangular oscillation indicated that the error was small so that triangular element model could be used without losing significant accuracy.

Linearized stability analysis indicated that the implicit method for time integration was stable. However, the system of equations is nonlinear so that the time step should be carefully determined based on various conditions such as slope and discretization level. In model evaluation with 60 second time step and a value of 0.5 for overrelaxation factor, runoff processes were simulated reasonably.

4.2.2 Verification of Sediment Transport Models

Sediment transport models were tested using the analytical solutions provided by Singh and Regl (1983) and Singh (1983). Since prediction of sediment transport is based on the simulation results from runoff model, runoff models' results were also compared with their analytical solutions. The analytical procedure, based on kinematic approximations for runoff, were obtained by the method of characteristics for simulating the runoff and sediment transport.

4.2.2.1 Input conditions and method

In deriving the solutions for runoff and sediment transport, Singh and Regl (1983) used the following form of kinematic wave equation :

$$\frac{\partial h}{\partial t} + \alpha n h^{n-1} \frac{\partial h}{\partial x} = q \qquad (4\text{-}41)$$

That is, flow rate per unit width is represented by αh^n. Where h is flow depth and q is rainfall excess and α and n are depth-discharge coefficient and exponent, respectively. In describing the continuity relationship for sediment transport, Singh and Regl (1983) used simple equations for rill and interrill erosion :

$$\frac{\partial (Ch)}{\partial t} + \frac{\partial Q_s}{\partial x} = Bq + \gamma (Kh^n - CQ) \qquad (4\text{-}42)$$

where C = sediment concentration
Q_s = sediment load
B = interrill erosion coefficient
γ = coefficient for sediment exchange
K = coefficient for sediment transport capacity

For comparing the model predictions with the analytical solutions, the following conditions were used (Table 4-3).

Table 4-3. Simulation conditions for analytical solutions

n	α	B	γ	K	rainfall
1.5	5	4 kg/m^3	0.03 m^{-1}	1.5 $kg/s.m^{2.5}$	10 cm/hr

With the assumption that rainfall rate equals the rainfall excess, a 200 m long overland flow was simulated by both 1-D and 2-D models. Since the parameters used in analytical solutions do not explicitly give surface parameters such as slope and Manning's coefficient, they were derived based on the uniform flow relationship. In addition, other parameters required in sediment transport capacity equations were also computed in a similar way. The computed values of parameters used in analytical solution are shown in Table 4-4. K_{USLE} indicates soil erodibility factor in USLE equation and D_{50} is the mean diameter of soil particle. ϕ_f and ϕ_r are reduction factors due to mulching or soil surface conditions in splash and hydraulic erosion, respectively.

Table 4-4. Parameters for simulation models.

slope	Manning's n	K_{USLE}	ϕ_f	ϕ_r	D_{50}
1 %	0.017	0.4	0.5	0.1	0.05 mm

Both the 1-D and 2-D models used 60 second time step for runoff and sediment transport simulations. In order to give the same discretization level, the area was discretized into 10 element with 11 nodes for the 1-D and 20 elements with 22 nodes for the 2-D simulations.

Additional simulations were made to compare the effects of different source and sink terms in transport models. In addition to Engelund and Hansen's equation (1967), Meyer and Wischmeier's (1969) equations were also used to compare model predictions.

4.2.2.2 Comparison of analytical solutions with model predictions

Four different equations for sediment transport capacity were briefly discussed in the literature review chapter. One of their common characteristics was that the sediment transport capacity increases with an increase in flow velocity. However, there were some contradictions among the relationships. Some equations predicted an increase while the other equations predicted a decrease in sediment transport capacity with an increase in flow depth. These contradictions suggest difficulties which exist in estimating sediment transport capacity and simulating soil erosion processes. Among the equations, Meyer and Wischmeier's (Equation 2-31) and Engelund and Hansen's (Equation 2-36) equations were used in the model verification to compare the equation used in the analytical solution.

Simulation results of the 1-D and 2-D models were compared with the analytical solutions obtained by the Singh's (1983) method. For each simulation, three different source and sink equations were incorporated. As shown in Figure 4-6, runoff flows were simulated reasonably well by both 1-D and 2-D model. However, the flow rate obtained by the analytical procedure reached equilibrium or peak much faster than those predicted by the models.

Sediment concentrations also showed good agreement between the analytical solutions and models' predictions (Figure 4-7). Figure 4-7 shows sediment concentration changes estimated by the 1-D model over time. There was no differences in sediment concentrations between the 1-D and 2-D estimations. Slight differences in sediment concentration between the analytical and models' results seems to be due to the differences in the runoff amount provided by runoff simulation models as well as differences in the representation of source and sink terms. At initial stages, the analytical solution shows exponential decrease in sediment concentrations. Meanwhile, model predictions show some increase in sediment concentration values for short time period before the decrease in the concentration show in the analytical solution. The reason for this increase is that sediment source at the initial stage in the simulation model is mainly determined by splash rather than hydraulic erosion. In other word, sediment supply by rainfall splash at the initial stage of runoff event is greater than the amount settling down. Experimental results presented in the literature also show that sediment concentrations increase slightly at the initial stage of runoff (Laguna and Giraldez, 1993)

When the source and sink terms were represented in the models by Meyer and Wischmeier's (1969) or Engelund and Hansen's (1967) equations, sediment concentrations did not show the sudden decrease as was the case in the analytical method (Figures 4-7). It is because the initial sediment concentration in the models was much lower than that in the analytical solution. In the simulation models, the effect of splash erosion was significantly reduced by the parameter, k(h) in Equation (3-43) which is an exponential function. The parameter exponentially decrease as flow depth increases.

In this study, the equations for sediment transport capacity were not compared with each other since source and sink term used in the analytical method was different in describing erosion factors. As shown in the right hand side of Equation (4-42), the source and sink term is a combined one which include both rill and interrill processes. The simulation models, however, have different algorithm to evaluate splash and hydraulic erosion processes rather than rill and

interrill erosion. Model verification in this section was intended to evaluate the models' performance in simulating soil erosion and sediment transport processes, as compared with the analytical solutions.

In comparing 1-D and 2-D simulation results, there was no significant differences in either concentration or sediment loading. The overland flow was one-dimensional without side directional slope and hence model predictions between the 1-D and 2-D were expected to be the same.

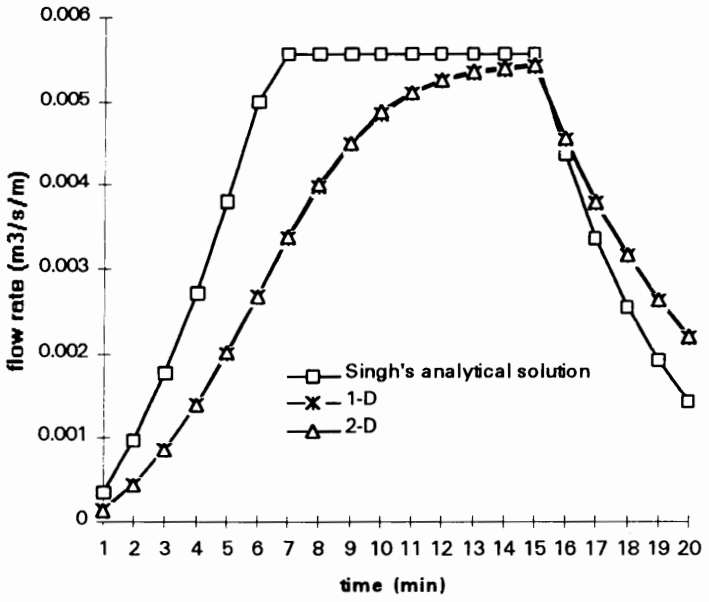

Figure 4-6. Comparison of flow rates between Singh's analytical solution and 1-D simulation.

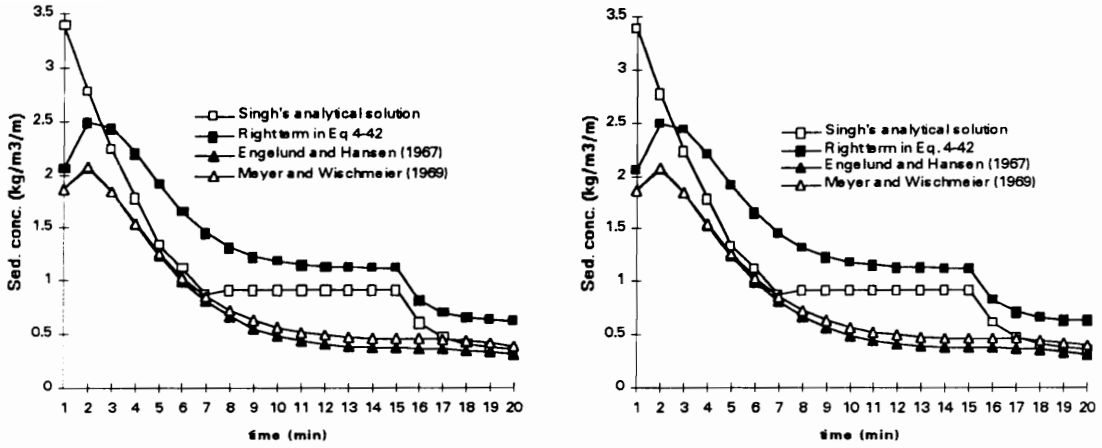

a) 1-D estimations b) 2-D estimations

Figure 4-7. Comparison of sediment concentrations between Singh's analytical solution and 1-D simulations by different source and sink terms.

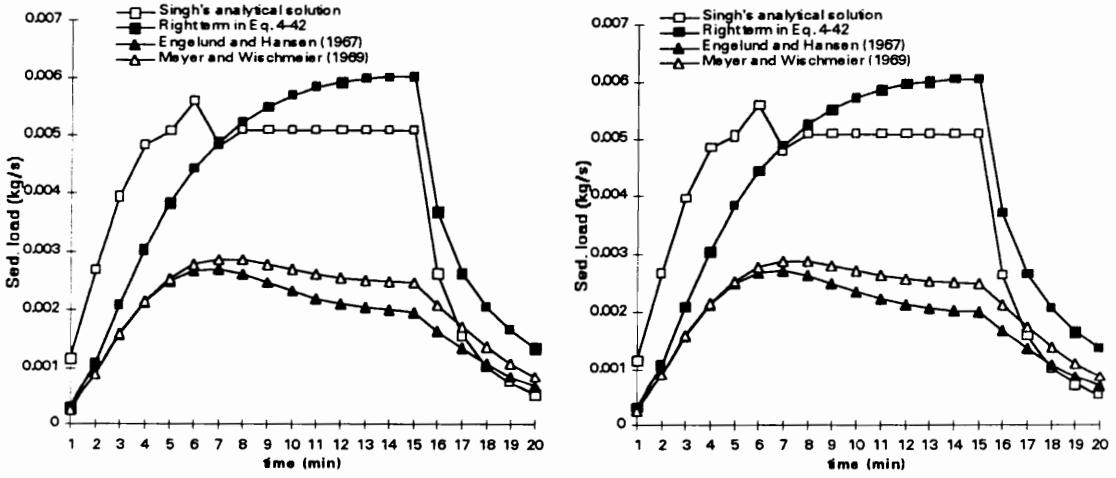

a) 1-D estimations b) 2-D estimations

Figure 4-8. Comparison of sediment load between Singh's analytical solution and 1-D simulations.

4.2.3 Summary of sediment transport model testing

The comparison of simulation results and analytical solutions indicated that the sediment transport processes were simulated reasonably well by either Meyer and Wischmeier's or Engelund and Hansen's equation based on the continuity relationship for sediment. However, some

differences existed depending on which source and sink terms were used in the simulation results. Specifically, the equation for sediment transport capacity was different and hence model results were also different.

There was no significant differences between 1-D and 2-D predictions since the problem area was one-dimensional. Sediment loadings estimated by the models showed differences depending upon the choice of source and sink equations. In this study, the effects of changes in runoff characteristics on sediment transport processes were investigated. Characteristics of the sediment transport capacity and related parameters are not discussed here.

Based on the comparison of model predictions with analytical solutions, it could be concluded that both the 1-D and 2-D models could simulate runoff and sediment transport processes reasonably well. Along with runoff model verifications using the Izzard method, comparison of model predictions with analytical solutions suggested that runoff and sediment transport models for both 1-D and 2-D were successfully developed.

4.3 Sensitivity Analysis for the 1-D models

Sensitivity analysis can be defined as a procedure for investigating the change in model responses to the changes in model parameters. A certain parameter can affect model results in a dramatic way while the change in another parameter may not significantly affect model predictions. Thus, sensitivity analysis is important in understanding the model characteristics and appropriately applying the model. Such analysis guides the preparation of input data and selection of an accurate value for more sensitive parameters. In this section, selected parameters such as Manning's coefficient, slope, hydraulic conductivity, and initial moisture condition were tested to evaluate their sensitivities on the models' results. The analyses were performed only for the 1-D runoff and sediment transport models since the 2-D model predictions are significantly affected by cross slopes. Cross slope effects on model prediction in the 2-D model are discussed in the following chapter.

4.3.1 Model parameters for the sensitivity analysis

A simple hypothetical overland area was used for the sensitivity analysis. Overland area for the sensitivity analysis was assumed to be 50 m long with uniform slope. In runoff simulations, the major parameters analyzed were Manning's roughness coefficient (n), saturated hydraulic conductivity (K_S), a parameter (B) related with initial water content, slope, time step (Δt), and mesh size (Δx). In addition, the ratio of mesh sizes in each direction, $\Delta x/\Delta y$ was also tested in the 2-D model. The base values for selected parameters are listed in Table 4-5. The analyses were performed for ± 10% and ± 30% changes in the parameters, and total runoff volume and peak flow rate were compared. For all model runs, a rainfall event with intensity of 10 cm/hr and 25 minute duration was assumed. Simulations were performed for a duration of 30 minutes.

Table 4-5. Base values for sensitivity analysis of runoff simulation models.

K_S, m/s	n	slope,%	B	Δt, sec	Δx,m	$\Delta x/\Delta y$
7.0E-7	0.02	2	0.1	60	5	1.0*

* only for 2-D model

Using the above parameters, sediment transport models were also applied for a fixed set of mean diameter of soil particle (D_{50}), coefficient for splash erosion (c_f), transfer rate coefficient for hydraulic erosion (c_g), and reduction factor for splash erosion. The reduction factor is a function of flow depth. The total sediment load was compared in order to evaluate the sensitivities of these parameters. Both runoff and sediment transport models were applied for a period of 30 minutes with a rainfall duration of 20 minutes. The base values for these parameters are listed in Table 4-6.

Table 4-6. Basis values for sensitivity analysis of sediment transport models.

D_{50}, mm	c_g	c_f	c_h
0.05	80	0.003	203

In reality, c_g is a function of USLE soil erosivity factor and a reduction factor considering mulch or other effects on soil erosion, as described in the last chapter, and c_f is a function of the clay content and other reduction factors explaining the resistance of soil to detachment. However, the sensitivity analysis was not performed for the parameters related with soil erosion processes

such as mean diameter of soil particle or fall velocity. In this study, the effects of hydraulic characteristics on sediment transport was mainly investigated. Thus, only parameters related to runoff processes are discussed in this sensitivity analysis.

4.3.2 Sensitivity of runoff model parameters

The most sensitive parameters in runoff simulation were K_s and B. As shown in Figure 4-9, total runoff volume was increased by about 10% when either hydraulic conductivity or the parameter, B, were reduced by 30%. Such increase in runoff volume was reasonable since the infiltration amount decreases as the hydraulic conductivity becomes small. Also, runoff volume increased as B decreased since B has a higher value when the initial water content is low. Parameters such as Manning's coefficient and slope showed little changes in the runoff volume. These parameters are mainly related to flow resistance or gravity effects therefore changes in total runoff volume is not significant. Peak flow rate was affected more by the hydraulic conductivity and initial water content than the roughness coefficient and slope. Figure 4-10 shows that peak flow rate increased about 5% when the conductivity decreased or initial water content increased by 30%.

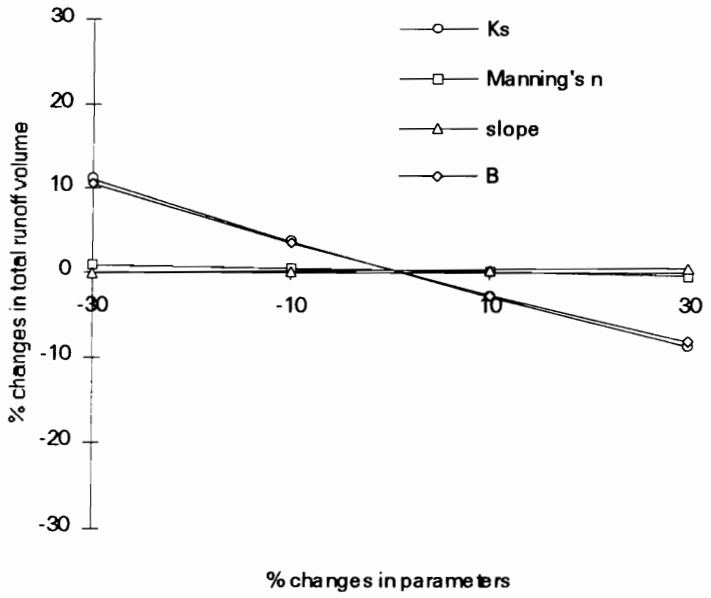

Figure 4-9. Percent changes of total runoff volume

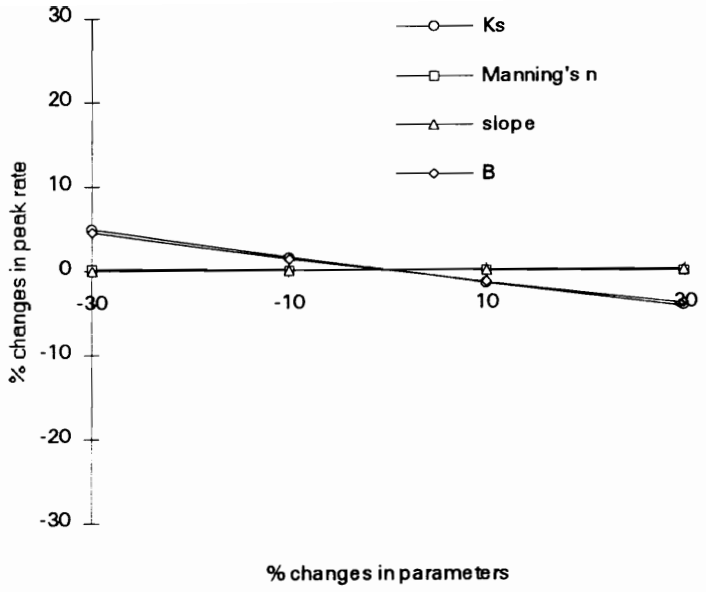

Figure 4-10. Percent changes of peak flow rate

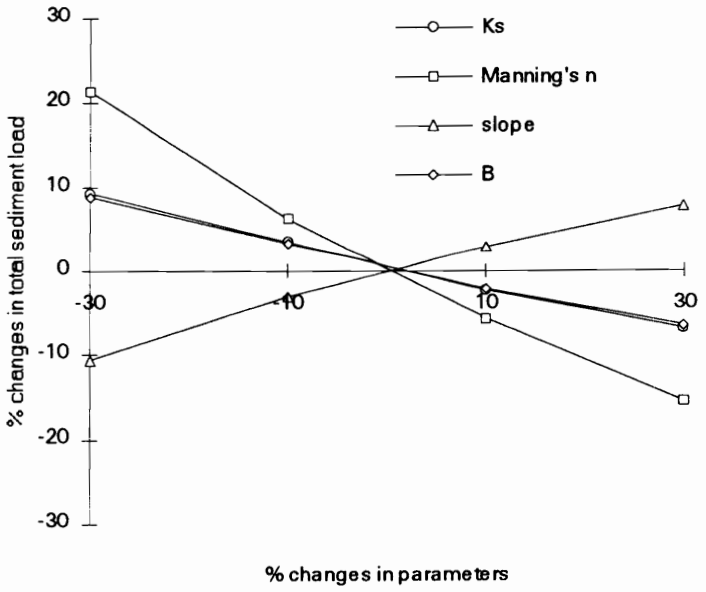

Figure 4-11. Percent changes of total sediment load

Compared to runoff simulation results, sediment loading was more sensitive to the changes in all the selected parameters (Figure 4-11). Total sediment load showed at least about 10% change for 30% change in every parameter analyzed. Overall, Manning's coefficient resulted in more changes in total sediment load than any other parameter used in the sensitivity analysis. A 30% reduction in the roughness coefficient resulted in over 20% increase in sediment loads. These results are supported by the findings reported in the literature (Borah, 1989; Meyer and Harman, 1985).

Meyer and Harmon (1985) investigated the effects of several parameters including slope from furrows under bare soil conditions on sediment loads. The experiment was performed for only runoff inflow added onto the upper end of plots. When the rainfall intensity was 2.6 cm/hr, sediment load was not significantly affected by the change in plot slope. When the plot slopes were between 2% and 5%, there were no significant changes in sediment load due to the slope changes. The sediment load, however, increased very rapidly as slope increased in the range of less than 2% or greater than 5%.

Based on the model testing, it could be seen that the changes in parameters related to the roughness and slope are sensitive when simulating sediment transport. Manning's coefficient defines flow resistance such that at higher n values, reduction in flow velocity and increased depth could occur. In fact, Manning's coefficient did not affect total runoff volume and peak flow rate predictions. The roughness coefficient does not affect gross runoff characteristics but changes flow depth and velocities over the area on which runoff flows. Figure 4-12 shows that flow depth is most sensitive to the Manning's coefficient. A 30% change in the roughness coefficient resulted in about 20% change in flow depth. These results suggest that sediment transport capacity would change the same magnitude when the capacity is represented by a linear function of flow depth. Flow depth is also affected more by surface slope than by K_s and initial water content which are major factors affecting total runoff volume and peak flow rate. As flow depth increases, detachment of soil particles by splash erosion and transport decrease significantly (Woolhiser, 1990). It is worthwhile to note that changes in the Manning's coefficient and slope do not affect predictions of total runoff volume or peak flow rate. Flow depth was most sensitive to the Manning's coefficient. Thus, it is expected that the sediment load could be affected by these parameters.

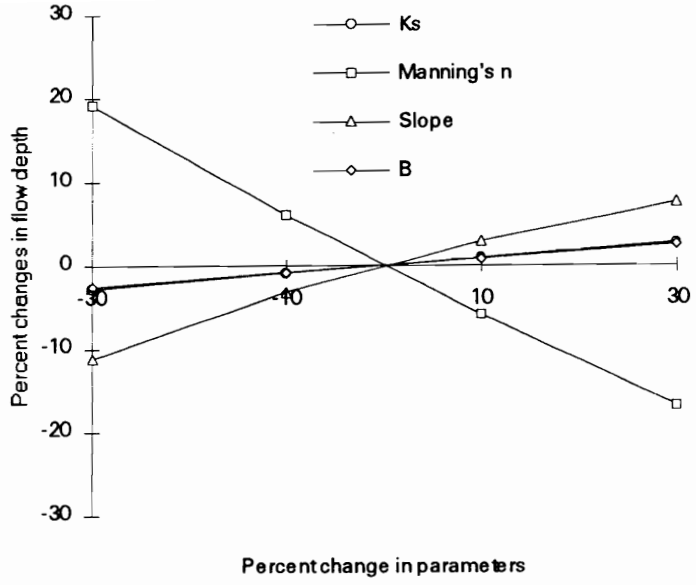

Figure 4-12. Percent changes in flow depth.

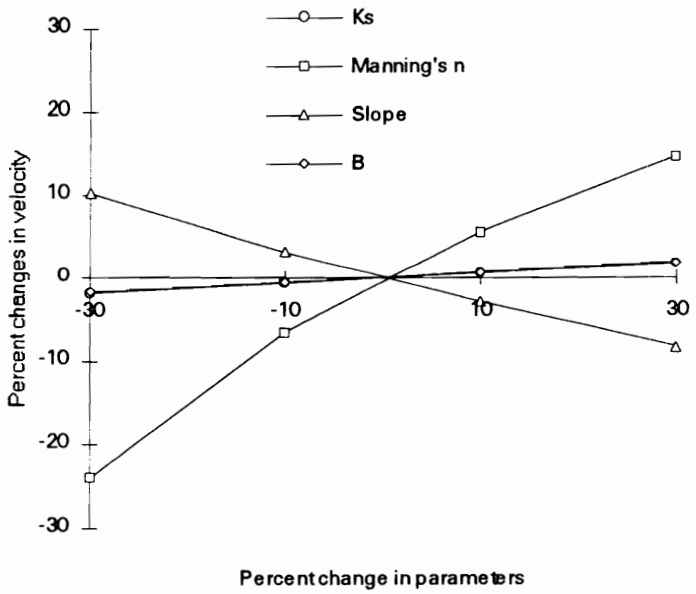

Figure 4-13. Percent changes in velocity

Another important variable in estimating sediment load is flow velocity. As shown in Figure 4-13, the Manning's coefficient and slope affect flow velocity more than any other parameter. A 30% changes in Manning's coefficient resulted in over 20% changes in flow velocity. Literature also supports the importance of slope and other parameter in studying soil erosion processes in overland area (Rose, et al., 1984; Rose et al., 1992, Meyer and Harmon, 1985).

These results suggest that sensitive parameters to total runoff volume and peak flow rate may not affect sediment transport estimations. Since flow depth and velocities are major variables used in determining sediment transport capacity, Manning's coefficient and slope should be appropriately estimated to achieve accurate estimation of sediment transport.

Sensitivity analysis was also performed on discretization levels in both space and time. In theory, the solutions obtained by numerical techniques such as finite element or finite difference methods become equal to the exact solutions when the problem domain is close to zero. However, domain can not be divided into extremely small meshes because of machine round-off errors and feasibility. In most engineering applications, a compromise should be made between the inexpensive approximate and expensive more accurate solutions. In reality, the quality of approximate solutions is not improved after a certain level of discretization.

Model predictions were compared for different levels of discretization in both time and space (Figures 4-14 and 15). For the base discretization, an element size was chosen to be a 10% of the whole overland reach. In other words, 5 meter element size was used for the 50 m whole reach. Figure 4-14 shows the changes in model predictions for 2.5, 4.167, 6.25, and 10 m of element size at the 60 second time step. Discretization levels for the sizes are 0.05, 0.083, 0.125, and 0.2, respectively. For this range of discretization level, the model predictions was not affected.

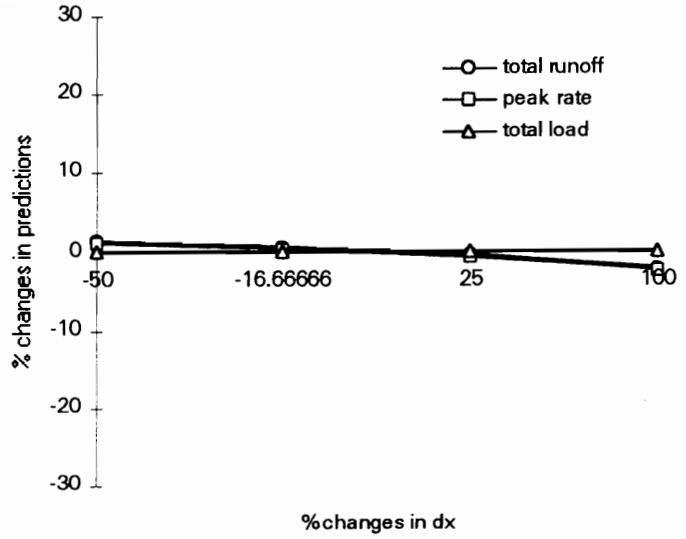

Figure 4-14. Percent changes in model predictions due to mesh size changes

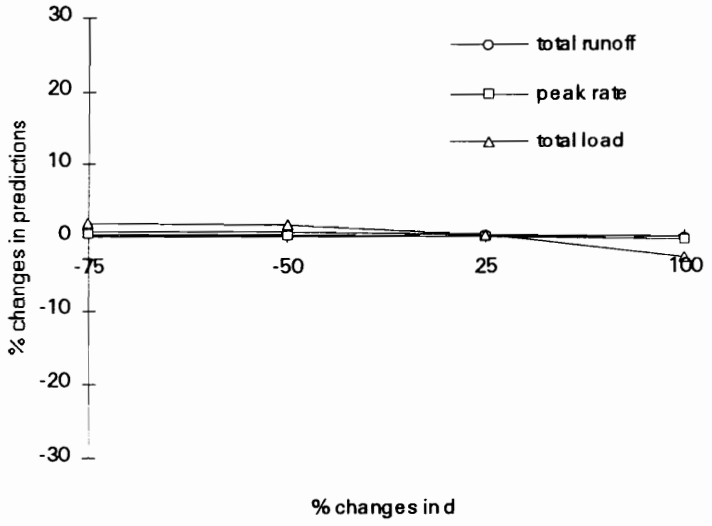

Figure 4-15. Percent changes in velocity due to time step changes

With spatial discretization level of 0.1 of the whole reach, model predictions were compared at different time steps. Temporal discretization level was also defined in a similar way. When time step was 60 seconds, temporal discretization level was 0.033 for the total simulation time of 30 minutes. When time step sizes were 15, 30, 75, and 120 seconds, the temporal discretization levels were 0.00833, 0.01667, 0.04, and 0.067, respectively, for the same total simulation time. Similar to the spatial discretization, for this range of temporal discretization, the models predictions were not significantly affected.

4.3.3 Summary of Sensitivity Analysis

Saturated hydraulic conductivity and initial moisture content significantly affected total runoff volume and peak flow rate. Manning's roughness coefficient and slope did not affect the total runoff and peak flow rate, but significantly affected flow depth and velocities at the outlet. In other words, total runoff and peak flow rate are sensitive to hydraulic conductivity and initial moisture content, while Manning's coefficient and slope were sensitive to local hydraulic characteristics such as flow depth and velocity. Meanwhile, sediment loads were sensitive to all the parameters used in this analysis. Particularly, Manning's coefficient and slope were the most sensitive parameters in simulating sediment loads. These results suggest that flow characteristics such as depth and velocity more significantly affect the simulation of sediment transport.

4.4 Summary and Conclusions

Flow rates obtained by the Izzard method were compared with predictions by both the 1-D and 2-D runoff models to evaluate their performance in simulating runoff processes. To provide the same level of discretization, the overland slope was discretized by 7 and 13 node meshes for the 1-D and 14 and 26 node meshes for the 2-D model applications. The 7 node and 13 node meshes for 1-D were equivalent to the 14 node and 26 node meshes for 2-D model. At the same level of discretization, there were no significant differences in flow rate estimations between 1-D and 2-D models. Both the 1-D and 2-D models estimated peak flow rate about 2% less than that calculated by the Izzard method.

In order to test sediment transport models, analytical solutions presented by Singh and Regl (1983) and Singh (1983) were compared with model predictions. The source and sink terms used by Singh and Regl (1983) were different from the ones chosen in this study, therefore, there were differences in the predictions of sediment load among the various source and sink equations. In general, simulation models predicted sediment transport processes reasonably well, compared to the analytical solutions. However, there were significant differences in sediment concentration at the initial stage of rainfall. Model predictions, regardless of the type of source and sink equation used, commonly showed increase in sediment concentrations at the initial stage of runoff while the analytical solution showed consistent decrease. The difference at the initial stage may be due to the reason that simulation models take flow depth impacts on soil erosion processes into account. Overall, the comparison of model's predictions and analytical solutions indicated that sediment transport models could reasonably simulate soil erosion and sediment transport processes.

The sensitivity analysis suggests that Manning's roughness coefficient is more sensitive in simulating sediment transport processes. Hydraulic conductivity and initial water content were sensitive in determining total runoff volume or peak flow rate but they had little effect on flow depth and velocity. Meanwhile, Manning's coefficient and slope were sensitive in determining runoff characteristics which subsequently affected total sediment load.

5. MODEL APPLICATIONS

5.1 Introduction

Through model validation and sensitivity analysis presented in the previous chapter, it was found that both runoff and sediment transport models were properly developed and gave reasonable predictions. The sensitivity analysis showed the importance of surface conditions described by Manning's coefficient and slope in simulating sediment loadings. However, the results was based on the one-dimensional process. In actual field conditions, topography is complex so that more detailed simulations may be required. When cross slopes exist, flow may converge and flow characteristics would become more complex. Thus, it is important to investigate various situations with complex topography where secondary slopes exist.

This chapter describes applications of the models to several hypothetical overland cases and actual field plots where runoff flow was measured. Application of the models to the hypothetical overland areas were conducted to investigate the effects of cross slope and element shape on runoff and sediment load. In these simulations, model predictions were compared for each different set of hypothetical slopes. The 1-D and 2-D models were applied to investigate the effects of flow depth, velocity, and flow rate on sediment loadings at the outlet area as well as the spatial distribution of sediment concentration. Simulation results were compared with the data obtained from the experimental studies performed by Dillaha et al. (1986) and Storm (1991).

The 1-D and 2-D models were compared to test their ability in simulating sediment loadings. The 2-D model was not always superior to 1-D model in runoff and sediment transport simulations. In this chapter, the differences between the 1-D and 2-D models are discussed and explained in terms of runoff characteristics. As shown in the previous chapter, sediment transport processes were more sensitive to runoff characteristics such as flow depth and velocity than total runoff volume. Thus, model predictions are compared with respect to these runoff characteristics and spatial distribution of sediment concentration. An assessment is made to determine whether the 2-D approach improves model predictions over the 1-D approach for various situations.

5.2 Criteria for comparing model predictions

The 1-D and 2-D models' predictions were compared to evaluate their abilities in simulating runoff and pollutant transport processes. The steps involved in the simulation process included the definition of equations based on physical processes, numerical formulation, and preparation of input data for describing the problem domain. An objective comparison of model predictions by the 1-D and 2-D approaches can not be achieved when any of these steps is different. Therefore, it is very important to provide the same computational conditions and input data when comparing the simulation results of the 1-D and 2-D models.

The computational conditions in this study included time step and mesh size. Both time step and mesh size are related to the stability of the solutions. The time step is important in solving time-dependent problems by a numerical technique. It is related to the stability of solution. Particularly, explicit method requires strict stability conditions determined by the time step to achieve appropriate solutions. The time step is not a problem in comparing model predictions since it is defined by the user in the input files. Meanwhile, the spatial discretization process for the two models is more complicated and are not identical. When it comes to comparing the number of nodal points in meshes, 2-D simulation requires at least twice as many nodes as those of the 1-D model, since it uses areal elements that require at least three nodal points. For example, 2-D requires at least 10 nodes for simple overland to provide the same level of discretization, whereas 5 nodes may be enough in 1-D simulations. In reality, the spatial discretization level is determined by the availability of topographic information, while time discretization can be determined by the model user. In this study, the same level of spatial discretization for the 1-D and 2-D applications indicates the same number of nodal points along the slope. The spatial discretization level could be determined by the amount of information of topography in actual field applications.

Another important consideration in comparing the 1-D and 2-D models is the computational cost. The 2-D model has three degrees of freedom per node while the 1-D has two since the former has secondary directional flow velocity. Thus, the 2-D model requires more computational time than the 1-D to solve a problem with the same number of nodes. Dealing with an engineering problem, one should consider cost-benefit relationships. In other words, the

question should be asked if model predictions can be improved by 2-D over 1-D approach with reasonable additional computational cost.

When comparing model predictions between the 1-D and 2-D models, one should properly define what variables are to be compared and how they are compared. In this study, the comparison is conducted for the simulation results such as runoff rate and sediment concentration, which are spatially different and transient. They can be compared in terms of their variations over time and space, or at a specific time and space. Hydrograph, for example, provides runoff changes over time, and contour maps illustrate spatial distribution of results at a certain time.

To compare predictions by the 1-D and 2-D models, the following simulation results were evaluated :

- Flow rate and sediment loading rate at the outlet,
- Peak flow rates,
- Spatial distribution of the flow depth and sediment concentration,
- Average flow depth and sediment concentrations at a specific time,
- Computational costs and requirement of additional computational efforts, and
- Ratio of cross slope to main slope.

Percent difference (PD) between the 1-D and 2-D estimations was used to compare the model predictions. The PD was calculated by the following relationship :

$$PD = \frac{(E_{1D} - E_{2D})}{\left(\frac{E_{1D} + E_{2D}}{2}\right)} \qquad (5\text{-}1)$$

where PD = percent difference between the 1-D and 2-D estimations
E_{1D} = 1-D estimation
E_{2D} = 2-D estimation

5.3 Hypothetical Cases

Four hypothetical case studies were performed to investigate the effects of element shape, cross slope, and field size on model predictions. The first case study was for an arbitrary shape overland area without cross slope, and the second through fifth cases were of rectangular shape area where cross slopes as well as main slope existed. The first case was chosen to investigate the effect of element shape in the 1-D model. Model applications were made for different levels of discretization along the main slope. The second and third hypothetical scenarios were used to evaluate the effects of cross slope on runoff and sediment transport simulations. The last case study was performed to investigate the effect of field size on the model predictions.

5.3.1 Hypothetical Case Study #1 :Effects of Discretization Level on Model Predictions

5.3.1.1 Input requirement and Computational Conditions

For 1-D simulations, rectangular elements were assumed. Model predictions could be affected by the discretization level when overland area is difficult to be represented by a rectangle. In this study, each element in 1-D model was represented by a rectangular area. The area was determined based on actual shape, and the flow length was estimated by an average value or representative length. In the 2-D model, the elements were represented by nodal points and their connectivity without determining flow length as in the 1-D model.

In the first case, a hypothetical overland area of about 0.8 ha was used (Figure 5-1, b). A 4.8 cm/hr rainfall event was applied for 25 minutes. The overland area was discretized to have 2, 5, 8, and 11 nodes for 1-D and 4, 7, 9, 11, and 20 node for 2-D simulations. The input conditions for these simulations are given in Table 5-1.

Table 5-1. Description of hypothetical overland area

Area, m^2	Slope, %	K_s, cm/hr	Manning's n	D_{50}, mm	B*	time step
7757.4	5	1.3	0.02	0.05	0.002	60 sec

* B is a parameter indicating the saturation deficit of the soil multiplied by the effective net capillary drive.

Additional model applications were also made for three different choices of representative flow length, using the 5 node mesh in 1-D model, in order to investigate the effects of flow length on model predictions. An average flow length in which an element was represented by mean width and mean length was selected for simulation. This approach is most common in 1-D simulations. Two additional simulations were made for flow lengths of 10% shorter and 10% longer than the average length. Since different flow lengths can be chosen by the users for the same element in actual model applications, it is worthwhile to investigate the effects of various flow lengths on the 1-D model predictions. Figure 5-1 shows an example of 1-D and 2-D meshes for the hypothetical overland area.

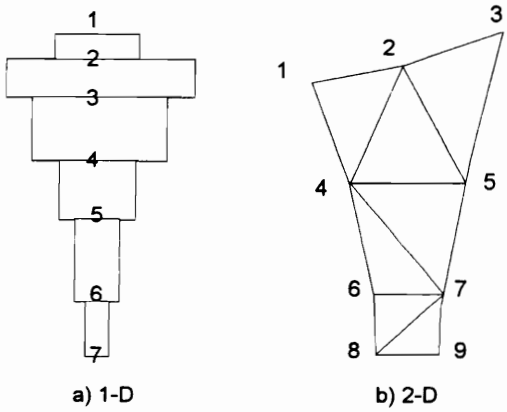

(not in scale)

Figure 5-1. Example of meshes for the first hypothetical overland area for both 1-D and 2-D simulations.

5.3.1.2 Results and Analysis

Comparisons were made at several different levels of spatial discretization for the 1-D and 2-D models. Model's predictions obtained from the 11-node mesh for 1-D were considered closer to the exact solution than any other meshes since numerical solutions approach the exact solutions as the discretization level increases. The 1-D model results showed that peak flow rates computed by 2- and 5-node meshes were 35% and 20% less, respectively, than the values estimated by the 11-node mesh. A 2-node mesh did not describe the actual shape of the overland area since it

considers the area as a rectangle. Simulation results from the 2-D model also showed similar tendencies with respect to discretization level. The 4-node mesh of the 2-D simulations are

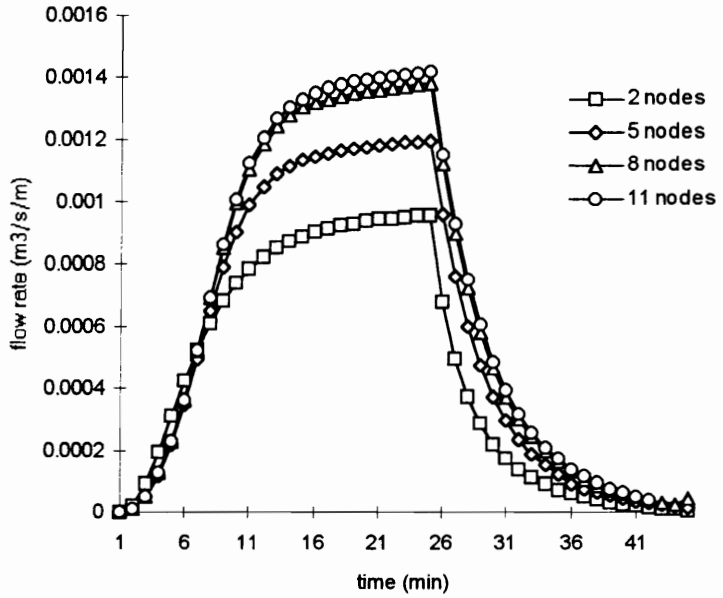

Figure 5-2. Effect of different discretization level on peak flow rate simulations by the 1-D model.

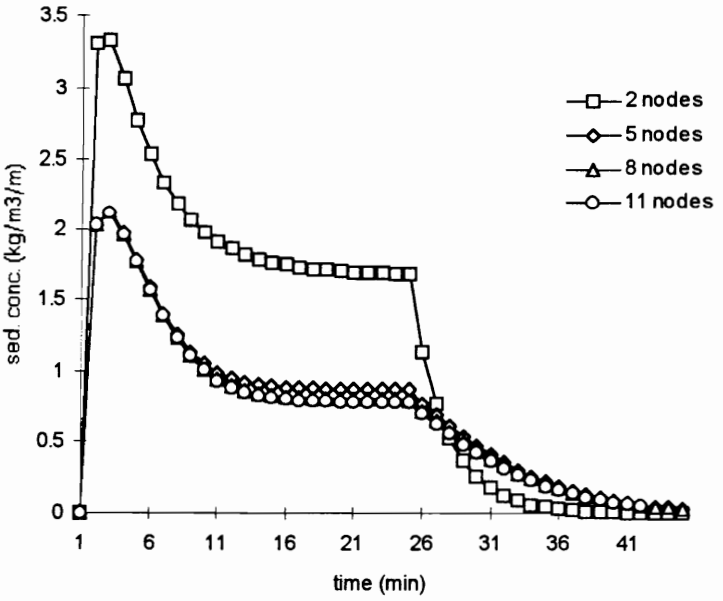

Figure 5-3. Effect of different discretization level on sediment concentration simulations by the 1-D model.

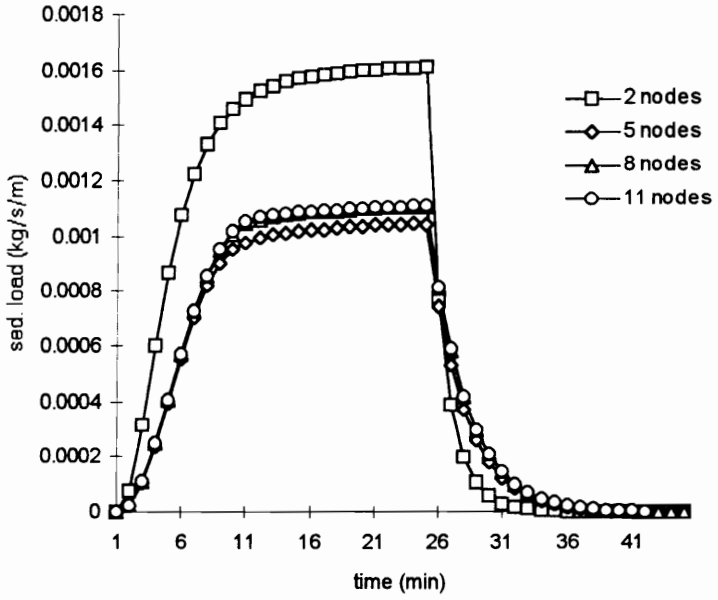

Figure 5-4. Effect of different discretization level on sediment load simulations by the 1-D model.

comparable to the 2-node mesh of 1-D in terms of discretization level. The flow rates estimated by the 2-D model with 4 nodes are nearly the same as those predicted by the 1-D model with 2 nodes (Figures 5-2, 5-8).

The predictions obtained from the 2-node mesh in the 1-D model showed remarkable differences from any other scenarios. The sediment concentrations predicted from the 2-node mesh were two times as high as those estimated from other meshes. However, in most applications overland area should be discretized with a larger number of nodes to satisfy stability conditions. The hydrographs shown in Figure 5-2 indicate some differences among 5, 8, and 11 node meshes, but estimated sediment loads were not substantially different. The peak flow rate predicted from 11-node mesh was 15% higher than 5-node prediction, while 11-node estimation of sediment load was only 6% higher at the time of peak flow. Based on the simulation results of the 1-D model, reasonable predictions could not be expected when the area is not sufficiently discretized to describe actual shape of overland area.

The 5-node mesh size was used to investigate the effects of different representation of flow length on model predictions and results were illustrated in Figures 5-5, 5-6, and 5-7. Changes in the

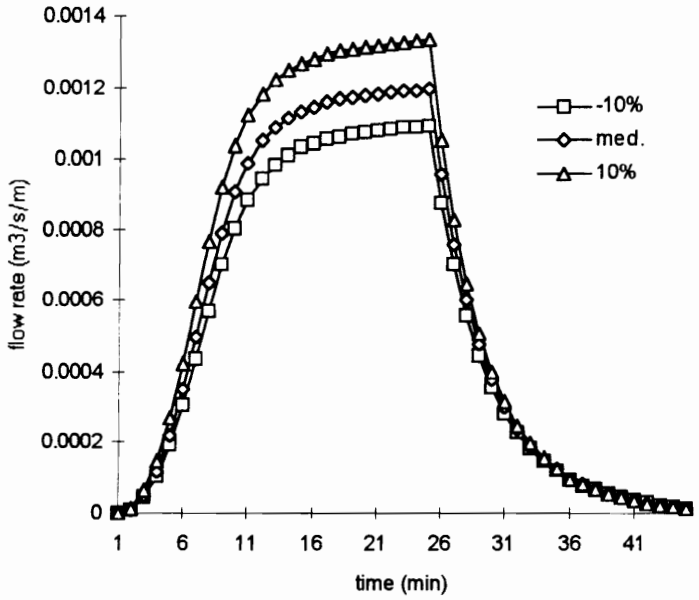

Figure 5-5. Effects of different flow lengths on peak flow rate simulation by 1-D model.

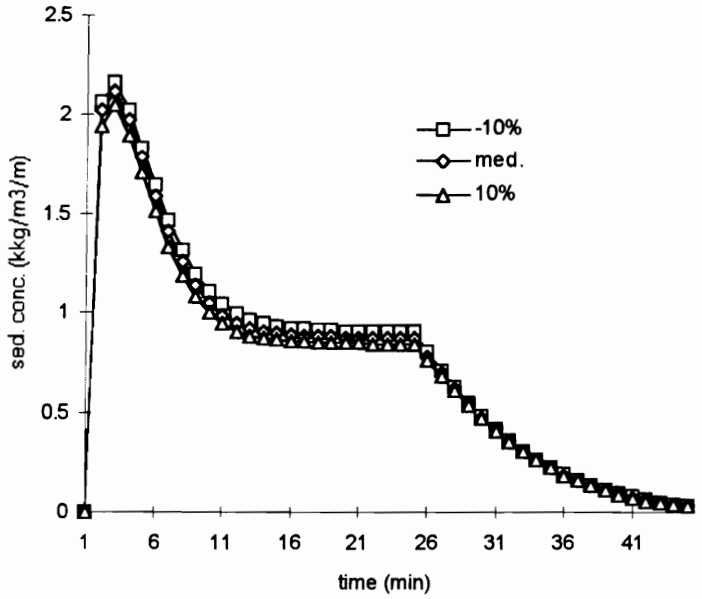

Figure 5-6. Effects of different flow lengths on sediment concentration simulation by 1-D model.

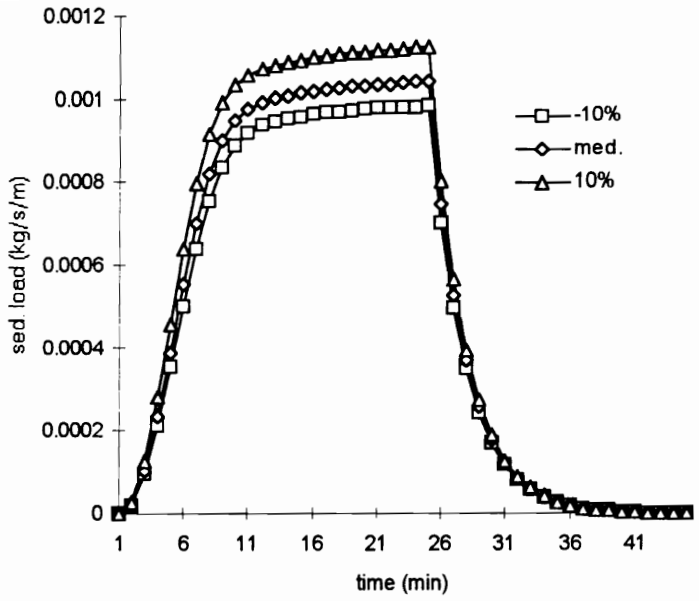

Figure 5-7. Effects of different flow lengths on sediment load simulation by 1-D model.

prediction of runoff flow rate were about the same as the changes in flow lengths. When the flow length of 10% longer than the average value was used, the flow rate also increased by 10%. In the meanwhile, sediment concentration did not change notably as a result of various representation of flow length even though a slight decrease in concentrations was observed when flow length was increased (Figure 5-6). Figure 5-7 illustrates that the differences in sediment loads are mainly due to the differences in flow rate estimations.

Compared to the 1-D predictions, runoff estimations by the 2-D model showed that the equilibrium state was reached in early time stages after the start of runoff (Figure 5-8). A comparison of Figures 5-8 and 5-2 showed that the 2-D model resulted in a slightly higher flow rate than 1-D at the same level of spatial discretization. The peak flow rate predicted by the 11-node mesh in the 2-D was 19% higher than that predicted by 11-node mesh in 1-D. The 11-node mesh for the 2-D model was obtained by placing two additional nodal points on the 2-D mesh illustrated in Figure 5-1. However, the 11-node mesh in 1-D has a higher discretization level than that in 2-D. The main reason for the differences in the peak flow rate may be due to the difference

in the representation of the overland area since other input conditions were the same. Sediment concentrations estimated by the 2-D model were not substantially different from those simulated by 1-D (Figures 5-3 and 5-9). Predictions obtained from the 4-node mesh showed a large difference from those obtained from other meshes. The 4-node mesh has the same level of discretization as the 2-node mesh in the 1-D model.

The sediment load predictions by the 2-D model were about 30 to 40% greater than those simulated by the 1-D when discretization level in both time and space was approximately the same (Table 5-2). The reason for this difference was mainly due to the assignment of open boundary condition to the side boundary nodes, which had no constraints such as zero flow velocity or flow depth. More about the effects of different boundary conditions are discussed in the second hypothetical study.

Table 5-2. Comparison of 1-D and 2-D model predictions for different level of discretization

Discretization level*	model dimension	No. of nodes	Peak flow, (m^2/s)	Sed. load at peak flow, (kg/m/s)	Runoff Vol. (m^3/m)	Sed. Yield (kg/m)
1	1-D	2	9.56E-4	1.61E-3	1.21	2.02
1	2-D	4	1.30E-3	1.50E-3	1.93	2.26
4	1-D	5	1.19E-3	1.04E-3	1.52	1.35
4	2-D	7	1.46E-3	1.41E-3	2.16	2.06
7	1-D	8	1.38E-3	1.10E-3	1.75	1.44
5	2-D	9	1.72E-3	1.36E-3	2.55	2.00
10	1-D	11	1.414E-3	1.11E-3	1.79	1.442
6	2-D	11	1.71E-3	1.39E-3	2.53	2.04

* Discretization level was defined as the number of elements in the direction of slope.

From this hypothetical application, it was concluded that no substantial differences existed between 1-D and 2-D models in simulating runoff and sediment transport when discretization level was approximately the same. Even though the 1-D runoff model resulted in different peak flow rates for the different choices of the flow length of element, the effects of the flow length on the 1-D model predictions could be ignored when enough discretization was provided such that the actual shape of the overland area could be reasonably described.

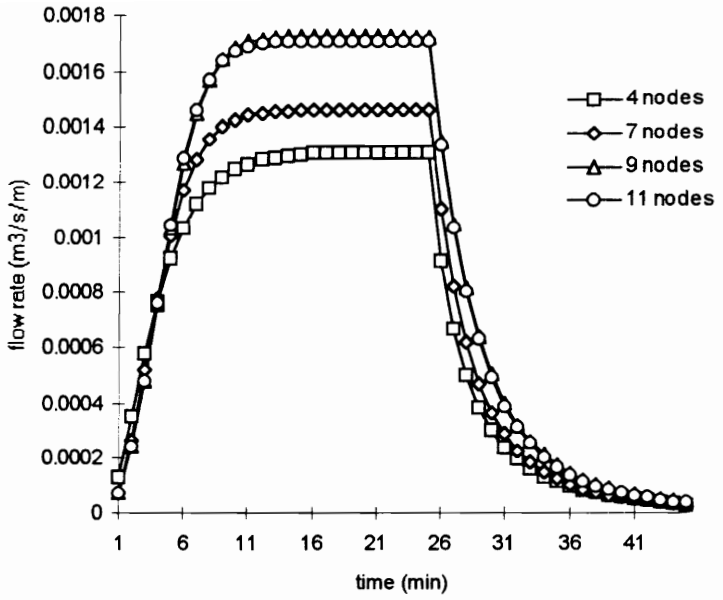

Figure 5-8. Effects of different flow lengths on peak flow rate simulation by the 2-D model.

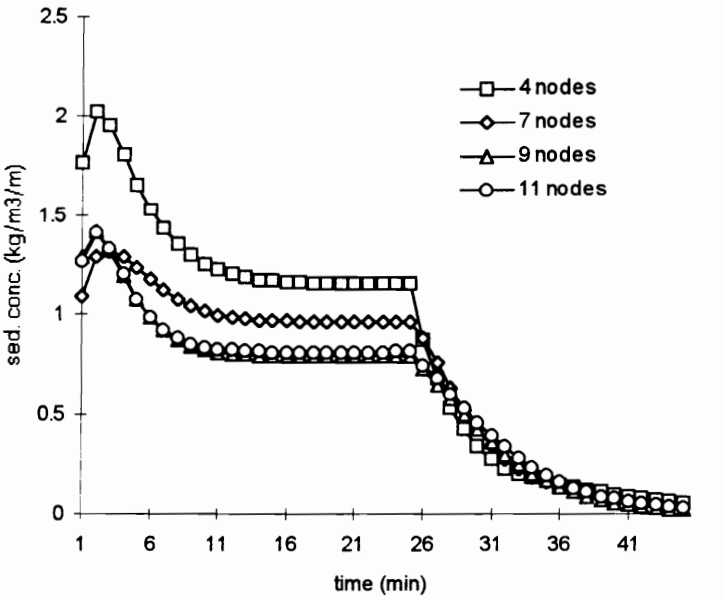

Figure 5-9. Effects of different flow lengths on sediment concentration simulation by the 2-D model.

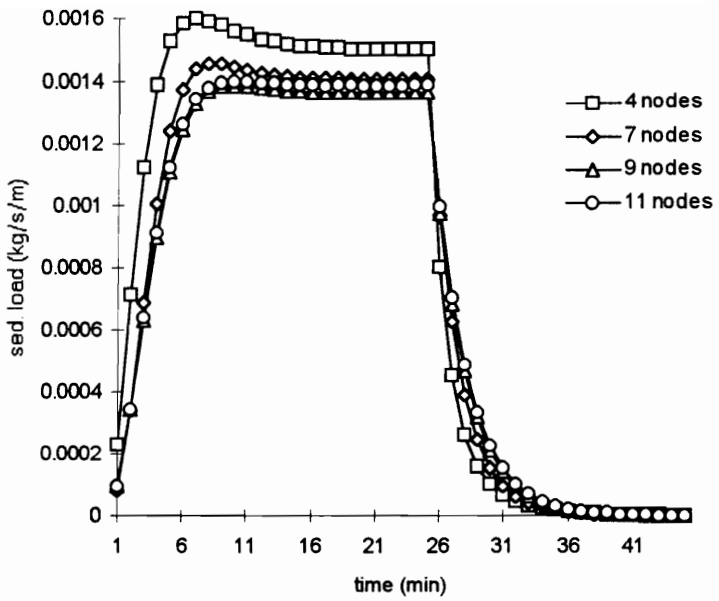

Figure 5-10. Effects of different flow lengths on sediment load simulation by the 2-D model.

5.3.2 Hypothetical Case Study #2 : Cross Slope Effects on Model Predictions

5.3.2.1 Input and Computational Conditions

Surface slope is an important factor in describing both runoff and sediment transport processes. It determines the shear stress which is considered to represent a direct force to detach and transport soil particles from the bed. As discussed in the previous chapter, surface slope plays a more important role in simulating sediment transport process than in the runoff process. The surface slope is more closely related with flow velocity and runoff depth.

In order to investigate the effects of slope on sediment transport, a second hypothetical study was conducted where cross slope as well as a main directional slope existed. When the cross slopes are ignored, as in 1-D simulation, the model may not adequately simulate runoff and sediment transport processes. In this hypothetical case study, overland processes were simulated

by both the 1-D and 2-D models to compare the effects of cross slope on model predictions. Cross slope was assumed to be zero, 1, and 2% while the main slope was assumed to be 5%. The cross slopes were directed toward the center of the plot. Zero cross slope was simulated by the 1-D model and 1 and 2% cross slopes were simulated by the 2-D model. For all simulations, a rainfall event of 4.8 cm/hr was applied on a rectangular area of 80m x 100 m for 25 minutes, and simulations were performed for a 30-minute duration. The overland area was discretized to have 30 nodal points. All the input conditions except the representation of slope, were exactly the same as those given in Table 5-1.

5.3.2.2 Results and Analysis

When cross slopes exist, side boundary conditions should be considered. As in upstream boundary nodes, no lateral inflow was assumed at the side boundary nodes. That is, either flow depth or velocity should be zero. This is often called a closed boundary condition (Zhang and Cundy, 1989). The closed boundary condition was assigned to upstream boundary nodes for all simulations in this study. Meanwhile, the side boundary nodes are assigned according to whether cross slope existed or not. When cross slopes exist, side boundary nodes should also be considered as zero flow flux nodes, or closed boundary nodes. Otherwise, model solution might not converge. In fact, when cross slope was 2%, the solution in the 2-D model did not converge until over 100 iterations after the end of rainfall, if proper boundary conditions were not imposed to side boundary nodes. As runoff receded, the model did not converge for this case since side boundary points had negative flow depths. When both upstream and side boundaries were assigned zero flow conditions, the convergence problem disappeared. With zero flow conditions on both upstream and side boundary nodes on 1% and 2% cross slopes for 2-D simulations, model predictions were compared with the 1-D simulation results (Figures 5-11, 12, and 13).

Models' results indicated that there were differences in all predictions between cross slopes and zero cross slope. The average peak flow rates simulated for 1% and 2% cross slope at the outlet area were about 26% and 17% less than those obtained from the 1-D uniform slope (zero cross slope), respectively (Figure 5-11). The average sediment concentrations at the outlet predicted by the 1-D model was 18% and 29% greater than those estimated by the 2-D model, respectively, for 1% and 2% cross slopes (Figure 5-12). There was no difference in sediment

concentration between the 1% and 2% cross slopes. Average sediment loads at the time of peak flow showed 18 to 29% differences between zero and non-zero cross slopes (Figure 5-13, Table 5-3).

The differences in model predictions for various slopes resulted from the differences in flow characteristics due to the existence of cross slopes. The 2-D model simulated flow convergence along the lower elevation nodes so that the distribution of flow depths was substantially different. The maximum flow depth for 2% cross slope was about 27% higher than that simulated for the 1% cross slope. The 1-D model prediction, meanwhile, showed rather uniform distribution of flow depth along the main slope. Flow velocities along the slope also showed uniform distribution. In addition, spatial distributions of the resulting sediment concentrations were substantially different between the 1-D and 2-D predictions since the flow characteristics determine sediment transport capacity. Meanwhile, the average values of flow depth and sediment concentration at the outlet were not substantially different among the slopes.

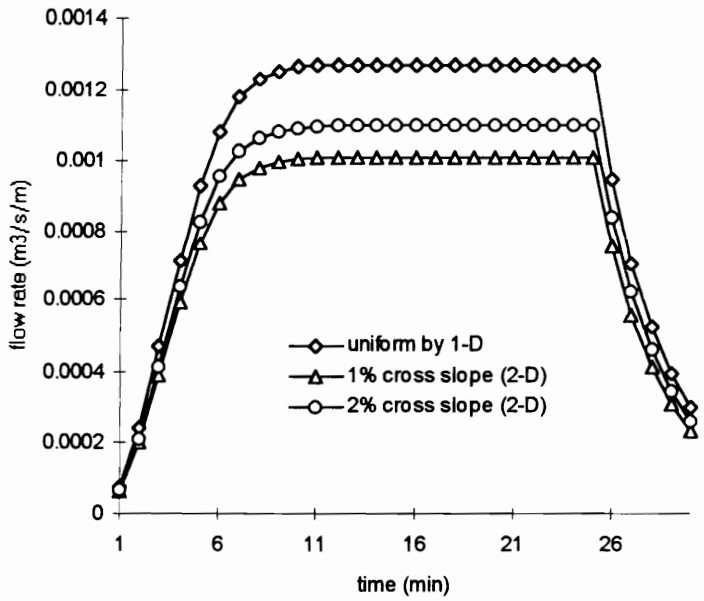

Figure 5-11. Comparison of hydrograph for different slope conditions

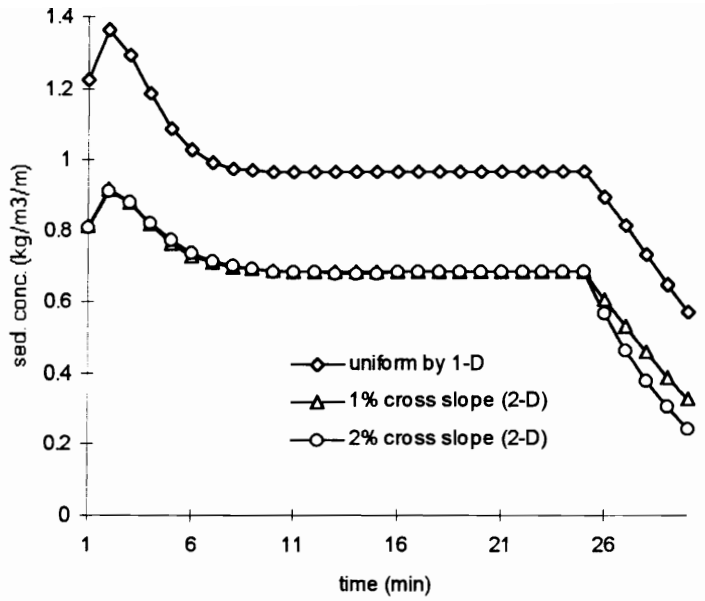

Figure 5-12. Comparison of sediment concentrations for different slope conditions

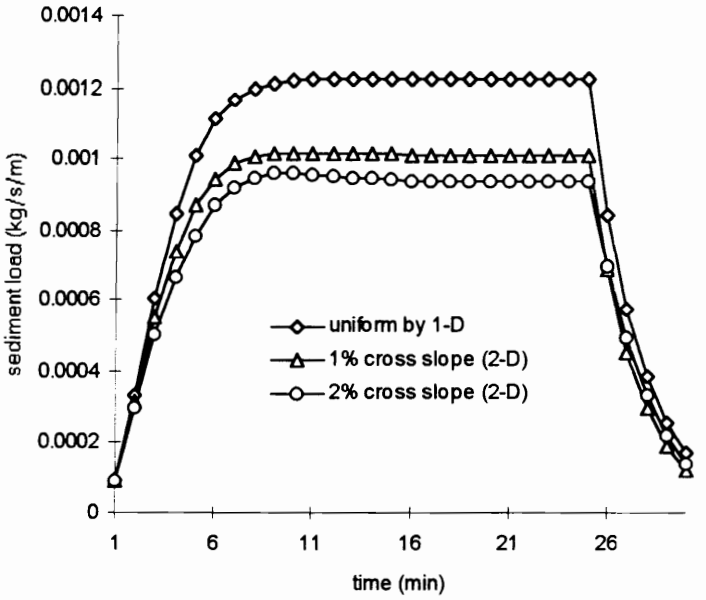

Figure 5-13. Comparison of sediment loads for different slope conditions

The results suggested that the differences in model predictions of both runoff and sediment transport, were not substantial due to the existence of cross slope. Based on these results, it was found that the 1-D simulations, without the consideration of cross slope, resulted in about 20% higher estimations for both runoff flow rate and sediment loads, compared with the 2-D model predictions (Table 5-3).

Table 5-3. Comparison of 1-D and 2-D model predictions for different cross slopes.

	1-D	2-D 1% cross	PD	2-D 2% cross	PD
Peak flow rate ($m^3/s/m$)	0.0013	0.0010	26	0.0011	17
Sed. loads at peak flow, (kg/m/s)	0.0012	0.0010	18	0.0009	29
Total runoff volume, (m^3)	145.6	116.3	22	126.6	14
Sediment yield, (kg)	140.8	117.4	18	110.4	24

PD: percent difference (Equation 5-1).

5.3.2.2.1 Effects of boundary conditions on prediction results

Since the boundary conditions could affect both runoff and sediment transport processes, it is worthwhile to investigate their impacts on model predictions. Hence, simulation results from 1% cross slope were also compared for the different boundary conditions to investigate their effects on model predictions. In simulating plots with cross slopes, side boundary points need to be set to zero flow depth. Otherwise, side boundary nodes would have negative flow depths after rain has stopped, which will not allow the overall solutions to converge. Boundary conditions may be imposed in three different ways: fully closed, half closed, and open boundary conditions. Fully closed condition indicates all zero boundary condition for both flow depth and velocity, and open condition is free condition for both variables. The half closed condition can be defined as free flow depth but zero flow velocity. The half closed condition is often used in simulating overland flow processes (Tayfur et al., 1993).

With the same input conditions as in the previous simulations, the 1% cross slope was tested for three different boundary conditions for side boundary nodes. The flow rates were affected by the assignment of zero boundary conditions (Figure 5-14). When fully open conditions were imposed to both upstream and side boundary nodes, the peak flow rate estimation was about

20% higher than those from the fully-closed condition. When non-zero depth conditions were imposed, flow rates increased without reaching equilibrium state. The fully open condition is not appropriate when the side boundary nodes are separated (e.g. watershed boundary) If fully open condition is imposed, the nodes have non-zero flow and simulation cannot be performed properly as estimated flow rates become larger than the actual ones. This can be easily shown by comparing prediction results with 1-D model between open and closed conditions for upstream boundary nodes. In many model applications, half-closed or fully-closed conditions rather than fully open condition are frequently used (Tayfur et al., 1993; Woolhiser and Liggett, 1967; Zhang and Cundy, 1989).

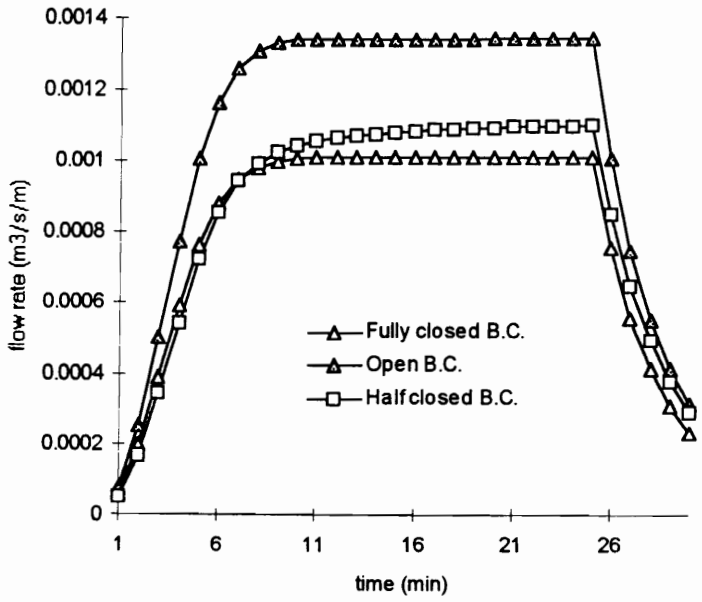

Figure 5-14. Comparison of hydrograph for different boundary conditions

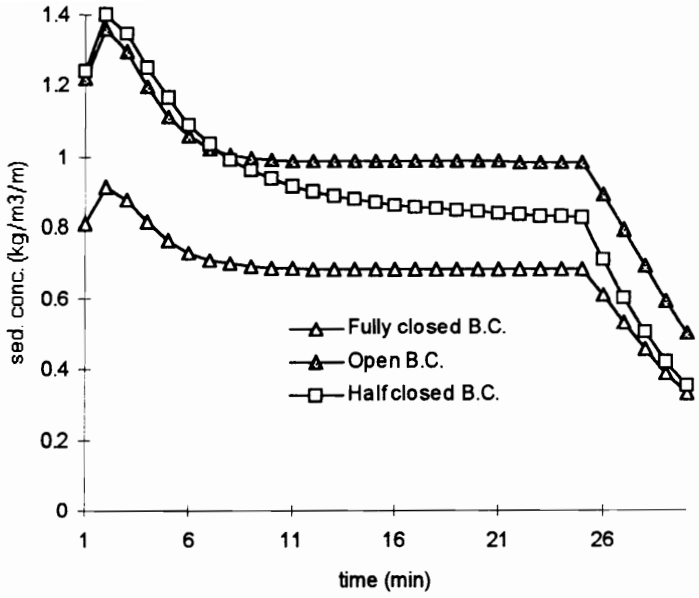

Figure 5-15. Comparison of sediment concentrations for different boundary conditions

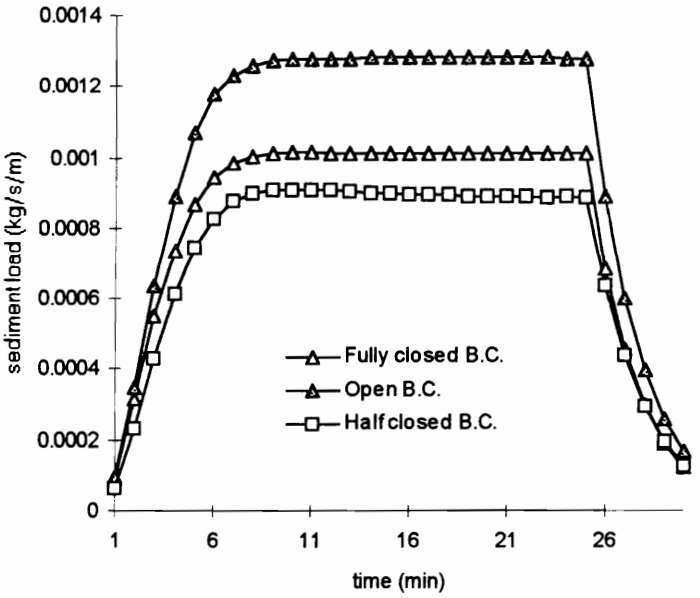

Figure 5-16. Comparison of sediment loads for different boundary conditions

The peak flow rate estimation was about 10% different between the fully-closed and the half-closed boundary conditions. Since side boundary nodes under closed boundary condition have no flow, open boundary condition showed consistently higher flow rates than other conditions. The half-closed boundary condition resulted estimations in between fully closed and open boundary conditions. Sediment concentrations also showed similar tendencies. Open condition showed higher sediment concentrations over time than any other conditions. Under the half-closed boundary conditions, the sediment concentrations were closer to those values estimated under open boundary condition, mainly because half closed condition had non-zero flow depth at side boundary nodes so that they had non-zero sediment concentrations. Figure 5-16 shows that sediment load under open condition is about 30% higher than that under the fully-closed condition at the outlet area. The half-closed boundary condition showed slightly greater estimations of both flow rate and sediment concentration than the fully-closed condition. Whereas, the prediction of sediment loading under the fully-closed condition was 10% higher than under the half-closed condition. The reason for greater prediction of sediment loading under the fully-closed condition, in spite of less flow rate and lower sediment concentration, is that flow rates at the boundary nodes were computed by zero. The half-closed condition was assigned to have zero flow velocity. Even though non-zero sediment concentrations existed at the boundary nodes, the average sediment load decreased since sediment load at the boundary nodes became zero. It could be seen that the choice of boundary condition could result in about 10% difference in sediment loading.

Figures 5-17 illustrates the spatial distributions of model predictions over the outlet area. There were no differences in flow depth between the open boundary and half-closed boundary conditions. Flow rate predictions were also nearly identical between fully closed and half closed conditions. Sediment concentrations had a similar distribution for open and half-closed boundary conditions. Figure 5-17 (a) illustrates that fully closed condition resulted in a slight different flow depth distribution compared to the other two. However, a comparison of spatial distribution among three different conditions suggests that the model predictions were essentially the same. Open boundary condition is an inappropriate boundary condition since it allows non-zero flow at the side boundaries where flow rate should be ideally zero. The literature supports this approach for boundary conditions (Tayfur et al., 1993; Zhang and Cundy, 1989; Liggett and Woolhiser, 1967). The forced fully-closed condition may be also undesirable when the boundary nodes are

artificially separated. Around the separated boundaries by plywood, for example, there could exist enough flow depth and hence nonzero flow flux even though no flow velocity is assumed right on the nodes. In this study, fully-closed conditions are imposed when cross slopes are directed toward the center of the plot.

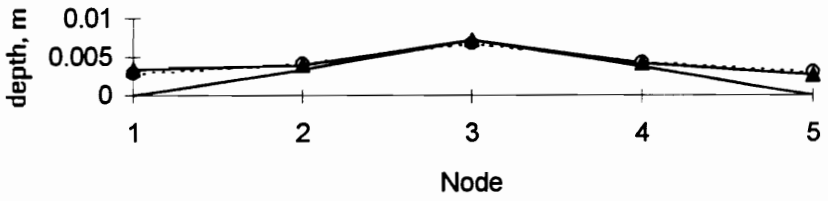

a) Flow depth distribution

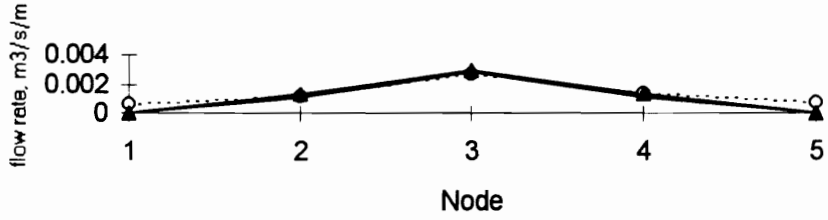

b) Flow rate distribution

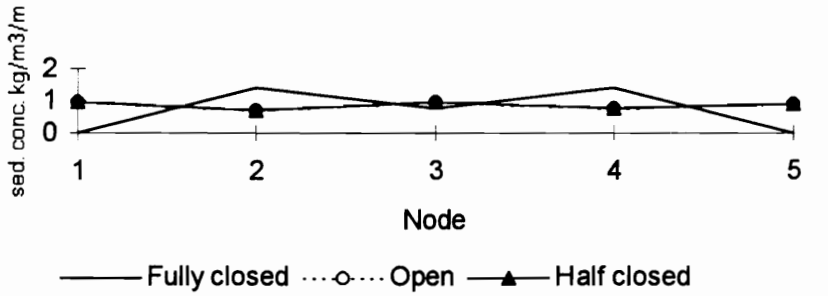

c) Sediment concentration distribution

Figure 5-17. Comparison of model predictions for different boundary conditions

This hypothetical case study showed that representation of cross slopes by the 2-D model resulted in about 20% underestimation of sediment yield compared to the 1-D estimations. However, the differences were not considered critical because the 2-D model itself produced about 10% differences in model predictions for the different boundary conditions. Model predictions of sediment transport could vary by 20% by using alternative input parameters as shown in the sensitivity analysis.

5.3.3 Hypothetical Case Study #3 : Channelized Flow

In most field conditions, channelized overland flows are easily observed. The channelized runoff could occur even on the overland area where cross slope is relatively small, compared to its main slope. To investigate the effects of the channelized runoff on sediment transport processes, another set of hypothetical overland slopes was generated.

The hypothetical area was assumed to be 50 m x 75 m with a main slope of 5% (H505 and H510) or 1% (H102 and H103) as shown in Figure 5-18. The cross slopes were assumed to be 10, 20, or 30 % of the main slope. Figure 5-18 shows the contours of generated hypothetical elevations used in this case study. A total of 176 nodal points were used for both 1-D and 2-D applications.

5.3.3.1 Input Data and Computational Conditions

For both the 1-D and 2-D simulations, a 10 second time step was used. A rainfall rate of 50 mm/hr was assumed for a 30-minute duration. Zero depth and velocity boundary conditions were used for both upstream and side boundary nodal points. The input parameters for runoff and sediment transport models are presented in Table 5-4.

Table 5-4. Input conditions for hypothetical case study #3.

Parameters	
Init. soil moisture	saturation
Manning's n	0.013
D_{50}, mm	0.01
Fall velocity, mm/s	0.06

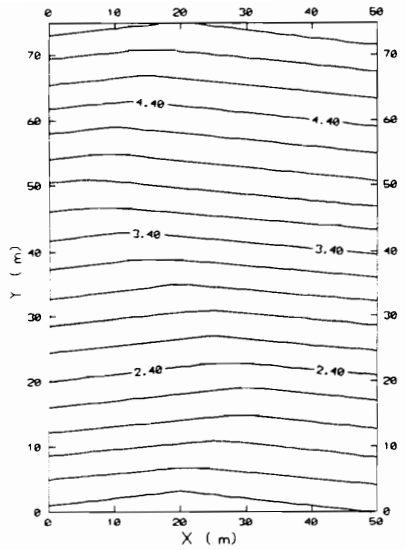

a) 5% main with 0.5% cross slope (H505)

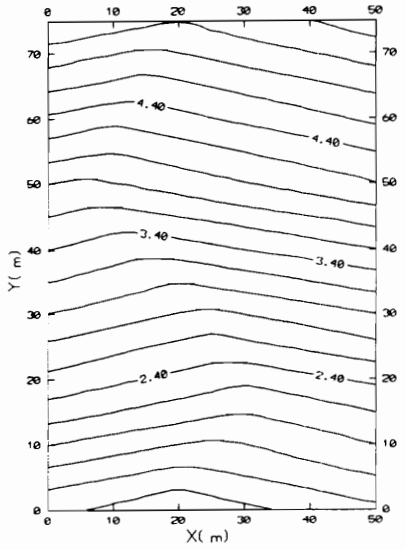

b) 5% main with 1% cross slope (H510)

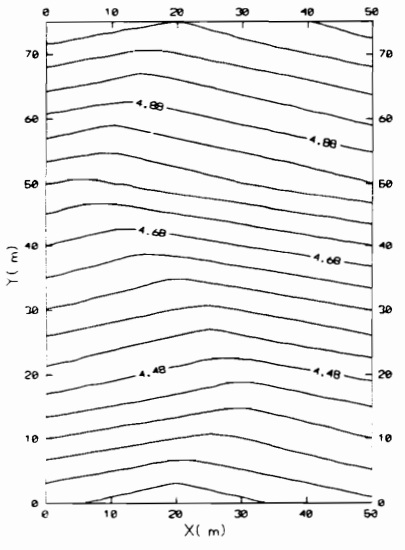

c) 1% main with 0.2% cross slope (H102)

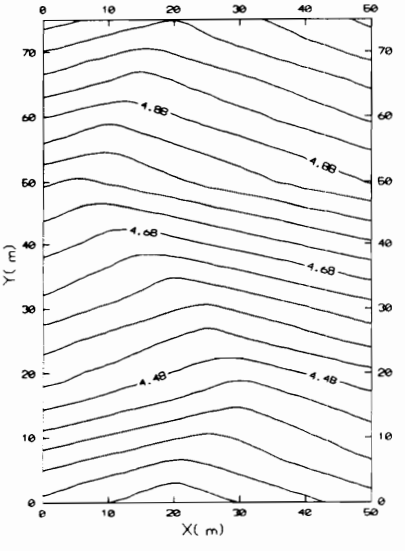

d) 1% main with 0.3% cross slope (H103)

Figure 5-18. Elevation contours for the hypothetical case study # 3.

5.3.3.2 Results and Analysis

In this hypothetical case study, the models' results were compared in terms of spatial and temporal distribution of runoff and sediment loading rates. Runs H103 could not be completed after rain stopped because of development of negative flow depths. Therefore, only model predictions before the solution failed to converge were compared in this hypothetical case study.

The distribution of flow depth predicted by the 2-D model was similar to the elevation contour maps presented in Figure 5-18. Compared to the spatial distribution of the 2-D flow depths, the 1-D model showed rather uniform distribution along the main slope. The 2-D model simulated flow convergence phenomena along the lower elevation points of the plot while the 1-D model did not show much differences in flow depth in cross slope direction (Figures 5-19 and 20). Meanwhile, the differences in the spatial distribution of estimated sediment concentration were not remarkable between 1-D and 2-D, compared to the distribution of flow depth. The 1-D estimation of sediment concentration did have the approximate features of 2-D distribution.

As the cross slope increased, the 1-D model showed a slight improvement in spatial distribution of flow depth. Compared to the run H102, flow depth for the run H103 showed increase along the lower elevation points (Figure 5-20 a.). However, the 1-D estimated spatial distribution of sediment concentration was not affected at the increase of cross slope.

A major difference in models' predictions between the 1-D and 2-D models was that the 1-D model predictions were rather uniform along the cross section of slope while the 2-D estimations showed increased flow depth and sediment concentration at the lower elevation nodes.

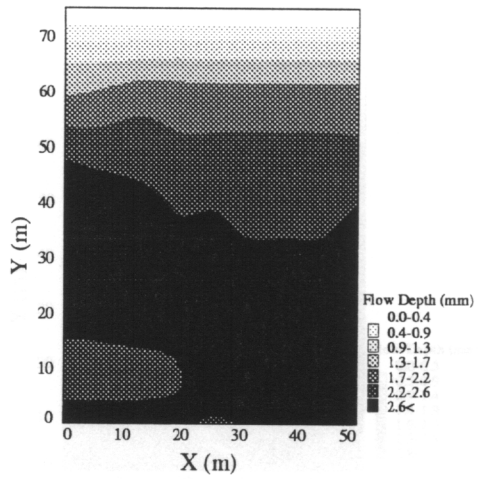

a)1-D estimated depth distribution

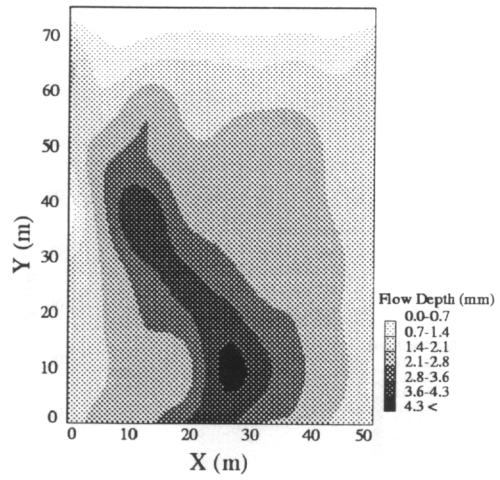

b) 2-D estimated depth distribution

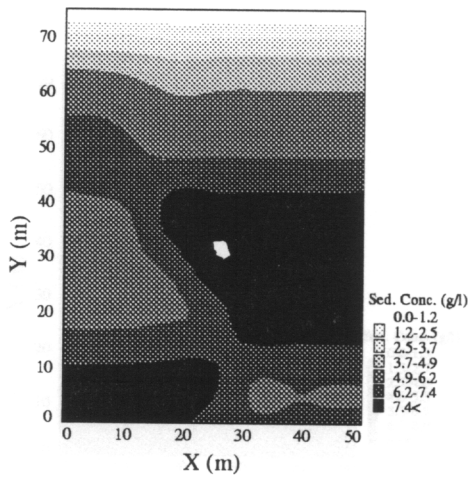

c) 1-D sediment concentration distribution

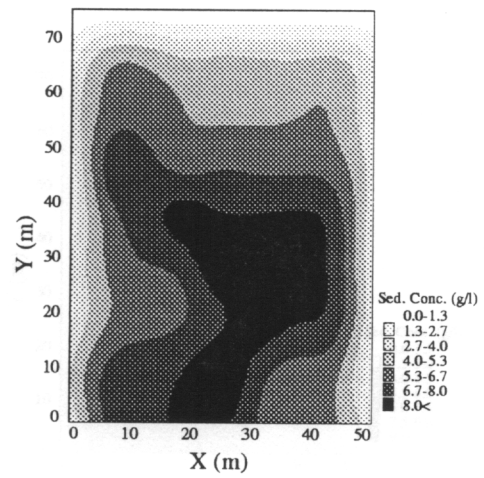

d) 2-D sediment concentration distribution

Figure 5-19. Spatial distribution of model predictions for the 1% main slope with 0.2% cross slope after 200 seconds .

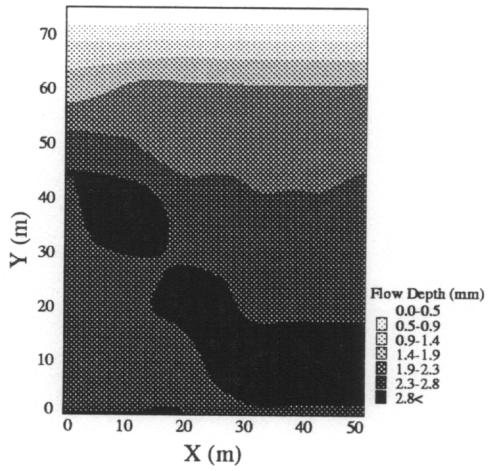

a) 1-D depth distribution

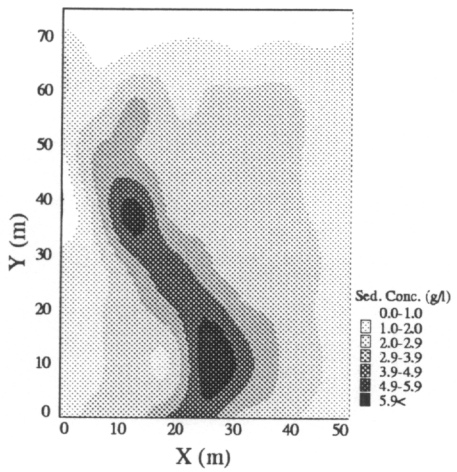

b) 2-D depth distribution

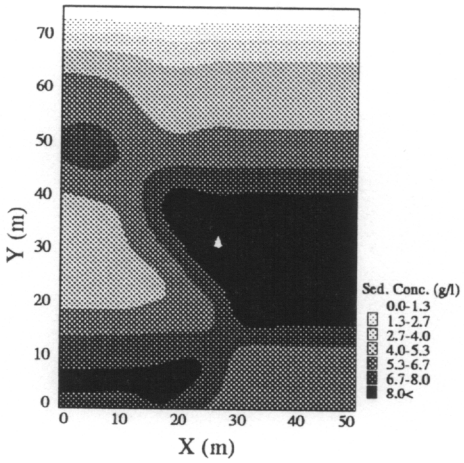

c)1-D sediment concentration distribution

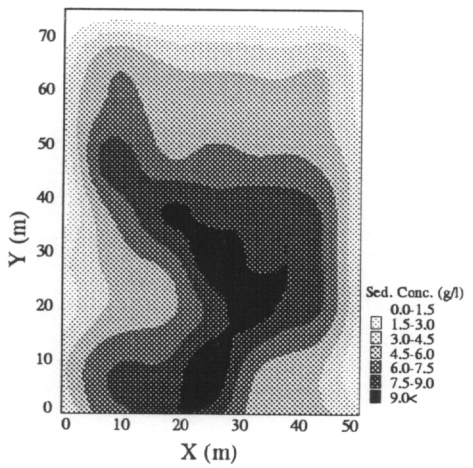

d) 2-D sediment concentration distribution

Figure 5-20. Spatial distribution of model predictions for the 1% main slope with 0.2% cross slope after 200 seconds

Spatial distributions of velocity and flow rate for runs H505 and H510 were also compared (Figure 5-18), where the main slope was 5% and cross slopes were 0.5% and 1%, respectively. The vectors shown in Figures 5-21 through 24 indicates direction and magnitude of velocity or flow rate by its length.

From the 1-D results for H505 (Figure 5-21), no changes in the magnitude of velocity and flow rate due to the existence of cross slopes were observed among the nodal points in cross slope directions. Meanwhile, the 2-D estimations show differences in both flow directions and their magnitude among the downstream nodal points (Figure 5-22). The maximum flow velocities estimated by the 1-D and 2-D models were 0.3 and 0.4 m/s, respectively. The maximum flow rate at the lowest elevation node was 0.14 m^2/s for the 2-D model which was twice greater than that estimated by the 1-D model.

The spatial distributions of the H510 results are illustrated in Figures 5-23 and 24. The 1-D model predictions for the H510 were not different from those for H505 (Figures 5-21 and 5-23). The maximum flow velocity and flow rate for H510 were nearly identical to those from H505 estimations. However, the 2-D estimations for both flow velocity and flow rate for H510 were significantly increased compared to those for H505. The maximum flow velocity increased by about 23% and maximum flow rate by about 93%.

The comparison showed that the 2-D model simulated the increase in velocity and flow rate along the lower elevation nodes reasonably well. The 2-D model simulated the effects of changes in cross slope on flow characteristics while the 1-D model did not.

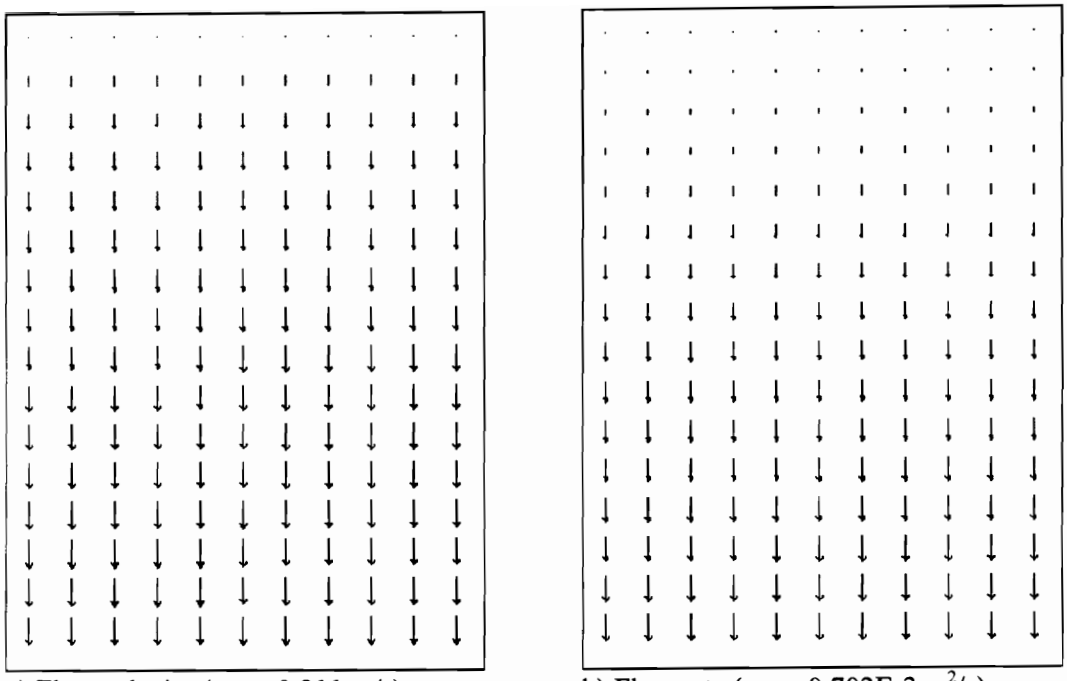

a) Flow velocity (max. 0.311 m/s) b) Flow rate (max. 0.702E-3 m^2/s)

Figure 5-21. Spatial distributions of 1-D estimations for the 5% main slope with 0.5% cross slope (H505).

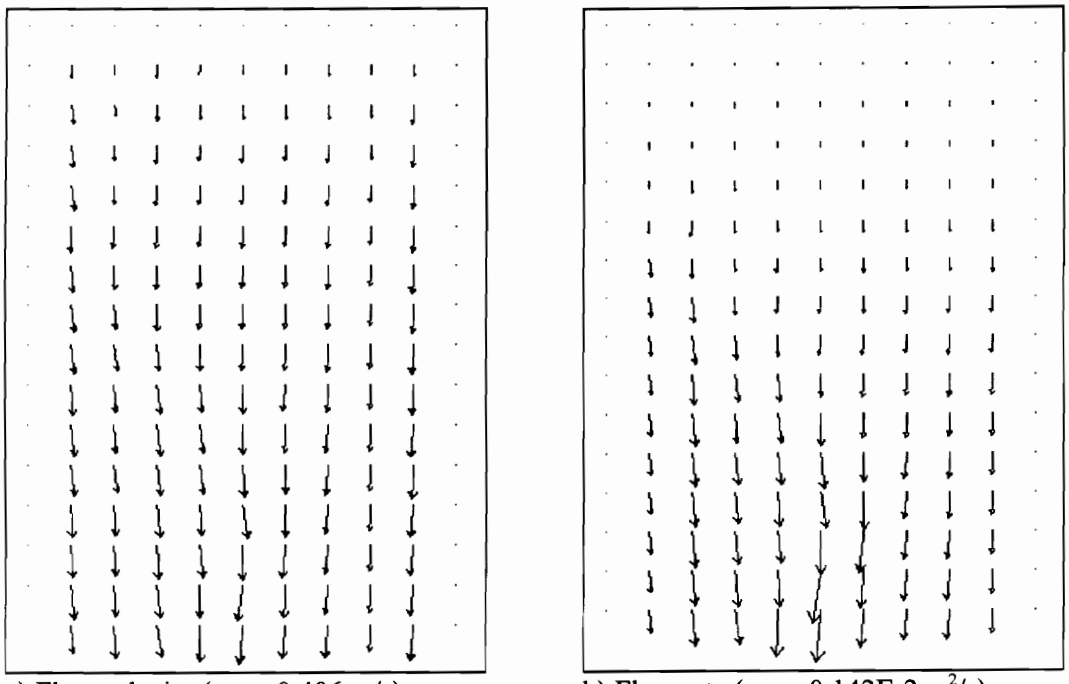

a) Flow velocity (max. 0.406 m/s) b) Flow rate (max. 0.142E-2 m^2/s)

Figure 5-22. Spatial distributions of 2-D estimations for the 5% main slope with 0.5% cross slope (H505).

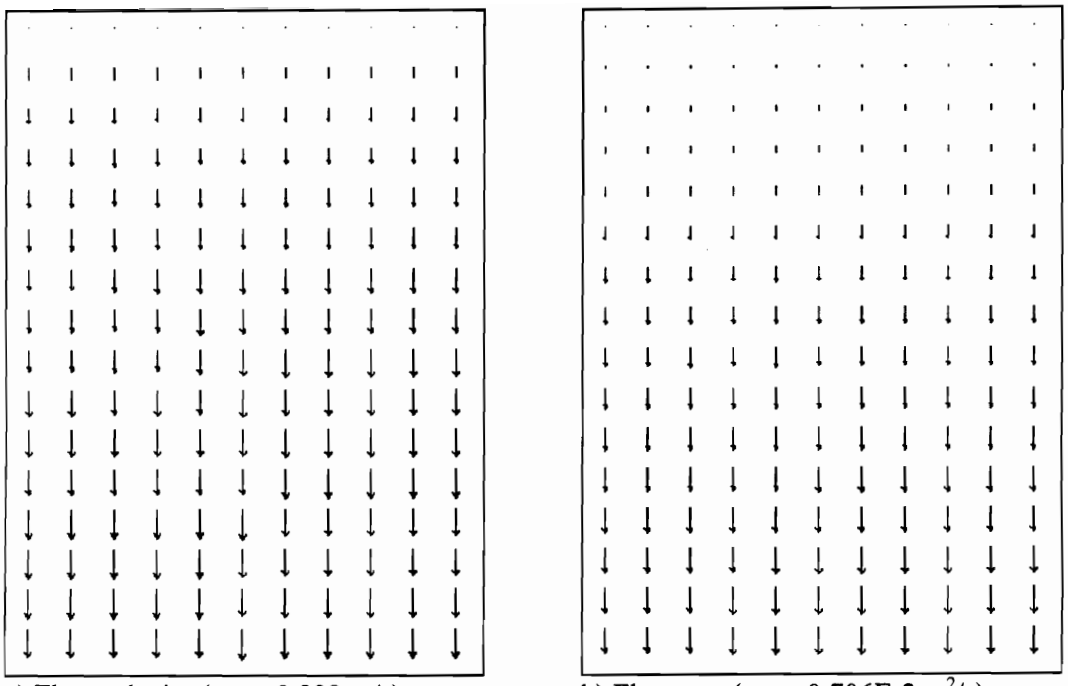

a) Flow velocity (max. 0.322 m/s) b) Flow rate (max. 0.706E-3 m^2/s)

Figure 5-23. Spatial distribution of 1-D estimations for the 5% main slope with 1% cross slope (H510).

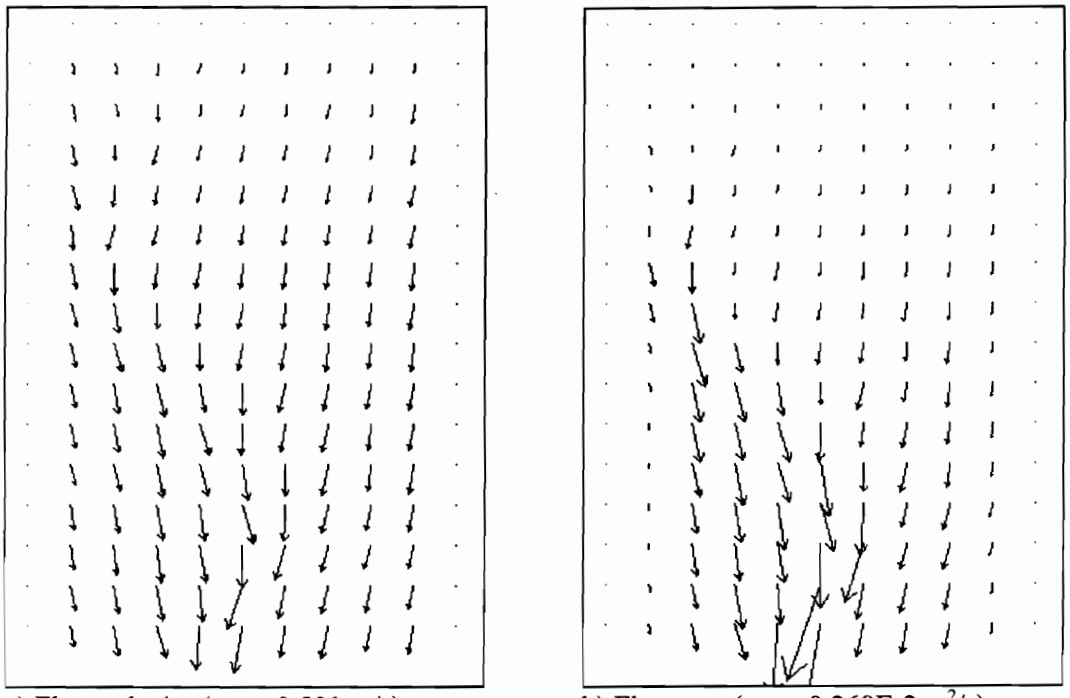

a) Flow velocity (max. 0.501 m/s) b) Flow rate (max. 0.268E-2 m^2/s)

Figure 5-24. Spatial distribution of 2-D estimations for the 5% main slope with 1% cross slope (H510).

When runoff rates reached a steady state for H505 scenario, runoff and sediment loading rates estimated by the 1-D model were about 8% and 2% higher than those predicted by the 2-D model, respectively. At the rising limb of both hydrograph and sedi-graph, however, the 2-D estimations had higher values than the 1-D simulations (Figures 5-25 and 26). When the cross slope increased from 0.5% to 1%, the peak flow rate estimations changed slightly in both 1-D and 2-D models (Figures 5-27 and 28). The 2-D estimated sediment loading rate at the time of peak flow for the 1% cross slope showed an increase of 8% compared to 0.5% cross slope. This change could be explained by the development of flow convergence due to increased cross slope. However, the magnitude of the differences in the predictions between the 1-D and 2-D model was insignificant. In addition, peak flow and sediment concentrations were not significantly affected by the change in the cross slope in both the 1-D and 2-D predictions.

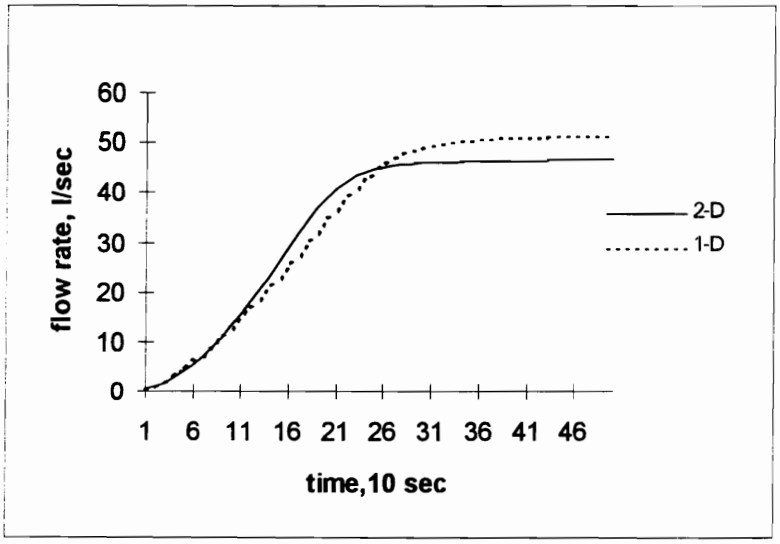

Figure 5-25. A comparison of runoff hydrograph predicted by the 1-D and 2-D models for H505 (5% main and 0.5% cross slope)

In the hydrographs (Figure 5-25 and 27), the 2-D results showed higher flow rates during the rising limb of hydrograph when cross slopes existed. The 2-D model reached the equilibrium flow rate before the 1-D model which could mean that the 2-D model simulated runoff processes along the steepest paths to the outlet. Meanwhile, the 1-D model simulated runoff processes along the strips defined by the main slope. The strips, however, could not be actual flow paths when

cross slopes existed. Even though cross slopes were very small, the downstream nodal points, defined by the main slope, could not be the lowest elevation points in the surrounding nodes. Therefore, the 1-D model required more time to reach the equilibrium flow rate.

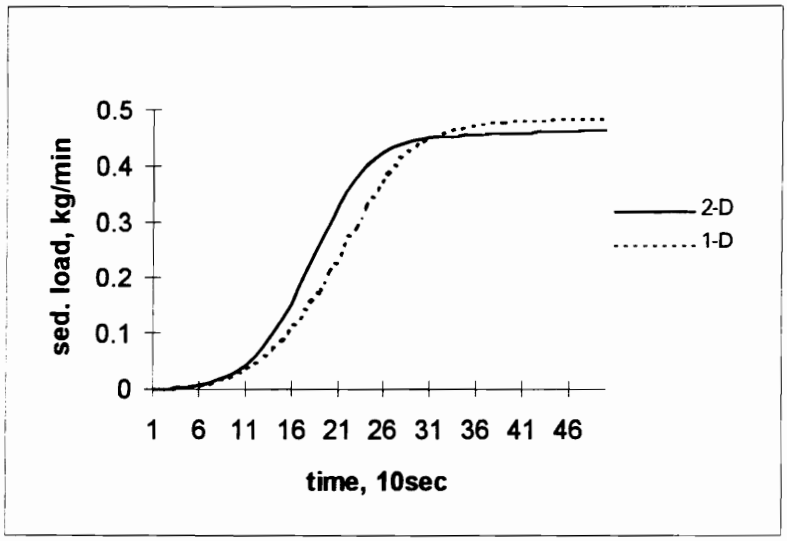

Figure 5-26. A comparison of sediment loading rate predicted by the 1-D and 2-D models for H505 (5% main and 0.5% cross slope)

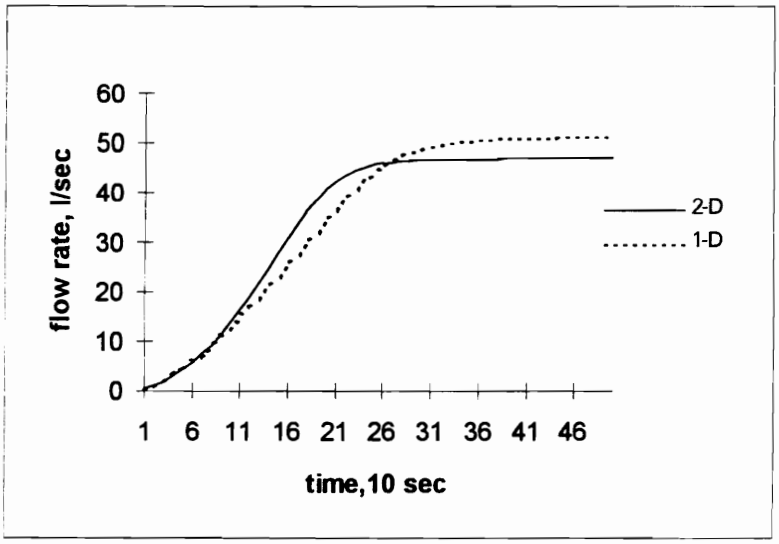

Figure 5-27. A comparison of runoff hydrograph predicted by the 1-D and 2-D models for H510 (5% main and 1.0% cross slope)

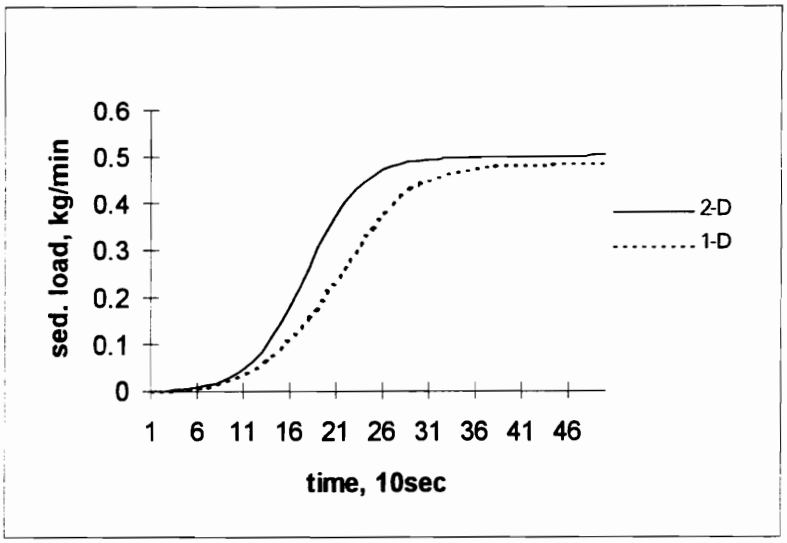

Figure 5-28. A comparison of sediment loading rate predicted by the 1-D and 2-D models for H505 (5% main and 1.5% cross slope)

Table 5-5. Comparison of 1-D and 2-D estimations for different slope conditions in the hypothetical study #3.

	model	H505	H510	H102	H103
main slope, (%)		5	5	1	1
cross slope, (%)		0.5	1	0.2	0.3
Peak flow, (l/s)	1-D	51	51	51	51
	2-D	47	47	47	48
Sed. load at	1-D	0.48	0.49	0.05	0.05
peak, (kg/min)	2-D	0.47	0.51	0.05	-
Total runoff	1-D	90	90	87	87
volume, (m^3)	2-D	83	83	80	83
Sed. yield, (kg)	1-D	13.7	13.8	1.25	1.27
	2-D	13.4	14.5	1.29	-
Average flow	1-D	1.66	1.66	2.26	2.27
depth.,(mm)	2-D	1.76	1.73	2.27	2.28
Average sed.	1-D	64	65	6.09	6.14
conc.(g/l)	2-D	65	62	5.91	-
Computation	1-D	5	5	5	5
time*, (min)	2-D	12	12	12	-

* On Sun workstation.

- not provided due to convergence problem.

Runoff and sediment transport processes were also compared in terms of average flow depth and concentration. As shown in Table 5-5, however, the average sediment concentration was not substantially different for the 1-D and 2-D simulations. For the run H102, the average concentration estimated by the 2-D model was only about 2% less than that predicted by the 1-D model. When the cross slope increased, the difference in model predictions increased. However, the magnitude of difference was still not significant. For the run H103, the difference in the average sediment concentration between the 1-D and 2-D model was 6%.

Runoff volumes and sediment yields at the plot outlet showed little differences between the 1-D and 2-D models. Even though much greater flow rates and sediment concentrations were estimated at the lowest elevation nodes of the outlet, the average values were not substantially different between the two models. In fact, other nodal points at the outlet showed much smaller flow rate and sediment concentrations compared to the lowest elevation nodes in the 2-D estimations. The results indicate that model estimations of total runoff volume and sediment yield at the outlet were not affected by the model dimension even though spatial distribution of flow depth and sediment concentrations were substantially different for the 1-D and 2-D models.

As the cross slope increased from 10% (H505) to 20% (H510) of the main slope, the 2-D model showed a slight increase in sediment concentration. The peak flow rate increased by only 1% while sediment concentration showed an 8% increase in the 2-D predictions. Meanwhile, the 1-D model showed little differences in its predictions. As the cross slope increased from 20% (H102) to 30% (H103), the peak flow rate by the 2-D model increased by 3%. However, little changes in the 1-D model predictions were observed. These comparison suggested that the 2-D model could simulate the changes in runoff and sediment transport processes due to the cross slope. In fact, the 1-D model did not show any significant changes in its predictions. In a quantitative measure, the effect of the cross slope on model predictions was not significant under the conditions presented in this case study.

The 2-D model required computational time over twice as much as the 1-D model. In addition, the 2-D model did not converge after thirty time steps when cross slope was 0.3% or 30 percent of the main slope of 1%. Therefore, it is difficult to justify additional computational cost and increased number of input parameters required from the 2-D model due to the insignificant differences between the 1-D and 2-D model predictions.

5.3.4 Hypothetical Case Study #4 : Effects of field size

The hypothetical case studies presented in the previous sections were for small fields with less than one hectare in size. There is a need to investigate if the differences in predictions between the models might be changed when the size of a field is larger. Therefore, another hypothetical case study was analyzed to investigate the effect of the size of a field on the model predictions.

In this case study, two fields were used to compared models' predictions: a small and a large field. The large field was generated using the topography of the small field.

5.3.4.1 Input Data and Computational Conditions

For the small field, a 48.8m x 24.4m area was used. The field had a 39% main slope as well as cross slopes ranging from 3% to 6%. Elevation was measured at 153 points in the field. The elevation points were used for the discretization of the model applications. The contour lines are shown in Figure 5-29.

A large field was generated using the topographic information of the plot shown in Figure 5-29. Each dimension was multiplied by 10, while keeping the same topographic conditions. Therefore, the large field was of 488m x 244 m with the same main and cross slopes. The field

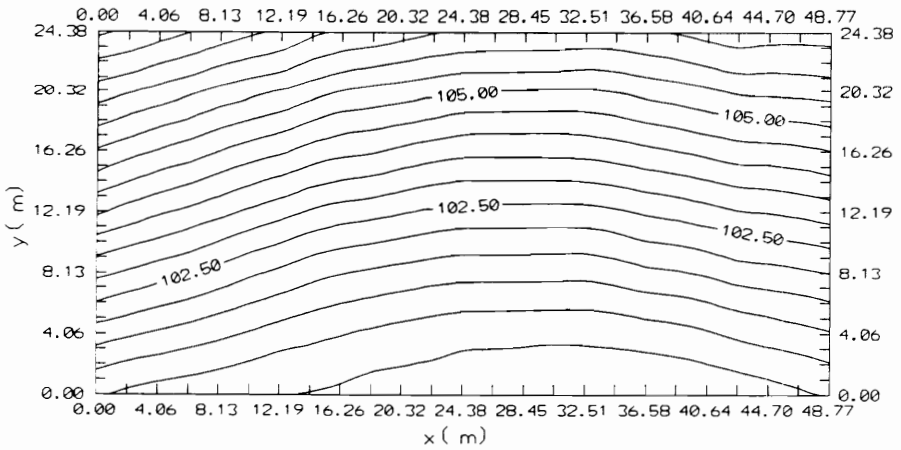

Figure 5-29. Contours of elevations for the hypothetical case study #4.

discretization was also performed with the same number of nodal points. Using the 153 nodal points, 136 and 256 element meshes were generated for the 1-D and 2-D models, respectively.

A rainfall rate of 18 mm/hr for 200 seconds was assumed for the small field. For the large field, a duration of 600 seconds were assumed for the same rainfall intensity. A time step of 10 seconds was used. The other soil and surface conditions were the same as those used in the hypothetical case study #3.

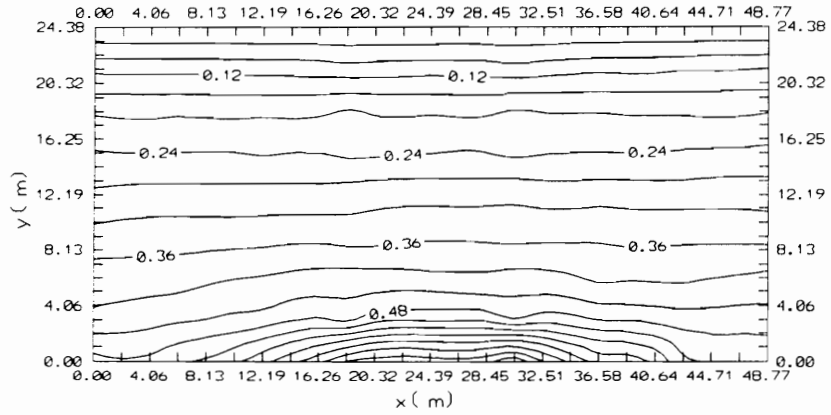

a) Flow depth (mm) distribution predicted by the 1-D model at 200th second

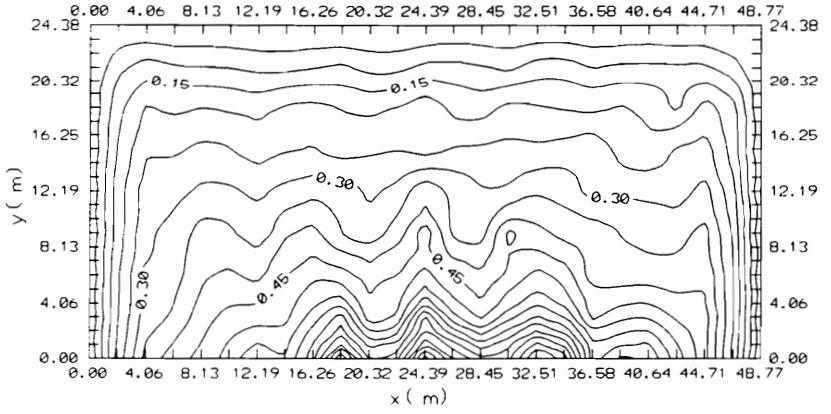

b) Flow depth (mm) distribution predicted by the 2-D model at 200th second

Figure 5-30. Contours for flow depths for the small field in the hypothetical case #4.

5.3.4.2 Results and Analysis

The contours for flow depths show the spatial distribution of models' predictions (Figure 5-30). Both 1-D and 2-D models simulated the increase in flow depth at the downstream area reasonably well. Even though the 1-D model could not simulate the flow convergence, the increase in flow depth at the outlet was well defined. Meanwhile, the contours of the 2-D estimated flow depths show more complex distributions than the 1-D results.

For both fields, the 2-D results showed that the equilibrium flow rate reached within the end of the duration. Meanwhile, flow rates predicted by the 1-D model continued to increase until rainfall stopped. The peak flow rate estimated by the 1-D model was 9% larger than that estimated by the 2-D model (Figure 5-31). Sediment loading at the peak flow rate was also 9% larger than the 2-D prediction. When the size of field was increased, the time to reach the equilibrium flow rate by the 2-D model was also increased (Figure 5-32). Unlike the small field, the peak flow rate predicted by the 2-D model was 8% larger than that estimated by the 1-D model.

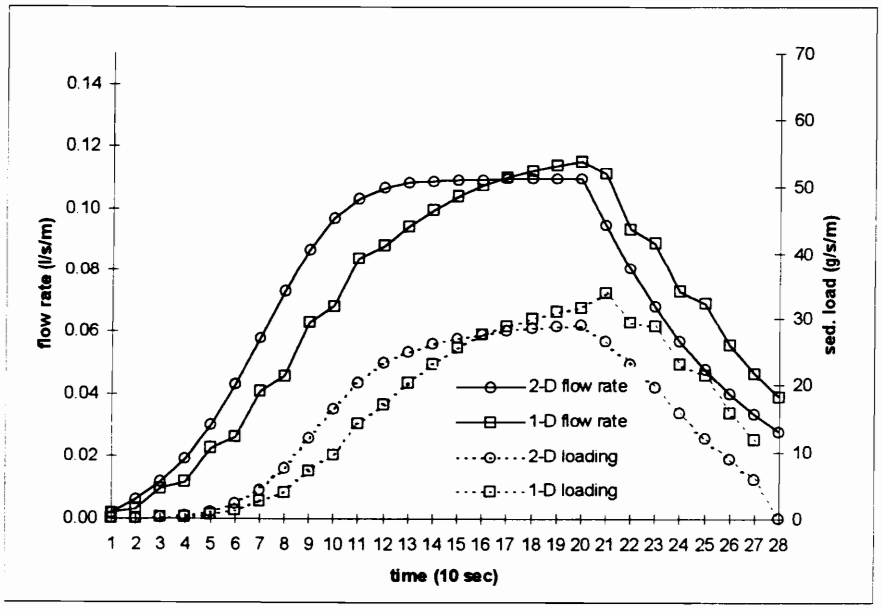

Figure 5-31. Comparison of flow rate and sediment loading for the small field.

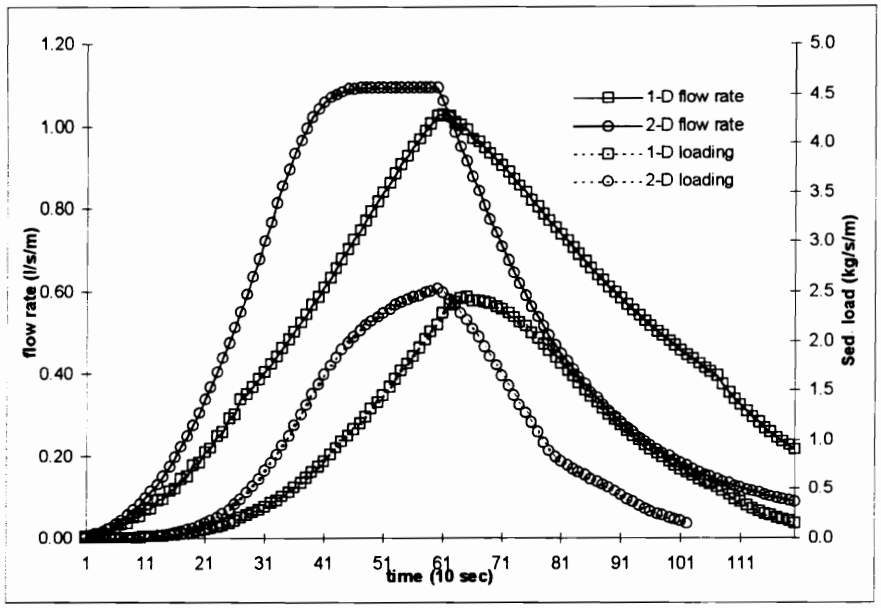

Figure 5-32. Estimated flow rate and sediment loading for the large field.

The differences in model's predictions between the 1-D and 2-D models were not affected by the field size. Models' predictions are summarized and compared in Table 5-6.

Table 5-6. Comparison of model predictions for different field size

	Small Field (0.12 ha)			Large Field (12 ha)		
	1-D	2-D	PD*	1-D	2-D	PD*
Peak flow (l/s/m)	0.12	0.11	9	1.02	1.10	8
Peak sed. load	31.7 g	29.0 g	9	2.16 kg	2.52 kg	15
Total runoff (m^3)	0.91	0.94	3	277	289	4
Sed. yield	214 kg	205 kg	4	518 ton	499 ton	4

* Percent difference between the 1-D and 2-D predictions (Equation 5-1)

As the field size increased, the differences in sediment loading rate at the peak flow were increased from 9% to 15%. However, the differences in total runoff volume remained the same level. The total runoff volume from the large field was about 300 times larger than that from the small field. The difference in runoff volume was due to the difference in the size of the plots and the rainfall duration. Meanwhile, total sediment yield from the large field was about two thousand times larger than that from the small field. This significant increase at the large field may be

explained by the fact that the topographic factor (LS) in USLE dramatically increases as slope length increases, particularly when slope is larger than 20% (Schwab et al., 1981). The slope used in this case study was 39% and the slope length was increased by 10 times.

The differences in the predictions of sediment yield between the 1-D and 2-D models also remained the same level of 4%, even though the size of field increased. Therefore, it could be concluded from this hypothetical case study that the size of field did not affect the differences in the models' predictions between the 1-D and 2-D models.

This hypothetical case study also showed that 2-D model reached the equilibrium flow rate before the 1-D model. When the field size increased, 1-D model did not show equilibrium flow rate while the 2-D mode showed a distinctive equilibrium flow rate after about 400 seconds.

5.3.5 Summary and Discussion of Hypothetical Case Studies

Four hypothetical case studies were investigated in this chapter. The objective of the first case was to investigate the effects of the element shapes on model predictions. The second and third cases were used to determine how cross slopes affected model predictions. The fourth hypothetical case study was to investigate the effect of field size on differences in model predictions.

Based on the results of the first hypothetical case study, no significant differences in model predictions were found between the 1-D and 2-D models when discretization level was the same. Even though the 1-D estimation of peak flow rate was affected by the choice of different element length, its effect on the 1-D model predictions could be ignored when discretization level was sufficient to reasonably describe the shape of the surface.

The second case study involved the investigation of the effects of cross slope. The cross slope was assumed to be zero, 1%, and 2% while the main slope was kept at 5%. The average flow rates resulted from 1% and 2% cross slopes at the outlet were about 23% and 14% less than those obtained from the 1-D uniform slope. The 1-D with no cross slope showed over 30% greater average sediment concentration than the 2-D estimations from the cross sloped areas.

The third case study was also related to cross slopes. This case study was included to investigate the effects of rather complex flow convergence due to the cross slope on model predictions. The spatial distributions of flow depth and sediment concentration estimated by the 2-

D model were significantly different from the 1-D results. The greater flow depths estimated by the 2-D model, for example, were located along the lower elevation points on the contour maps. The 1-D model did not simulate flow convergences along the lower elevation points.

The results of the second and third hypothetical case studies indicated that the effects of cross slope on runoff and sediment transport processes were not significant. Even though the ratio of cross slope to the main slope increased by up to 30%, the model predictions did not show substantial differences.

The fourth hypothetical case study indicated that the differences in predictions between the 1-D and 2-D models were not affected by the size of the field. With the same main and cross slope conditions, the differences in models' predictions were not changed when the field size increased from 0.12 to 12 ha.

No substantial differences were found in the predictions of runoff volume and sediment yield by the 1-D and 2-D models. Since runoff rate or sediment concentration is averaged at the outlet, the predictions between the 1-D and 2-D models were only slightly different. When cross slope was 10% to 20% of the main slope, differences in both runoff volume and sediment yield were less than 8% between the 1-D and 2-D approaches. The 2-D model required much more computational time compared to the 1-D model in solving the same problems. Moreover, the 2-D model frequently failed to converge due to negative flow depths. The hypothetical case studies did not show any improvements in predictions by the 2-D model compared to the 1-D model.

5.4 Field Applications

Both the 1-D and 2-D models were applied to real field situations in order to compare their predictions with the field measurements. For this purpose, two experimental data sets were chosen: one reported by Storm (1991) and the other by Dillaha et al. (1986). Storm (1991) performed a comprehensive soil erosion experiment including measurements of rill geometry before and after rainfall simulation. Field experiments performed by Dillaha et al. (1986) were on vegetative filter strips. The plots used in their experiments had 5 to 16% main slope as well as about 1% to 4% cross slopes. In both experiments runoff and sediment concentrations were measured.

5.4.1 Storm's Experimental Study

In his field study, Storm (1991) performed soil erosion experiments on the University of Kentucky Coldstream Farm. The field experiment included measurements of runoff and sediment concentrations under rainfall simulations. He also measured surface profiles using a surface profile meter which used pins to locate soil surface with a 1.27 cm spacing. The experiments were performed for two different soil types and two different surface treatments of smooth and rough conditions. The soil types were McAfee silt loam for top soil and Maury silty clay loam for subsoil condition. Two types of surface conditions were prepared : rough and smooth conditions. The smooth surfaces were created by roto-tilling and then hand raking cross slope with a garden rake. The rough surfaces were created by performing a one pass disking operation.

Each plot was 4.57 m wide and 22.1 m long, and was graded to have a uniform 8.7 percent slope. The plots were prepared to have minimal cross slope. However, the measured surface profile showed that local cross slopes existed. Surface cross section measurements were taken every 0.61 m in the main slope and 1.27 cm in the cross-slope direction. The rainfall intensity was 78 mm/hr in most cases with duration of either 90 or 120 minutes.

5.4.1.1 Input Conditions

The plots were discretized to have 80 nodal points each. To provide the same level of discretization for both 1-D and 2-D applications, the same number of nodal points was used. Out of a total of 12 experiments reported by Storm (1991), three topsoil conditions (T1R2, T1V2, and T2V2) were used in this study. Input parameter such as Manning's coefficient and saturated hydraulic conductivity were determined by the calibration based on experimental data (Storm, 1991) and a simulation study presented by Tayfur et al. (1993). Saturated hydraulic conductivity was calibrated for the 1-D model predictions using T1R2 observations (Table 5-7).

Input parameters could be calibrated based on either the 1-D or 2-D model prediction. When the 1-D model predictions are used for the calibration, the input parameters may not be the best choice for the 2-D mode and vice versa. Therefore, it seems worthwhile to investigate if any differences exist between the models' predictions rather than to find which model gives better or closer predictions to the observed data. In fact, a series of model calibrations showed that the differences in model predictions between the 1-D and 2-D model was not changed regardless of

which model's results were used for the calibration. For the plot T1R2, the differences in peak flow rate and total runoff volume between the 1-D and 2-D models were always 14% for different values of the saturated hydraulic conductivity. The input parameters are summarized in Table 5-7.

Table 5-7. Input parameters for Storm's experimental field plots

Run code	Surface treatment	Main slope, %	Cross slope, %	Rainfall intensity, mm/hr	Sat. hyd. conductivity, mm/hr	Manning's coefficient
T1R2	rough	8.7	< 0.5	78	6.7	0.013
T1V2	smooth	8.8	< 0.5	78	6.7	0.013
T2V2	smooth	8.7	< 0.5	79	6.7	0.013

For all simulations, the initial moisture content was assumed to be at saturation since these experiments were performed after initial rainfall applications. Boundary conditions for the 2-D runoff simulations were assigned to have zero flow depth and velocity. However, for these boundary conditions, negative flow depths were resulted after some time steps. Even though the cross slopes were very small, compared to the main slope of 8.7%, a number of nodal points resulted in negative flow depth, causing instability problems. For this reason, the nodal points which had negative flow depths were also assigned a very small flow depth of about 0.1×10^{-3} mm in T1R2 simulation. However, this non-zero flow depth assignment did not affect the 2-D model prediction. When the non-zero flow depth was assigned to those nodal points where negative flow depths developed, the flow rates were increased by just 1%, compared to that obtained by the simulation with the zero flow depth assignment.

For T1V2 and T2V2 simulations, surface profiles in cross slope directions were modified to have average slopes. The average slope was obtained by interpolation using elevation data along the cross slope. When the measured surface profiles were used, the solution did not converge due to the negative flow depths. This approach has also been used in simulating runoff processes by Tayfur et al. (1993). Tayfur et al. (1993) used the same data sets presented by Storm (1991) in evaluating their 2-D runoff simulation model. Figure 5-33 illustrates elevation distribution for plot T1R2. Even though there exist elevation changes in cross slope direction, the contour lines apparently do not show any topographic complexity.

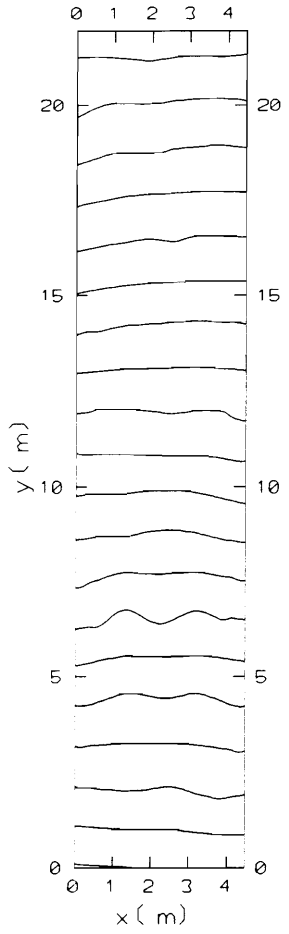

Figure 5-33. Elevation contour for T1R2 at 30th minute

5.4.1.2 Results and Discussions

While the elevation contour map for T1R2 does not show topographic complexity, the distribution of flow depths estimated by the 2-D model was significantly different from that predicted by the 1-D model (Figure 5-34). The contour maps presented in Figure 5-34 are for flow depths predicted at the 30th minute. The distribution of 1-D flow depth was rather uniform along the direction of slope and no flow convergence was found. The maximum flow depth was 1.2 mm in 1-D predictions while the 2-D model resulted in 2.5 mm due to the flow convergence. It is

notable that the flow depths estimated by the 2-D model were highly localized around the lower elevation points and over half of outlet area also showed flow depth less than 1 mm which was the typical value observed in the upstream nodes. The average flow depth at the outlet, however, was not substantially different between the 1-D and 2-D estimations. The average flow depth at the outlet was estimate to be 1.2 mm and 1.0 mm, respectively, for the 1-D and 2-D models. Even though the maximum flow depth in the 2-D prediction was about twice greater than the 1-D estimation, the difference in average flow depth was not significant between the 1-D and 2-D models.

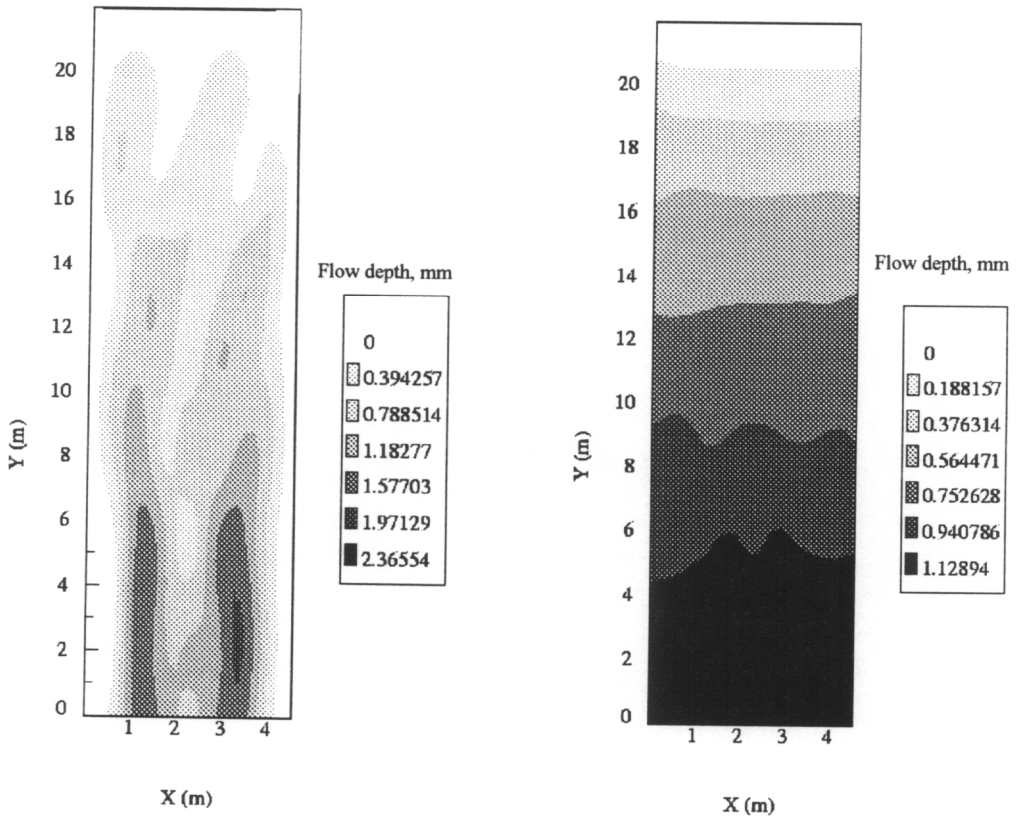

a) 2-D distribution

b) 1-D distribution

Figure 5-34. Flow depth distribution for T1R2

Figures 5-35 and 5-36 illustrate flow rate and sediment loading rate changes over time, respectively. With the calibrated saturated hydraulic conductivity, the root-mean-square differences between estimated and measured flow rates were 19.5 and 19.7 l/min for the 1-D and 2-D models, respectively As described in the previous section (5.4.1.1), the difference in the predictions between the 1-D and 2-D model was not changed regardless of which model was used for the calibration. For T1R2, therefore, the models were compared with respect to their differences in their predictions.

The model predictions for T1R2 indicated 15% differences in peak flow rate and 21% differences in sediment loading rate at the time of peak flow between the 1-D and 2-D models. The runoff volume and sediment yield for 90 minutes were also 15% and 26% different, respectively, between the 1-D and 2-D estimations. The 1-D estimated peak flow rate was about 15% greater than the value predicted by the 2-D model. Meanwhile, the 2-D estimation for sediment loading at the time of peak flow was about 20% greater than the 1-D model.

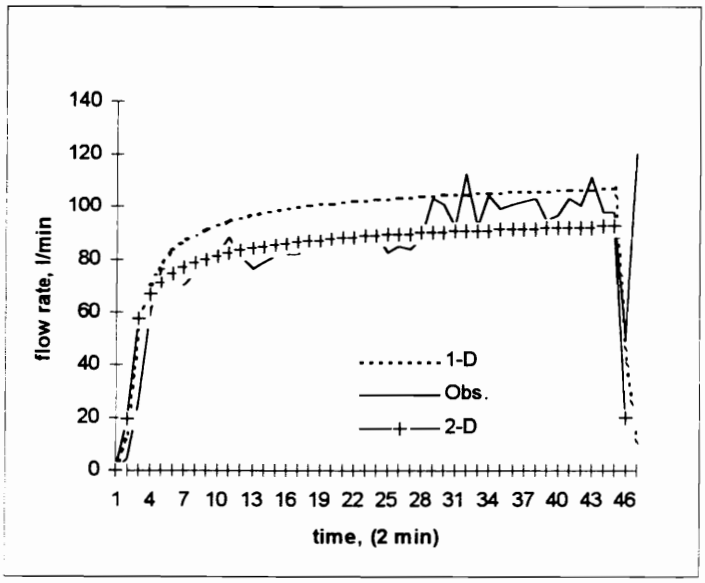

Figure 5-35. Runoff hydrograph for T1R2

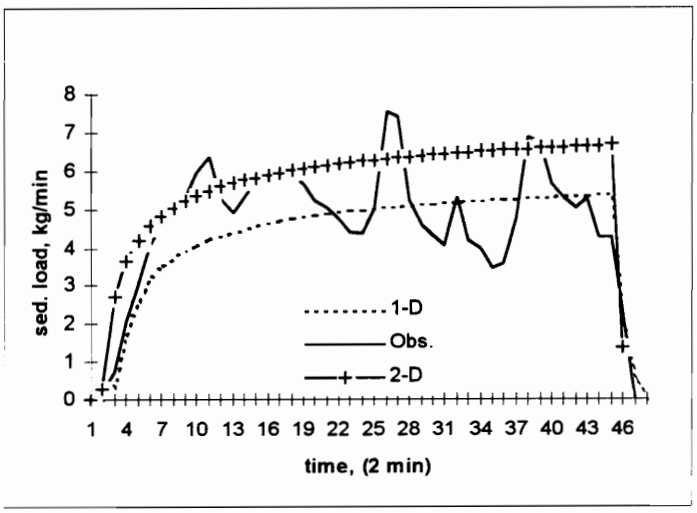

Figure 5-36. Time distribution of sediment loadings for T1R2

Simulation results for T1V2 indicated that the simulated peak flow rates were not substantially different between 1-D and 2-D. The difference was only 5%. The total runoff volume estimations for 125 minutes, by the 1-D and 2-D models, were about 28% and 20% greater compared to the observed value, respectively. Figure 5-35 shows that the estimated runoff rates by the 1-D and 2-D models were much greater than the observed in the rising limb of the hydrograph. Flow rate by the two models reached the peak more quickly than the observed one, thus resulting in a higher estimations of total runoff volume than observed by both 1-D and 2-D models.

The estimated sediment load rates were also higher than the observed values. The loading rates at the time of peak flow were 6.3 kg/min and 5.8 kg/min for 1-D and 2-D, respectively. These values are 47% and 35%, respectively, higher than the observed one. The total runoff volumes at the 125th minute were estimated to be 653 and 605 kg by the 1-D and 2-D models, respectively, which are about 36% and 26% higher estimations than the observed values. High fluctuations are observed in measurements of sediment concentrations while models' predictions indicate a rather steady concentration after about 30 minutes (Figure 5-37). No substantial differences in predictions of sediment concentrations existed between the 1-D and 2-D models.

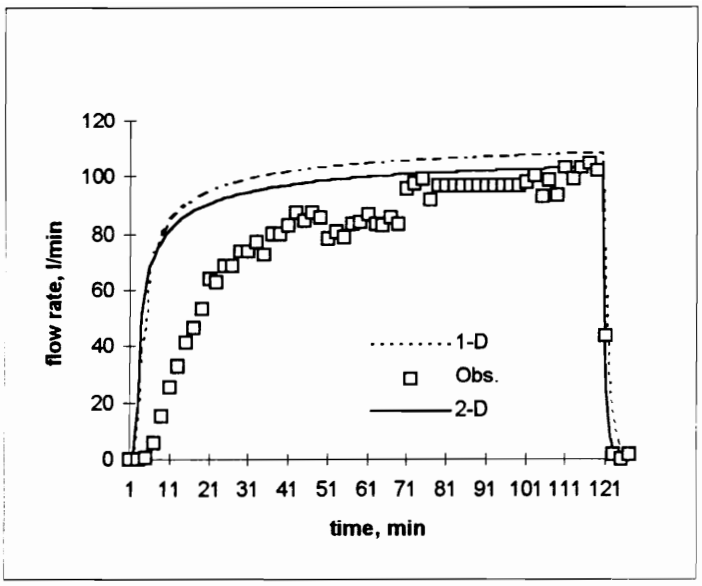

Figure 5-37. Runoff hydrograph for T1V2

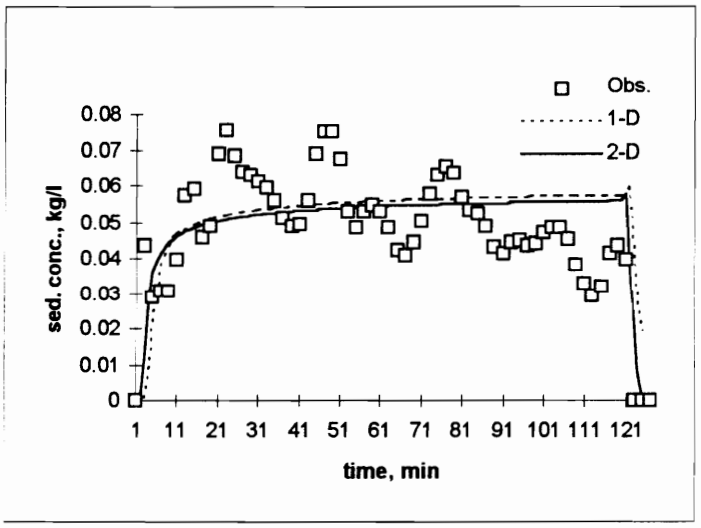

Figure 5-38. Sediment concentration changes for T1V2

Overall, the prediction for T2V2 run were very similar to those for T1V2. Both the 1-D and 2-D models overestimated total runoff volumes and sediment yield. Total runoff volumes at 125th minutes were overestimated by 20% and 21% and sediment yield by 67% and 72% by the 1-D and 2-D models, respectively. Figure 5-38 shows that the simulated flow rates by the two

models approached the peak quickly at the initial stage. For the first 20 minutes of simulation, therefore, runoff rates estimated by the models were higher than the observed values. Neither the 1-D and 2-D model simulated sediment transport processes very well. The observed sediment concentration shows a consistent decrease over time while model predictions by the both models indicate steady sediment concentrations, except during the initial stage of simulation (Figure 5-39). The observed sediment concentration decreased over the time while model predictions showed a consistent increase.

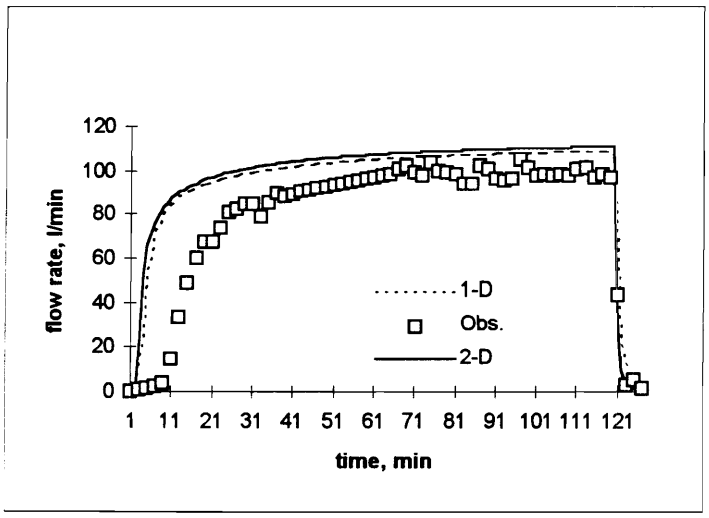

Figure 5-39. Runoff hydrographs for T2V2

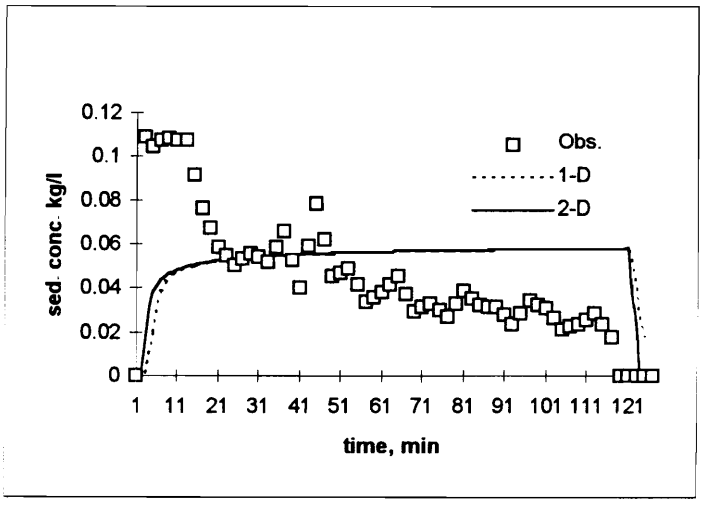

Figure 5-40. Sediment concentration changes for T2V2

Compared with T1R2 results, the model predictions for T2V2 showed less differences between the 1-D and 2-D predictions. One reason may be that the surface profiles were averaged for T2V2 runs rather than using the measured surface profiles. When original measurements of surface profile were used, the 2-D model did not converge. This suggests that the 1-D approach is computationally advantageous over the 2-D model. With the same level of information on a plot, the 1-D model could be applied easily without much difficulty while the 2-D model required additional pre-processing procedures to prevent convergence problems due to the development of negative flow depth. The total runoff volume and total sediment yield for 120 minute run resulted in 0.8% and 2.9% differences, respectively, between the 1-D and 2-D model predictions.

The models' applications to the experimental study presented by Storm (1991) suggested that no substantial differences in the prediction of runoff and sediment transport existed between the 1-D and 2-D simulations. The model predictions were compared and are summarized in Table 5-8. Similar to the results of the third hypothetical case study, estimations at the outlet showed little differences between the 1-D and 2-D simulations, even though spatial distributions of flow depth and sediment concentrations were substantially different.

When comparing total runoff volumes and sediment yields, no substantial differences could be found between the 1-D and 2-D models. Compared to the observed data, total runoff volumes were about 20% overestimated by the two models for both T1V2 and T2V2 (Table 5-8). Sediment yields were also overestimated by about 30% for T1V2 and 70% for T2V2. Considering these magnitude of overpredictions, the differences in model predictions between the 1-D and 2-D models could be negligible.

In spite of the differences in spatial distribution, average values of flow depths were the same for both T1V2 and T2V2. The average flow depth over the whole plot was the same for both models. Average sediment concentrations, meanwhile, showed 19.4% and 56% differences between the 1-D and 2-D models, respectively, for T1V2 and T2V2 (Table 5-8.

Table 5-8 Comparison model estimations and observations for different slope conditions in the field application # 1.

	Models	T1R2	PD*	T1V2	PD*	T2V2	PD*
Peak flow,	1-D	107.3	4.4	108.8	4.0	108.7	3.4
(l/min)	2-D	92.8	17.3	103.3	-1.2	110.7	5.3
	Obs.	112.2	-	104.6	-	105.1	-
Sed. load at	1-D	5.4	1.9	6.3	46.5	6.3	75.0
peak,	2-D	6.7	26.4	5.8	34.9	6.4	77.8
(kg/min)	Obs.	5.3	-	4.3	-	3.6	-
Total runoff	1-D	8.7	19.2	12.0	27.7	12.0	20.0
volume, (m^3)	2-D	7.5	2.7	11.3	20.2	12.1	21.0
	Obs.	7.3	-	9.4	-	10.0	-
Sed. yield, (kg)	1-D	397.5	4.4	653.5	35.7	659.4	66.8
	2-D	515.2	23.8	605.4	25.7	678.9	71.7
	Obs.	416.0	-	481.6	-	395.3	-
Average flow	1-D	0.79	-	0.79	-	0.79	-
depth.,(mm)	2-D	0.69	-	0.79	-	0.79	-
	PD_o	13.5	-	0.0	-	0.0	-
Average sed.	1-D	31.49	-	44.60	-	41.98	-
conc. (g/l)	2-D	34.11	-	36.73	-	23.61	-
	PD_o	8.0	-	19.4	-	56.0	-

PD* : Percent difference between the prediction and the observed data (PD=(Pre.-Obs.)/Obs.*100).
PD_o : Percent difference between the 1-D and 2-D predictions (Equation 5-1).

Another comparison for model predictions could be made between the two plots, T1V2 and T2V2. The main slopes were 8.8% and 8.7% for T1V2 and T2V2, respectively. Cross slopes were less than 0.5% for both plots. The two plots were not substantially different in terms of their topographic features. Table 5-8 indicates that the 1-D model predictions were nearly identical for the two plots. Total runoff volumes were estimated by 12 m^3 for both T1V2 and T2V2 by the 1-D model. Sediment yield estimations by the 1-D model showed just 0.9% difference between the plots. Meanwhile, the 2-D model showed greater differences in both total runoff volume and

sediment yield than the 1-D model. An 11.4% difference in sediment yields between T1V2 and T2V2 was shown by the 2-D model. It suggests that the 1-D model did not simulate changes in runoff and sediment transport processes due to the topographic changes inside the plots.

Compared with the observed values, the 2-D model did not show any improvements in model predictions over the 1-D model. Both the 1-D and 2-D model showed from 20 to 70% differences in model predictions from the observed data. However, the differences in model predictions between the models were not substantial. Based on the model applications to Storm's experiments (1991), it could be concluded that the 2-D approach did not provide substantial improvements in simulating runoff and sediment transport processes over the 1-D approach, even though the 2-D approach could simulate the changes in runoff and sediment transport processes due to the slight changes in elevation of the plots.

5.4.2 Vegetative Filter Strip Experimental Study

An experimental plot study conducted on vegetative filter strips by Dillaha et al. (1986) was used to demonstrate the applicability of the models in predicting BMP impacts as well as assessing their performance against field data. Nine field plots were prepared and a rainfall simulator was used in this study. The experimental field plots were constructed to have bare area and filter strip area. The bare area of each plot was 5.5 m wide and 18.3 m long (Dillaha et al., 1986). One plot in each set had no filter, another a 4.5 m filter, and the third had a 9.1 m filter. Three different main slopes were used. Soil type was Groseclose silt loam and orchard grass was used for the filter strip vegetation. Manure was later spread on the bare area that had previously been under no-till corn. Manure was applied to the plots at a rate of 7500 and 15000 kg/ha for two different experimental sets, respectively. The intensity of simulated rainfall was 50 mm/hr for a 30-minute duration. Runoff samples were collected every 3 minutes after the start of runoff to determine runoff rate and sediment concentration.

Two out of a total of three rainfall simulation runs were used in this study. Run 1 was used for calibrating saturated hydraulic conductivity and Run 2 was used for model applications (Table 5-9).

Table 5-9. Plot characteristics for filter strip simulations.

	Run 1		Run 2	
	QF5	QF6	QF2	QF3
Plot lenth, m	18.3	18.3	18.3	18.3
Filter length, m	4.6	0.0	4.6	0.0
Slope, %	16	16	11	11
Cross slope, %	0.7	0.7	0.7	0.7

5.4.2.1 Input data conditions

Filter strips were assumed to have larger values of Manning's coefficient and greater resistance against both splash and hydraulic erosion. Ninety six node meshes were used for no-filter simulation but additional finer meshes were provided around the boundary between filter strip and upstream area because of numerical oscillations due to the discontinuity of element characteristics. When mesh size of about 1 m was used in a uniform mesh net, stable solutions could not be obtained. The data collected from Run 1 was used for model calibration. Zero boundary conditions were assigned to upstream boundary nodes. Since the plots had cross slopes, additional boundary conditions were necessary for the 2-D applications. Runoff flowed down to a side border which was installed to separate other plots. Therefore, nodal points located on the border were also assigned to have zero flow velocity in cross-slope direction. The input parameters obtained from calibration of both bare and the filter strip plots are summarized in Table 5-10. A large value was assumed for the fall velocity of soil particle in order to represent the increased deposition of soil particles. The rate coefficient for deposition was represented by a function of fall velocity of soil particle and flow depth in this study.

Table 5-10. Input parameters used in simulation of filter strips.

Parameters	Bare field	Filter strip
Sat. hydraulic conductivity, K_s	18 mm/hr	18 mm/hr
Init. soil moisture	saturation	saturation
Manning's n	0.013	0.053
Fall velocity, m/s	5.1 E-8	5.1 E-8 <

5.4.2.2 Results and Discussion

The observed data indicated that 4.5 m filter strips with 16% and 11% slope resulted in reductions of 72 % and 75%, respectively, in total sediment loadings, compared to the plots with no filter strips.

The 2-D model estimated both runoff and sediment losses reasonably well (Figures 5-40 and 5-41). Simulation results also showed that flow depth increased by over 70% on the filter strip area while velocity decreased by about 50% compared with those at the outlet area of the plot with no-filter strips (Figures 5-42 and 5-43). The filter strip was represented in the model by changing Manning's coefficient and reduction factors which control erosion rates by rain drop or runoff flow. The reduction in sediment loading by filter strips could be due to surface protection from rainfall or runoff as well as retardation of runoff flow by the vegetation. Sediment concentration was reduced by over 60% due to the installation of the vegetative filter strips (Figure 5-44). The observed sediment concentrations showed high fluctuations over time (Figure 5-45).

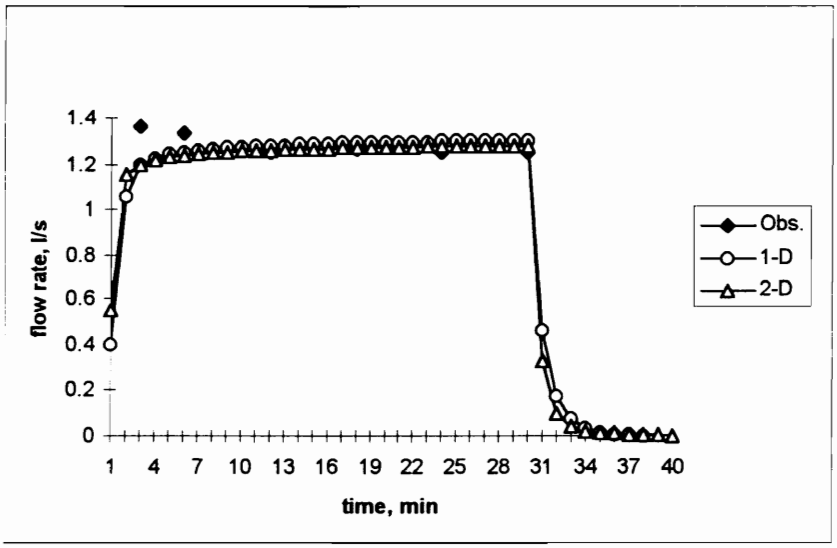

Figure 5-41. Comparison of hydrographs for QF3.

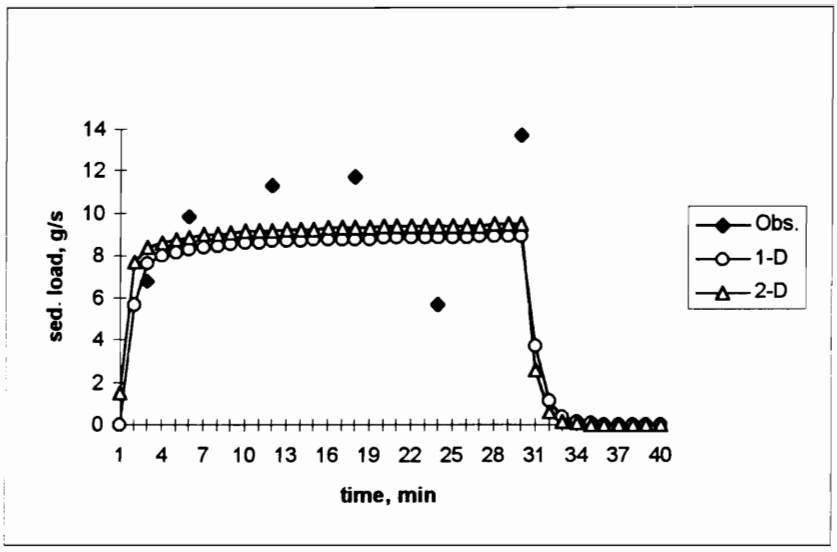

Figure 5-42. Comparison of sediment loading rates for QF3.

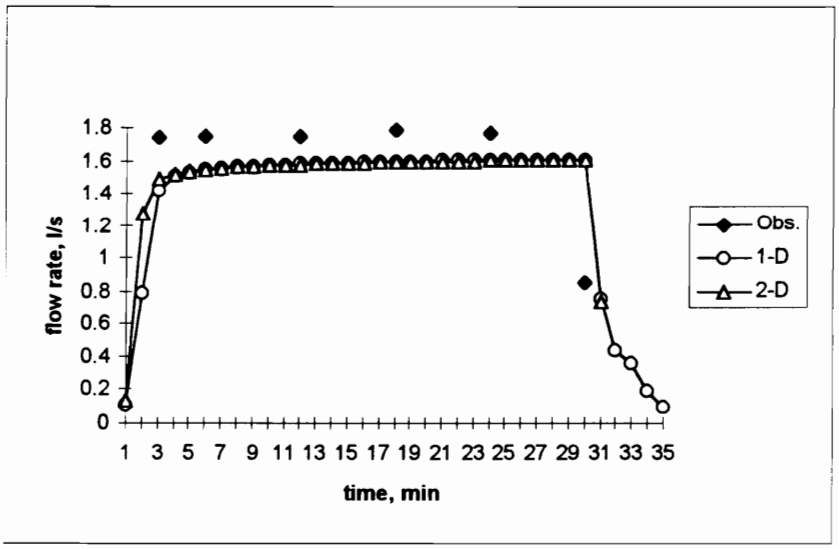

Figure 5-43. Comparison of hydrographs for QF2.

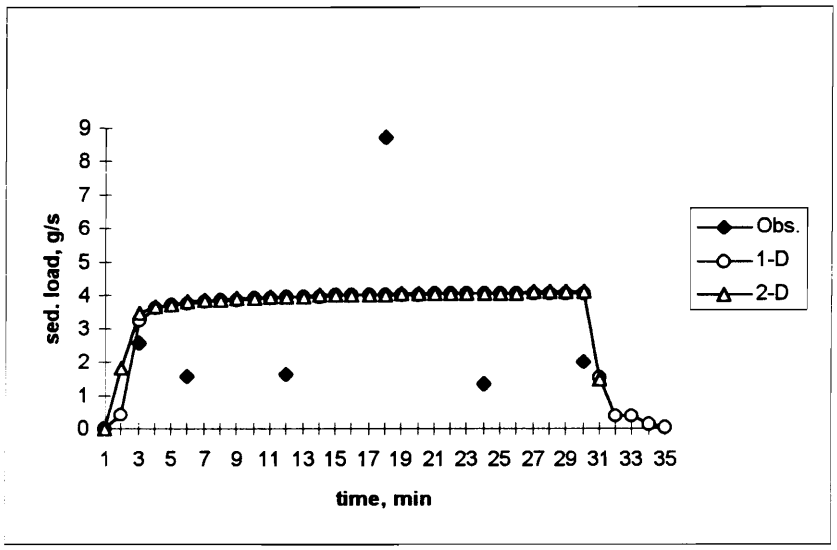

Figure 5-44. Comparison of sediment loading rate for QF2.

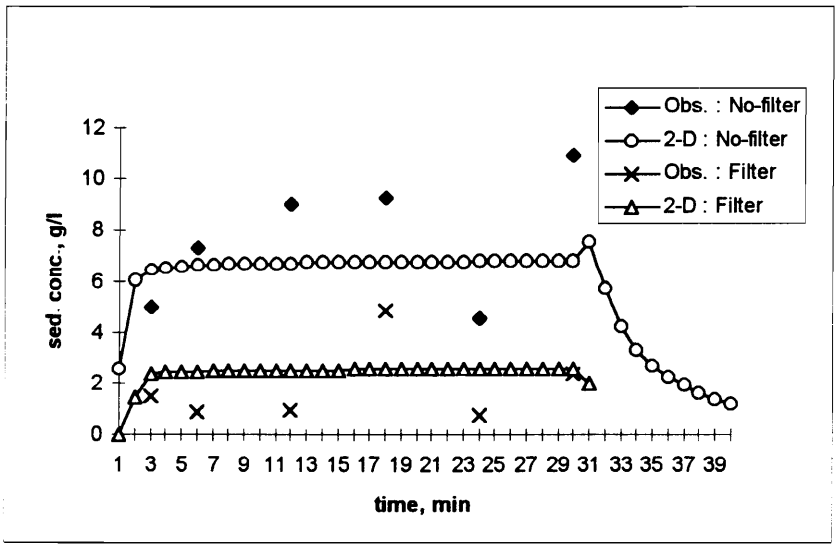

Figure 5-45. Sediment concentration changes between filter and no-filter fields.

There were no significant reductions in runoff volumes due to installation of filter strips. The simulation results indicated that filter strips provided less than 1% reduction in depth of runoff volume compared to no-filter plots. The observed field data presented by Dillaha et al.

(1986) also did not show any consistent reductions in runoff volume due to installation of filter strips. Sediment yields from filter strip plot were 6.6 and 6.8 kg for the 1-D and 2-D models, respectively, about 55% less than those from no-filter plots (Table 5-11). The observed sediment yield from filter strip plot was 4.2kg which was 25% of the sediment yield from the no-filter strip.

Table 5-11. Comparison of model predictions of the impact of filter strips on runoff and sediment losses.

	model	No-filter	Filter
Peak flow, (l/s)	1-D	1.3	1.6
	2-D	1.3	1.6
	Obs.	2.2	1.8
Sed. load at peak, (g/s)	1-D	8.9	4.1
	2-D	9.4	4.1
	Obs.	8.5	2.2
Total runoff volume, (m^3)	1-D	22.3	21.6
	2-D	22.4	21.8
	Obs.	20.1	22.7
Sed. yield, (kg)	1-D	14.9	6.6
	2-D	15.0	6.8
	Obs.	16.6	4.2

Under the field conditions presented in this study, there were no significant differences in predictions between the 1-D and 2-D models. The consideration of 0.7% cross slope in the 2-D simulation had little effect on runoff and sediment transport processes. Even though the 2-D model produced a maximum flow rate of 0.5 E-3 m^2/s at an outlet node, which was twice greater than the 1-D estimation, the average flow rates were the same for both models. Sediment concentration also showed similar variations. That is, flow convergence simulated by the 2-D model did not affect overall sediment transport processes.

5.4.3 Summary and Discussions of Field Applications

Two different field studies were used to compare the models' ability in simulating runoff and sediment transport processes. Soil erosion experiment performed by Storm (1991) and a vegetative filter strip study reported by Dillaha et al. (1986) were used. Since Storm's experimental study provided extensive measurements of surface profiles, detailed elevation could be used in the model applications. For the model applications for the vegetative filter strip study,

meanwhile, elevations were generated using slopes since elevation data inside the plot was not reported.

In applying the 2-D runoff model to Storm's field experiments, convergence problems limited the models' applications. Simulation of plot T1R2, which was used for input parameter calibration, used actual surface profiles for elevation information. For the other two plots, T1V2 and T2V2, average cross slopes were used because of the difficulty in obtaining stable solutions. For T1R2, total runoff volume and sediment yield for 90 minutes showed 15% and 26% differences, respectively, between the 1-D and 2-D predictions. Both T1V2 and T2V2 runs showed no differences in predictions between the 1-D and 2-D models. Runoff processes were simulated well but sediment transport processes were overestimated by both models. For T2V2, estimated runoff volumes for a duration of 125 minutes by the 1-D and 2-D models were 20% and 21%, respectively, larger than the observed values. The observed sediment yields were also overestimated by 67 and 72% by 1-D and 2-D models, respectively. As shown in the hypothetical case studies, in spite of different spatial distribution of flow depth and sediment concentration between the two models, the model predictions were not substantially different from each other.

Model estimations for field experiments performed by Dillaha et al. (1986) also showed only slight differences between the 1-D and 2-D models. Consideration of 0.7% cross slope in 2-D simulations had little effects on both runoff and sediment transport processes.

A major limitation in model applications may be that the fields used in both hypothetical and experimental studies were small in size and rather uniform with minimum spatial variability. As the field size increases, more spatial variability could be expected. Therefore, a larger difference in model predictions may be expected between the 1-D and 2-D models, particularly when runoff flow converges on the highly erodible areas of a field as an extreme case. In this case, the differences in sediment loading between the two models could be much larger than those found in the hypothetical cases or experimental studies presented here, since the 1-D model do not simulate flow convergence due to cross slopes. However, this study did not include those extreme cases but dealt with the effects of cross slopes, discretization level, and field size, on the differences in model predictions between the 1-D and 2-D models for small overland areas.

5.5 Summary and Conclusions

In this chapter, the 1-D and 2-D models were applied to four hypothetical case studies and two field experiments to investigate the differences in their estimations of runoff and sediment transport. The hypothetical case studies were performed to study the effects of element size, the existence of cross slopes, and the size of field. It was found that both the 1-D and 2-D models resulted in similar estimations at the same level of discretization. When cross slope was 1% and 2% with the main slope of 5%, the 2-D prediction resulted in 23% and 14% less average peak flow rates than the corresponding 1-D estimations. The 1-D prediction which did not consider cross slope showed 30% greater average sediment concentration than the 2-D cross slope estimations. The third hypothetical case study suggested that average models' predictions at the outlet between the 1-D and 2-D were slightly different even though there existed significantly different spatial distributions of flow depth and sediment concentrations. The 2-D model simulated the spatial distribution of flow depth well along the generated flow paths. The 2-D runoff volume and sediment yield predictions, however, were not substantially different from the 1-D estimations. The fourth hypothetical case study showed that the differences in model predictions between the 1-D and 2-D models were not affect by the change in field size.

The model applications to field experiments also supported the conclusions derived from the hypothetical case studies. Simulation results for Storm's (1991) experiments also showed significantly different spatial distribution in flow depth and sediment concentration, but runoff volume and sediment yield were about 13% and 26% different, respectively, between the 1-D and 2-D models. However, the convergence problem due to negative flow depths limited the 2-D model applications to the field plots. When the average slope was used to overcome computational difficulties, model predictions between the two were nearly the same.

Based on the hypothetical case studies and field applications, the differences in models' predictions in both runoff volume and sediment yield were approximately 20%. In most cases, no substantial differences in prediction were found between the 1-D and 2-D models. Field application results showed that both the 1-D and 2-D models overestimated runoff volume and sediment yield.

Model application results showed about 30% maximum differences in predictions between the 1-D and 2-D. Meanwhile, the 2-D model resulted in 10 to 20% differences in model

predictions when different boundary conditions were used. The 1-D model predictions were also affected by the choice of element length and its geometry. In this context, the differences in total runoff volume and sediment yield at the outlet, shown in the hypothetical and experimental case studies, could not be considered significant. Meanwhile, the 2-D modeling approach could be advantageous over the 1-D model in identifying critical areas where higher concentration of sediment and other associated pollutants was expected. The 2-D model predictions simulated flow convergences and resulting high concentrations along the lower elevation region due to the cross slope, reasonably well.

Throughout the model applications, the 2-D results showed higher flow rates during the rising limb of hydrograph when cross slopes existed. In addition, the 2-D model reached the equilibrium flow rate before the 1-D model, in most cases where cross slopes existed. This early reach of equilibrium flow rate could mean that the 2-D model simulated runoff processes along the steepest paths to the outlet. Meanwhile, the 1-D model simulated runoff processes along the strips defined by the main slope. The strips could not be actual flow paths when cross slopes existed. Even though cross slopes were very small, the downstream nodal points, defined by the main slope, could not be the lowest elevation points in the surrounding nodes. Therefore, the 1-D model required more time to reach the equilibrium flow rate.

The 2-D model required more computational time and additional computational efforts, particularly when the solutions did not converge. For the cases investigated in this study, the 2-D model did not provide significant advantage over the 1-D approach in predicting runoff and sediment at the outlet. However, the 2-D model gave better representation of spatial distributions of flow depth and sediment concentrations.

6. SUMMARY AND CONCLUSIONS

The goal of this study was to investigate whether the 2-D modeling approach could improve the predictions of runoff and sediment transport processes over 1-D approach. Both the 1-D and 2-D simulation models were developed to accomplish the objective. The models were formulated to provide the same mathematical representation of physical processes of runoff and sediment transport. Runoff processes were described by the St. Venant dynamic equations which consisted of the continuity and momentum equations. Runoff and sediment transport processes were simulated only for overland processes, excluding channel processes for which the 1-D approach was considered sufficient. Sediment transport was described based on the continuity relationship. Source and sink terms in the sediment transport model were evaluated by the procedures presented by Woolhiser et al. (1990), which included splash and hydraulic erosion by rainfall and overland runoff, respectively.

The finite element method was used to solve the governing equations for both runoff and sediment transport processes. The linear triangular element was used as the interpolation function for the 2-D model, and the linear line element was employed for the 1-D model. The finite element method based on the interpolation functions was used to solve the governing equations for both runoff and sediment transport processes. The finite element formulation resulted in a discrete system of equations. The system equation for runoff process became nonlinear since the stiffness matrix included dependent variables such as flow depth and velocity. A substitution method was used to solve the nonlinearity. A value of less than 1.0 was used for the over-relaxation factor. For time differences, the implicit method was used. Stability analysis was performed based on the linearized system. Discrete Fourier method was employed for this analysis. The linearized system was unconditionally stable regardless of the discretization level. However, model application could be limited depending upon field conditions because the actual system was nonlinear.

The models were tested using the data reported in the literature. For testing runoff models, the Izzard method (Chow, 1959) was used. Results showed that both the 1-D and 2-D models

provided good estimations of runoff. When discretization level was the same for both the 1-D and 2-D meshes, models' predictions were almost identical. In fact, the overland area used for this comparison had a 1-D slope with no cross slopes. Therefore, no differences in model predictions were expected between the 1-D and 2-D models. Meanwhile, the 2-D estimations showed a certain type of oscillation due to the shape of elements. The 2-D runoff estimations varied corresponding to the element connectivity. The oscillation problem was unique in triangular meshes since the solutions obtained by quadrilateral meshes did not show this oscillation. However, the oscillation problem could be considered to be negligible in terms of accuracy of the results. Only about 1% of difference in model predictions could be attributed to the orientation of meshes.

The analytical solutions obtained by Singh and Regl (1983) and Singh (1983) were also used for model evaluation. Their analytical solutions were based on the method of characteristics for both runoff and sediment transport. Since the governing equations used for runoff and sediment transport were different from those presented in this study, the input parameters were changed so that the same steady solution for simple cases could be obtained. The simulation results showed that both the 1-D and 2-D models estimated runoff processes reasonably well. The analytical solutions for runoff reached the steady state faster than those by the simulation models. Sediment transport estimation varied depending upon the choice of sediment transport capacity equation. When a transport capacity relationship similar to Singh and Regl's (1983) was used, model predictions were closer to the analytical solutions than any other transport capacity equations. The results of the models' evaluation indicated that both the 1-D and 2-D models performed appropriately and simulated runoff and sediment transport processes reasonably well.

Sensitivity analysis was performed to investigate the models' characteristics. Since this study was intended to compare the 1-D with 2-D models in terms of their prediction of hydraulic characteristics and sediment transport, the parameters related with only runoff processes were used for the analysis. The results indicated that the hydraulic conductivity and a parameter related with initial moisture content were most sensitive to total runoff volume and peak flow rate. Manning's roughness coefficient and slope slightly affected the runoff volume and peak rate. Compared to the runoff estimations, sediment loading was more sensitive to these parameters. The most sensitive parameter for estimation of sediment loading was the Manning's coefficient. About 20 percent change in the loading was resulted from over 30 percent changes in the coefficient.

After the model testing and sensitivity analysis were completed, the models were applied to three different hypothetical case studies and two field experiments to investigate the differences in predictions by the 1-D and 2-D models. The first hypothetical case study was conducted to evaluate the effects of the element shapes on the model predictions and the second and the third case studies investigated the impact of various cross slopes on simulation results.

The results of the first case study suggested that the 1-D simulation could be affected by the selection of representative flow length when it was difficult to describe the element by rectangles. However, model predictions did not show significant differences between the 1-D and 2-D when discretization level was sufficient. In particular, sediment concentration was not affected by the choice of the element length in 1-D. The second hypothetical case study investigated the effects of cross slopes on the 5% main slope. The 2-D estimated average flow rates at the outlet from 1% and 2% cross slope areas were, respectively, 23 and 14 percent less than those obtained from the 1-D model which did not consider cross slopes. The 1-D model, however, predicted an average sediment concentration which was over 30% greater than the value estimated by the 2-D model. When the path of lower elevation points was not parallel to the main slope, as in the third hypothetical case study, spatial distribution of flow depth and sediment concentrations were significantly different between the 1-D and 2-D models. The 2-D model simulated the increase in flow depths and sediment concentrations reasonably well along the lower elevation points. The 1-D model results did not show the localization of the increase in flow depths or sediment concentrations. That is, 1-D approach could not simulate the changes in runoff and sediment transport processes due to the cross slope. However, models' predictions at the outlet were not substantially different from each other, as expected from the spatial distribution of flow depth and sediment concentrations. Even though higher sediment concentrations and flow depths were predicted at the lower elevation nodes by the 2-D model, the average values at the outlet were almost the same as those estimated by the 1-D model.

Field experiments were also used to investigate the differences in models' predictions. Storm's (1991) soil erosion experiments provided detailed surface profiles so that real field processes could be simulated and compared with the observed data. When the actual surface profiles were used, however, convergence problems limited the 2-D model applications due to negative flow depths. Additional conditions were assigned to the nodes at which negative flow

depths resulted. Therefore, average surface profiles were used for model applications to the other plots.

When the original profiles were used (T1R2), spatial distribution of flow depths and sediment concentration was significantly different between the 1-D and 2-D models. Even though the elevation contour map did not show any possible flow paths with lower elevation, the 2-D prediction showed notable flow convergences. Greater sediment concentration was also estimated along the path with greater flow depths. Meanwhile, flow rate and sediment loading at the outlet were not substantially different between the 1-D and 2-D models, which is similar to the results of the third hypothetical case study. When the average slopes were used (T1V2 and T2V2), the differences in model predictions between the 1-D and 2-D approaches became much smaller.

Model predictions for vegetative filter strip experiments also showed similar results to the Storm's erosion experiments. The 0.7% uniform cross slope considered in the 2-D estimations did not affect overall model predictions. Both runoff volume and sediment yield did not show any significant differences between the 1-D and 2-D predictions.

Model application results showed about 30% of maximum differences in predictions between the 1-D and 2-D. Meanwhile, the 2-D model resulted in 10 to 20% differences in model predictions when different boundary conditions were used. The 1-D model predictions were also affected by the choice of element length. In this context, the differences in total runoff volume and sediment yield at the outlet, shown in the hypothetical and experimental case studies, could not be considered significant.

Meanwhile, the 2-D modeling approach is advantageous in locating critical areas where higher concentration is expected, compared to the 1-D model. 2-D model predictions simulated flow convergences and resulting high concentrations along the lower elevation region due to the cross slope reasonably well.

Throughout the model applications, the 2-D results showed higher flow rates in the rising limb of hydrograph when cross slopes existed. In the field application to Storm's experiments (1991), 2-D estimated flow rates were slightly larger than those by the 1-D model in the rising limb of hydrograph even though equilibrium flow rate predicted by the 1-D model was higher than that by the 2-D model. The 2-D model reached the equilibrium flow rate before the 1-D model, in most cases where cross slopes existed. This early reach of equilibrium flow rate in the 2-D model could mean that the 2-D model simulated runoff processes along the steepest paths to the outlet.

Meanwhile, the 1-D model simulated runoff processes along the strips defined by the main slope. The strips could not be actual flow paths when cross slopes existed. Even though cross slopes were very small, the downstream nodal points defined by the main slope could not be the lowest elevation points in the surrounding nodes. Therefore, the 1-D model could require more time to reach the equilibrium flow rate.

With regard to the computational costs, the 1-D model was overwhelmingly advantageous over the 2-D approach. The computational time for the 2-D model application was over twice longer than for the 1-D model. Each nodal point in the 2-D runoff model has three unknowns while the 1-D model has two. When the number of nodal points is the same, therefore, the 2-D runoff model has 1.5 times more number of unknowns that the 1-D runoff model has. In addition, overland areas can be discretized with less number of nodes in 1-D meshes than 2-D since 2-D discretization requires area elements. For the same overland area, therefore, the 2-D model requires much longer computational time.

Another computational shortcoming of the 2-D model is that its applications were often limited by convergence problems when surface profile was complex. When solution did not converge, additional processes, such as generation of average slope or additional boundary conditions, were required by the 2-D model.

In summary, the following conclusions could be made based on models' application results of hypothetical case studies and field experiments in this study:

1. When sufficient discretization level was used to reasonably describe the actual surface shape, the 1-D model predications were not affected by the element shape even though overland area was difficult to describe by rectangular elements. The simulation results were not significantly different between the 1-D and 2-D models for the same level of discretization.

2. The 2-D estimations of runoff and sediment yield with cross slopes of 20% and 40% of the main slope were slightly less than the 1-D model results with no cross slopes. However, these differences were not significant since the 2-D model resulted in 10 to 20% differences in model predictions when different boundary conditions were used and the 1-D model predictions were also affected by the choice of element length.

3. When cross slopes existed, the 2-D model predicted spatial distribution of flow depth and sediment concentration along the area of lower elevations . However, quantitatively speaking, there were no significant differences in model predictions for total runoff volume and sediment yield between the 1-D and 2-D models. Both hypothetical and field experimental applications indicated that model predictions at the outlet were almost identical between the two approaches even though the 2-D model provided substantially different spatial distribution of flow depth and sediment concentration from the 1-D. Therefore, it could be concluded that detailed representation of local hydraulic characteristics achieved by the 2-D model did not improve model predictions of total runoff volume and sediment yield at the outlet.

4. Compared with the 1-D model, the 2-D model required much more computational time and effort to simulate the same problems. In addition, convergence problems due to negative flow depths limited the 2-D model applications. The 2-D simulations required more than twice the computational time needed for the 1-D simulations. For predicting the sediment yield and runoff volume at the outlet, much greater computational costs and efforts could not justify the use of the 2-D approach over the 1-D model.

5. For the conditions investigated in this study, the 2-D model did not provide any significant benefit compared with the 1-D model, in predicting runoff volume and sediment yield at the outlet. However, it is expected that the 2-D model would be beneficial for applications where spatial variability is significant.

7. Recommendations for Future Studies

There were several limitations in applying the models, developed in this study, to various situations because of the convergence problems. In many cases, the 2-D model did not provide the solutions since negative flow depths were developed. Therefore, the following recommendations are suggested :

1. In formulating the governing equations for runoff flow processes, different sets of dependent variables could be used. Flow velocity and depth were used in this study. Alternative variables include flow rate and elevation of water surface. When the elevation of water surface is used as a dependent variable, it may include surface topography. Cunge et al. (1980) pointed out that one choice of dependent variables is advantageous to the other in terms of its numerical integration and accompanying computational errors.

The overland runoff characteristics are quite different from river or channel flow situations. Overland runoff flows are assumed as sheet flow and the flow depth is shallow. Two-dimensional representation of fields could result in convex areas in which flow depth is close to zero. Therefore, modeling approaches used in simulating estuary or lake processes may not be valid for overland runoff simulations. In the concave area, the basic assumptions of the continuity and momentum equations will not hold. Shock wave could occur in the concave area, where dependent variables are not continuous any more.

The convergence problems are reported by many studies dealing with the 2-D simulation of overland runoff processes (Zhang and Cundy, 1989; Tayfur et al., 1993). Zhang and Cundy (1989) used extremely small time steps of 0.001 seconds and Tayfur et al. (1993) employed average slope rather than using the actual topography to overcome the convergence problems. Therefore, it is recommended to investigate which set of dependent variables is advantageous to others in simulating overland runoff processes as well as related computational characteristics. Such investigation would help simulate runoff processes on more complex topographic conditions.

2. The digital information tools can provide enormous amount of geographic information which is required in simulating runoff and NPS pollutant transport. In addition, they have

functions to help with watershed discretization and division of subsheds. One example of coupling runoff simulation model with a geographic information system is the study presented by Vieux (1989). The study showed that a function in ARC/INFO, a vector based geographic information system, could be used in watershed discretization for runoff simulation. The function employed in his study was the triangular irregular network (TIN), a digital elevation model. The study showed a possibility of incorporation of simulation model with digital information system.

However, the 2-D modeling approach requires much more computational costs that the 1-D as shown in this study. In addition, the 2-D model does not provide any significant improvements in estimating runoff and sediment transport compared to the 1-D results. Therefore, it is recommended that the 1-D model be used for simulating runoff and sediment transport. It seems desirable that the 1-D model be coupled with digital information tools in preparing model input data such as discretization of fields or watersheds.

3. Sophisticated numerical tools are being used in simulating runoff and sediment transport. The finite element method was used in this study. The finite difference method is also frequently used. Any numerical technique is expected to produce reasonable results. In most cases, at least the second order of error rate is required (Sod, 1984).

However, a major problem in simulating runoff and sediment transport is that accurate determination of input parameters is difficult. The sensitivity analysis and model applications indicated that input parameters such as roughness coefficient and saturated hydraulic conductivity affected the model predictions. Even though the numerical scheme is highly accurate and could provide the exact solutions, the difficulties in determining the input parameters could prevent improvement in model predictions. In other words, when the accuracy of determination of input parameter is of the first order of error rate, the accuracy of model predictions is also of the first order even though the numerical scheme has the second or higher order of error rate.

Input parameters and relationship which determine soil erosion rate and sediment transport capacity are more empirical and affect the accuracy of model predictions. In addition, most currently available relationships for the sediment transport capacity were developed under the stream flow conditions. Therefore, improvement in model predictions of sediment transport could be achieved by providing improved relationship for soil erosion and sediment transport processes and better determination of the related parameters.

REFERENCES

Akan, A. O. and B. C. Yen. 1981. Effect of rain intensity on infiltration and surface runoff rates. Advances in Infiltration : Proceedings of the National Conference on Advances in Infiltration, December 12-13, 1983, Hyatt Regency Illinois Center, Chicago, Illinois. ASAE. pp. 324-331.

Beasley, D. B., L. F. Huggins, and E. J. Monke. 1980. ANSWERS: A model for watershed planning. *Trans. of ASAE.* 23(4):938-944.

Bennett, J. P. 1974. Concepts of mathematical modeling sediment yield. *Water Resources Research* 10(3):485-492.

Blandford, G.E. and L.E. Ormsbee. 1993. A diffusion wave finite element model for channel networks. *Journal of Hydrology* 142:99-120.

Blau, J.B., D.A. Woolhiser and J.J. Lane. 1988. Identification of erosion model parameters. *Trans. of ASAE* 31:859-864,854.

Borah, D. K. 1989. Sediment discharge model for small watersheds. *Trans. of ASAE.* 32(3):874-880.

Cathers, B and B.A. O'Connor. 1993. Picard iteration convergence analysis in a Galerkin finite element approximation of the one-dimensional shallow water equations. *Numerical Methods for Partial Differential Equations* 9(1):77-92.

Chow, V.T. 1959. Open Channel Hydraulics, McGraw-Hill Co. New York.

Chow, Ven Te and Arie Ben-Zvi. 1973. Hydrodynamic modeling of two-dimensional watershed flow. *ASCE Journal of Hydraulic Engineering division.* 99(11):2023-2040.

Chung, W-H., A.A. Aldama and J.A. Smith. 1993. On the effects of downstream boundary conditions on diffusive flood routing. *Advances in Water Resources.* 16(5):259-275.

Connor, J.J. and C.A. Brebbia. 1976. Finite Element Techniques for Fluid Flow. Newnes-Butterworths Co. Ltd. London.

Cooley, R. L. and S. A. Moin. 1976. Finite element solution of Saint-Venant equations. *ASCE Journal of Hydraulic Engineering* 102(6):759-775.

Croley Jr., T.S. 1982. Unsteady overland sedimentation. *Journal of Hydrology* 56:325-346.

Croley, T.E. Jr., G.R. Foster. 1984. Unsteady sedimentation in nonuniform rills. *Journal of Hydrology* 70:101-122.

Cuhadaroglu, M. S., D. R. Maidment and L. J. Hayes. 1992. Integrating a finite element model for storm water prediction with a geographic information system. *Computational Methods in Water Resources IX.* Volume 2: Mathematical Modeling in Water Resources. Computational Publications, Boston. MA.

Cunge, J.A., F.M. Holly, Jr. and A. Verwey. 1980. Principal Aspects of Computational River Hydraulics. Pitman Pub. Ltd.

Dhatt, G. and G. Touzot. 1984. The Finite Element Method Displayed, translated by G. Cantin. John and Wiley and Sons.

Dillaha, T.A. and D.B. Beasley. 1983. Distributed parameter modeling of sediment movement and particle size distributions. *Trans. of ASAE 26(6)*:1766-1777.

Dillaha, T. A., J. H. Sherrad, D. Lee, V. O. Shanholtz, S. Mostaghimi and W. L. Magette. 1986. Use of Vegetative Filter Strips and Phosphorous Losses from Feedlots : Phase I. Experimental Plot Studies. Virginia Water Resources Research Center. Bulletin 151. Virginia Tech.

Engelund, F. and E. Hansen. 1967. A monograph on sediment transport in alluvial streams. Teknisk Vorlag, Copenhagen.

Foster, G.R. 1982. Modeling the erosion process. In C.T. Haan, H.P. Johnson, and D.L. Brakensiek, eds., Hydrologic Modeling of Small Watersheds, ASAE monograph 5. pp: 297-380. ASAE, St. Joseph, MI.

Foster, G.R., L.J. Lane, J.D. Nowlin, J.M. Laflen, R.A. Young. 1981. Estimating erosion and sediment yield on field-sized areas. *Trans. of ASAE* 24:1253-1262.

Goodrich, C.G., D.A. Woolhiser and T.O. Keefer. 1991. Kinematic routing using finite elements on a triangular irregular network. *Water Resources Research* 27(6):995-1003.

Green, W.H. and G.A. Ampt. 1911. Studies on soil physics: Part I. The flow of air and water through soil. *Journal of Agricultural Science* 4:1-24.

Hairsine, P.B. and C.W. Rose. 1992. Modeling water erosion due to overland flow using physical principles: 1. Rill flow. *Water Resources Research* 28(1):245-250.

Haverkamp, R.M., V.J. Touma, P.J. Wierenga and G. Vachaud. 1977. A comparison of numerical simulation models for one-dimensional infiltration. *Soil Sci. Soc. Am. J.* 41:285-294.

Henderson, F.M. 1966. Open Channel Flow. The McMillan Co. New York.

Holtan, H.N. 1961. A concept for infiltration estimates in watershed engineering. *Trans. of ASAE* 10(3):407-410.

Jayawardena, A. W. and J. K. White. 1977. A finite element distributed catchment model, I. Analytical basis. *Journal of Hydrology* 34:269-286.

Judah, O.M., V.O. Shanholtz, and D.N. Contractor. 1975. Finite element simulation of flood hydrographs. *Trans. of ASAE.* 18:518-522.

Julien, P.Y. and D.B. Simons. 1985. Sediment transport capacity of overland flow. *Trans. of ASAE* 28(3):755-762.

Kawahara, Mutsuto and Teruyuki Yokoyama. 1980. Finite element method for direct runoff flow. *ASCE Hydraulic Engineering division.* 106(4):519-534.

Knisel, D. R. 1980. CREAMS: A Field Scale Model for Chemical, Runoff, and Erosion from Agricultural Management Systems. Conservation Research Report No.26, USDA-SEA.

Laguna, A. and J. V. Giraldez. 1993. The description of soil erosion through a kinematic wave model. *Journal of Hydrology* 145:65-82.

Laursen, E. M. 1956. Sediment transport mechanics in stable channel design. *ASCE Journal of Hydraulic Engineering* ():195-206.

Liggett, J.A. and D.A. Woolhiser. 1967. Difference solutions of the shallow-water equation. *ASCE Journal of the Engineering Mechanics Division.* 93(2):39-71.

Mein, R.G. and C.L. Larson. 1973. Modeling infiltration during a steady rain. *Water Resources Research* 9(2):384-394.

Meyer, L.D. and W.C. Harmon. 1985. Sediment loss from cropland furrows of different gradient. *Trans. of ASAE* 28:448-452.

Meyer, L.D., W.H. Wischmeier. 1969. Mathematical simulation of the process of soil erosion by water. *Trans. of the ASAE* 12:754-762.

Moor, I.D. 1981. Infiltration equations modified for surface effects. *ASCE Journal of Irrigation and Drainage Division* 107(1):71-86.

Morel-Seytoux, H.J. and J. Khanji. 1974. Derivation of an equation of infiltration. *Water Resources Research* 10(4):795-800.

Nearing, M.A., G.R. Foster, L.J. Lanes, and S.C. Finkner. 1989. A process-based soil erosion model for USDA- water erosion prediction project technology. *Trans. of ASAE* 32(5):1587-1593.

Overton, D.E. and M. E. Meadows. 1976. *Stormwater Modeling.* Academic Press, New York.

Parlange, J. Y., I. Lisle, R. D. Braddock and R. E. Smith. 1982. The three parameter infiltration equation. *Soil Science* 133(6):337-341.

Pinder, G.F. and W.G. Gray. 1977. Finite Element Simulation in Surface and Subsurface Hydrology. Academic Press, New York.

Ponce, V.M., R.M. Li and D.B. Simons. 1978. Applicability of kinematic and diffusion models. *ASCE Journal of Hydraulic Engineering division* 104(3):353-360.

Rallison, R.E. and N. Miller. 1981. Past, present, and future SCS Soil Conservation Service runoff procedure rural watershed areas. In proceedings of International Symposium on rainfall-runoff modeling, edited by V.P. Singh, pp. 353-364.

Rawls, W.J., D.L. Brakensiek and K.E. Saxton. 1982. Estimation of soil water properties. *Trans. of ASAE* 25(5):1316-1320.

Rose, C. W. 1985. Developments in soil erosion and deposition models. *Adv. Soil Sci. 2:1-63.*

Rose, C. W., J. R. Williams, C. Sanders and D. A. Barry. 1983a. A mathematical model of soil erosion and deposition processes: I. Theory for a plane land element. *Soil Sci. Soc. Am. J.* 47:991-995.

Rose, C. W., J. R. Williams, C. Sanders and D. A. Barry. 1983b. A mathematical model of soil erosion and deposition processes: II. Application to data from an arid-zone catchment. *Soil Sci. Soc. Am. J.* 47:996-1000.

Ross, B. B. 1978. A spatially response catchment model for predicting storm water runoff from ungaged watersheds. Ph.D Thesis. Dept. of Agri. Eng. Virginia Tech. Blacksburg, VA.

Ross, B.B. and V.O. Shanholtz. 1979. A one-dimensional finite element structure for modeling the hydrology of small upland watersheds. In. the Proceedings of the Hydrologic Transport Modeling symposium, publised by ASAE. St. Joseph, MI.

Schwab, G. O., R. K. Frevert, T. W. Edminster and K. K Barnes. 1981. Soil and Water Conservation Engineering. John and Wiley and Sons, Inc. New York.

Sharda, V.N. and S.R. Singh. 1994. A finite element model for simulating runoff and soil erosion from mechanically treated agricultural lands : 1. Governing equations and solutions. *Water Resources Research* 30(7):2287-2298.

Shirley, E.D. and J.J. Lane. 1978. A sediment yield equation from an erosion simulation model. *Hydrol. Water Resources Arizona Southwest*, 8:90-96.

Singh, V.P. 1983. Analytical solutions of kinematic equations for erosion on a plain : II. Rainfall of finite duration. *Advances in Water Resources* 6:88-95.

Singh, V.P. and R. R. Regl. 1983. Analytical solutions of kinematic equations for erosion on a plain: I. Rainfall of indefinite duration. *Advances in Water Resources* 6:2-10.

Singh, V.P. and S.N. Prasad. 1982. Explicit solutions to kinematic equations for erosion on an infilration plane. In V.P. Singh ed., Modeling Components of Hydrologic Cycle. Water Resources, Littleton, CO., pp.515-538.

Smith, R. E. and J. Y. Parlange. 1978. A parameter efficient hydrologic infiltration model. *Water Resources Research* 14(3):533-538.

Smith, R. E., C. Corradini and F Melone. 1993. Modeling infiltration for multistorm runoff events. *Water Resources Research* 29(1):133-144.

Sod, G.A. 1989. Numerical Methods in Fluid Dynamics. Cambridge University Press, Cambridge.

Stephenson, D. and M. E. Meadows. 1986. *Kinematic Hydrology and Modeling*. Elsevier Sci. Pub. NY.

Storm, D.E. 1991. Modeling Dynamic Rill Networks from Random Surfaces on Moderate Slopes. Ph.D. Thesis, The University of Kentucky. Lexington, Kentucky. U.S.A.

Szymkiewicz,R. 1991. Finite element method for the solution of the Saint Venant equations in an open channel network. *Journal of Hydrology*. 122:275-287.

Tayfur, G., M. L. Kavvas, R. S. Govindaraju and D. E. Storm. 1993. Applicability of St. Venant equations for two-dimensional overland flows over rough infiltration surfaces. *Journal of Hydraulic Engineering* 119(1):51-63.

Taylor, C., G. Al-Mashidani and J. H. Davis. 1974. A finite element approach to watershed runoff. *Journal of Hydrology* 21:231-246.

Thomas, D.L., M.L. Griffin and D.B. Beasley. 1989. ANSWERS : Areal Nonpoint Source Watershed Environment Response Simulation, In Application of Water Quality Models for Agricultural and Forested Watersheds, Southern Cooperative Series Bulletine No. 338. pp. 5-13.

U.S. Soil Conservation Service. 1972, Hydrology : National Engineering Handbook, Section 4. Washinton, D.C. USDA-ARS.

Vieira, J. H. 1983. Conditions governing the use of approximations for the Saint-Venant equations for shallow surface water flow. *Journal of Hydrology* 60:43-58.

Vieux, B.E. 1989. Finite Element Analysis of Hydrologic Response Areas using Geographic Information Systems, Ph.D. thesis. Michigan State University, East Lansing, MI.

Wells, L. G., A. D. Ward, I. D. Moore and R. E. Phillips. 1986. Comparison of four infiltration models in characterizing infiltration through surface mine profiles. *Tans. of ASAE.* 29(3):785-793.

Wolfe, M. L. 1982. Sediment detachment and transport functions to simulate soil loss from reclaimed mine soils. M.S. thesis. Department of Agricultural Engineering, Virginia Tech. Blacksburg, VA.

Woodruff, P. H. 1993. Water quality for the 21st century. *Water Environment and Technology* 5(3):64-67.

Woolhiser, D. A., R. E. Smith and D. C. Goodrich. 1990. KINEROS, A Kinematic Runoff and Erosion Model. USDA-ARS, ARS-77.

Wu, T. H., J. A. Hall and J. V. Bonta. 1993. Evaluation of runoff and erosion model. *Journal of Irrigation and Drainage Engineering* 119(4):364-382.

Yalin, M. S. 1963. An expression for bed load transportation. *ASCE Journal of Hydraulic Engineering* 89(3):221-249.

Yang, C.T. 1973. Incipient motion and sediment transport. *ASCE Journal of Hydraulic Engineering* 99(10):1679-1704.

Young, R. A., C. A. Onstad, D. D. Bosch, and W. P. Anderson. 1987, AGNPS, Agricultural Non-Point-Source Pollution Model. A Watershed Analysis Tool. Conservation Research Report 35.

Young, R. A., C. A. Onstad, D. D. Bosch, and W. P. Anderson. 1989, AGNPS : a nonpoint source pollution model for evaluating agricultural watershed. *Journal Soil and Water Conservation.* 44(2):168-173

Zhang, W. and T. W. Cundy. 1989. Modeling of two-dimensional overland flow. *Water Resources Research.* 25(9):2019-2035.

Appendix I

Glossary of Model Variables

1. Reading of coordinates and number of degrees of freedom of all the nodes (COOR)

Variables	Columns	Format	Description
NNT	1-5	I5	total number of nodes
NDLN	6-10	I5	number of degrees of freedom
NDIM	11-15	I5	number of dimension
FAC(1)	16-25	F10.0	scale factor in direction x
FAC(2)	26-35	F10.0	scale factor in direction y
IN1	1-5	I5	Nodal id number
X1(1)	6-15	F10.0	x coordinate
X2(1)	16-25	F10.0	y coordinate

2. Reading of boundary conditions (COND)

Variables	Columns	Format	Description
ICOD	1-10	10I1	for each degree of freedom 2 if non-zero prescribed 1 if zero prescribed 0 if free
V	11-80	7F10.0	values for prescribed degree of freedom
KV	1-80	16I5	node numbers for boundary condition

3. Reading of nodal properties (PRND)

Variables	Columns	Format	Description
NPRN	1-5	I5	number of properties per node
VPRNG	1-80	8F10.0	values of nodal properties

4. Reading of element properties (PREL)

Variables	Columns	Format	Description
NGPE	1-5	I5	number of groups of element properties
NPRE	6-10	I5	number of properties per group
IGPE	1-5	I5	group number
V1	6-75	7F10.0	successive values of properties

5. Reading of elements (ELEM)

Variables	Columns	Format	Description
NELT	1-5	I5	total number of elements
NNEL	6-10	I5	number of nodes per element
NTPE	11-15	I5	number of element type by default
NGRE	16-20	I5	number of element group by default
NSYM	21-25	I5	indicator for stiffness matrix 0 if symmetric 1 if non-symmetric
IEL	1-5	I5	element number
ITPE	6-10	I5	element type number
IGPE	11-15	I5	element properties group number
IGRE	16-20	I5	element group number
KNE	21-35	3I5	node number of the element

6. Reading of general computational criteria and rainfall data (TEMP)

Variables	Columns	Format	Description
DPAS	1-10	F10.0	time step
NPAS	11-15	I5	number of time steps
NITER	15-20	I5	maximum iterations
IMETH	21-25	I5	1 for computing stiffness matrix at each iteration
EPSDL	26-35	F10.0	admissible error of the norm
OMEGA	36-45	F10.0	coefficient of Euler method : 1
BETA	46-55	F10.0	machine zero : 0.1E-14
HULA	46-55	F10.0	over-relaxation factor : 0.5
IPRINT	56-60	I5	frequency of step for printing
ISIMM	61-65	I5	0 if runoff simulation 1 if sediment transport simulation

Appendix II

Computer Programs for Runoff and Sediment transport models

1. Main Program (main.f)

```
C
C...   FORTRAN PROGRAM FOR TRANSIENT NONLINEAR PROBLEM
C      The source code is originated from  'The Finite Element Method Displayed'
C...     by Gouri Dhatt and Gilbert Totzot (1984)
C
      IMPLICIT REAL*8 (A-H,O-Z)
      CHARACTER*4 BLOC,BLOCS(21)
      character*50 infile
      COMMON/ALLOC/NVA,IVA,IVAMAX,NREEL,NTBL
      COMMON/ES/M,MR,MP,MLUN(10)
      COMMON VA(30000)
      DATA BLOCS/'IMAG','COMT','COOR','DLPN','COND','PRND','PREL',
     *           'ELEM','SOLC','SOLR','LINM','LIND','NLIN','TEMP',
     *           'VALP','....','....','....','....','....','STOP'/
      DATA NB/21/
C
C...  LENGTH OF BLANK COMMON IN REAL WIRDS (TABLE VA)
C
      NVA=30000
C
C...  HEADING
C
      MR=4
      WRITE(6,*) ' TYPE INPUT FILE NAME'
      READ(5,51) infile
 51   format(a50)
      MP=7
      OPEN(UNIT=4,FILE=infile)
      OPEN(UNIT=MP,FILE='one6.out')
      OPEN(UNIT=10,FILE='one10.out',form='unformatted')
      open(unit=20,file='ovel.out')
      open(unit=30,file='ohyd.out',form='unformatted')
      open(unit=50,file='oinf.out',form='unformatted')
      WRITE(MP,2000)
2000  FORMAT(1H1,30X,' Runoff and sediment transport model'////)
C
C...  READ BLOCK TITLE
C
10    READ(MR,1000) BLOC,M,MLUN
1000  FORMAT(A4,I6,10I5)
C
C...  SEARCH FOR THE BLOVK TO BE EXECUTED
C
      DO 20 I=1,NB
         IF(BLOC.EQ.BLOCS(I)) GOTO 30
20    CONTINUE
      WRITE(MP,2010)
2010  FORMAT(' ******* ERROR , MISSING BLOCK CALLING CARD')
      GOTO 10
30    GO TO (110,120,130,140,150,160,170,
     *       180,190,200,210,220,230,240,
     *       250,260,270,280,290,300,999) I
C
C...  BLOCK PRINT IMAGES OF DATA CARDS ----- 'IMAG'
C
110   CONTINUE
C     CALL BLIMAG
      GOTO 10
C
C...  BLOCK READ AND PRINT COMMENTS    ----- 'COMT'
C
120   CALL BLCOMT
      GOTO 10
C
C...  BLOCK TO READ NODAL POINTS COORDINATES-'COOR'
```

```
C
130   CALL BLCOOR
      GOTO 10
C
C...  BLOCK TO READ DOF PER NODE       ----- 'DLPN'
C
140   CONTINUE
C     CALL BLDLPN
      GOTO 10
C
C...  BLOCK TO READ BOUNDARY CONDITION ----- 'COND'
C
150   CALL BLCOND
      GOTO 10
C
C...  BLOCK TO READ NODAL PROPERTIES   ----- 'PRND'
C
160   CONTINUE
      CALL BLPRND
      GOTO 10
C
C...  BLOCK TO READ ELEMENT PROPERTIES ----- 'PREL'
C
170   CALL BLPREL
      GOTO 10
C
C...  BLOCK TO READ ELEMENT DATA       ----- 'ELEM'
C
180   CALL BLELEM
      GOTO 10
C
C...  BLOCK TO READ CONCENTRATED LOADS ----- 'SOLC'
C
190   CONTINUE
C     CALL BLSOLC
      GOTO 10
C
C...  BLOCK TO READ DISTRIBUTD LOADS   ----- 'SOLR'
C
200   CONTINUE
C     CALL BLSOLR
      GOTO 10
C
C...  BLOCK FOR IN CORE ASSEMBLING AND
C...  LINEAR SOLUTION ---------------------- 'LINM'
C
210   CONTINUE
C     CALL BLLINM
      GOTO 10
C
C...  BLOCK FOR ON DISK ASSEMBLING AND LINEAR
C...  SOLUTION                -------------- 'LIND'
C
220   CONTINUE
C     CALL BLLIND
      GOTO 10
C
C...  BLOCK FOR NONLINEAR SOLUTION      ----- 'NLIN'
C
230   CONTINUE
C     CALL BLNLIN
      GOTO 10
C
C...  BLOCK FOR UNSTEADY PROBLEM       ----- 'TEMP'
C
240   CALL BLTEMP
      GOTO 10
C
C...  BLOCK TO COMPUTE EIGENVALUE      ----- 'VALP'
C
```

```
250   CONTINUE
C     CALL BLVALP
      GOTO 10
C
C...  UNDEFINED BLOCKS
C
260   CONTINUE
270   CONTINUE
280   CONTINUE
290   CONTINUE
300   CONTINUE
      GOTO 10
C
C...  END OF PROBLEM
999   WRITE(MP,2020) IVAMAX, NVA
2020  FORMAT(//' END OF PROBLEM :',I10,' UTILIZED REAL WORDS OVER',I10)
      STOP
      END
C
C-------------------------------------
C
C...  BLOCK DATA SUBROUTINE
      BLOCK DATA
C
C...  INITIALIZE LABELLED COMMONS
      IMPLICIT REAL*8 (A-H,O-Z)
C
      COMMON/COOR/NDIM,NNT,NDLN,NDLT,FAC(3)
      COMMON/COND/NCLT,NCLZ,NCLNZ
      COMMON/PRND/NPRN
      COMMON/PREL/NGPE,NPRE
      COMMON/ELEM/NELT,NNEL,NTPE,NGRE,ME,NIDENT,NPG
      COMMON/ASSE/NSYM,NKG,NKE,NDLE
      COMMON/RESO/NEQ,NRES,MRES
      COMMON/RGDT/IEL,ITPE,ITPE1,IGRE,IDLE,ICE,IPRNE,IPREE,INEL,IDEG,
     1            IPG,ICOD,IDLE0,INEL0,IPG0
      COMMON/LIND/NLBL,NBLM,MKG1,MKG2
      COMMON/NLIN/EPSDL,XNORM,OMEGA,XPAS,DPAS,DPAS0,NPAS,IPAS,NITER,
     1            ITER,IMETH
      COMMON/VALP/NITER1,NMDIAG,EPSLB,SHIFT,NSS,NSWM,TOLJAC,NVALP
      COMMON/ES/M,MR,MP,MLUN(10)
      COMMON/ALLOC/NVA,IVA,IVAMAX,NREEL,NTBL
      COMMON/LOC/LCORG,LDLNC,LNEQ,LDIMP,LPRNG,LPREG,LLD,LLOCE,LCORE,
     1           LNE,LPRNE,LPREE,LDLE,LKE,LFE,LKGS,LKGD,LKGI,LKG,LRES
     2          ,LDLG,LME,LDLE0,LDLG0,LFG0
      DIMENSION LXX(25)
      EQUIVALENCE (LXX(1),LCORG)
C
C...  COMMON DATA
C
      DATA NNT,NDLN,NDIM,FAC/20,2,2,3*1.D0/
      DATA NPRN/0/
      DATA NGPE,NPRE/0,0/
      DATA NELT,NNEL,NTPE,NGRE,ME,NIDENT/20,8,1,1,1,0/
      DATA NSYM/0/
      DATA NRES, MRES/0,2/
      DATA ITPE1/0/
      DATA MKG1,MKG2/4,7/
      DATA EPSDL,OMEGA,DPAS,NPAS,NITER,IMETH/1.D-2,1.D0,.2D0,1,5,1/
      DATA NITER1,NMDIAG,EPSLB,SHIFT,NSS,NSWM,TOLJAC,NVALP
     * /10,0,1.D-3,0.D0,5,12,1.D-12,3/
      DATA MR,MP/5,7/
      DATA IVA,IVAMAX,NTBL/1,1,25/
      DATA NREEL/2/
      DATA LXX/25*1/
      END
C
C-----------------------------------------------
C...  ERREUR SUBROUTINE
C
```

```
      SUBROUTINE ERREUR(IERR,I1,I2,INIV)
      IMPLICIT REAL*8 (A-H,O-Z)
      COMMON/ES/M,MR,MP,MNUL(10)
C
      IF(IERR.GT.19) GOTO 200
      IE=IERR-10
      GOTO (110,120,130,140,150,160,160,180) IE
110   WRITE(MP,2110) I1,I2
2110  FORMAT(' ERROR 1ST NODE NUMBER',I4,' IS GREATER THAN NNT=',I4)
      GOTO 900
120   WRITE(MP,2120) I1,I2
2120  FORMAT(' ERROR 2ND NODE NUMBER',I4,' IS GREATER THAT NNT=',I4)
      GOTO 900
130   WRITE(MP,2130) I1,I2
2130  FORMAT(' ERROR NODAL NUMBER OF DOF',I4,' GREATER THAN MDLN=',I4)
      GOTO 900
140   WRITE(MP,2140)
2140  FORMAT(' ERROR, 1ST AND 2ND NODE NUMBER ARE INCOMPATIBLE WITH',
     *' THE GENERATION PARAMETER')
      GOTO 900
150   WRITE(MP,2150) I1
2150  FORMAT(' ERROR, NODE',I4,' IS DEFINED MORE THAN ONCE')
      GOTO 900
160   WRITE(MP,2160) I1
2160  FORMAT(' ERROR NODE',I4,' IS NOT DEFINED')
      GOTO 900
180   WRITE(MP,2180) I2,I1
2180  FORMAT(' ERROR, GENERATED NODES NUMBER',I4,',IS LESS THAN NNT=',
     *I4)
      GOTO 900
C
C...  BLOCK "DLPN"
C
200   IF(IERR.GT.29) GOTO 300
      IE=IERR-20
      GOTO (210,220), IE
210   WRITE(MP,2210) I1,I2
2210  FORMAT(' ERROR NUMBER OF DOF',I2,' IS GREATER THAN NDLN=',I2)
      GOTO 900
220   WRITE(MP,2220) I1,I2
2220  FORMAT(' ERROR, NODE NUMBER ',I4,'IS GREATER THAN NNT=',I4)
      GOTO 900
C
C...  BLOCK "COND"
C
300   IF(IERR.GT.39) GOTO 400
      IE=IERR-30
      GOTO (900,320,900),IE
320   GOTO 220
C
C...  BLOCK 'PREL'
C
400   IF(IERR.GT.49) GOTO 500
      IE=IERR-40
      GOTO (410,900),IE
410   WRITE(MP,2410) I1,I2
2410  FORMAT(' ERROR, GROUP NUMBER',I3,' IS GREATER THAN NGPE=',I3)
      GOTO 900
C
C...  BLOCK 'ELEM'
C
500   IF(IERR.GT.59) GOTO 900
      IE=IERR-50
      GOTO (510,900,530,540,550,560,570),IE
510   WRITE(MP,2510) I1,I2
2510  FORMAT(' ERROR, NUMBER OF NODE',I3,' IS GREATER THAN NNEL=',I3)
      GOTO 900
530   WRITE(MP,2530) I1,I2
2530  FORMAT(' ERROR, PROPERTY NUMBER',I3,' IS GREATER THAT NGPE=',I3)
      GOTO 900
```

```
540   WRITE(MP,2540) I1,I2
2540  FORMAT(' ERROR, GROUP NUMBER',I4,' GREATER THAN NGRE=',I4)
      GOTO 900
550   WRITE(MP,2550) I1,I2
2550  FORMAT(' ERROR, ELEMENT NUMBER ',I3,' GREATER THAN NELT=',I2)
      GOTO 900
560   GOTO 220
570   WRITE(MP,2570) I1,I2
2570  FORMAT(' ERROR, NUMBER OF ELEMENT',I4,' IS GGREATER THAN NELT=',
     *       I4)
C
C...  END
C
900   I1=I2
      IF(INIV.GE.2) STOP
      RETURN
      END
C
C-----------------------------------------
C
C----------SUBROUTINE BLCOMT
      SUBROUTINE BLCOMT
      IMPLICIT REAL*8 (A-H,O-Z)
      CHARACTER*4 BLANC,CART,CNUL
      COMMON/ES/M,MR,MP,MNUL(10)
      COMMON/TRVL/CART(20),ITNUL(66)
      DATA BLANC/'    '/
      WRITE(MP,2000)
2000  FORMAT(//' COMMENTS'/' ',10('=')/)
10    READ(MR,1000) CART
1000  FORMAT(20A4)
      DO 20 I=1,20
      IF(CART(I).NE.BLANC) GOTO 30
20    CONTINUE
      RETURN
30    WRITE(MP,2010) CART
2010  FORMAT(1X,20A4)
      GOTO 10
      END
C
C-----------------------------------------
C...  SUBROUTINE ESPACE
      SUBROUTINE ESPACE(ILONG,IREEL,TBL,IDEB)
      IMPLICIT REAL*8 (A-H,O-Z)
      COMMON/ES/M,MR,MP,MNUL(10)
      COMMON/ALLOC/NVA,IVA,IVAMAX,NREEL,IHONG
      COMMON VA(1)
      CHARACTER*4 TBL
      DIMENSION KA(1)
      EQUIVALENCE (VA(1),KA(1))
      DATA ZERO/0.D0/
C
C...  CALCULATE THE TABLE LENGTH IN REAL WORDS
      ILGR=ILONG
      IF(IREEL.EQ.0) ILGR=(ILONG+NREEL-1)/NREEL
      IVA1=IVA+ILGR
C...  CHECK IF ENOUGH SPACE IS AVAILABLE
      IF(IVA1.LE.NVA) GOTO 20
C...  ALLOCATION ERROR
10    WRITE(MP,2000) TBL,IVA1,NVA
2000  FORMAT('*** ALLOCATION ERROR, TABLE',A4,/' REQUIRED SPACE'/
     1       I9,'REAL WORDS, AVAILABLE SPACE:',I9,' REAL WORDS')
      STOP
C...  ALLOCATE TABLE
20    IDEB=IVA+1
      IVA=IVA1
      IF(IVA.GT.IVAMAX) IVAMAX=IVA
      IF(M.GT.0) WRITE(MP,2010) TBL,IDEB,IVA1
2010  FORMAT(60X,'TABLE',A4,' GOES FROM VA(',I7,')TO VA(',I7,')')
C...  INITIALIZE THE ALLOCATED TABLE TO ZERO
```

```
      I1=IDEB
      IF(IREEL.EQ.0) I1=(I1-1)*NREEL+1
      I2=I1+ILONG-1
      IF(IREEL.EQ.0) GOTO 40
      DO 30 I=I1,I2
30    VA(I)=ZERO
      RETURN
40    DO 50 I=I1,I2
50    KA(I)=0
      RETURN
      END
C
C-----------------------------------------------
C     SUBROUTINE VIDE -- ALSO FOR PSEUDO-DYNAMIC MEMORY ALLOCATION
      SUBROUTINE VIDE(IDEB,IREEL,TBL)
      IMPLICIT REAL*8 (A-H,O-Z)
      COMMON/ES/M,MR,MP,MNUL(10)
      CHARACTER*4 TBL
      COMMON/ALLOC/NVA,IVA,IVAMAX,NREEL,NTBL
      COMMON/LOC/LXX(25)
      COMMON VA(1)
C
C...  SEARCH FOR THE 1ST POSITION OF NEXT TABLE
      I1=IVA+1
      DO 10 I=1,NTBL
      IF(LXX(I).LE.IDEB) GOTO 10
      IF(LXX(I).LT.I1) I1=LXX(I)
10    CONTINUE
C...  SHIFT ALL TABLES AFTER THIS
      ID=I1-IDEB
      IF(I1.EQ.IVA+1) GOTO 40
      DO 20 I=1,NTBL
      IF(LXX(I).GT.IDEB) LXX(I)=LXX(I)-ID
20    CONTINUE
      DO 30 I=I1,IVA
      J=I-ID
30    VA(J)=VA(I)
C...  PRINT
40    IVA=IVA-ID
      IF(M.GT.0) WRITE(MP,2000) TBL,ID,IDEB
2000  FORMAT(60X,' DELETED TABLE',A4,' COMPACTING',I7,' REAL WORDS',
     &       ' AFTER VA(',I7,')')
      RETURN
      END
C
C---------
      SUBROUTINE BLCOND
      IMPLICIT REAL*8 (A-H,O-Z)
      CHARACTER*4 TBL(2)
      COMMON/COOR/NDIM,NNT,NDLN,NDLT,ONG1(3)
      COMMON/COND/NCLT,NCLZ,NCLNZ
      COMMON/ALLOC/NVA,IVA,IHONG(3)
      COMMON/ES/M,MR,MP,M1,MNUL(9)
      COMMON/LOC/LCORG,LDLNC,LNEQ,LDIMP,LOCNUL(21)
      COMMON VA(1)
      DATA TBL/'NEQ ','DIMP'/
C...
      IF(M1.EQ.0) M1=MR
      WRITE(MP,2000) M
2000  FORMAT(//' INPUT OF B.C. M=',I2)
      IF(LNEQ.EQ.1) CALL ESPACE(NDLT,0,TBL(1),LNEQ)
      IF(LDIMP.EQ.1) CALL ESPACE(NDLT,1,TBL(2),LDIMP)
      CALL EXCOND(VA(LCORG),VA(LDLNC),VA(LNEQ),VA(LDIMP))
      CALL VIDE(LDIMP+NCLT,1,TBL(2))
      RETURN
      END
C
C--------
      SUBROUTINE EXCOND(VCORG,KDLNC,KNEQ,VDIMP)
      IMPLICIT REAL*8 (A-H,O-Z)
```

```
      COMMON/COOR/NDIM,NNT,NDLN,NDLT,ONG(3)
      COMMON/COND/NCLT,NCLZ,NCLNZ
      COMMON/RESO/NEQ,NUL3(2)
C     COMMON/LOC/LCORG,LDLNC,LNEQ,LDIMP,LOCNUL(21)
      COMMON/ES/M,MR,MP,M1,MNUL(9)
      COMMON/TRVL/KV(16),V(10),H(20),ICOD(10)
C,TNUL(68),ITNUL(13)
      DATA L7,L8,L16,X1,X2,X3,ZERO/7,8,16,0.D0,0.D0,0.D0,0.D0/
      COMMON/LOC/LCORG,LDLNC,LNEQ,LDIMP,LPRNG,LPREG,LLD,LLOCE,LCORE,LNE,
     1   LPRNE,LPREE,LDLE,LKE,LFE,LKGS,LKGD,LKGI,LFG,LRES,LDLG,LME,
     1   LDLE0,LDLG0,LFG0
      DIMENSION VCORG(LDLNC-LCORG+1),KDLNC(LDIMP-LDLNC+1),
     1 VDIMP(LNEQ-LDIMP+1),KNEQ(LLD-LNEQ+1)
C
C     CUMULATIVE TABLE KDLNC
C
      DO 10 IN=1,NNT
10    KDLNC(IN+1)=KDLNC(IN)+KDLNC(IN+1)
      I1=NNT+1
      IF(M.GT.0) WRITE(MP,2000) (KDLNC(IN),IN=1,I1)
2000  FORMAT(//'NUMBER OF DOF PRECEEDING EACH NODE',/2X,10I10)
C
C...  INITIALIZE
C
      NCLT=0
      NCLNZ=0
      NCLZ=0
      IF(M.GE.0) WRITE(MP,2010)
2010  FORMAT(//'B.C. CARDS')
20    READ(M1,1000) ICOD,(V(I),I=1,L7)
1000  FORMAT(10I1,7F10.0)
      IF(M.GE.0) WRITE(MP,2020) ICOD,(V(I),I=1,L7)
2020  FORMAT('>>>'/10I1,7F10.5)
C...  CHECK FOR A BLANK CARD
      J=0
      DO 30 I=1,10
30    J=J+ICOD(I)
      IF(J.EQ.0) GOTO 110
C...  READ ADDITIONAL CARD ID REQUIRED
      I2=0
      DO 40 ID=1,NDLN
      IF(ICOD(ID).LT.2) GOTO 40
      I2=I2+1
      IF(I2.NE.L8) GOTO 40
      READ(M1,1010) (V(I),I=L8,NDLN)
1010  FORMAT(10X,7F10.0)
      IF(M.GE.0) WRITE(MP,2030) (V(I),I=L8,NDLN)
2030  FORMAT('>>>'/7F11.5)
40    CONTINUE
C...  READ NODE CARDS
50    READ(M1,1020) (KV(IN),IN=1,L16)
1020  FORMAT(16I5)
      IF(M.GE.0) WRITE(MP,2040) (KV(IN),IN=1,L16)
2040  FORMAT('>>>'/16I5)
C...  FORM NEQ
      DO 100 IN=1,L16
         I2=KV(IN)
C...  END OF GROUP OF B.C. OR END OF NODES OR ANALYSIS OF NODE
         IF(I2)  20,20,60
60       IF(I2.GT.NNT) CALL ERREUR(32,I2,NNT,1)
         I1=KDLNC(I2)
         IDN=KDLNC(I2+1)-I1
C...  GENERATE VDIMP, PUT IT IN KNEQ
         IV=0
         DO 90 ID=1,IDN
            I1=I1+1
            IC=ICOD(ID)-1
            IF(IC) 90,70,80
70          NCLT=NCLT+1
            VDIMP(NCLT)=ZERO
```

```
            NCLZ=NCLZ+1
            KNEQ(I1)=-NCLT
            GOTO 90
80          NCLT=NCLT+1
            IV=IV+1
            VDIMP(NCLT)=V(IV)
            NCLNZ=NCLNZ+1
            KNEQ(I1)=-NCLT
90        CONTINUE
100     CONTINUE
C..     ADDITIONAL CARD OF NODE NUMBER
        GOTO 50
C..     GENERATE EQUATION NUMBERS IN NEQ
110     I1=0
        DO 150 IN=1,NNT
        ID=KDLNC(IN)
120     ID=ID+1
        IF(ID.GT.KDLNC(IN+1)) GOTO 150
        IF(KNEQ(ID)) 120,130,120
130     I1=I1+1
        KNEQ(ID)=I1
        GOTO 120
150     CONTINUE
        NEQ=I1
C...    OUTPUT
        IF(M.LT.0) GOTO 170
        WRITE(MP,2050) NNT,NDLT,NEQ,NCLNZ,NCLZ,NCLT
2050    FORMAT('TOTAL NUMBER OF NODE=',I5,/
       1        'TOTAL NUMBER OF DOF =',I5,/
       2        ' NUMBER OF EQUATIONS=',I5,/
       3        ' NUMBER OF PRESCRIBED NON ZERO DOF',I5,/
       4        ' NUMBER OF PRESCRIBED ZERO DOF',I5,/
       5        ' TOTAL NUMBER OF PRESCRIBED DOF',I5)
        IF(M.GE.2.AND.NCLT.GT.0) WRITE(MP,2060)(VDIMP(I),I=1,NCLT)
2060    FORMAT(//'PRESCRIBED VALUES'/(10X,10E12.5))
        WRITE(MP,2070)
2070    FORMAT(//'NODAL COORDINATE     NO D.L.    X    Y    Z  NEQ')
        I2=0
        DO 160 IN=1,NNT
        I1=I2+1
        I2=I2+NDIM
        ID1=KDLNC(IN)+1
        ID2=KDLNC(IN+1)
        ID=ID2-ID1+1
        IF(ID2.LT.ID1) ID2=ID1
        X1=VCORG(I1)
        IF(NDIM.GE.2) X2=VCORG(I1+1)
        IF(NDIM.GE.3) X3=VCORG(I1+2)
160     WRITE(MP,2080) IN,ID,X1,X2,X3,(KNEQ(I),I=ID1,ID2)
2080    FORMAT(2I6,3E12.5,10X,10I6)
170     RETURN
        END
C
C---------------
        SUBROUTINE BLPRND
        IMPLICIT REAL*8 (A-H,O-Z)
        CHARACTER*4 TBL
        COMMON/COOR/NDIM,NNT,NDLN,NDLT,FAC(3)
        COMMON/PRND/NPRN
        COMMON/ES/M,MR,MP,M1,MLUN(9)
        COMMON/LOC/LXX(4),LPRNG,LPREG,LLD,LLOCE,LCORE,
       1           LNE,LPRNE,LPREE,LDLE,LKE,LFE,LKGS,LKGD,LKGI,LKG,LRES
       2          ,LDLG,LME,LDLE0,LDLG0,LFG0
        COMMON VA(1)
        DATA TBL/'PRNG'/
C
        IF(M1.EQ.0) M1=MR
        READ(M1,1000) NPRN
1000    FORMAT(I5)
        WRITE(MP,2000) M,NPRN
```

```
2000  FORMAT(//'INPUT NODAL PROPERTIES',I2,' NO. OF PROPERTIES PER',
     &' NODE=',I5)
      IF(LPRNG.EQ.1) CALL ESPACE(NNT*NPRN,1,TBL,LPRNG)
      CALL EXPRND(VA(LPRNG))
      RETURN
      END
C
C------------------
      SUBROUTINE EXPRND(VPRNG)
      IMPLICIT REAL*8 (A-H,O-Z)
      COMMON/COOR/NDIM,NNT,NDLN,NDLT,FAC(3)
      COMMON/PRND/NPRN
      COMMON/ES/M,MR,MP,M1,MLUN(9)
      DIMENSION VPRNG(1)
C
      I1=NNT*NPRN
      READ(M1,1000) (VPRNG(I),I=1,I1)
1000  FORMAT(8F10.0)
      IF(M.GE.0) WRITE(MP,2000) (VPRNG(I),I=1,I1)
2000  FORMAT('>>>'/8F12.5)
      RETURN
      END
C
C-----------------
      SUBROUTINE BLPREL
      IMPLICIT REAL*8 (A-H,O-Z)
      CHARACTER*4 TBL(2)
      COMMON/PREL/NGPE,NPRE
      COMMON/ES/M,MR,MP,M1,MNUL(9)
      COMMON/LOC/LXX(5),LPREG,LOCNUL(19)
      COMMON/TRVL/IN(2),ITNUL(84)
      COMMON VA(1)
      DATA TBL/'PREG','V   '/
C
      IF(M1.EQ.0) M1=MR
      READ(M1,1000) IN
1000  FORMAT(2I5)
      IF(IN(1).GT.0) NGPE=IN(1)
      IF(IN(2).GT.0) NPRE=IN(2)
      WRITE(MP,2000) M,NGPE,NPRE
2000  FORMAT(' INPUT OF ELEMENT PROPERTIES=',I2/
     1       'NO OF GROUPS OF PEORPERTIES=',I5/
     2       'NO OF PROPERTIES PER GROUP=',I5)
      IF(LPREG.EQ.1) CALL ESPACE(NGPE*NPRE,1,TBL(1),LPREG)
      CALL ESPACE(NPRE,1,TBL(2),L1)
      CALL EXPREL(VA(LPREG),VA(L1))
      CALL VIDE(L1,1,TBL(2))
      RETURN
      END
C
C--------
      SUBROUTINE EXPREL(VPREG,V1)
      IMPLICIT REAL*8 (A-H,O-Z)
      COMMON/PREL/NGPE,NPRE
      COMMON/ES/M,MR,MP,M1,MNUL(9)
      DIMENSION VPREG(1),V1(1)
C
      WRITE(MP,2000)
2000  FORMAT(//'CARDS OF ELEMENT PROPERTIES')
      I1=MIN(7,NPRE)
      J=1
10    READ(MR,1000) IGPE,(V1(I),I=1,I1)
1000  FORMAT(I5,7F10.0)
      WRITE(MP,2010) IGPE,(V1(I),I=1,I1)
2010  FORMAT('>>>',I5,7E12.5)
      IF(IGPE.LE.0) GOTO 40
      IF(IGPE.GT.NGPE) CALL ERREUR(41,IGPE,NGPE,1)
      IF(NPRE.LE.7) GOTO 20
C.... READ THE PROPERTIES
      READ(MR,1010) (V1(I),I=8,NPRE)
```

```
1010  FORMAT(5X,7F10.0)
      WRITE(MP,2020) (V1(I),I=8,NPRE)
2020  FORMAT('>>>>>',5X,7E12.5)
20    DO 30 I=1,NPRE
      VPREG(J)=V1(I)
30    J=J+1
      GOTO 10
40    RETURN
      END
C
C=======================
      SUBROUTINE  ASSEL(IKG,IFG,IDLE,NSYM,KLOCE,KLD,VKE,VFE,VKGS,
     1  VKGD,VKGI,VFG)
      IMPLICIT REAL*8 (A-H,O-Z)
C==========
C     TO ASSEMBLE  AN ELEMENT MATRIX  AND/OR VECTOR
C     (MATRIX SYMMETRICAL  OR NOT)
C       INPUT
C          IKG       IF IKG.EQ.1  ASSEMBLE ELEMENT  MATRIX KE
C          IFG       IF IFG.EQ.1  ASSEMBLE ELEMENT  VECTOR FE
C          IDLE      ELEMENT NUMBER  OF D.O.F.
C          NSYM      O=SYMMETRIC  PROBLEM, 1=UNSYMMETRIC  PROBLEM
C          KLOCE     ELEMENT LOCALIZATION  VECTOR
C          KLD       CUMULATIVE  COLUMN HEIGHTS  OF KG
C          VKE       ELEMENT MATRIX  KE (FULL OR  UPPER TRIANGLE  BY
C                    DESCENDING  COLUMNS)
C          VFE       ELEMENT VECTOR  FE
C       OUTPUT
C          VKGS,VKGD,VKGI      GLOBAL MATRIX (SKYLINES) C
C   (SYMMETRIC  OR NOT)
C          VFG       GLOBAL LOAD  VECTOR
C==
      COMMON/LOC/LCORG,LDLNC,LNEQ,LDIMP,LPRNG,LPREG,LLD,LLOCE,LCORE,LNE,
     1   LPRNE,LPREE,LDLE,LKE,LFE,LKGS,LKGD,LKGI,LFG,LRES,LDLG,LME,
     1   LDLE0,LDLG0,LFG0
      DIMENSION  KLD(LLOCE-LLD+1),
     1 KLOCE(LCORE-LLOCE+1),
     1                                    VKE(LME-LKE+1),
     2 VFE(LDLE-LFE+1),                   VKGS(LKGD-LKGS+1),
     2 VKGD(LKGI-LKGD+1),
     2  VKGI(LFG-LKGI+1),VFG(LRES-LFG+1)
C     DIMENSION  KLOCE(1),KLD(1),VKE(1),VFE(1),VKGS(1),VKGD(1),
C    1  VKGI(1),VFG(1)
C-----------------------------------------------------------------------
C
C-------   ASSEMBLE ELEMENT MATRIX
C
      IF(IKG.NE.1)  GOTO  100
      IEQ0=IDLE
      IEQ1=1
C-------   FOR EACH COLUMN OF  KE
      DO  90 JD=1,IDLE
      IF(NSYM.NE.1)  IEQ0=JD
      JL=KLOCE(JD)
      IF(JL)  90,90,10
10    I0=KLD(JL+1)
      IEQ=IEQ1
      IQ=1
C-------   FOR EACH ROW OF KE
      DO  80 ID=1,IDLE
      IL=KLOCE(ID)
      IF(NSYM.EQ.1)  GO TO 30
      IF(ID-JD)  30,20,20
20    IQ=ID
30    IF(IL)  80,80,40
40    IJ=JL-IL
      IF(IJ)  70,50,60
C-------   DIAGONAL TERMS OF  KG
50    VKGD(IL)=VKGD(IL)+VKE(IEQ)
      GO  TO 80
```

```
C-------   UPPER TRIANGLE TERMS  OF KG
60     I=I0-IJ
       VKGS(I)=VKGS(I)+VKE(IEQ)
       GO  TO 80
C-------   LOWER TRIANGLE TERMS  OF GG
70     IF(NSYM.NE.1)  GO TO 80
       I=KLD(IL+1)+IJ
       VKGI(I)=VKGI(I)+VKE(IEQ)
80     IEQ=IEQ+IQ
90     IEQ1=IEQ1+IEQ0
C
C-------   ASSEMBLE ELEMENT LOAD  VECTOR
C
100    IF(IFG.NE.1)  GO TO 130
       DO 120 ID=1,IDLE
       IL=KLOCE(ID)
       IF(IL) 120,120,110
110    VFG(IL)=VFG(IL)+VFE(ID)
120    CONTINUE
130    RETURN
       END
C=========================
       SUBROUTINE  PRSOL(KDLNC,VCORG,VDIMP,KNEQ,VFG)
C=============================================================

C      TO PRINT  THE SOLUTION
C=
       IMPLICIT REAL*8 (A-H,O-Z)
       COMMON/COOR/NDIM,NNT,IHONG1(2),ONG(3)
       COMMON/ADD/VL,BETA,HULA,ISIMM
       COMMON/ES/M,MR,MP,MNUL(10)
       COMMON/TRVL/V(10),FX(10),ITNUL(46)
       COMMON/LOC/LCORG,LDLNC,LNEQ,LDIMP,LPRNG,LPREG,LLD,LLOCE,LCORE,LNE,
      1   LPRNE,LPREE,LDLE,LKE,LFE,LKGS,LKGD,LKGI,LFG,LRES,LDLG,LME,
      1   LDLE0,LDLG0,LFG0
C      DIMENSION VCORG(LDLNC-LCORG+1),KDLNC(LDIMP-LDLNC+1),
C     1 VDIMP(LNEQ-LDIMP+1),KNEQ(LLD-LNEQ+1),
C     2                    VFG(LRES-LFG+1)
       DIMENSION  VDIMP(1),KDLNC(1),VCORG(1),KNEQ(1),VFG(1)
       CHARACTER*4 RF,RL,FX
       DATA ZERO/0.D0/
C-------------------------------------------------------------------------
       RF=' *  '
       RL='    '
       X2=ZERO
       X3=ZERO
       WRITE(MP,2000)
2000   FORMAT(/'NODES',4X,'X',11X,'Y',11X,'Z',10X,'DEGREES OF FREEDOM (*
      1  = PRESCRIBED)'/)
       I2=0
       DO  50 IN=1,NNT
       I1=I2+1
       I2=I2+NDIM
       ID1=KDLNC(IN)+1
       ID2=KDLNC(IN+1)
       ID=ID2-ID1+1
       IF(ID2.LT.ID1)  GO  TO 50
       X1=VCORG(I1)
       IF(NDIM.GE.2)  X2=VCORG(I1+1)
       IF(NDIM.GE.3)  X3=VCORG(I1+2)
       J=ID1
       DO 40 I=1,ID
       JJ=KNEQ(J)
       IF(JJ)  10,20,30
10     V(I)=VDIMP(-JJ)
       FX(I)=RF
       GOTO 40
20     V(I)=ZERO
       FX(I)=RF
       GOTO 40
```

```
30      V(I)=VFG(JJ)
C
        FX(I)=RL
40      J=J+1
C
C
        WRITE(20,5010) X1,X2,(V(IJ),IJ=2,ID),V(1)
5010    FORMAT(2F10.4,3F10.7)
        WRITE(MP,2010)IN,X1,X2,X3,(V(II),FX(II),II=1,ID)
C WRITE RESULTS FOR READING IN TRANSPORT MODEL
        IF(ISIMM.EQ.0) THEN
           WRITE(30) (V(IJ),IJ=2,ID),V(1)
        ENDIF
2010    FORMAT(1X,I5,3E12.5,5X,5(E12.5,A4)/47X,5(E12.5,A4))
50      CONTINUE
        RETURN
        END
C================================================
      SUBROUTINE DLELM(KLOCE,VDLG,VDIMP,VDLE)
C==============
C     TO GENERATE ELEMENT D.O.F.
C=====
      IMPLICIT REAL*8 (A-H,O-Z)
      COMMON/RGDT/IEL,INUL(3),IDLE,NUL4(10)
      COMMON/ES/M,MR,MP,MNUL(10)
      DIMENSION KLOCE(1),VDLG(1),VDIMP(1),VDLE(1)
      DATA ZERO/0.D0/
C---------------------------------------------------------------------
       DO 40 ID=1,IDLE
       IL=KLOCE(ID)
       IF(IL) 10,20,30
10     VDLE(ID)=VDIMP(-IL)
       GO TO 40
20     VDLE(ID)=ZERO
       GO TO 40
30     VDLE(ID)=VDLG(IL)
40     CONTINUE
       IF(M.GE.2)  WRITE(MP,2000)  IEL,(VDLE(ID),ID=1,IDLE)
2000   FORMAT('  DEGREES OF FREEDOM  OF ELEMENT ',I5/(1X,10E12.5))
       RETURN
       END
C
C===
      SUBROUTINE  INIT(X,N,V)
C===
C     INITIALIZE  VECTOR V  TO VALUE X
C=====================================================================
      IMPLICIT REAL*8 (A-H,O-Z)
      DIMENSION V(1)
      DO 10  I=1,N
10    V(I)=X
      RETURN
      END
C=======
      SUBROUTINE  MAJ(X1,X2,N,V1,V2)
C================
C     EXECUTE  THE VECTOR  OPERATION: V2=XL*V1  + X2*V2
C        XL,X2:SCALARS    VL,V2:VECTORS
C=
      IMPLICIT REAL*8 (A-H,O-Z)
      DIMENSION  V1(1),V2(1)
C---------------------------------------------------------------------
      DO 10  I=1,N
10    V2(I)=X1*V1 (I)+X2*V2(I)
      RETURN

      END
C=============================
      SUBROUTINE  NORME(N,VDEL,V,XNORM)
C==========
```

```
C     COMPUTE  THE LENGTHS  RATIO OF VECTORS  VDEL AND V
C===
      IMPLICIT REAL*8 (A-H,O-Z)
      DIMENSION  VDEL(1),V(1)
      DATA  ZERO/0.0D0/,UN/1.00D0/,FAC/1.00D-3/
C-------------------------------------------------------------------------
      C1=ZERO
      C2=ZERO
      DO  10 I=1,N
      C1=C1+VDEL(I)*VDEL(I)
10    C2=C2+V(I)*V(I)
      C=C1*FAC
      IF(C2.LE.C)  C2=UN
      XNORM=SQRT(C1/C2)
      RETURN
      END
C
      SUBROUTINE  BLTEMP
C============
C     TO CALL  BLOCK 'TEMP'
C     TO SOLVE  AN UNSTEADY PROBLEM  (LINEAR  OR NOIJ
C===
      IMPLICIT REAL*8 (A-H,O-Z)
      CHARACTER*4 TBL(13)
      COMMON/ELEM/NUL(4),ME,NUL1(2)
      COMMON/ASSE/NSYM,NKG,NKE,NDLE
      COMMON/RESO/NEQ,NUL3(2)
      COMMON/NLIN/EPSDL,XNORM,OMEGA,XPAS,DPAS,DPAS0,NPAS,IPAS,NITER,
     1   ITER,IMETH
      COMMON/ES/M,MR,MP,M1,M2,M3,M4,MNUL(6)
      COMMON/LOC/LCORG,LDLNC,LNEQ,LDIMP,LPRNG,LPREG,LLD,LLOCE,LCORE,LNE,
     1   LPRNE,LPREE,LDLE,LKE,LFE,LKGS,LKGD,LKGI,LFG,LRES,LDLG,LME,
     1   LDLE0,LDLG0,LFG0
      COMMON  VA(1)
      DIMENSION  IN(2),XIN(3)
      DATA  TBL/'KGS ','KGD ','KGI ','FG  ','KE  ',
     1   'FE  ','RES ','DLE ','DLG ','ME  ','DLE0','DLG0','FG0 '/
C--------------------------  '
      IF(M1.EQ.0)  M1=MR
      IF(M2.EQ.0)   M2=ME
      WRITE(MP,2000)   M
2000  FORMAT(//'   UNSTEADY SOLUTION  (M=',I2,')'/1X,23('='))
C-------   TO ALLOCATE SPACE
      IF(LKGS.EQ.1)   CALL ESPACE(NKG,1,TBL(1),LKGS)
      IF(LKGD.EQ.1)   CALL ESPACE(NEQ,1,TBL(2),LKGD)
      IF(NSYM.EQ.1.AND.LKGI.EQ.1)    CALL ESPACE(NKG,1,TBL(3),LKGI)
      IF(LFG.EQ.1)   CALL  ESPACE (NEQ,1,TBL(4),LFG)
      IF(LKE.EQ.1)   CALL  ESPACE(NKE,1,TBL(5),LKE)
      IF(LFE.EQ.1)   CALL  ESPACE(NDLE,1,TBL(6),LFE)
      IF(LRES.EQ.1)   CALL  ESPACE(NEQ,1,TBL(7),LRES)
      IF(LDLE.EQ.1)   CALL  ESPACE(NDLE,1,TBL(8),LDLE)
      IF(LDLG.EQ.1)   CALL  ESPACE(NEQ,1,TBL(9),LDLG)
      IF(LME.EQ.1)    CALL ESPACE(NKE,1,TBL(10),LME)
      IF(LDLE0.EQ.1)    CALL ESPACE(NDLE,1,TBL(11),LDLE0)
      IF(LDLG0.EQ.1)    CALL ESPACE(NEQ,1,TBL(12),LDLG0)
      IF(LFG0.EQ.1)   CALL  ESPACE(NEQ,1,TBL(13),LFG0)
C-------  TO  EXECUTE THE BLOCK
      CALL   EXTEMP(VA(LCORG),VA(LDLNC),VA(LDIMP),VA(LNEQ),VA(LLD),
     1VA(LLOCE),VA(LCORE),VA(LPRNE),VA(LPREE),VA(LNE),VA(LKE),VA(LME),
     2  VA(LFE),VA(LDLE),VA(LKGS),VA(LKGD),VA(LKGI),VA(LFG),VA(LRES),
     3  VA(LDLG),VA(LDLE0),VA(LDLG0),VA(LFG0))
        RETURN
        END
C=======================
      SUBROUTINE  EXTEMP(VCORG,KDLNC,VDIMP,KNEQ,KLD,KLOCE,VCORE,VPRNE,
     1   VPREE,KNE,VKE,VME,VFE,VDLE,VKGS,VKGD,VKGI,VFG,VRES,VDLG,
     2  VDLE0,VDLG0,VFG0)
C==
C      TO EXECUTE BLOCK 'TEMP'
C      TO SOLVE AN UNSTEADY  PROBLEM (LINEAR  OR NOLJ
```

```
C=============
      IMPLICIT REAL*8 (A-H,O-Z)
       COMMON/ADD/VL,BETA,HULA,ISIMM
       COMMON/COOR/NDIM,NNT,NDLN,NDLT,FAC(3)
       COMMON/RESO/NEQ,NUL3(2)
       COMMON/COND/NCLT,NCLZ,NCLNZ
       COMMON/ASSE/NSYM,NUL2(3)
      COMMON/NLIN/EPSDL,XNORM,OMEGA,XPAS,DPAS,DPAS0,NVAS,IPAS,NITER,
     1  ITER,IMETH
      COMMON/ES/M,MR,MP,M1,M2,M3,M4,MNUL(6)
      DIMENSION  VCORG(1),KDLNC(1),VDIMP(1),KNEQ(1),KLD(1),KLOCE(1),
     1  VCORE(1),VPRNE(1),VPREE(1),KNE(1),VKE(1),VME(1),VFE(1),VDLE(1),
     2  VKGS(1),VKGD(1),VKGI(1),VFG(1),VRES(1),VDLG(1),VDLE0(1),
     3  VDLG0(1),VFG0(1)
      COMMON/LOC/LCORG,LDLNC,LNEQ,LDIMP,LPRNG,LPREG,LLD,LLOCE,LCORE,LNE,
     1    LPRNE,LPREE,LDLE,LKE,LFE,LKGS,LKGD,LKGI,LFG,LRES,LDLG,LME,
     1    LDLE0,LDLG0,LFG0
C
      COMMON/TRANS/DEPG0(500),XVELG0(500),YVELG0(500)
      COMMON/INF/AINF(500),IEXCESS,IZINF
      COMMON/SOLINI/CMLR1(100)
C
       DATA ZERO/0.D0/,UN/1.D0/
C-------------------------------"'
C       OPEN(M4,FILE='TMP3',FORM='UNFORMATTED')
       DPAS0=ZERO
       XPAS=ZERO
       IPAS=0
       IEXCESS=0
       IZINF=0
C-------   READ INITIAL  D.O.F. ON FILE  M3
       IF(M3.EQ.0) GO TO 5
       CALL MAJ(UN,ZERO,NEQ,VDLG,VDLG0)
C
C-------   SAVE THE  REFERENCE LOAD  CONDITIONS
C
5      CALL MAJ(UN,ZERO,NEQ,VFG,VFG0)
C
C-------   READ A  CARD DEFINING A SET  OF IDENTICAL  STEPS
10     READ(M1,1000)  DPAS,I1,I2,I3,X1,X2,BETA,HULA,IPRINT,ISIMM
1000   FORMAT(F10.0,3I5,4F10.0,2I5)
       IF(DPAS.EQ.ZERO)  GO TO 140
       IF(I1.GT.0)  NPAS=I1
       IF(I2.GT.0)  NITER=I2
       IF(I3.GT.0)  IMETH=I3
       IF(X1.GT.ZERO)  EPSDL=X1
       IF(X2.NE.ZERO)  OMEGA=X2
C
C-------  LOOP  OVER THE STEPS
C
      WRITE(11,5444)
5444  FORMAT(' NODE',2X,'   WATER DEPTH',' X-DIR VELOCITY',
     &'  Y-DIR VELOCITY',' FLOW RATE(L>2/T)')
C
C.....  START THE SIMULATIONS
C
      CALL INIT(ZERO,500,AINF)
C
C
      DO 130  IP=1,NPAS
      CALL  INIT(ZERO,NEQ,VFG)
      IPAS=IPAS+1
      XPAS=XPAS+DPAS
      WRITE(MP,2000)  IPAS,DPAS,XPAS,NITER,IMETH,EPSDL,OMEGA
2000  FORMAT(/1X,13('-'),'STEP   NUMBER (IPAS):',I5//
     1                14X,'INCREMENT                    (DPAS)=',E12.5/
     2                14X,'TOTAL  LEVEL                 (XPAS)=',E12.5/
     3                14X,'NUMBER  OF ITERATIONS       (NITER)=',I12/
     4                14X,'METHOD  NUMBER              (IMETH)=',I12/
     5                14X,'TOLERANCE                   (EPSDL)=',E12.5/
```

```
     6                14X,'COEFFICIENT   ALPHA          (OMEGA)=',E12.5/)
C
C-------   LOOP OVER EQUILIBRIUM  ITERATIONS
C
      IF(ISIMM.EQ.1) THEN
       DO 3000 IRUN=1,NNT
          IF(NDIM.EQ.1) THEN
           READ(30) DEPG0(IRUN),XVELG0(IRUN)
          ENDIF
          IF(NDIM.EQ.2) READ(30) XVELG0(IRUN),YVELG0(IRUN),DEPG0(IRUN)
3000   ENDDO
      ENDIF
C
       DO 110 ITER=1,NITER
C     WRITE(10,*) ' ITERATION NUMBER', ITER
C-------   CHOOSE THE  METHOD
       IF(IMETH.GT.3)  GO TO 20
C-------   EULER TYPE  METHODS
      CALL EULER(VCORG,KDLNC,VDIMP,KNEQ,KLD,KLOCE,VCORE,VPRNE,VPREE,
     1 KNE,VKE,VME,VFE,VDLE,VKGS,VKGD,VKGI,VFG,VRES,VDLG,
     2 VDLE0,VDLG0,VFG0)
      GO TO 100
C-------   OTHER METHODS  ......
20     CONTINUE
       WRITE(MP,2010)  IMETH
2010   FORMAT('  ** ERROR, METHOD:',I3,'  UNKNOWN')
       STOP
C
C-------   COMPUTE  THE NORM
C... FOR ZERO INFILTRATION : UNTIL PONDING INITIATES
100    IF(IZINF.LE.0) GOTO 120
C
C..  TREATMENT FOR NEGATIVE FLOW DEPTH
C
      IF(ISIMM.NE.0) GOTO 109
      DO INEG=1,NNT
       IF(NDIM.EQ.2) THEN
         NNEG1=KNEQ(NDLN*(INEG-1)+1)
         NNEG2=KNEQ(NDLN*(INEG-1)+2)
         NNEG3=KNEQ(NDLN*(INEG-1)+3)
         IF(NNEG1.GT.0.AND.VDLG(NNEG1).LE.0.0D0) THEN
            VDLG(NNEG1)=0.0D0
            IF(NNEG2.GT.0) VDLG(NNEG2)=0.0D0
            IF(NNEG3.GT.0) VDLG(NNEG3)=0.0D0
         ENDIF
       ELSEIF(NDIM.EQ.1) THEN
         NNEG=KNEQ(NDLN*(INEG-1)+2)
         IF(NNEG.GT.0.AND.VDLG(NNEG).LE.0.0D0) THEN
            VDLG(NNEG)=0.0D0
            IF(KNEQ(NDLN*(INEG-1)+1).GT.0) VDLG(NNEG-1)=0.0D0
         ENDIF
       ENDIF
      ENDDO
C
109    CALL NORME(NEQ,VRES,VDLG,XNORM)
       IF(XNORM.LE.EPSDL.OR.ITER.EQ.NITER) THEN
          WRITE(MP,2020)  ITER,XNORM
       ENDIF
C      WRITE(6,2020) ITER,XNORM
2020   FORMAT(5X,'ITERATION  (ITER):',I6,'  NORM (XNORM)=',E12.5)
       IF(M.GE.2)  CALL PRSOL(KDLNC,VCORG,VDIMP,KNEQ,VDLG)
       IF(XNORM.LE.EPSDL)  GO  TO 120
110    CONTINUE
C
C-------   END  OF STEP
C
120   CONTINUE
      IF(NDIM.EQ.2.AND.ISIMM.EQ.0.AND.IZINF.LE.0) THEN
       DO INEG=1,NEQ
          IF(VDLG(INEG).LT.0.1E-25) THEN
```

```
C             WRITE(6,*) ' NEGATIVE FLOW DEPTH',VDLG(INEG)
              VDLG(INEG)=0.1E-30
              VDLG(INEG+1)=0.1E-30
              VDLG(INEG+2)=0.1E-30
           ENDIF
         ENDDO
        ENDIF
C
        IF(NDIM.EQ.1.AND.ISIMM.EQ.0.AND.IZINF.LE.0) THEN
         DO INEG=1,NEQ
           IF(VDLG(INEG+1).LT.0.1E-30) THEN
C             WRITE(6,*) ' NEGATIVE OR ZERO FLOW DEPTH',VDLG(INEG+1)
              VDLG(INEG)=0.1E-30
              VDLG(INEG+1)=0.1E-30
           ENDIF
         ENDDO
        ENDIF
C......
         CALL MAJ(ZERO,ZERO,NEQ,VFG,VFG0)
         DPAS0=DPAS
         CALL  MAJ(UN,ZERO,NEQ,VDLG,VDLG0)
C.... PRINT FOR INTERPRETATION
         IF(IP.EQ.1.OR.(IP/IPRINT)*IPRINT.EQ.IP) THEN
          IF(NDIM.EQ.2) THEN
           WRITE(11,9010) ((1+(IM-1)/3),VDLG(IM),VDLG(IM+1),VDLG(IM+2),
     &    SQRT(VDLG(IM+2)*VDLG(IM+2)+VDLG(IM+1)*VDLG(IM+1))*VDLG(IM),
     &    IM=1,NEQ,3)
          ELSE
           WRITE(11,9011) ((1+(IM-1)/2),VDLG(IM),VDLG(IM+1),
     &    VDLG(IM)*VDLG(IM+1), IM=1,NEQ,2)
          ENDIF
9010      FORMAT(I5,2X,4F15.8)
9011      FORMAT(I5,2X,3F15.8)
          WRITE(20,*) ' STEP =', IP
          CALL  PRSOL(KDLNC,VCORG,VDIMP,KNEQ,VDLG)
         ENDIF
130      CONTINUE
         GO TO 10
C-------   SAVE  THE SOLUTION  ON FILE M4
140      IF(M4.NE.0)  WRITE(M4)  (VDLG(I),I=1,NEQ)
         RETURN
         END
C=====================================
       SUBROUTINE  EULER(VCORG,KDLNC,VDIMP,KNEQ,KLD,KLOCE,VCORE,VPRNE,
      1  VPREE,KNE,VKE,VME,VFE,VDLE,VKGS,VKGD,VKGI,VFG,VRES,VDLG,
      2  VDLE0,VDLG0,VFG0)
       IMPLICIT REAL*8 (A-H,O-Z)
CMS==================================
C      ALGORITHM  FOR EULER TYPE  METHODS (IMPLICIT,  EXPLICIT  OR BOTH
C      ACCORDING  TO OMEGA) FOR  LINEAR OR NON  LINEAR PRO8LEMS.
C      THE NON  LINEAR PROBLEM IS  SOLVED BY A  NEWTON-RAPHSON
C      METHOD          EULE   8
C        IMETH.EQ.L    STANDARD NEWTON-RAPHSON
C        IMETH.EQ.2    K IS CONSTANT
C        IMETH.EQ.3    K IS RECOMPUTED  AT THE BEGINNING  OF EACH  STEP
C=========================================
       COMMON/ADD/DUMM1,DUMM2,HULA,ISIMM
       COMMON/ASSE/NSYM,NKG,NUL2(2)
       COMMON/RESO/NEQ,NUL3(2)
       COMMON/NLIN/EPSDL,XNORM,OMEGA,XPAS,DPAS,DPAS0,NPAS,IPAS,NITER,
      1  ITER,IMETH
        COMMON/COOR/NDIM,NNT,NDLN,NDLT,FAC(3)
        COMMON/ES/M,MR,MP,MNUL(10)
       COMMON/LOC/LCORG,LDLNC,LNEQ,LDIMP,LPRNG,LPREG,LLD,LLOCE,LCORE,LNE,
      1   LPRNE,LPREE,LDLE,LKE,LFE,LKGS,LKGD,LKGI,LFG,LRES,LDLG,LME,
      1   LDLE0,LDLG0,LFG0
       DIMENSION VCORG(1),KDLNC(1),VDIMP(1),KNEQ(1),KLD(1),KLOCE(1),
      1  VCORE(1),VPRNE(1),VPREE(1),KNE(1),VKE(1),VME(1),VFE(1),
      2  VDLE(1),VKGS(1),VKGD(1),VKGI(1),VFG(1),VRES(1),VDLG(1),
      3  VDLE0(1),VDLG0(1),VFG0(1)
```

```
      DATA ZERO/0.D0/,UN/1.D0/
C-----------------------------------------------------------------
C-------   DECIDE IF GLOBAL  MATRIX IS  TO BE REASSEMBLED
       IKT=0
       IF(IMETH.EQ.1)  GO TO 10
       IF(DPAS.NE.DPAS0.AND.ITER.EQ.1)   GO TO 10
       IF(IMETH.EQ.3.AND.ITER.EQ.1)  GO  TO 10
       GO TO 20
10     IKT=1
C-------   INITIALIZE  GLOBAL MATRIX TO  ZERO IF NECESSARY
20     IF(IKT.EQ.0) GO  TO 30
       CALL INIT(ZERO,NKG,VKGS)
       CALL INIT(ZERO,NEQ,VKGD)
       IF(NSYM.EQ.1) CALL  INIT(ZERO,NKG,VKGI)
C-------   ASSEMBLE RESIDUALS  AND GLOBAL  MATRIX IF REQUIRED
30     CALL MAJ(UN,ZERO,NEQ,VFG0,VRES)
       CALL ASEULR(IKT,VCORG,KDLNC,VDIMP,KNEQ,KLD,KLOCE,VCORE,VPRNE,
     1   VPREE,KNE,VKE,VME,VFE,VDLE,VKGS,VKGD,VKGI,VFG,VRES,VDLG,
     2   VDLE0,VDLG0,VFG0)
       C1=UN
       IF(ITER.GT.1) C1=C1-OMEGA
       DO 40 I=1,NEQ
40     VRES(I)=DPAS*(VRES(I)-C1*VFG(I))
7030   FORMAT(E15.8)
7035  FORMAT(6E13.3)
C-------   SOLVE
       CALL SOL(VKGS,VKGD,VKGI,VRES,KLD,NEQ,MP,IKT,1,NSYM,ENERG)
C-------   UPDATE THE SOLUTION
       CALL MAJ(HULA,UN,NEQ,VRES,VDLG)
C..  CHECK THE NEGATIVE FLOW DEPH
       RETURN
       END
C=======
C
      SUBROUTINE SOL(VKGS,VKGD,VKGI,VFG,KLD,NEQ,MP,IFAC,ISOL,NSYM,ENERG)
      IMPLICIT REAL*8 (A-H,O-Z)
C=
C     TO SOLVE A  LINEAR SYSTEM (SYMMETRICAL OR NOT).
C     THE MATRIX  IS STORED IN CORE BY SKYLINES  IN ARRAYS
C     VKGS,VKGD,VKGI
C       INPUT
C          VKGS,VKGD,VKGI      SYSTEM MATRIX : UPPER, DIAGONAL AND
C                              LOWER PARTS
C          VFG                 SECOND MEMBER
C          KLD                 ADDRESSES OF COLUMN TOP TERMS
C          NEQ                 NUMBER OF EQUATIONS
C          MP                  OUTPUT DEVICE NUM8ER
C          IFAC                IF IFAC.EQ.L TRIANGULARIZE THE
C                              MATRIX
C          ISOL                IF ISOL.EQ.L COMPUTE THE SOLUTION FROM
C                              TRIANGULARIZED MATRIX
C          NSYM                INDEX FOR NONSYMMETRIC PROBLEM
C       OUTPUT
C          VKGS,VKGD,VKGI      TRIANGULARIZED MATRIX (IF IFAC.EQ.L)
C          VFG                 SOLUTION (IF ISOL.EQ.1)
C          ENERG               SYSTEM ENERGY (IF NSYM.EQ.O)
C
C
C     DIMENSION  VKGS(1),VKGD(1),VKGI(1),VFG(1),KLD(1)
      COMMON/LOC/LCORG,LDLNC,LNEQ,LDIMP,LPRNG,LPREG,LLD,LLOCE,LCORE,LNE,
     1   LPRNE,LPREE,LDLE,LKE,LFE,LKGS,LKGD,LKGI,LFG,LRES,LDLG,LME,
     1   LDLE0,LDLG0,LFG0
      DIMENSION
     1                                      KLD(LLOCE-LLD+1),
     2                                    VKGS(LKGD-LKGS+1),
     2 VKGD(LKGI-LKGD+1),
     2  VKGI(LFG-LKGI+1),VFG(LRES-LFG+1)
      DATA  ZERO/0.0D0/
C------
7030  FORMAT(6E13.4)
```

```
      IK=1
      IF(VKGD(1).NE.ZERO)   GO TO 10
      WRITE(MP,2000)  IK
      STOP
10    ENERG=ZERO
C
C-----  FOR EACH COLUMN IK TO BE MODIFIED
C
       JHK=1
       DO 100 IK=2,NEQ
C-----   ADDRESS OF THE  NEXT COLUMN  TOP TERM IK+1
       JHK1=KLD(IK+1)
C-----   HEIGHT OF COLUMN  IK (INCLUDE  UPPER AND DIAGONAL  TERMS)
       LHK=JHK1-JHK
       LHK1=LHK-1
C-----   ROW OF FIRST  TERM TO BE  MODIFIED IN COLUMN  IK
       IMIN=IK-LHK1
       IMIN1=IMIN-1
C-------   ROW  OF LAST TERM TO  BE MODIFIED IN  COLUMN IK
       IMAX=IK-1
       IF(LHK1.LT.0)  GO TO 100
       IF(IFAC.NE.1)  GO TO 90
       IF(NSYM.EQ.1)  VKGI(JHK)=VKGI(JHK)/VKGD(IMIN1)
       IF(LHK1.EQ.0)  GO TO 40
C
C-----  MODIFY NON-DIAGONAL TERM IN COLUMN IK
C
      JCK=JHK+1
      JHJ=KLD(IMIN)
C-----  FOR  EACH TERM LOCATED  AT JCK AND  CORRESPONDING  TO COLUMN IJ
      DO  30 IJ=IMIN,IMAX
      JHJ1=KLD(IJ+1)
C-----  NUMBER  OF MODIFICATIVE  TERMS FOR  COEFFICIENT  LOCATED AT JCK
      IC=MIN(JCK-JHK,JHJ1-JHJ)
      IF(IC.LE.0.AND.NSYM.EQ.0)   GO TO  20
      C1=ZERO
      IF(IC.LE.0)  GO  TO 17
      J1=JHJ1-IC
      J2=JCK-IC
      IF(NSYM.EQ.1)   GO TO 15
      VKGS(JCK)=VKGS(JCK)-SCAL(VKGS(J1),VKGS(J2),IC)
      GOTO 20
15    VKGS(JCK)=VKGS(JCK)-SCAL(VKGI(J1),VKGS(J2),IC)
      C1=SCAL(VKGS(J1),VKGI(J2),IC)
17       VKGI(JCK)=(VKGI(JCK)-C1)/VKGD(IJ)
20    JCK=JCK+1
30    JHJ=JHJ1
C
C---- MODIFY DIAGONAL TERM
C
40    JCK=JHK
      CDIAG=ZERO
      DO 70 IJ=IMIN1,IMAX
      C1=VKGS(JCK)
      IF(NSYM.EQ.1) GOTO 50
      C2=C1/VKGD(IJ)
      VKGS(JCK)=C2
      GOTO 60
50    C2=VKGI(JCK)
60    CDIAG=CDIAG+C1*C2
C
C
70    JCK=JCK+1
      VKGD(IK)=VKGD(IK)-CDIAG
      IF(VKGD(IK)) 90,80,90
80    WRITE(MP,2000) IK
2000  FORMAT(' *** ERROR,ZERO  PIVOT EQUATION ',I5)
      STOP
C
C-----  SOLVE LOWER  TRIANGULAR SYSTEM
```

```
C
90      IF(ISOL.NE.1) GO TO 100
        IF(NSYM.NE.1) VFG(IK)=VFG(IK)-SCAL(VKGS(JHK),VFG(IMIN1),LHK)
        IF(NSYM.EQ.1) VFG(IK)=VFG(IK)-SCAL(VKGI(JHK),VFG(IMIN1),LHK)
100     JHK=JHK1
        IF(ISOL.NE.1) RETURN
C
C------- SOLVE DIAGONAL TERM
C
      IF(NSYM.EQ.1)  GO TO 120
      DO  110 IK=1,NEQ
      C1=VKGD(IK)
      C2=VFG(IK)/C1
      VFG(IK)=C2
110   ENERG=ENERG+C1*C2*C2
C
C-----  SOLVE DIAGONAL SYSTEM
C
120   IK=NEQ+1
      JHK1=KLD(IK)
130   IK=IK-1
      IF(NSYM.EQ.1)  VFG(IK)=VFG(IK)/VKGD(IK)
      IF(IK.EQ.1)  RETURN
      C1=VFG(IK)
      JHK=KLD(IK)
      JBK=JHK1-1
      IF(JHK.GT.JBK) GO TO 150
      IJ=IK-JBK+JHK-1
      DO 140  JCK=JHK,JBK
      VFG(IJ)=VFG(IJ)-VKGS(JCK)*C1
140   IJ=IJ+1
150   JHK1=JHK
      GO TO 130
      END
C
      FUNCTION  SCAL(X,Y,N)
C========
C     INNER  PRODUCT OF VECTORS  X AND Y  OF LENGTH N
C        (FUNCTION TO BE  WRITTEN EVENTUALLY  IN ASSEM8LER)
C=
      IMPLICIT REAL*8 (A-H,O-Z)
      DIMENSION  X(1),Y(1)
      DATA  ZERO/0.0D0/
C---------------------------------------------------------------------
      SCAL=ZERO
      DO  10 I=1,N
      SCAL=SCAL+X(I)*Y(I)
10    CONTINUE
      RETURN
      END
      SUBROUTINE PNINV(VKSI,KEXP,VP,K1,VPN)
C=
C     EVALUATE  THE PN-INVERSE MATRIX WHICH
C     CONTAINS THE COEFFICIENTS OF FUN[TIONS N
C       INPUT        VKSI,KEXP,INEL,IDLE,ITPE,M,MP
C       WORKSPACE    VP,K1
C       OUTPUT       VPN
C=
      IMPLICIT REAL*8 (A-H,O-Z)
      COMMON/COOR/NDIM,IHONG1(3),ONG1(3)
      COMMON/RGDT/IEL,ITPE,ITPE1,IGRE,IDLE,ICE,IPRNE,IPREE,INEL,IDEG,IPG
     &,NUL4(4)
      COMMON/ES/M,MR,MP,MNUL(10)
      DIMENSION VKSI(1),KEXP(1),VP(1),K1(1),VPN(1),KDER(3)
      DATA ZERO/0.D0/,KDER/3*0/
C---------------------------------------------------------------------
C
C.......  FORM PN MATRIX !FOR ANY LAGRANGE TYPE ELEMENT)
C
C
```

```
      I0=1
      I1=1
      DO 20 IN=1,INEL
      CALL BASEP(VKSI(I1),KEXP,KDER,VP)
      I2=I0
      DO 10 IJ=1,INEL
      VPN(I2)=VP(IJ)
10    I2=I2+INEL
      I0=I0+1
20    I1=I1+NDIM
C
C..... ENDOFPNFORMATION
C
C-------  PRINT  THE PN MATRIX
      IF(M.LT.4)  GO TO 40
      WRITE(MP,2000)
2000  FORMAT(/'  PN MATRIX'/)
      ID=(INEL-1)*INEL
      DO 30 I0=1,INEL
      I1=I0+ID
30    WRITE(MP,2010)  (VPN(IJ),IJ=I0,I1,INEL)
2010  FORMAT(1X,10E13.5/(14X,9E13.5))
C-------  INVERSE  THE PN MATRIX
40    CALL INVERS(VPN,INEL,INEL,K1,DET)
      IF(DET.NE.ZERO) GO TO 50
      WRITE(MP,2020) ITPE
2020  FORMAT(' *** ERROR, PN SINGULAR,  ELEMENT TYPE: ',I3)
      STOP
C-------  PRINT  THE PN-INVERSE  MATRIX
50    IF(M.LT.4) GO TO 70
      WRITE(MP,2030)
2030  FORMAT(/' PN-INVERSE  MATRIX'/)
      DO 60 I0=1,INEL
      I1=I0+ID
60    WRITE(MP,2010)  (VPN(IJ),IJ=I0,I1,INEL)
70    RETURN
      END
C
C-----------------------------------------------------------------
      SUBROUTINE  NI(VKSI,KEXP,KDER,VP,VPN,VNI)
C
C     TO EVALUATE FUNCTIONS N OR  THEIR DERIVATIVES
C     AT POINT VKSI ON THE REFERENCE ELEMENT
C       INPUT    VKSI,KEXP,KDER,VP,VPN,IDLE,M,MP
C       OUTPUT   VNI
C=
      IMPLICIT REAL*8 (A-H,O-Z)
      COMMON/COOR/NDIM,IHONG1(3),ONG1(3)
      COMMON/RGDT/IEL,ITPE,ITPE1,IGRE,IDLE,ICE,IPRNE,IPREE,INEL,IDEG,IPG
     &,NUL4(4)
      COMMON/ES/M,MR,MP,MNUL(10)
      DIMENSION VKSI(1),KEXP(1),KDER(1),VP(1),VPN(1),VNI(1)
      DATA ZERO/0.D0/
C-----------------------------------------------------------------------
C-------  COMPUTE THE POLYNOMIAL BASIS AT POINT VKSI
      CALL BASEP(VKSI,KEXP,KDER,VP)
C-------  P*(PN-INVERSE) PRODUCT
      I0=1
      DO 20 IJ=1,INEL
      I1=I0
      C=ZERO
      DO 10 II=1,INEL
      C=C+VP(II)*VPN(I1)
10    I1=I1+1
      VNI(IJ)=C
20    I0=I0+INEL
C-------  PRINT FUNCTIONS N
      IF(M.LT.3) GO TO 30
      WRITE(MP,2000) (KDER(I),I=1,NDIM)
2000  FORMAT(/' DERIVATIVE OF N WITH ORDER ',3I2)
```

```
      WRITE(MP,2010) (VKSI(I),I=1,NDIM)
2010  FORMAT(14X,'AT POINT ',3E13.5)
      WRITE(MP,2020) (VNI(I),I=1,INEL)
2020  FORMAT(/(1X,10E13.5))
30    RETURN
      END
C
C-------------------------------------------------------
      SUBROUTINE  BASEP(VKSI,KEXP,KDER,VP)
C====================
C   TO EVALUATE THE POLYNOMIAL BASIS  AND ITS DERIVATIVES AT POINT VKSI
C       INPUT     VKSI,KEXP,KDER,IDLE,IDEG,NDIM,M,MP
C       OUTPUT    VP
C=======
      IMPLICIT REAL*8 (A-H,O-Z)
      COMMON/COOR/NDIM,IHONG1(3),ONG1(3)
      COMMON/RGDT/IEL,ITPE,ITPE1,IGRE,IDLE,ICE,IPRNE,IPREE,INEL,IDEG,IPG
     &,NUL4(4)
      COMMON/ES/M,MR,MP,MNUL(10)
      DIMENSION VKSI(1),KEXP(1),KDER(1),VP(1)
      DIMENSION PUISS(2,3)
      DATA ZERO/0.D0/,UN/1.D0/
C-------------------------------------------------------------------------
C-------  FORM SUCCESSIVE  POWERS OF  KSI,ETA,DZETA
      DO 10 I=1,NDIM
      PUISS(I,1)=UN
      DO 10 ID=1,IDEG
10    PUISS(I,ID+1)=PUISS(I,ID)*VKSI(I)
C-------  DERIVATIVES  OF ORDER KDER  WITH RESPECT TO KSI,ETA,DZETA
      DO 50 IDL=1,INEL
      C1=UN
      I0=(IDL-1)*NDIM
      DO 30 I=1,NDIM
      IDR=KDER(I)
      I0=I0+1
      IXP=KEXP(I0)+1
      J=IXP-IDR
      IF(J.LE.0) GO  TO 40
      IF(IDR.LE.0)  GO TO 30
      DO 20 ID=1,IDR
20    C1=C1*(IXP-ID)
30    C1=C1*PUISS(I,J)
      GO TO 50
40    C1=ZERO
50    VP(IDL)=C1
C-------   PRINT POLYNOMIAL  BASIS
C
       IF(M.LT.4) GO TO 60
       WRITE(MP,2000)  (KDER(I),I=1,NDIM)
2000   FORMAT(/' POLYNOMIAL  BASIS, DERIVATIVE  OF ORDER ',3I2)
       WRITE(MP,2010)  (VKSI(I),I=1,NDIM)
2010   FORMAT(19X,'AT  POINT ',3E13.5)
       WRITE(MP,2020) (VP(I),I=1,INEL)
2020   FORMAT(/(1X,10E12.5))
60     RETURN
       END
C
C-------------------------------------------------
       SUBROUTINE INVERS(VP,N,IVP,K,DET)
      IMPLICIT REAL*8 (A-H,O-Z)
C=====
C      TO INVERT A NON-SYMMETRIC MATRIX WITH SEARCH OF A
C      NON-ZERO PIVOT IN A COLUMN
C       INPUT
C           VP      MATRIX TO BE INVERTED
C           N       ORDER OF THE MATRIX
C           IVP     DIMENSION OF THE MATRIX IN THE CALLING PROGRAM
C           K       INTEGER WORKING ARRAY WITH LENGTH N
C       OUTPUT
C          VP       INVERSE MATRIX
```

```
C           DET      DETERMINANT
C
       DIMENSION VP(IVP,IVP),K(N)
       DATA ZERO/0.D0/,UN/1.D0/,EPS/1.D-13/
C-----------------------------------------------------------------
       DET=UN
       DO 5 I=1,N
5      K(I)=I
C-------   START INVERSION
       DO 80 II=1,N
C-------   SEARCH FOR NON-ZERO PIVOT IN COLUMN II
       DO 10 I=II,N
       PIV=VP(I,II)
       IF(ABS(PIV).GT.EPS) GO TO 20
10     CONTINUE
       DET=ZERO
       RETURN
C-------   EXCHANGE LINES II AND I
20     DET=DET*PIV
       IF(I.EQ.II) GO TO 40
       I1=K(II)
       K(II)=K(I)
       K(I)=I1
       DO 30 J=1,N
       C=VP(I,J)
       VP(I,J)=VP(II,J)
30     VP(II,J)=C
       DET=-DET
C-------   NORMALIZE PIVOT LINE
40     C=UN/PIV
       VP(II,II)=UN
       DO 50 J=1,N
50     VP(II,J)=VP(II,J)*C
C-------  ELIMINATION
       DO 70 I=1,N
       IF(I.EQ.II) GO TO 70
       C=VP(I,II)
       VP(I,II)=ZERO
       DO 60 J=1,N
60    VP(I,J)=VP(I,J)-C*VP(II,J)
70    CONTINUE
80    CONTINUE
C------- REORDER  THE COLUMNS OF INVERSE MATRIX
       DO 120 J=1,N
C------- FIND J1  SUCH THAT K(J1)=J
       DO 90 J1=J,N
       JJ=K(J1)
       IF(JJ.EQ.J) GO TO 100
 90    CONTINUE
100    IF(J.EQ.J1) GO TO 120
C-------  EXCHANGE COLUMNS J AND  J1
       K(J1)=K(J)
       DO 110 I=1,N
       C=VP(I,J)
       VP(I,J)=VP(I,J1)
110    VP(I,J1)=C
120    CONTINUE
       RETURN
       END
C-------------------------------------------------
C
C      SUBROUTINE FOR READING NODAL COORDINATES
       SUBROUTINE BLCOOR
       IMPLICIT REAL*8 (A-H,O-Z)
       CHARACTER*4 TBL(2)
       COMMON/COOR/NDIM,NNT,NDLN,NDLT,FAC(3)
       COMMON/ES/M,MR,MP,M1,MNUL(9)
       COMMON/ALLOC/NVA,IHONG(4)
       COMMON/LOC/LCORG,LDLNC,LOCNUL(23)
       COMMON/TRVL/FAC1(3),IN(3),ITNUL(77)
```

```
      COMMON VA(1)
      DIMENSION KDLNC(1)
      DATA ZERO/0.D0/, TBL/'CORG','DLNC'/
C
C...  BLOCK HEADING
C
      IF(M1.EQ.0) M1=MR
      READ(M1,1000) IN,FAC1
1000  FORMAT(3I5,3F10.0)
C...  DEFAULT OPTION
      IF(IN(1).GT.0) NNT=IN(1)
      IF(IN(2).GT.0) NDLN=IN(2)
      IF(IN(3).GT.0) NDIM=IN(3)
      DO 10 I=1,3
         IF(FAC1(I).NE.ZERO) FAC(I)=FAC1(I)
10    CONTINUE
C...  PRINT BLOCK PARAMETERS
      WRITE(MP,2000) M,NNT,NDLN,NDIM,FAC,NVA
2000  FORMAT(/' INPUT OF NODES =',I5,
     *       /' MAX. NUMBER OF NODES =',I5,
     1       /' MAX. NUMBER OF DOF PER NODES =',I5,
     2       /' DIMENSIONS OF PROBLEM =',I5,
     3       /' COORDINATE SCALE FACTORS =',3E12.5,
     4       /' WORKSPACE IN REAL WORDS =',I10)
C...  ALLOCATE SPACE
      IF(LCORG.EQ.1) CALL ESPACE(NNT*NDIM,1,TBL(1),LCORG)
      IF(LDLNC.EQ.1) CALL ESPACE(NNT+1,0,TBL(2),LDLNC)
C
C...  READ NODAL INPUT DATA
C
      DO 900 IND=LCORG,(LCORG+(NNT*NDIM)-1),NDIM
         READ(MR,500) ID,VA(IND),VA(IND+1)
C       READ(MR,500) ID,VA(IND)
        WRITE(20,500) ID,VA(IND),VA(IND+1)
500     FORMAT(I5,2F10.2)
900   CONTINUE
C
      CALL MKKDLNC(VA(LDLNC))
      RETURN
      END
C
      SUBROUTINE MKKDLNC(KDLNC)
      IMPLICIT REAL*8 (A-H,O-Z)
      DIMENSION FAC(3)
      COMMON/COOR/NDIM,NNT,NDLN,NDLT,FAC
      DIMENSION KDLNC(1)
      NDLT=0
      DO 901 IND=2,NNT+1
        KDLNC(IND)=NDLN
901     NDLT=NDLT+KDLNC(IND)
      RETURN
      END
      SUBROUTINE BLELEM
C=======================================================================
C     TO CALL BLOCK 'ELEM'
C     TO READ ELEMENT  DATA
C=======================================================================
      IMPLICIT REAL*8 (A-H,O-Z)
      CHARACTER*4 TBL(6)
      COMMON/COOR/NDIM,NNT,NDLN,INUL,ONG1(3)
      COMMON/PRND/NPRN
      COMMON/PREL/NGPE,NPRE
      COMMON/ELEM/NELT,NNEL,NTPE,NGRE,ME,NIDENT,NPG
      COMMON/ASSE/NSYM,NKG,NUL2(2)
      COMMON/RESO/NEQ,NUL3(2)
      COMMON/ES/M,MR,MP,M1,M2,MNUL(8)
      COMMON/LOC/LCORG,LDLNC,LNEQ,LDIMP,LPRNG,LPREG,LLD,LLOCE,LCORE,LNE,
     1  LPRNE,LPREE,LDLE,LKE,LFE,LKGS,LKGD,LKGI,LFG,LRES,LDLG,LOCNUL(4)
      COMMON VA(1)
      DIMENSION  IN(6)
```

```
      DATA TBL/'LD  ','LOCE','CORE','NE  ' ,'PRNE','PREE'/
C-----------------------------------------------
C     IF(M1.EQ.0) THEN
        M1=MR
        M2=MP
      READ(M1,1000)IN
1000  FORMAT(6I5)
      IF(IN(1).GT.0)  NELT=IN(1)
      IF(IN(2).GT.0)  NNEL=IN(2)
      IF(IN(3).GT.0)  NTPE=IN(3)
      IF(IN(4).GT.0)  NGRE=IN(4)
      IF(IN(5).NE.0)  NSYM=1
      IF(IN(6).NE.0)  NIDENT=1
      WRITE(MP,2000) M,NELT,NNEL,NTPE,NGRE,NSYM,NIDENT
2000  FORMAT(//'  INPUT OF  ELEMENTS (M=',I2,')'/'  ',20('=')/
     1  15X,'MAX.  NUMBER  OF ELEMENTS              (NELT)=',I5/
     2  15X,'MAX.  NUMBER  OF NODES PER ELEMENT     (NNEL)=',I5/
     3  15X,'DEFAULT  ELEMENT  TYPE                 (NTPE)=',I5/
     4  15X,'NUMBER  OF GROUPS  OF ELEMENTS         (NGRE)=',I5/
     5  15X,'INDEX  FOR NON  SYMMETRIC PROBLEM      (NSYM)=',I5/
     6  15X,'INDEX  FOR IDENTICAL  ELEMENTS       (NIDENT)=',I5/)
      IF(LLD.EQ.1)  CALL  ESPACE(NEQ+1,0,TBL(1),LLD)
      IF(LLOCE.EQ.1)  CALL  ESPACE(NNEL*NDLN,0,TBL(2),LLOCE)
      IF(LCORE.EQ.1)  CALL  ESPACE(NNEL*NDIM,1,TBL(3),LCORE)
      IF(LNE.EQ.1)  CALL ESPACE(NNEL,0,TBL(4),LNE)
      IF(NPRN.GT.0.AND.LPRNE.EQ.1) CALL ESPACE(NNEL*NPRN,1,TBL(5),LPRNE)
      IF(NPRE.GT.0.AND.LPREE.EQ.1)   CALL  ESPACE(NPRE,1,TBL(6),LPREE)
      CALL  EXELEM(VA(LCORG),VA(LDLNC),VA(LPRNG),VA(LPREG),VA(LLOCE),
     1       VA(LCORE),VA(LNE),VA(LPRNE),VA(LPREE),VA(LNEQ),VA(LLD))
      WRITE(MP,2010) NKG,NPG
2010  FORMAT(15X,'LENGTH OF A TRIANGLE IN KG          (NKG)=',I10/,
     1      15X,'NUMBER  OF INTEGRATION POINTS        (NPG)=',I10/)
      RETURN
      END
C
      SUBROUTINE EXELEM(VCORG,KDLNC,VPRNG,VPREG,KLOCE,VCORE,KNE,VPRNE,
     1                  VPREE,KNEQ,KLD)
C=======================================================================
C     TO EXECUTE BLOCK 'ELEM'
C     READ ELEMENTS DATA
C=======================================================================
      IMPLICIT REAL*8 (A-H,O-Z)
      COMMON/COOR/NDIM,NNT,IHONG1(2),ONG1(3)
      COMMON/PRND/NPRN
      COMMON/PREL/NGPE,NPRE
      COMMON/ELEM/NELT,NNEL,NTPE,NGRE,ME,NIDENT,NPG
      COMMON/ASSE/NSYM,NKG,NKE,NDLE
      COMMON/RGDT/IEL,ITPE,ITPE1,IGRE,IDLE,ICE,IPRNE,IPREE,INEL,IDEG,IPG
     1  ,ICODE,IDLE0,INEL0,IPG0
      COMMON/RESO/NEQ,NUL3(2)
      COMMON/ES/M,MR,MP,M1,M2,MNUL(8)
      DIMENSION VCORG(1),KDLNC(1),VPRNG(1),VPREG(1),KLOCE(1),VCORE(1),
     1          KNE(1),VPRNE(1),VPREE(1),KNEQ(1),KLD(1)
      DATA I10/10/,I15/15/
C-----------------------------------------------------------------------
C-------  INITIALIZE
      NDLE=0
      IELT=0
      M2=10
      NPG=0
      REWIND M2
      IF(M.GT.0) WRITE(MP,2000)
2000  FORMAT(//' ELEMENTS CARDS'/)
C-------  READ AN ELEMENT  CARD
10    READ(M1,1000) IEL,ITPE,IGPE,IGRE,(KNE(IN),IN=1,I10)
1000  FORMAT(16I5)
      WRITE(20,1000) IEL, (KNE(IN),IN=1,NNEL)
C     IF(M.GT.0) WRITE(MP,2010) IEL,ITPE,IGPE,IGRE,
C    1                          (KNE(IN),IN=1,I10)
2010  FORMAT(' >>>>>',16I5)
```

```
        IF(IEL) 80,80,20
C-------  NUMBER  OF NODES AND ADDITIONNAL CARDS AS REQUIRED
20      INEL=0
        I1=1
        I2=I10
30      DO 40 IN=I1,I2
        IF(KNE(IN).EQ.0) GO TO 50
        INEL=INEL+1
40      CONTINUE
        I1=I2+1
        I2=I1+I15
        READ(M1,1000) (KNE(IN),IN=I1,I2)
C        IF(M.GT.0) WRITE(MP,2010) (KNE(IN),IN=I1,I2)
         GO TO 30
C-------  CHECKING
50      IF(INEL.GT.NNEL) CALL ERREUR(51,INEL,NNEL,1)
C         IF(INCR.EQ.0) INCR=1
         IF(ITPE.EQ.0) ITPE=NTPE
         IF(IGPE.GT.NGPE) CALL ERREUR(53,IGPE,NGPE,1)
         IF(IGPE.EQ.0) IGPE=1
         IF(IGRE.GT.NGRE) CALL ERREUR(54,IGRE,NGRE,1)
        IF(IEL.GT.NELT) CALL ERREUR(55,IEL,NELT,1)
       CALL  LOCELD(KDLNC,KNE,KNEQ,KLOCE,KLD)
C-------   GENERATE ELEMENT  COORDINATES AND  PROPERTIES
       CALL  XTRELM(IGPE,VCORG,VPRNG,VPREG,KNE,VCORE,VPRNE,VPREE)
C-------   UPDATE TOTAL  NUMBER OF INLEGRATION  POINTS
55     NPG=NPG+IPG0
C-------   STORE ON  ELEMENT FILE
       CALL WRELEM(M2,KLOCE,VCORE,VPRNE,VPREE,KNE)
       IELT=IELT+1
C-------   PRINT ELEMENT  CHARACTERISTICS
C      CALL  PRELEM(KLOCE,VCORE,VPRNE,VPREE,KNE)
C-------   NEXT ELEMENT  TO BE GENERATED  OR READ
C       DO  60 IN=1,INEL
C60     KNE(IN)=KNE(IN)+INCR
       IF(IDLE.GT.NDLE)   NDLE=IDLE
C70     IEL=IEL+1
       GO  TO 10
C-------   CHECK  IF TOTAL NUMBER  OF ELEMENT IS EXCEEDED
80     IF(IELT.NE.NELT)   CALL ERREUR(57,IELT,NELT,1)
C-------   PRINT  BAND HEIGHTS
       IMA=0
       IMO=0
       I1=NEQ+1
       DO  90 I=2,I1
       J=KLD(I)
       IF(J.GT.IMA)IMA=J
90     IMO=IMO+J
       C=IMO
       C=C/NEQ
       WRITE(MP,2030)   C,IMA
2030   FORMAT(/15X,'MEAN   BAND  HEIGHT=',F8.1,'  MAXIMUM=',I5)
       IF(M.GE.2)   WRITE(MP,2040)  (KLD(I),I=1,I1)
2040   FORMAT(//'   TABLE OF  BAND HEIGHTS'/(10X,20I5))
C-------   TRANSFORM KLD INTO  ADDRESSES  OF COLUMN TOP TERM
       IF(NSYM.EQ.0)   NKE=(NDLE*(NDLE+1))/2
       IF(NSYM.EQ.1)   NKE=NDLE*NDLE
       KLD(1)=1
       DO 100 ID=2,I1
 100   KLD(ID)=KLD(ID-1)+KLD(ID)
       NKG=KLD(I1)-1
       IF(M.GE.2)   WRITE(MP,2050)  (KLD(ID),ID=1,I1)
 2050 FORMAT(//'   TABLE  OF ADDRESSES  OF COLUMN TOP TERMS   (LD)'/
      1           (10X,20I6))
       RETURN
       END
C
       SUBROUTINE   LOCELD(KDLNC,KNE,KNEQ,KLOCE,KLD)
C=======================================================================
C    TO   FORM THE ELEMENT  LOCALIZATION  TABLE (LOCE)
```

```
C    AND   UPDATE COLUMN  HEIGHTS FOR  A GIVEN ELEMENT
C=======================================================================
      IMPLICIT REAL*8 (A-H,O-Z)
      COMMON/COOR/NDIM,NNT,IHONG1(2),ONG(3)
      COMMON/RGDT/NUL(4),IDLE,NUL1(3),INEL,NUL4(6)
      DIMENSION   KDLNC(1),KNE(1),KNEQ(1),KLOCE(1),KLD(1)
      DATA  NDLMAX/32000/

C-------------------------------------------------------
C-------   GENERATE KLOCE  FROM KNEQ
       IDLE=0
       LOCMIN=NDLMAX
        DO 20 IN=1,INEL
        INN=KNE(IN)
        IF(INN.GT.NNT) CALL ERREUR(56,INN,NNT,1)
        IEQ=KDLNC(INN)
        IEQ1=KDLNC(INN+1)
10      IF(IEQ.GE.IEQ1) GO TO 20
        IEQ=IEQ+1
        IDLE=IDLE+1
        J=KNEQ(IEQ)
        KLOCE(IDLE)=J
        IF(J.LT.LOCMIN.AND.J.GT.0) LOCMIN=J
        GO TO 10
20      CONTINUE
C-------  UPDATE TABLE OF COLUMN HEIGHTS (KLD)
        DO 30 ID=1,IDLE
        J=KLOCE(ID)
        IF(J.LE.0) GO TO 30
        IH=J-LOCMIN
        IF(IH.GT.KLD(J+1))KLD(J+1)=IH
30      CONTINUE
        RETURN
        END

      SUBROUTINE XTRELM(IGPE,VCORG,VPRNG,VPREG,KNE,VCORE,VPRNE,VPREE)
C=======================================================================
C     TO GENERATE ELEMENT COORDINATES AND PROPERTIES FROM
C     GLOBAL ARRAYS
C     (IGPE: GROUP NUMBER FOR ELEMENT PROPERTIES)
C=======================================================================
      IMPLICIT REAL*8 (A-H,O-Z)
      COMMON/COOR/NDIM,IHONG1(3),ONG(3)
      COMMON/PRND/NPRN
      COMMON/PREL/NGPE,NPRE
      COMMON/RGDT/NUL(5),ICE,IPRNE,IPREE,INEL,NUL4(6)
      DIMENSION VCORG(1),VPRNG(1),VPREG(1),KNE(1),VCORE(1),
     1  VPRNE(1),VPREE(1)
C-----------------------------------------------------------------------X
C-------  GENERATE ELEMENT COORDINATES
      IPRNE=0
      ICE=0
      DO 30 IN=1,INEL
      IC=(KNE(IN)-1)*NDIM
      DO 10 I=1,NDIM
      ICE=ICE+1
      IC=IC+1
   10 VCORE(ICE)=VCORG(IC)
C-------  GENERATE ELEMENT NODAL  PROPERTIES
      IF(NPRN.EQ.0) GO TO 30
      IC=(KNE(IN)-1)*NPRN
      DO 20 I=1,NPRN
      IPRNE=IPRNE+1
      IC=IC+1
   20 VPRNE(IPRNE)=VPRNG(IC)
   30 CONTINUE
C-------  GENERATE ELEMENT PROPERTIES
      IPREE=0
      IF(NPRE.EQ.0) GO TO 50
      IC=(IGPE-1)*NPRE
```

```
      DO 40 I=1,NPRE
      IPREE=IPREE+1
      IC=IC+1
40    VPREE(IPREE)=VPREG(IC)
50    RETURN
      END
C
C-----------=======
      SUBROUTINE  PRELEM(KLOCE,VCORE,VPRNE,VPREE,KNE)
C=====================================================================
C     PRINT  DATA DEFINING AN ELEMENT
C
      IMPLICIT REAL*8 (A-H,O-Z)
      COMMON/PRND/NPRN
      COMMON/PREL/NGPE,NPRE
      COMMON/RGDT/IEL,ITPE,ITPE1,IGRE,IDLE,ICE,IPRNE,IPREE,INEL
     &,NUL4(6)
      COMMON/ES/M,MR,MP,MNUL(10)
      DIMENSION  KLOCE(1),VCORE(1),VPRNE(1),VPREE(1),KNE(1)
C-------------------------------------------
C     IF(M.GE.0)  WRITE(MP,2000) IEL,ITPE,INEL,IDLE,IPRNE,IPREE,IGRE
2000  FORMAT(10X,'ELEMENT:',I5,' TYPE:',I2,' N.P.:',I2,'  D.O.F.:',
     1  I3,' N. PROP:',I3,' EL. PROP:',I3,' GROUP:',I3)
C     IF(M.GE.0)  WRITE(MP,2010) (KNE(I),I=1,INEL)
2010  FORMAT(15X,'CONNECTIVITY  (NE)',20I5/(32X,20I5))
      IF(M.LT.1)  GO TO 10
C     WRITE(MP,2020)  (KLOCE(I),I=1,IDLE)
2020  FORMAT(15X,'LOCALIZATN  (LOCE)',20I5/(32X,20I5))
C     WRITE(MP,2030)  (VCORE(I),I=1,ICE)
2030  FORMAT(15X,'COORDINATES(CORE)',8E12.5/(32X,8E12.5))
C     IF(NPRN.GT.0)  WRITE(MP,2040)  (VPRNE(I),I=1,IPRNE)
2040  FORMAT(15X,'NOD.PROP.   (PRNE)',8E12.5/(32X,8E12.5))
C     IF(IPREE.GT.0)  WRITE(MP,2050)  (VPREE(I),I=1,IPREE)
2050  FORMAT(15X,'ELEM.   PROP.(PREE)',8E12.5/(32X,8E12.5))
10    RETURN
      END
C=======================
      SUBROUTINE   WRELEM(ME,KLOCE,VCORE,VPRNE,VPREE,KNE)
C======
C     WRITE   ELEMENT PROPERTIES ON FILE ME
C====
      IMPLICIT REAL*8 (A-H,O-Z)
      COMMON/RGDT/IEL,ITPE,ITPE1,IGRE,IDLE,ICE,IPRNE,IPREE,INEL,
     &NUL4(6)
      DIMENSION   KLOCE(1),VCORE(1),VPRNE(1),VPREE(1),KNE(1)
C-----------------------------------------"
      IPRNE1=IPRNE
      IF(IPRNE1.EQ.0)   IPRNE1=1
      IPREE1=IPREE
      IF(IPREE1.EQ.0)   IPREE1=1
      WRITE(ME) IEL,ITPE,IGRE,IDLE,ICE,IPRNE1,IPREE1,INEL,
     1          (KLOCE(I),I=1,IDLE),(VCORE(I),I=1,ICE),
     2          (VPRNE(I),I=1,IPRNE1),(VPREE(I),I=1,IPREE1),
     3          (KNE(I),I=1,INEL)
      RETURN
      END
C=====================
      SUBROUTINE   RDELEM(ME,KLOCE,VCORE,VPRNE,VPREE,KNE)
C=
C   READ   ELEMENT PROPERTIES FROM FILE ME
C====
      IMPLICIT REAL*8 (A-H,O-Z)
      COMMON/RGDT/IEL,ITPE,ITPE1,IGRE,IDLE,ICE,IPRNE,IPREE,INEL,
     &            NUL4(6)
      DIMENSION   KLOCE(1),VCORE(1),VPRNE(1),VPREE(1),KNE(1)
C---------------------------------------
      READ(ME)   IEL,ITPE,IGRE,IDLE,ICE,IPRNE,IPREE,INEL,
     1          (KLOCE(I),I=1,IDLE),(VCORE(I),I=1,ICE),
     2          (VPRNE(I),I=1,IPRNE),(VPREE(I),I=1,IPREE),
     3          (KNE(I),I=1,INEL)
```

```
      RETURN
      END
C=============================
```

2. 2-D subprogram for runoff simulation (elemt.f)

```
      SUBROUTINE ELEM01(VCORE,VPRNE,VPREE,VDLE,VKE,VFE,VME)
C=======================================================================
      IMPLICIT REAL*8(A-H,O-Z)
      COMMON/COOR/NDIM,IHONG1(3),ONG1(3)
      COMMON/ADD/VL,BETA,HULA
      COMMON/RGDT/IEL,ITPE,ITPE1,IGRE,IDLE,ICE,IPRNE,IPREE,INEL,IDEG,IPG
     1  ,ICODE,IDLE0,INEL0,IPG0
      COMMON/ES/M,MR,MP,MNUL(10)
      DIMENSION X(3),Y(3),U(3),V(3),H(3),ALPHX(3),ALPHY(3),F(3,3)
      DIMENSION VCORE(1),VPRNE(1),VPREE(1),VDLE(1),VKE(1),VFE(1),VME(1)
      DATA ONE,TWO,THREE,FOUR,G/1.0D0,2.D0,3.D0,4.0D0,9.8060/
      DATA F/4.0D0,2.0D0,2.0D0,2.0D0,4.0D0,2.0D0,2.0D0,2.0D0,4.0D0/
      DATA RP/1.3333333333333333/
C.......
       DATA ZERO/0.D0/
      IKE=IDLE*IDLE
C
C-------  INITIALIZE  VKE
C
300   DO  310 I=1,IKE
310   VKE(I)=ZERO
C
C.. BETA IS TO GIVE A DEPTH FOR DEPRESSION STORAGE
C...  VL : AREA OF THE ELEMENT
      X1=VCORE(1)
      Y1=VCORE(2)
      X2=VCORE(3)
      Y2=VCORE(4)
      X3=VCORE(5)
      Y3=VCORE(6)
      H1=VDLE(1)
      U1=VDLE(2)
      V1=VDLE(3)
      H2=VDLE(4)
      U2=VDLE(5)
      V2=VDLE(6)
      H3=VDLE(7)
      U3=VDLE(8)
      V3=VDLE(9)
C
      U(1)=TWO*U1+U2+U3
      U(2)=U1+TWO*U2+U3
      U(3)=U1+U2+TWO*U3
      V(1)=TWO*V1+V2+V3
      V(2)=V1+TWO*V2+V3
      V(3)=V1+V2+TWO*V3
      H(1)=TWO*H1+H2+H3
      H(2)=H1+TWO*H2+H3
      H(3)=H1+H2+TWO*H3
      X(1)=X3-X2
      X(2)=X1-X3
      X(3)=X2-X1
      Y(1)=Y2-Y3
      Y(2)=Y3-Y1
      Y(3)=Y1-Y2
      VL=0.5D0*(X2*Y3-X3*Y2+X1*Y2-X2*Y1+X3*Y1-X1*Y3)
C
C  ..  TO AVOID FLOATING POINT OVERFLOW ERROR
C.. X- DIRECTION
C
      UV1=DSQRT(U1*U1+V1*V1)
      UV2=DSQRT(U2*U2+V2*V2)
      UV3=DSQRT(U3*U3+V3*V3)
C
      IF(H1.LT.BETA.OR.UV1.LT.BETA) THEN
       ALPHX(1)=0.0D0
```

```
        ELSE
        ALPHX(1)=UV1*VPREE(2)*VPREE(2)/(1.0D0*H1**RP)
       ENDIF
       IF(H2.LT.BETA.OR.UV2.LT.BETA) THEN
        ALPHX(2)=0.0D0
        ELSE
        ALPHX(2)=UV2*VPREE(2)*VPREE(2)/(1.0D0*H2**RP)
       ENDIF
       IF(H3.LT.BETA.OR.UV3.LT.BETA) THEN
        ALPHX(3)=0.0D0
       ELSE
        ALPHX(3)=UV3*VPREE(2)*VPREE(2)/(1.0D0*H3**RP)
       ENDIF
C
C... CONSTRUCTING [K] MATRIX FOR TRIANGULAR ELEMENT
C
       COEF=ONE/24.0D0
C
C..  THE FIRST DIAGONAL
       I=1
       DO I1=1,3
          DO J=1,3
             VKE(I)=(U(J)*Y(I1)+V(J)*X(I1))*COEF
             VKE(I+10)=VKE(I)+F(I1,J)*G*ALPHX(I1)*VL*COEF
             VKE(I+20)=VKE(I)+F(I1,J)*G*ALPHX(I1)*VL*COEF
             I=I+3
          ENDDO
          I=I+18
       ENDDO
C
C... SECONDARY DIAGONALS
C
       DO I=2,8,3
          VKE(I)=FOUR*G*Y(1)*COEF
          VKE(I+27)=FOUR*G*Y(2)*COEF
          VKE(I+54)=FOUR*G*Y(3)*COEF
          VKE(I+1)=FOUR*G*X(1)*COEF
          VKE(I+28)=FOUR*G*X(2)*COEF
          VKE(I+55)=FOUR*G*X(3)*COEF
       ENDDO
C
C...  TERTIAL DIAGONALS
C
       I=10
       DO I1=1,3
          DO J=1,3
             VKE(I)=H(J)*Y(I1)*COEF
             VKE(I+9)=H(J)*X(I1)*COEF
             I=I+3
          ENDDO
          I=I+18
       ENDDO
C
C=================================
C-------  MASS MATRIX [C] =========
C=================================
C
500    DO 510 I=1,IKE
510    VME(I)=ZERO
C
       COEF=VL/12.0D0
C
       I1=0
       I2=7
       I3=22
       VME(I2)=COEF
       VME(I3)=COEF
       DO I=1,9
          I1=I1+I
          VME(I1)=TWO*COEF
```

```
C
         IF(I.GE.5) THEN
            I2=I2+I
            VME(I2)=COEF
         ENDIF
C
         IF(I.GE.8) THEN
            I3=I3+I
            VME(I3)=COEF
         ENDIF
      ENDDO
C
C-------  EVALUATE THE ELEMENT  RESIDUAL [K]*[U] MATRIX
C
600   DO 605 I=1,IDLE
605   VFE(I)=ZERO
      DO 610 J=1,IDLE
         SUM=0.0D0
         DO 620 I=1,IDLE
            SUM=SUM+VKE((I-1)*IDLE+J)*VDLE(I)
620      CONTINUE
610   VFE(J)=SUM
      RETURN
      END
C
C
C...SUBPROGRAM MATRIX CALCULATION (SYMMETRIC * NON-SYNNETRIC)
      SUBROUTINE MATMUL(A,B)
      IMPLICIT REAL*8 (A-H,O-Z)
      DIMENSION A(9,9),B(1),B1(9,9),C(9,9)
C
      M=0
      DO 10 I=1,9
         DO 10 J=1,I
            M=M+1
            B1(I,J)=B(M)
10    B1(J,I)=B(M)
C
      DO 30 I=1,9
         DO 30 J=1,9
30    C(I,J)=A(I,J)+B1(I,J)
C
      DO 50 I=1,9
         DO 50 J=1,9
            A(I,J)=C(I,J)
50    CONTINUE
      RETURN
      END
C
       SUBROUTINE ASEULR(IKT,VCORG,KDLNC,VDIMP,KNEQ,KLD,KLOCE,VCORE,
     1  VPRNE,VPREE,KNE,VKE,VME,VFE,VDLE,VKGS,VKGD,VKGI,VFG,VRES,
     2  VDLG,VDLE0,VDLG0,VFG0)
C=
C      TO ASSEM8LE THE RESIDUALS  AND THE GLOBAL  MATRIX (IF IKT.EQ.1)
C      WHILE LOOPING OVER THE  ELEMENTS (FOR EULER  METHOD)
C==
       IMPLICIT REAL*8(A-H,O-Z)
       COMMON/ELEM/NELT,NNEL,NTPE,NGRE,ME,NIDENT,NUL1
       COMMON/ASSE/NSYM,NUL2(3)
       COMMON/RESO/NEQ,NUL3(2)
       COMMON/INF/AINF(600),IEXCESS,IZINF
      COMMON/RGDT/IEL,ITPE,ITPE1,IGRE,IDLE,ICE,IPRNE,IPREE,INEL,IDEG,IPG
     1  ,ICOD,NUL4(3)
       COMMON/NLIN/EPSDL,XNORM,OMEGA,XPAS,DPAS,DPAS0,NPAS,IPAS,NITER,
     1  ITER,IMETH
      COMMON/ES/M,MR,MP,M1,M2,MNUL(8)
      COMMON/ADD/VL,BETA,HULA
      DIMENSION  VCORG(1),KDLNC(1),VDIMP(1),KNEQ(1),KLD(1),KLOCE(1),
     1 VCORE(1),VPRNE(1),VPREE(1),KNE(1),VKE(1),VME(1),VFE(1),VDLE(1),
     2 VKGS(1),VKGD(1),VKGI(1),VFG(1),VRES(1),VDLG(1),VDLE0(1),
```

```
     3 VDLG0(1),VFG0(1)
      DIMENSION VRE(9),RAIN(700)
      DATA  UN/1.D0/
      DATA G/9.806/
C-------------------------------------------------------------------------
      CC=DPAS*OMEGA
      M2=2
      IFE=0
      IF(ITER.GT.1)  IFE=1
C-------   REWIND ELEMENT  FILE (ME)
      CLOSE(UNIT=M2)
      OPEN(UNIT=M2,FILE='tri10.out',form='unformatted')
C     REWIND  M2
C-------   LOOP OVER THE  ELEMENTS
C...  READ RAINFALL DATA
      IF(ITER.EQ.1) THEN
        READ(MR,505) RAIN0
        DO I=1,NELT
         RAIN(I)=RAIN0
        ENDDO
      ENDIF
505   FORMAT(8F10.4)
      DO  90 IE=1,NELT
C-------   READ AN ELEMENT
      CALL  RDELEM(M2,KLOCE,VCORE,VPRNE,VPREE,KNE)
C-------   FIND ELEMENT  D.O.F. FROM  VFG
10    CALL  DLELM(KLOCE,VDLG,VDIMP,VDLE)
C-------   COMPUTE THE  RESIDUAL K.U. AND [M], [K]
C
      CALL ELEM01(VCORE,VPRNE,VPREE,VDLE,VKE,VFE,VME)
C
C-------   RESIDUALS  OF THE FIRST ITERATION  IN EACH  STEP (LINEAR)
15    IF(ITER.GT.1)   GO TO 20
      VRAIN=RAIN(IE)
C
      IF(VPREE(4).LT.0.0D0) GOTO 5090
C...  ESTIMATION OF RAINFALL EXCESS
C
      ALB=VPREE(3)
      FMIN0=VPREE(4)
C...  CALLING SUBROUTINE FOR ACCUMULATIVE INFILTRATION
      IF(VRAIN.LE.FMIN0) THEN
          FMIN=VRAIN
        ELSE
          FMIN=FMIN0
      ENDIF
C     WRITE(*,*) 'FMIN',FMIN
C
      CALL INFCAP(AINF(IE),F1,DPAS,FMIN,ALB,0.8)
C
      IF((VRAIN*DPAS).LT.(F1-AINF(IE))) THEN
          AINF(IE)=VRAIN*DPAS+AINF(IE)
          VRAIN=0.0D0
        ELSE
          VRAIN=(VRAIN*DPAS-F1+AINF(IE))/DPAS
          AINF(IE)=F1
      ENDIF
C
5090  WRITE(50) VRAIN
      IF(VRAIN.GT.0.1E-30) IZINF=IZINF+1
5010  FORMAT(10F10.0)
      DO IRAIN=1,9
         VRE(IRAIN)=0.0D0
      ENDDO
      A1=VCORE(1)-VCORE(3)
      B1=VCORE(1)-VCORE(5)
      A2=VCORE(2)-VCORE(4)
      B2=VCORE(2)-VCORE(6)
      A3=VPRNE(1)-VPRNE(2)
      B3=VPRNE(1)-VPRNE(3)
```

```
C.. SLOPE IN X AND Y DIRECTION
      S0X=(A2*B3-A3*B2)/(A1*B2-A2*B1)
      S0Y=(A3*B1-A1*B3)/(A1*B2-A2*B1)
C..
      DO IR=1,7,3
         VRE(IR)=VL*VRAIN/3.0D0
         VRE(IR+1)=VL*S0X*G/3.0D0
         VRE(IR+2)=VL*S0Y*G/3.0D0
      ENDDO
C
      CALL  ASSEL(0,1,IDLE,NSYM,KLOCE,KLD,VKE,VRE,VKGS,VKGD,VKGI,VFG0)
      CALL  ASSEL(0,1,IDLE,NSYM,KLOCE,KLD,VKE,VRE,VKGS,VKGD,VKGI,VRES)
C
      CALL  ASSEL(0,1,IDLE,NSYM,KLOCE,KLD,VKE,VFE,VKGS,VKGD,VKGI,VFG)
7010  FORMAT(F15.10)
20    CONTINUE
      CALL  DLELM(KLOCE,VDLG0,VDIMP,VDLE0)
      DO  30 I=1,IDLE
      VDLE(I)=(VDLE0(I)-VDLE(I))/DPAS
30    VFE(I)=-OMEGA*VFE(I)
C-------   PRODUCT  M . U
      VFE(1)=VFE(1)+VME(1)*VDLE(1)
      II=1
      DO  50 J=2,IDLE
      J1=J-1
      DO  40 I=1,J1
      II=II+1
      VFE(I)=VFE(I)+VME(II)*VDLE(J)
40    VFE(J)=VFE(J)+VME(II)*VDLE(I)
      II=II+1
50    VFE(J)=VFE(J)+VME(II)*VDLE(J)
C
C----------RLATRIX M + DPAS.OMEGA. K
60    CONTINUE
C      IF(IKT.EQ.0)   GO  TO 80
      II=0
      DO  70 I=1,IDLE
      DO  70 J=1,IDLE
      II=II+1
70    VKE(II)=VKE(II)*CC
C
      CALL MATMUL(VKE,VME)
C
C------- ASSEMBLE  THE RESIDUAL  AND  THE GLOBAL MATRIX
C
7020  FORMAT(6E12.5)
C
80    CALL ASSEL(IKT,IFE,IDLE,NSYM,KLOCE,KLD,VKE,VFE,VKGS,VKGD,VKGI,
     1  VRES)
C
90    ITPE1=ITPE
      RETURN
      END
C
        SUBROUTINE INFCAP(F0,F1,DELT,FMIN,AL,ALPH)
      IMPLICIT DOUBLE PRECISION (A-H,O-Z)
C
C  THIS SUBROUTINE CALCULATES ACCUMULATED INFILTRATION AT EACH CHANNEL
C  NODE.
C
C    F1 = ACCUM. INFILT. AT TIME T+DELT IN FT. (OUTPUT)
C    F0 = ACCUM.     "    AT TIEM T      IN FT. (INPUT)
C    AL = B IN THE FORMULA
C    DELT = TIME INTERVAL
C    FMIN = HYDRAULIC CONDUCTIVITY
C    ALPH = INTERPOLATING COEFFICIENT
C
C-------------------------------------------------------------------------
C
      DATA TOL /0.0005/
```

```
C
      FX = F0 + FMIN*DELT
      IF (FX .GT. 2.) GO TO 20
C
      DO 16 K=1,990
         ERF = FX/(1-ALPH) + AL/(ALPH-1)*LOG(ALPH-1+EXP(FX*ALPH/AL))
     &       - FMIN*DELT
     &       - F0/(1-ALPH) - AL/(ALPH-1)*LOG(ALPH-1+EXP(F0*ALPH/AL))
C        WRITE(*,*) ' ALPH,FX,AL=',ALPH,FX,AL
         DERFDX = 1.0 - ALPH / ( ALPH - 1 + EXP(FX*ALPH/AL) )
         CORR = ERF/DERFDX
         FX = FX - CORR
         IF(ABS(CORR/FX) .LT. TOL) GO TO 20
C
   16 CONTINUE
C     NO CONVERGENCE AFTER 30 ITERATIONS
C
   20 CONTINUE
      F1 = FX
      RETURN
      END
```

3. 1-D subprogram for runoff simulation (elemo.f)

```
C=======
      SUBROUTINE ASEULR(IKT,VCORG,KDLNC,VDIMP,KNEQ,KLD,KLOCE,VCORE,
     1  VPRNE,VPREE,KNE,VKE,VME,VFE,VDLE,VKGS,VKGD,VKGI,VFG,VRES,
     2  VDLG,VDLE0,VDLG0,VFG0)
C=
C      TO ASSEM8LE THE RESIDUALS  AND THE GLOBAL  MATRIX (IF IKT.EQ.1)
C      WHILE LOOPING OVER THE  ELEMENTS (FOR EULER  METHOD)
C==
      IMPLICIT REAL*8(A-H,O-Z)
      COMMON/ELEM/NELT,NNEL,NTPE,NGRE,ME,NIDENT,NUL1
      COMMON/ASSE/NSYM,NUL2(3)
      COMMON/RESO/NEQ,NUL3(2)
     COMMON/RGDT/IEL,ITPE,ITPE1,IGRE,IDLE,ICE,IPRNE,IPREE,INEL,IDEG,IPG
     1  ,ICOD,NUL4(3)
      COMMON/NLIN/EPSDL,XNORM,OMEGA,XPAS,DPAS,DPAS0,NPAS,IPAS,NITER,
     1  ITER,IMETH
      COMMON/ES/M,MR,MP,M1,M2,MNUL(8)
      COMMON/ADD/VL,BETA,HULA
      COMMON/INF/AINF(500),IEXCESS,IZINF
      DIMENSION  VCORG(1),KDLNC(1),VDIMP(1),KNEQ(1),KLD(1),KLOCE(1),
     1 VCORE(1),VPRNE(1),VPREE(1),KNE(1),VKE(1),VME(1),VFE(1),VDLE(1),
     2 VKGS(1),VKGD(1),VKGI(1),VFG(1),VRES(1),VDLG(1),VDLE0(1),
     3 VDLG0(1),VFG0(1)
      DIMENSION VRE(4),VRAIN(500)
      DATA  UN/1.D0/
C-------------------------------------------------------------------------
      CC=DPAS*OMEGA
      M2=2
      IFE=0
      IF(ITER.GT.1)  IFE=1
C-------   REWIND ELEMENT  FILE (ME)
      CLOSE(UNIT=M2)
      OPEN(UNIT=M2,FILE='one10.out',form='unformatted')
C     REWIND  M2
C.... READ RAINFALL DATA FOR EACH ELEMENT
      IF(ITER.EQ.1) THEN
       READ(MR,5010) VRAIN0
        DO IR=1,NELT
         VRAIN(IR)=VRAIN0
        ENDDO
5010   FORMAT(8E10.5)
      ENDIF
C-------   LOOP OVER THE  ELEMENTS
      DO  90 IE=1,NELT
C-------   READ AN ELEMENT
      CALL  RDELEM(M2,KLOCE,VCORE,VPRNE,VPREE,KNE)
C-------   FIND ELEMENT  D.O.F. FROM  VFG
10    CALL  DLELM(KLOCE,VDLG,VDIMP,VDLE)
C-------   COMPUTE THE  RESIDUAL K.U. AND [M], [K]
      CALL ELEM01(VCORE,VPRNE,VPREE,VDLE,VKE,VFE,VME)
C
C-------   RESIDUALS  OF THE FIRST ITERATION  IN EACH  STEP (LINEAR)
15    IF(ITER.GT.1)   GO TO 20
      DO IRAIN=1,4
         VRE(IRAIN)=0.0D0
      ENDDO
      S0=(VPRNE(1)-VPRNE(2))/VL
C
C...  ESTIMATE INFILTRATION AMOUNT AND GET RAINFALL EXCESS
      IF(VPREE(5).LT.0.0) GOTO 5090
      ALB=VPREE(4)
      FMIN0=VPREE(5)
C
C... FOR ZERO RAINFALL
C
```

```
      IF(VRAIN(IE).LT.1.0E-30) THEN
           GOTO 5001
      ENDIF
C...  CALLING SUBROUTINE FOR ACCUMULATIVE INFILTRATION
      IF(VRAIN(IE).LE.FMIN0) THEN
         FMIN=VRAIN(IE)
       ELSE
         FMIN=FMIN0
      ENDIF
C
 5001  CALL INFCAP(AINF(IE),F1,DPAS,FMIN,ALB,0.8)
C
C...     AINF : ACCUMULATIVE INFILITRATION
C...     VRAIN(IE) : RAINFALL EXCESS
      IF((VRAIN(IE)*DPAS).LT.(F1-AINF(IE))) THEN
         IF(VRAIN(IE).LT.1.0E-30) THEN
           VRAIN(IE)=-FMIN0/10.0D0
          ELSE
           AINF(IE)=VRAIN(IE)*DPAS+AINF(IE)
           VRAIN(IE)=0.0D0
         ENDIF
        ELSE
         VRAIN(IE)=(VRAIN(IE)*DPAS+AINF(IE)-F1)/DPAS
         AINF(IE)=F1
      ENDIF
C   WRITE RAINFALL EXCESS
5090  WRITE(50) VRAIN(IE)
      IF(VRAIN(IE).GT.0.1E-30) IZINF=IZINF+1
C
      VRE(1)=S0*VL/2.0D0
      VRE(3)=S0*VL/2.0D0
      VRE(2)=VRAIN(IE)*VPREE(3)/(2.0D0*VPREE(1))
      VRE(4)=VRAIN(IE)*VPREE(3)/(2.0D0*VPREE(1))
      CALL  ASSEL(0,1,IDLE,NSYM,KLOCE,KLD,VKE,VRE,VKGS,VKGD,VKGI,VFG0)
      CALL  ASSEL(0,1,IDLE,NSYM,KLOCE,KLD,VKE,VRE,VKGS,VKGD,VKGI,VRES)
C
      CALL  ASSEL(0,1,IDLE,NSYM,KLOCE,KLD,VKE,VFE,VKGS,VKGD,VKGI,VFG)
C     WRITE(10,7010) (VFG(III),III=1,4)
7010  FORMAT(F15.10)
      GO  TO 60
C-------   RESIDUALS  AFTER FIRST ITERATION
20    CONTINUE
      CALL  DLELM(KLOCE,VDLG0,VDIMP,VDLE0)
      DO  30 I=1,IDLE
      VDLE(I)=(VDLE0(I)-VDLE(I))/DPAS
30    VFE(I)=-OMEGA*VFE(I)
C-------   PRODUCT  M . U
      VFE(1)=VFE(1)+VME(1)*VDLE(1)
      II=1
      DO  50 J=2,IDLE
      J1=J-1
      DO  40 I=1,J1
      II=II+1
      VFE(I)=VFE(I)+VME(II)*VDLE(J)
40    VFE(J)=VFE(J)+VME(II)*VDLE(I)
      II=II+1
50    VFE(J)=VFE(J)+VME(II)*VDLE(J)
C
C----------RLATRIX M + DPAS.OMEGA. K
60    CONTINUE
C      IF(IKT.EQ.0)   GO  TO 80
      II=0
      DO  70 I=1,IDLE
      K=I
      DO  70 J=1,IDLE
      II=II+1
      IF(I.LE.2) THEN
         K=K+(J-1)
      ENDIF
      IF(I.EQ.3) THEN
```

```
        IF(J.NE.IDLE) K=I+J
        IF(J.EQ.IDLE) K=I+J+2
      ENDIF
      IF(I.EQ.4) THEN
        K=I+J+2
      ENDIF
70    VKE(II)=VKE(II)*CC+VME(K)
C------- ASSEMBLE  THE RESIDUAL  AND  THE GLOBAL MATRIX
C
7020  FORMAT(4F15.10)
C
80    CALL ASSEL(IKT,IFE,IDLE,NSYM,KLOCE,KLD,VKE,VFE,VKGS,VKGD,VKGI,
     1  VRES)
C
90    ITPE1=ITPE
      RETURN
      END
C
      SUBROUTINE ELEM01(VCORE,VPRNE,VPREE,VDLE,VKE,VFE,VME)
C=======================================================================
      IMPLICIT REAL*8(A-H,O-Z)
      COMMON/COOR/NDIM,IHONG1(3),ONG1(3)
      COMMON/ADD/VL,BETA,HULA
      COMMON/RGDT/IEL,ITPE,ITPE1,IGRE,IDLE,ICE,IPRNE,IPREE,INEL,IDEG,IPG
     1  ,ICODE,IDLE0,INEL0,IPG0
      COMMON/ES/M,MR,MP,MNUL(10)
      DIMENSION VCORE(1),VPRNE(1),VPREE(1),VDLE(1),VKE(1),VFE(1),VME(1)
      DATA ONE,TWO,THREE,G/1.0D0,2.D0,3.D0,9.806D0/
C.......
       DATA ZERO/0.D0/
      IKE=IDLE*IDLE
C
C-------  CHOOSE  FUNCTION TO BE  EXECUTED
C-------  COMPUTE ELEMENT STIFFNESS MATRIX
C-------  INITIALIZE  VKE
300   DO  310 I=1,IKE
310   VKE(I)=ZERO
C.. BETA IS TO GIVE A DEPTH FOR DEPRESSION STORAGE
C
      VL=ABS(VCORE(2)-VCORE(1))
      U1=VDLE(1)
      U2=VDLE(3)
      H1=VDLE(2)
      H2=VDLE(4)
      AVH=(H1+H2)/TWO
      AVU=(U1+U2)/TWO
      IF(AVH.LT.BETA.OR.DABS(AVU).LT.BETA) THEN
          ALPH=0.0D0
          AVU=0.0D0
C          U1=0.0D0
C          U2=0.0D0
        ELSE
          ALPH=VPREE(2)*VPREE(2)/(1.0D0*AVH**(4.0D0/3.0D0))
      ENDIF
      COEF=ONE/(TWO*THREE)
      VKE(1)=COEF*((-TWO*U1-U2)/G+TWO*DABS(AVU)*VL*ALPH)
      VKE(2)=COEF*(-TWO*H1-H2)
      VKE(3)=COEF*((-U1-TWO*U2)/G+DABS(AVU)*VL*ALPH)
      VKE(4)=COEF*(-H1-TWO*H2)
      VKE(5)=COEF*(-THREE)
      VKE(6)=COEF*(-TWO*U1-U2)
      VKE(7)=COEF*(-THREE)
      VKE(8)=COEF*(-U1-TWO*U2)
      VKE(9)=COEF*((TWO*U1+U2)/G+DABS(AVU)*VL*ALPH)
      VKE(10)=COEF*(TWO*H1+H2)
      VKE(11)=COEF*((U1+TWO*U2)/G+TWO*DABS(AVU)*VL*ALPH)
      VKE(12)=COEF*(H1+TWO*H2)
      VKE(13)=COEF*THREE
      VKE(14)=COEF*(TWO*U1+U2)
      VKE(15)=COEF*(THREE)
```

```
      VKE(16)=COEF*(U1+TWO*U2)
1010  FORMAT(4F15.10)
C
C=================================
C-------  MASS MATRIX [C] =========
C=================================
C
500   DO 510 I=1,IKE
510   VME(I)=ZERO
C
      COEF=VL/6.0D0
      VME(1)=COEF*TWO/G
      VME(3)=COEF*TWO
      VME(4)=COEF*ONE/G
      VME(6)=COEF*TWO/G
      VME(8)=COEF*ONE
      VME(10)=COEF*TWO
C
C-------  EVALUATE THE ELEMENT  RESIDUAL [K]*[U] MATRIX
C
600   DO 605 I=1,IDLE
605   VFE(I)=ZERO
      DO 610 J=1,4
         SUM=0.0D0
         DO 620 I=1,4
            SUM=SUM+VKE((I-1)*4+J)*VDLE(I)
620      CONTINUE
610   VFE(J)=SUM
1020  FORMAT(F15.10)
      RETURN
      END
C
        SUBROUTINE INFCAP(F0,F1,DELT,FMIN,AL,ALPH)
      IMPLICIT DOUBLE PRECISION (A-H,O-Z)
C
C  THIS SUBROUTINE CALCULATES ACCUMULATED INFILTRATION AT EACH CHANNEL
C  NODE.
C
C    F1 = ACCUM. INFILT. AT TIME T+DELT IN FT. (OUTPUT)
C    F0 = ACCUM.    "    AT TIEM T      IN FT. (INPUT)
C    AL = B IN THE FORMULA
C    DELT = TIME INTERVAL
C    FMIN = HYDRAULIC CONDUCTIVITY
C    ALPH = INTERPOLATING COEFFICIENT
C
C-------------------------------------------------------------------------------
C     COMMON /IO/ IREAD, IWRITE, IDIAGN, JREAD, IPOND
C
      DATA TOL /0.0005/
C
      FX = F0 + FMIN*DELT
C** CHECK TO PREVENT UNDERFLOW (IF INFILTRATED VOLUME .GT. 2 FT)
      IF (FX .GT. 2.) GO TO 20
C
      DO 16 K=1,990
         ERF = FX/(1-ALPH) + AL/(ALPH-1)*LOG(ALPH-1+EXP(FX*ALPH/AL))
     &       - FMIN*DELT
     &       - F0/(1-ALPH) - AL/(ALPH-1)*LOG(ALPH-1+EXP(F0*ALPH/AL))
         DERFDX = 1.0 - ALPH / ( ALPH - 1 + EXP(FX*ALPH/AL) )
         CORR = ERF/DERFDX
         FX = FX - CORR
CD!      STOPPING CRITERIA OF WALRUS*5
         IF(ABS(CORR/FX) .LT. TOL) GO TO 20
C
   16 CONTINUE
20    CONTINUE
      F1 = FX
      RETURN
      END
```

3. 2-D subprogram for sediment transport (sedt.f)

```
C=======
      SUBROUTINE ASEULR(IKT,VCORG,KDLNC,VDIMP,KNEQ,KLD,KLOCE,VCORE,
     1  VPRNE,VPREE,KNE,VKE,VME,VFE,VDLE,VKGS,VKGD,VKGI,VFG,VRES,
     2  VDLG,VDLE0,VDLG0,VFG0)
C=
C       TO ASSEMBLE THE RESIDUALS  AND THE GLOBAL  MATRIX (IF IKT.EQ.1)
C       WHILE LOOPING OVER THE  ELEMENTS (FOR EULER  METHOD)
C==
       IMPLICIT REAL*8(A-H,O-Z)
       COMMON/ELEM/NELT,NNEL,NTPE,NGRE,ME,NIDENT,NUL1
       COMMON/COOR/NDIM,NNT,IHONG1(2),ONG1(3)
       COMMON/ASSE/NSYM,NUL2(3)
       COMMON/RESO/NEQ,NUL3(2)
      COMMON/RGDT/IEL,ITPE,ITPE1,IGRE,IDLE,ICE,IPRNE,IPREE,INEL,IDEG,IPG
     1  ,ICOD,NUL4(3)
       COMMON/NLIN/EPSDL,XNORM,OMEGA,XPAS,DPAS,DPAS0,NPAS,IPAS,NITER,
     1  ITER,IMETH
      COMMON/ES/M,MR,MP,M1,M2,MNUL(8)
      COMMON/ADD/VL,BETA,HULA,ISIMM
      COMMON/INF/AINF(600),IEXCESS,IZINF
      DIMENSION  VCORG(1),KDLNC(1),VDIMP(1),KNEQ(1),KLD(1),KLOCE(1),
     1 VCORE(1),VPRNE(1),VPREE(1),KNE(1),VKE(1),VME(1),VFE(1),VDLE(1),
     2 VKGS(1),VKGD(1),VKGI(1),VFG(1),VRES(1),VDLG(1),VDLE0(1),
     3 VDLG0(1),VFG0(1)
      DIMENSION VRE(3),VRAIN(600),XVELG(500),DEPG(500),XVELE(3),DEPE(3),
     1          YVELE(3),YVELG(500)
      COMMON/TRANS/ DEPG0(500),XVELG0(500),YVELG0(500)
      DATA  UN/1.D0/
C-------------------------------------------------------------------------
      CC=DPAS*OMEGA
      IFE=0
      IF(ITER.GT.1)  IFE=1
C-------   REWIND ELEMENT  FILE (ME)
C..   READ RUNOFF SIMULATION RESULTS
      M2=10
      REWIND M2
C.... READ RAINFALL DATA FOR EACH ELEMENT
      IF(ITER.EQ.1) THEN
        READ(MR,5010) RAIN0
         DO IR=1,NELT
          VRAIN(IR)=RAIN0
         ENDDO
5010     FORMAT(8E10.5)
      ENDIF
C-------   LOOP OVER THE  ELEMENTS
      DO  90 IE=1,NELT
      RAIN=VRAIN(IE)
C-------   READ AN ELEMENT
      CALL  RDELEM(M2,KLOCE,VCORE,VPRNE,VPREE,KNE)
        DO IVH=1,NNEL
             XVELE(IVH)=XVELG0(KNE(IVH))
             YVELE(IVH)=YVELG0(KNE(IVH))
              DEPE(IVH)=DEPG0(KNE(IVH))
        ENDDO
C-------   FIND ELEMENT  D.O.F. FROM  VFG
10    CALL  DLELM(KLOCE,VDLG,VDIMP,VDLE)
C-------   COMPUTE THE  RESIDUAL K.U. AND [M], [K]
C
      CALL ELEMS2(VCORE,VPRNE,VPREE,VDLE,VKE,VFE,VME,RAIN,XVELE,YVELE,
     1            DEPE)
C
C-------   RESIDUALS  OF THE FIRST ITERATION  IN EACH  STEP (LINEAR)
15    IF(ITER.GT.1)   GO TO 20
      READ(50) EXCES
      DO IRAIN=1,3
         VRE(IRAIN)=0.0D0
```

```
      ENDDO
C
C...  CALL SOURCE AND SINK
C
      A1=VCORE(1)-VCORE(3)
      B1=VCORE(1)-VCORE(5)
      A2=VCORE(2)-VCORE(4)
      B2=VCORE(2)-VCORE(6)
      A3=VPRNE(1)-VPRNE(2)
      B3=VPRNE(1)-VPRNE(3)
C.. SLOPE IN X AND Y DIRECTION
      S0X=(A2*B3-A3*B2)/(A1*B2-A2*B1)
      S0Y=(A3*B1-A1*B3)/(A1*B2-A2*B1)
      DMD=0.01E-3
      IF(EXCES.GT.0.1E-30) IZINF=IZINF+1
C
      CALL SEDSS(ES,XVELE,YVELE,DEPE,VDLE,RAIN,EXCES,S0X,S0Y,DMD)

C..   CONSTRUCT {F} MATRIX
      VRE(1)=ES*VL/3.0D0
      VRE(2)=ES*VL/3.0D0
      VRE(3)=ES*VL/3.0D0
      CALL  ASSEL(0,1,IDLE,NSYM,KLOCE,KLD,VKE,VRE,VKGS,VKGD,VKGI,VFG0)
      CALL  ASSEL(0,1,IDLE,NSYM,KLOCE,KLD,VKE,VRE,VKGS,VKGD,VKGI,VRES)
C
      CALL  ASSEL(0,1,IDLE,NSYM,KLOCE,KLD,VKE,VFE,VKGS,VKGD,VKGI,VFG)
7010  FORMAT(F15.10)
      GO  TO 60
C-------   RESIDUALS  AFTER FIRST ITERATION
20    CONTINUE
      CALL  DLELM(KLOCE,VDLG0,VDIMP,VDLE0)
      DO  30 I=1,IDLE
      VDLE(I)=(VDLE0(I)-VDLE(I))/DPAS
30    VFE(I)=-OMEGA*VFE(I)
C-------   PRODUCT  M . U
      VFE(1)=VFE(1)+VME(1)*VDLE(1)
      II=1
      DO  50 J=2,IDLE
      J1=J-1
      DO  40 I=1,J1
      II=II+1
      VFE(I)=VFE(I)+VME(II)*VDLE(J)
40    VFE(J)=VFE(J)+VME(II)*VDLE(I)
      II=II+1
50    VFE(J)=VFE(J)+VME(II)*VDLE(J)
C
C----------RLATRIX M + DPAS.OMEGA. K
60    CONTINUE
C      IF(IKT.EQ.0)   GO  TO 80
      II=0
      DO  70 I=1,IDLE
      DO  70 J=1,IDLE
      II=II+1
70    VKE(II)=VKE(II)*CC
C
      CALL MATMUL(VKE,VME)
C
C------- ASSEMBLE  THE RESIDUAL  AND  THE GLOBAL MATRIX
7020  FORMAT(4F15.10)
C
80    CALL ASSEL(IKT,IFE,IDLE,NSYM,KLOCE,KLD,VKE,VFE,VKGS,VKGD,VKGI,
     1  VRES)
C
90    ITPE1=ITPE
      RETURN
      END
C
C
      SUBROUTINE ELEMS2(VCORE,VPRNE,VPREE,VDLE,VKE,VFE,VME,RAIN,XVELE,
     &            YVELE,DEPE)
```

```
C=====================================================================
      IMPLICIT REAL*8(A-H,O-Z)
      COMMON/COOR/NDIM,IHONG1(3),ONG1(3)
      COMMON/ADD/VL,BETA,HULA
      COMMON/RGDT/IEL,ITPE,ITPE1,IGRE,IDLE,ICE,IPRNE,IPREE,INEL,IDEG,IPG
     1  ,ICODE,IDLE0,INEL0,IPG0
      COMMON/ES/M,MR,MP,MNUL(10)
      DIMENSION VCORE(6),VPRNE(1),VPREE(1),VDLE(1),VKE(9),VFE(1),VME(6)
     1         ,VCONE(1),XVELE(3),DEPE(3),YVELE(3),X(3),Y(3)
      DATA ONE,TWO,THREE,G/1.0D0,2.D0,3.D0,9.8060/
C.......
C.. IDLE : # OF DEGREE OF FREEDOM PER ELEMENT
C.. INEL : # OF NODAL POINTS PER ELEMENT
c..
       DATA ZERO/0.D0/
c-------  INITIALIZE  VKE
300   DO  310 I=1,INEL*INEL
310   VKE(I)=ZERO
C..
C...  VDLE IS THE CALCULATED WATER FLOW DEPTH AND VELOCITY
C...  AT THE TIME BETWEEN T AND T+DT
      X1=VCORE(1)
      Y1=VCORE(2)
      X2=VCORE(3)
      Y2=VCORE(4)
      X3=VCORE(5)
      Y3=VCORE(6)
      H1=DEPE(1)
      U1=XVELE(1)
      V1=YVELE(1)
      H2=DEPE(2)
      U2=XVELE(2)
      V2=YVELE(2)
      H3=DEPE(3)
      U3=XVELE(3)
      V3=YVELE(3)
C
      X(1)=X3-X2
      X(2)=X1-X3
      X(3)=X2-X1
      Y(1)=Y2-Y3
      Y(2)=Y3-Y1
      Y(3)=Y1-Y2
      VL=0.5D0*(X2*Y3-X3*Y2+X1*Y2-X2*Y1+X3*Y1-X1*Y3)
C
      QU1=U1*H1
      QU2=U2*H2
      QU3=U3*H3
      QV1=V1*H1
      QV2=V2*H2
      QV3=V3*H3
C
      QX1=TWO*QU1+QU2+QU3
      QX2=QU1+TWO*QU2+QU3
      QX3=QU1+QU2+TWO*QU3
      QY1=TWO*QV1+QV2+QV3
      QY2=QV1+TWO*QV2+QV3
      QY3=QV1+QV2+TWO*QV3
C
c...=================================
C...  CONSTTRUCTION OF [K] MATRIX IN 9 X 9
c   =================================
      COEF=ONE/24.0D0
      VKE(1)=COEF*(QX1*Y(1)+QY1*X(1)+VL*RAIN*4.0D0)
      VKE(2)=COEF*(QX2*Y(1)+QY2*X(1)+VL*RAIN*TWO)
      VKE(3)=COEF*(QX3*Y(1)+QY3*X(1)+VL*RAIN*TWO)
      VKE(4)=COEF*(QX1*Y(2)+QY1*X(2)+VL*RAIN*TWO)
      VKE(5)=COEF*(QX2*Y(2)+QY2*X(2)+VL*RAIN*4.0D0)
      VKE(6)=COEF*(QX3*Y(2)+QY3*X(2)+VL*RAIN*TWO)
      VKE(7)=COEF*(QX1*Y(3)+QY1*X(3)+VL*RAIN*TWO)
```

```
      VKE(8)=COEF*(QX2*Y(3)+QY2*X(3)+VL*RAIN*TWO)
      VKE(9)=COEF*(QX3*Y(3)+QY3*X(3)+VL*RAIN*4.0D0)
1010  FORMAT(4F15.10)
C
C==================================
C-------  MASS MATRIX [C] =========
C==================================
      COEF=VL/60.0D0
      VME(1)=COEF*(6.0D0*H1+2.0D0*H2+2.0D0*H3)
      VME(2)=COEF*(2.0D0*H1+2.0D0*H2+1.0D0*H3)
      VME(3)=COEF*(2.0D0*H1+6.0D0*H2+2.0D0*H3)
      VME(4)=COEF*(2.0D0*H1+1.0D0*H2+2.0D0*H3)
      VME(5)=COEF*(1.0D0*H1+2.0D0*H2+2.0D0*H3)
      VME(6)=COEF*(2.0D0*H1+2.0D0*H2+6.0D0*H3)
C
C ------  EVALUATE THE ELEMENT  RESIDUAL [K]*[U] MATRIX
C
600   DO 605 I=1,INEL
605   VFE(I)=ZERO
      DO 610 J=1,3
         SUM=0.0D0
         DO 620 I=1,3
            SUM=SUM+VKE((I-1)*3+J)*VDLE(I)
620      CONTINUE
610   VFE(J)=SUM
      RETURN
      END
C
C
C...SUBPROGRAM MATRIX CALCULATION (SYMMETRIC * NON-SYNNETRIC)
      SUBROUTINE MATMUL(A,B)
      IMPLICIT REAL*8 (A-H,O-Z)
      DIMENSION A(3,3),B(1),B1(3,3),C(3,3)
110   FORMAT(9F8.3)
      M=0
      DO 10 I=1,3
         DO 10 J=1,I
            M=M+1
            B1(I,J)=B(M)
10    B1(J,I)=B(M)
C
      DO 30 I=1,3
         DO 30 J=1,3
30    C(I,J)=A(I,J)+B1(I,J)
C
      DO 50 I=1,3
         DO 50 J=1,3
            A(I,J)=C(I,J)
50    CONTINUE
      RETURN
      END
C
      SUBROUTINE SEDSS(ES,XVELE,YVELE,DEPE,VDLE,RAIN,EXCES,S0X,S0Y,DMD)
      IMPLICIT DOUBLE PRECISION (A-H,O-Z)
      DIMENSION XVELE(1),YVELE(1),DEPE(1),VDLE(1)
C
C
      DEPTH=(DEPE(1)+DEPE(2)+DEPE(3))/3.0
      VELOX=(ABS(XVELE(1))+ABS(XVELE(2))+ABS(XVELE(3)))/3.0
      VELOY=(ABS(YVELE(1))+ABS(YVELE(2))+ABS(YVELE(3)))/3.0
      CONC=(VDLE(1)+VDLE(2)+VDLE(3))/3.0
C
C...  COMPUTING SPLASH EROSION
C         PARAMETERS 1)  CF = 422 K PHIF , K (VK)-> USLE FACTOR
C                                          PHIF -> REDUCTION FACTOR
C                    2)  K(H)=EXP(-CH*H) , CH -> 203 FOR 3MM RAINDROP
C                                          H -> FLOW DEPTH
C         SPLASH EROSION (SSE) = CF*K(H)*RAIN*EXCES
      VK=0.5
      PHIK=0.9
```

```
      CF=422.*VK*PHIK
C
      CH=203.0
      VKH=EXP(-CH*DEPTH)
      SSE=CF*VKH*RAIN*EXCES
C     SSE=4.0*RAIN
C     WRITE(*,*) 'SSE=',SSE
      FCL=0.25
      AT=130.0
C   IF  FCL < 0.22 , THEN AT = 188-468*FCL+907FCL*FCL
C    0.0 < PHIR < 1.0
      PHIR=0.40
      CG=5.6*VK*PHIR/AT
C... ESTIMATE SEDIMENT TRANSPORT CAPACITY
      CALL STCAP(DEPTH,VELOX,S0X,DMD,CMX1,VS)
      CALL STCAP(DEPTH,VELOY,S0Y,DMD,CMX2,VS)
      CMX12=CMX1*CMX1+CMX2*CMX2
      IF(CMX12.LT.1.0E-20) THEN
        CMX=0.0D0
       ELSE
        CMX=SQRT(CMX12)
      ENDIF
C
      IF(CMX.GE.CONC) THEN
         SHE=CG*(CMX-CONC)*DEPTH
        ELSE
         CG=VS*(1.0-(CMX/CONC))/DEPTH
         SHE=CG*(CMX-CONC)*DEPTH
      ENDIF
C
      VELO=SQRT(VELOX*VELOX+VELOY*VELOY)
C... NET SEDIMENT SOURCE AND SINK
      ES=SSE+SHE
C     IF(DEPTH.GT.1.0E-30.AND.CMX.LT.1.0E-30) ES=SSE
      IF(DEPTH.LE.1.0E-30) ES=0.0
      RETURN
      END
C
      SUBROUTINE STCAP(DU,V2,S,DMD,CMX,VS)
      IMPLICIT DOUBLE PRECISION (A-H,O-Z)
C      COMPUTING SEDIMENT SOURCE AND SINK TERMS
C.........................
C
C    * DU = FLOW DEPTH               * V2 = FLOW VELOCITY
C    * S = SLOPE                       SS = SPECIFIC WEIGHT OF GRAIN
C      RHOS = DENSTY OF PARTICLE       TW = TOP WIDTH
C      G = GRAVITATIONAL ACC.          VNU = KINEMATIC VISCOSITY
C    * DMD = MEDIAN DIAMETER OF PARTICLE
C
      S=ABS(S)
      SS=2.65
C  IN MEYER AND WISCHMEIER
C     CS=0.0001
C     CMX=CS*V2**4./DU
C     VS=2.0E-3
C     RETURN
C  ENGELUND AND HANSEN
C     WRITE(*,*) 'DU=',DU
      IF(DU.LE.0.0) THEN
         USTAR=0.0D0
       ELSE
         USTAR=SQRT(9.806*DU*S)
      ENDIF
      CMX=0.05*V2*USTAR**3./(9.806**2.*DMD*DU*(SS-1)**2)
c     CMX=0.05*V2**2*USTAR**3./(9.806**2.*DMD*(SS-1)**2)
C...  CHECK PARAMETER ----------------------     7)
      VS=0.06D-03
      RETURN
C
      RHOS=2645.23
```

```
      TW=1.0
      G=9.806
      VNU=1.007E-6
C     DMD=1.64E-4
C
      D=DU
      UB=V2
      S=ABS(S)
      IF(D.LE.1.0E-30) THEN
         CMX=0.0
         RETURN
      ENDIF
         HD=D/TW
         USTAR=SQRT(G*HD*S)
         REYP = USTAR*DMD/VNU
C ** UNIT STREAM POWER LAW
C... SETTLING VELOCITY
C
      VS=VSETL(SS,DMD,VNU)
      PA=REYP
      IF (PA-70.) 40,50,50
   40 IF (PA.LT.1.2) PA=1.20001
      VBW=2.5/(LOG10(PA)-0.06)+0.66
      GO TO 60
   50 VBW=2.05
   60 VPS=VS
      PB=VPS*DMD/VNU
      ALA=LOG10(PB)
C
C... FOR THE CASE OF SLOPE = 0.0
C
      IF(USTAR.GT.0.1E-50) THEN
         ALB=LOG10(USTAR/VPS)
        ELSE
         ALB=0.1E-50
      ENDIF
      FA=1.799-0.409*ALA-0.314*ALB
      EFB=UB*S/VPS-VBW*S
      IF (EFB) 170,170,70
   70 FB=LOG10(EFB)
      ALGCT=5.435-0.286*ALA-0.457*ALB+FA*FB
        CMX=10.**(ALGCT-6.)/RHOS
      RETURN
170   CMX=0.0
      RETURN
      END
C
C...  FUNCTION FOR CALCULATING SETTLING VELOCITY
C
      FUNCTION VSETL (SS,D,VNU)
      IMPLICIT DOUBLE PRECISION (A-H,O-Z)
C  ALL DIMENSIONS IN FT, SECONDS.
      ITER=0
      CA=24*VNU/D
      CK=42.91*(SS-1.)*D
      CB=3.*SQRT(VNU/D)
      CC=.34
      VS=2.8E05*D*D
   10  F=CA*VS+CB*VS**1.5+CC*VS*VS-CK
      FP=CA+1.5*CB*SQRT(VS)+2*CC*VS
      DVS=F/FP
      IF (ABS(DVS)-0.0001*VS) 30,30,20
   20 VS=VS-DVS
      ITER=ITER+1
      IF (ITER.GT.40) GO TO 40
      IF (VS.LE.0.) VS=0.5*(VS+DVS)
      GO TO 10
   30 VSETL=VS
      RETURN
   40 WRITE (6,50) SS,D,VNU,DVS
```

```
      STOP 9108
C
   50 FORMAT (36H 40 ITERS WITH SS, D, VNU, AND DVS =,4G13.5)
      END
```

4. 1-D subprogram for sediment transport (sedo.f)

```
C=======
      SUBROUTINE ASEULR(IKT,VCORG,KDLNC,VDIMP,KNEQ,KLD,KLOCE,VCORE,
     1  VPRNE,VPREE,KNE,VKE,VME,VFE,VDLE,VKGS,VKGD,VKGI,VFG,VRES,
     2  VDLG,VDLE0,VDLG0,VFG0)
C=
C       TO ASSEMBLE THE RESIDUALS  AND THE GLOBAL  MATRIX (IF IKT.EQ.1)
C       WHILE LOOPING OVER THE  ELEMENTS (FOR EULER  METHOD)
C==
      IMPLICIT REAL*8(A-H,O-Z)
      COMMON/ELEM/NELT,NNEL,NTPE,NGRE,ME,NIDENT,NUL1
      COMMON/COOR/NDIM,NNT,IHONG1(2),ONG1(3)
      COMMON/ASSE/NSYM,NUL2(3)
      COMMON/RESO/NEQ,NUL3(2)
     COMMON/RGDT/IEL,ITPE,ITPE1,IGRE,IDLE,ICE,IPRNE,IPREE,INEL,IDEG,IPG
     1  ,ICOD,NUL4(3)
      COMMON/NLIN/EPSDL,XNORM,OMEGA,XPAS,DPAS,DPAS0,NPAS,IPAS,NITER,
     1  ITER,IMETH
      COMMON/ES/M,MR,MP,M1,M2,MNUL(8)
      COMMON/ADD/VL,BETA,HULA,ISIMM
      COMMON/INF/AINF(500),IEXCESS,IZINF
      DIMENSION  VCORG(1),KDLNC(1),VDIMP(1),KNEQ(1),KLD(1),KLOCE(1),
     1 VCORE(1),VPRNE(1),VPREE(1),KNE(1),VKE(1),VME(1),VFE(1),VDLE(1),
     2 VKGS(1),VKGD(1),VKGI(1),VFG(1),VRES(1),VDLG(1),VDLE0(1),
     3 VDLG0(1),VFG0(1)
      DIMENSION VRE(2),VRAIN(500),XVELG(500),DEPG(500),XVELE(2),DEPE(2)
      COMMON/TRANS/ DEPG0(500),XVELG0(500),YVELG0(500)
      DATA  UN/1.D0/
C-----------------------------------------------------------------------
      CC=DPAS*OMEGA
      IFE=0
      IF(ITER.GT.1)  IFE=1
C-------   REWIND ELEMENT  FILE (ME)
C..   READ RUNOFF SIMULATION RESULTS
      M2=2
      open(unit=m2,file='onesed10.out',form='unformatted')
      REWIND M2
C...  RUNOFF VALUES AT TIME,T-T/2
C.... READ RAINFALL DATA FOR EACH ELEMENT
      IF(ITER.EQ.1) THEN
        READ(MR,5010) RAIN0
         DO IR=1,NELT
          VRAIN(IR)=RAIN0
         ENDDO
5010    FORMAT(8E10.5)
      ENDIF
C-------   LOOP OVER THE  ELEMENTS
      DO  90 IE=1,NELT
C-------   READ AN ELEMENT
      CALL  RDELEM(M2,KLOCE,VCORE,VPRNE,VPREE,KNE)
        DO IVH=1,NNEL
             XVELE(IVH)=XVELG0(KNE(IVH))
             DEPE(IVH)=DEPG0(KNE(IVH))
        ENDDO
      RAIN=VRAIN(IE)
C-------   FIND ELEMENT  D.O.F. FROM  VFG
10    CALL  DLELM(KLOCE,VDLG,VDIMP,VDLE)
C-------   COMPUTE THE  RESIDUAL K.U. AND [M], [K]
C
      CALL ELEMS1(VCORE,VPRNE,VPREE,VDLE,VKE,VFE,VME,RAIN,XVELE,DEPE)
C
C-------   RESIDUALS  OF THE FIRST ITERATION  IN EACH  STEP (LINEAR)
15    IF(ITER.GT.1)   GO TO 20
      DO IRAIN=1,2
         VRE(IRAIN)=0.0D0
      ENDDO
C
```

```
C...  CALL SOURCE AND SINK
C
      READ(50) EXCES
c     EXCES=RAIN
      IF(RAIN.GT.0.1E-30) IZINF=IZINF+1
      S0=(VPRNE(1)-VPRNE(2))/VL
      DMD=0.0100E-3
C
      CALL SEDSS(ES,XVELE,DEPE,VDLE,RAIN,EXCES,S0,DMD)
C
C..   CONSTRUCT (F) MATRIX
      VRE(1)=ES*VL/2.0D0
      VRE(2)=ES*VL/2.0D0
      CALL  ASSEL(0,1,IDLE,NSYM,KLOCE,KLD,VKE,VRE,VKGS,VKGD,VKGI,VFG0)
      CALL  ASSEL(0,1,IDLE,NSYM,KLOCE,KLD,VKE,VRE,VKGS,VKGD,VKGI,VRES)
C
      CALL  ASSEL(0,1,IDLE,NSYM,KLOCE,KLD,VKE,VFE,VKGS,VKGD,VKGI,VFG)
7010  FORMAT(F15.10)
      GO  TO 60
C-------   RESIDUALS  AFTER FIRST ITERATION
20    CONTINUE
      CALL  DLELM(KLOCE,VDLG0,VDIMP,VDLE0)
      DO  30 I=1,IDLE
      VDLE(I)=(VDLE0(I)-VDLE(I))/DPAS
30    VFE(I)=-OMEGA*VFE(I)
C--------   PRODUCT  M . U
      VFE(1)=VFE(1)+VME(1)*VDLE(1)
      II=1
      DO  50 J=2,IDLE
      J1=J-1
      DO  40 I=1,J1
      II=II+1
      VFE(I)=VFE(I)+VME(II)*VDLE(J)
40    VFE(J)=VFE(J)+VME(II)*VDLE(I)
      II=II+1
50    VFE(J)=VFE(J)+VME(II)*VDLE(J)
C----------RLATRIX M + DPAS.OMEGA. K
60    CONTINUE
C      IF(IKT.EQ.0)   GO  TO 80
      II=0
      DO  70 I=1,IDLE
      K=I
      DO  70 J=1,IDLE
      II=II+1
      IF(I.LE.2) THEN
         K=K+(J-1)
      ENDIF
      IF(I.EQ.3) THEN
        IF(J.NE.IDLE) K=I+J
        IF(J.EQ.IDLE) K=I+J+2
      ENDIF
      IF(I.EQ.4) THEN
        K=I+J+2
      ENDIF
70    VKE(II)=VKE(II)*CC+VME(K)
C------- ASSEMBLE  THE RESIDUAL  AND  THE GLOBAL MATRIX
7020  FORMAT(4F15.10)
C
80    CALL ASSEL(IKT,IFE,IDLE,NSYM,KLOCE,KLD,VKE,VFE,VKGS,VKGD,VKGI,
     1  VRES)
C
90    ITPE1=ITPE
      RETURN
      END
C
C
      SUBROUTINE ELEMS1(VCORE,VPRNE,VPREE,VDLE,VKE,VFE,VME,RAIN,XVELE,
     &                  DEPE)
C=======================================================================
      IMPLICIT REAL*8(A-H,O-Z)
```

```
      COMMON/COOR/NDIM,IHONG1(3),ONG1(3)
      COMMON/ADD/VL,BETA,HULA,ISIMM
      COMMON/RGDT/IEL,ITPE,ITPE1,IGRE,IDLE,ICE,IPRNE,IPREE,INEL,IDEG,IPG
     1  ,ICODE,IDLE0,INEL0,IPG0
      COMMON/ES/M,MR,MP,MNUL(10)
      DIMENSION VCORE(1),VPRNE(1),VPREE(1),VDLE(1),VKE(1),VFE(1),VME(1),
     1          VCONE(1),XVELE(2),DEPE(2)
      DATA ONE,TWO,THREE,G/1.0D0,2.D0,3.D0,9.806D0/
C.......
C.. IDLE : # OF DEGREE OF FREEDOM PER ELEMENT
C.. INEL : # OF NODAL POINTS PER ELEMENT
c..
       DATA ZERO/0.D0/
c-------  INITIALIZE  VKE
300   DO  310 I=1,INEL*INEL
310   VKE(I)=ZERO
C..
C...  VDLE IS THE CALCULATED WATER FLOW DEPTH AND VELOCITY
C...  AT THE TIME BETWEEN T AND T+DT
CC
      VL=ABS(VCORE(2)-VCORE(1))
      U1=XVELE(1)
      U2=XVELE(2)
      H1=DEPE(1)
      H2=DEPE(2)
      AVH=(H1+H2)/TWO
      AVU=(U1+U2)/TWO
      Q=AVU*AVH
c...=====================================
C...  CONSTTRUCTION OF [K] MATRIX IN 2 X 2
c   ====================================
      COEF=ONE/6.0d0
      VKE(1)=COEF*(-3.0D0*Q+TWO*RAIN*VL)
      VKE(2)=COEF*(-3.0D0*Q+RAIN*VL)
      VKE(3)=COEF*(3.0D0*Q+RAIN*VL)
      VKE(4)=COEF*(3.0D0*Q+TWO*RAIN*VL)
1010  FORMAT(4F15.10)
c
c==================================
c-------  MASS MATRIX [C] =========
c==================================
      COEF=VL*AVH/6.0D0
      VME(1)=COEF*TWO
      VME(2)=COEF
      VME(3)=COEF*TWO
C
C ------  EVALUATE THE ELEMENT  RESIDUAL [K]*[U] MATRIX
C
600   DO 605 I=1,INEL
605   VFE(I)=ZERO
      DO 610 J=1,2
         SUM=0.0D0
         DO 620 I=1,2
            SUM=SUM+VKE((I-1)*2+J)*VDLE(I)
620      CONTINUE
610   VFE(J)=SUM
      RETURN
      END
C
      SUBROUTINE SEDSS(ES,XVELE,DEPE,VDLE,RAIN,EXCES,S0,DMD)
      IMPLICIT DOUBLE PRECISION (A-H,O-Z)
      DIMENSION XVELE(2),DEPE(2),VDLE(2)
C
C
      DEPTH=(DEPE(1)+DEPE(2))/2.0
      VELO=(ABS(XVELE(1))+ABS(XVELE(2)))/2.0
      IF(VDLE(1)*VDLE(2).LT.1.0E-30) THEN
        CONC=VDLE(1)+VDLE(2)
       ELSE
        CONC=(VDLE(1)+VDLE(2))/2.0
```

```
      ENDIF
C
C...  COMPUTING SPLASH EROSION
C         PARAMETERS 1)  CF = 422 K PHIF , K (VK)-> USLE FACTOR
C                                      PHIF -> REDUCTION FACTOR
C                    2)  K(H)=EXP(-CH*H) , CH -> 203 FOR 3MM RAINDROP
C                                           H -> FLOW DEPTH
C         SPLASH EROSION (SSE) = CF*K(H)*RAIN*EXCES
      VK=0.50
      PHIK=0.9
      CF=422.*VK*PHIK
C
      CH=203.0
      VKH=EXP(-CH*DEPTH)
      SSE=CF*VKH*RAIN*EXCES
C
C     SSE=4.0*RAIN
      FCL=0.25
      AT=130.0
C   IF  FCL < 0.22 , THEN AT = 188-468*FCL+907FCL*FCL
C    0.0 < PHIR < 1.0
      PHIR=0.40
      CG=5.6*VK*PHIR/AT
C... ESTIMATE SEDIMENT TRANSPORT CAPACITY
      CALL STCAP(DEPTH,VELO,S0,DMD,CMX,VS)
C
      IF(CMX.GE.CONC) THEN
         SHE=CG*(CMX-CONC)*DEPTH
        ELSE
         CG=VS*(1.0-(CMX/CONC))/DEPTH
         SHE=CG*(CMX-CONC)*DEPTH
      ENDIF
C... NET SEDIMENT SOURCE AND SINK
      ES=SSE+SHE
      IF(DEPTH.LE.1.0E-29) ES=0.0
      RETURN
      END
C
      SUBROUTINE STCAP(DU,V2,S,DMD,CMX,VS)
      IMPLICIT DOUBLE PRECISION (A-H,O-Z)
C      COMPUTING SEDIMENT SOURCE AND SINK TERMS
C.........................
C
C     * DU = FLOW DEPTH                * V2 = FLOW VELOCITY
C     * S = SLOPE                       SS = SPECIFIC WEIGHT OF GRAIN
C       RHOS = DENSTY OF PARTICLE       TW = TOP WIDTH
C       G = GRAVITATIONAL ACC.          VNU = KINEMATIC VISCOSITY
C     * DMD = MEDIAN DIAMETER OF PARTICLE
C
      S=ABS(S)
      SS=2.65
C  IN MEYER AND WEISMEIER
c     CS=0.0001
c     CMX=CS*V2**4./DU
c     VS=2.0E-3
c     RETURN
C  ENGELUND AND HANSEN
      USTAR=SQRT(9.806*DU*S)
      IF(ABS(V2).LT.1.0E-25.OR.ABS(DU).LT.0.1E-30) THEN
       CMX=0.0D0
       ELSE
c     CMX=0.05*V2*V2*USTAR**3./(9.806**2.*DMD*(SS-1.)**2.)
      CMX=0.05*V2*USTAR**3./(9.806**2.*DMD*DU*(SS-1.)**2.)
      ENDIF
      VS=0.060E-3
      RETURN
C
      RHOS=2645.23
      TW=1.0
      G=9.806
```

```
      VNU=1.007E-6
C     DMD=1.64E-4
C
      D=DU
      UB=V2
      S=ABS(S)
      IF(D.LE.1.0E-30) THEN
         CMX=0.0
         RETURN
      ENDIF
         HD=D/TW
         USTAR=SQRT(G*HD*S)
         REYP = USTAR*DMD/VNU
C ** UNIT STREAM POWER LAW
C... SETTLING VELOCITY
C
C     VS=VSETL(SS,DMD,VNU)
      VS=70.E-3
C
      PA=REYP
      IF (PA-70.) 40,50,50
   40 IF (PA.LT.1.2) PA=1.20001
      VBW=2.5/(LOG10(PA)-0.06)+0.66
      GO TO 60
   50 VBW=2.05
   60 VPS=VS
      PB=VPS*DMD/VNU
      ALA=LOG10(PB)
      ALB=LOG10(USTAR/VPS)
      FA=1.799-0.409*ALA-0.314*ALB
      EFB=UB*S/VPS-VBW*S
      IF (EFB) 170,170,70
   70 FB=LOG10(EFB)
      ALGCT=5.435-0.286*ALA-0.457*ALB+FA*FB
        CMX=10.**(ALGCT-6.)/RHOS
C       CMX=10.**(ALGCT-6.)
      RETURN
170   CONTINUE
      CMX=0.0
      RETURN
      END
C
C...  FUNCTION FOR CALCULATING SETTLING VELOCITY
C
      FUNCTION VSETL (SS,D,VNU)
      IMPLICIT DOUBLE PRECISION (A-H,O-Z)
C  ALL DIMENSIONS IN FT, SECONDS.
      ITER=0
      CA=24.*VNU/D
      CK=42.91*(SS-1.)*D
      CB=3.*SQRT(VNU/D)
      CC=.34
      VS=2.8E05*D*D
   10  F=CA*VS+CB*VS**1.5+CC*VS*VS-CK
      FP=CA+1.5*CB*SQRT(VS)+2*CC*VS
      DVS=F/FP
      IF (ABS(DVS)-0.0001*VS) 30,30,20
   20 VS=VS-DVS
      ITER=ITER+1
      IF (ITER.GT.40) GO TO 40
      IF (VS.LE.0.) VS=0.5*(VS+DVS)
      GO TO 10
   30 VSETL=VS
      RETURN
   40 WRITE (6,50) SS,D,VNU,DVS
      STOP 9108
C
   50 FORMAT (36H 40 ITERS WITH SS, D, VNU, AND DVS =,4G13.5)
      END
```

Appendix III

Sample Input and Output Data

1. Sample input data for 2-D model

```
IMAG
COMT
 NONLINEAR TRANSIENT FE MODEL FOR ST. VENANT EQS.
 TRIAGULAR ELEMENT MODEL
Sample Run 1.

COOR
   56     3     2        1.0        1.0        1.0
    1     0.0000     0.0000
    2    10.0000     0.0000
    3    20.0000     0.0000
    4    30.0000     0.0000
    5    40.0000     0.0000
    6    50.0000     0.0000
    7    60.0000     0.0000
    8     0.0000    10.0000
    9    10.0000    10.0000
   10    20.0000    10.0000
   11    30.0000    10.0000
   12    40.0000    10.0000
   13    50.0000    10.0000
   14    60.0000    10.0000
   15     0.0000    20.0000
   16    10.0000    20.0000
   17    20.0000    20.0000
   18    30.0000    20.0000
   19    40.0000    20.0000
   20    50.0000    20.0000
   21    60.0000    20.0000
   22     0.0000    30.0000
   23    10.0000    30.0000
   24    20.0000    30.0000
   25    30.0000    30.0000
   26    40.0000    30.0000
   27    50.0000    30.0000
   28    60.0000    30.0000
   29     0.0000    40.0000
   30    10.0000    40.0000
   31    20.0000    40.0000
   32    30.0000    40.0000
   33    40.0000    40.0000
   34    50.0000    40.0000
   35    60.0000    40.0000
   36     0.0000    50.0000
   37    10.0000    50.0000
   38    20.0000    50.0000
   39    30.0000    50.0000
   40    40.0000    50.0000
   41    50.0000    50.0000
   42    60.0000    50.0000
   43     0.0000    60.0000
   44    10.0000    60.0000
   45    20.0000    60.0000
   46    30.0000    60.0000
   47    40.0000    60.0000
   48    50.0000    60.0000
   49    60.0000    60.0000
   50     0.0000    70.0000
   51    10.0000    70.0000
   52    20.0000    70.0000
   53    30.0000    70.0000
   54    40.0000    70.0000
   55    50.0000    70.0000
```

```
   56   60.0000   70.0000
COND
111
   56   55   54   53   52   51   50
    0
PRND
    1
   10.0000   10.0000   10.0000   10.0000   10.0000   10.0000   10.0000   11.0000
   11.0000   11.0000   11.0000   11.0000   11.0000   11.0000   12.0000   12.0000
   12.0000   12.0000   12.0000   12.0000   12.0000   13.0000   13.0000   13.0000
   13.0000   13.0000   13.0000   13.0000   14.0000   14.0000   14.0000   14.0000
   14.0000   14.0000   14.0000   15.0000   15.0000   15.0000   15.0000   15.0000
   15.0000   15.0000   16.0000   16.0000   16.0000   16.0000   16.0000   16.0000
   16.0000   17.0000   17.0000   17.0000   17.0000   17.0000   17.0000   17.0000
PREL
    8    4
    1    1.0000    0.2000    0.1000   1.0E-07
    2    1.0000    0.1000    0.1000   1.0E-07
    3    1.0000    0.0500    0.1000   1.0E-07
    4    1.0000    0.0700    0.1000   1.0E-07
    5    1.0000    0.1500    0.1000   1.0E-07
    6    1.0000    0.1250    0.1000   1.0E-07
    7    1.0000    0.0750    0.1000   1.0E-07
    8    1.0000    0.0600    0.1000   1.0E-07
    0
ELEM
   84    3    1    1    1
    1    1    3    1    1    9    8
    2    1    8    1    1    2    9
    3    1    8    1    2   10    9
    4    1    4    1    2    3   10
    5    1    4    1    3    4   10
    6    1    4    1    4   11   10
    7    1    4    1    4    5   11
    8    1    4    1    5   12   11
    9    1    4    1    5    6   12
   10    1    4    1    6   13   12
   11    1    4    1    6    7   13
   12    1    4    1    7   14   13
   13    1    3    1    8    9   15
   14    1    3    1    9   16   15
   15    1    3    1    9   10   16
   16    1    3    1   10   17   16
   17    1    3    1   10   18   17
   18    1    4    1   10   11   18
   19    1    4    1   11   12   18
   20    1    4    1   12   19   18
   21    1    4    1   12   13   19
   22    1    4    1   13   20   19
   23    1    4    1   13   14   20
   24    1    4    1   14   21   20
   25    1    3    1   15   16   22
   26    1    3    1   16   23   22
   27    1    3    1   16   17   23
   28    1    3    1   17   24   23
   29    1    3    1   17   18   24
   30    1    3    1   18   25   24
   31    1    3    1   18   26   25
   32    1    8    1   18   19   26
   33    1    8    1   19   27   26
   34    1    4    1   19   20   27
   35    1    4    1   20   21   27
   36    1    2    1   21   28   27
   37    1    3    1   22   23   29
   38    1    3    1   23   30   29
   39    1    3    1   23   24   30
   40    1    3    1   24   31   30
   41    1    3    1   24   25   31
   42    1    3    1   25   32   31
   43    1    3    1   25   26   32
```

```
   44     1     7     1    26    33    32
   45     1     7     1    26    27    33
   46     1     2     1    27    34    33
   47     1     2     1    27    28    34
   48     1     2     1    28    35    34
   49     1     1     1    29    37    36
   50     1     6     1    29    30    37
   51     1     6     1    30    38    37
   52     1     3     1    30    31    38
   53     1     3     1    31    32    38
   54     1     2     1    32    39    38
   55     1     2     1    32    33    39
   56     1     2     1    33    40    39
   57     1     2     1    33    34    40
   58     1     2     1    34    41    40
   59     1     2     1    34    35    41
   60     1     2     1    35    42    41
   61     1     1     1    36    37    43
   62     1     1     1    37    44    43
   63     1     1     1    37    38    44
   64     1     1     1    38    45    44
   65     1     1     1    38    46    45
   66     1     5     1    38    39    46
   67     1     5     1    39    47    46
   68     1     2     1    39    40    47
   69     1     2     1    40    41    47
   70     1     2     1    41    48    47
   71     1     2     1    41    42    48
   72     1     2     1    42    49    48
   73     1     1     1    43    44    50
   74     1     1     1    44    51    50
   75     1     1     1    44    45    51
   76     1     1     1    45    52    51
   77     1     1     1    45    46    52
   78     1     1     1    46    53    52
   79     1     1     1    46    47    53
   80     1     1     1    47    54    53
   81     1     1     1    47    55    54
   82     1     5     1    47    48    55
   83     1     5     1    48    56    55
   84     1     1     1    48    49    56
    0
TEMP
   10.0000    40    30     1 0.300E-01        1.0 0.100E-14        0.5     1     0
0.5000E-04
...
...
0.0000E+00
    0.0000
STOP
```

2. Sample input data for 1-D model

```
IMAG
COMT
 NONLINEAR TRANSIENT FE MODEL FOR ST. VENANT EQS.
 1-D MODEL
Sample Run 1.

COOR
   56    2    1       1.0       1.0       1.0
    1    0.0000
    2    0.0000
    3    0.0000
    4    0.0000
    5    0.0000
    6    0.0000
    7    0.0000
    8   10.0000
    9   10.0000
   10   10.0000
   11   10.0000
   12   10.0000
   13   10.0000
   14   10.0000
   15   20.0000
   16   20.0000
   17   20.0000
   18   20.0000
   19   20.0000
   20   20.0000
   21   20.0000
   22   30.0000
   23   30.0000
   24   30.0000
   25   30.0000
   26   30.0000
   27   30.0000
   28   30.0000
   29   40.0000
   30   40.0000
   31   40.0000
   32   40.0000
   33   40.0000
   34   40.0000
   35   40.0000
   36   50.0000
   37   50.0000
   38   50.0000
   39   50.0000
   40   50.0000
   41   50.0000
   42   50.0000
   43   60.0000
   44   60.0000
   45   60.0000
   46   60.0000
   47   60.0000
   48   60.0000
   49   60.0000
   50   70.0000
   51   70.0000
   52   70.0000
   53   70.0000
   54   70.0000
   55   70.0000
   56   70.0000
COND
11
```

```
   56   55   54   53   52   51   50
    0
PRND
    1
   10.0000   10.0000   10.0000   10.0000   10.0000   10.0000   10.0000   11.0000
   11.0000   11.0000   11.0000   11.0000   11.0000   11.0000   12.0000   12.0000
   12.0000   12.0000   12.0000   12.0000   12.0000   13.0000   13.0000   13.0000
   13.0000   13.0000   13.0000   13.0000   14.0000   14.0000   14.0000   14.0000
   14.0000   14.0000   14.0000   15.0000   15.0000   15.0000   15.0000   15.0000
   15.0000   15.0000   16.0000   16.0000   16.0000   16.0000   16.0000   16.0000
   16.0000   17.0000   17.0000   17.0000   17.0000   17.0000   17.0000   17.0000
PREL
   15    5
    1    1.0000    0.2000    10.000    0.1000   1.0E-07
    2    1.0000    0.1000    10.000    0.1000   1.0E-07
    3    1.0000    0.0500    10.000    0.1000   1.0E-07
    4    1.0000    0.0700    10.000    0.1000   1.0E-07
    5    1.0000    0.0533    10.000    0.1000   1.0E-07
    6    1.0000    0.0600    10.000    0.1000   1.0E-07
    7    1.0000    0.0550    10.000    0.1000   1.0E-07
    8    1.0000    0.0650    10.000    0.1000   1.0E-07
    9    1.0000    0.0760    10.000    0.1000   1.0E-07
   10    1.0000    0.0750    10.000    0.1000   1.0E-07
   11    1.0000    0.0800    10.000    0.1000   1.0E-07
   12    1.0000    0.0790    10.000    0.1000   1.0E-07
   13    1.0000    0.1250    10.000    0.1000   1.0E-07
   14    1.0000    0.1750    10.000    0.1000   1.0E-07
   15    1.0000    0.1500    10.000    0.1000   1.0E-07
    0
ELEM
   49    2    1    1    1
    1    1    5    1    1    8
    2    1    6    1    2    9
    3    1    4    1    3   10
    4    1    4    1    4   11
    5    1    4    1    5   12
    6    1    4    1    6   13
    7    1    4    1    7   14
    8    1    3    1    8   15
    9    1    3    1    9   16
   10    1    7    1   10   17
   11    1    8    1   11   18
   12    1    4    1   12   19
   13    1    4    1   13   20
   14    1    4    1   14   21
   15    1    3    1   15   22
   16    1    3    1   16   23
   17    1    3    1   17   24
   18    1    3    1   18   25
   19    1    6    1   19   26
   20    1    9    1   20   27
   21    1    2    1   21   28
   22    1    3    1   22   29
   23    1    3    1   23   30
   24    1    3    1   24   31
   25    1    3    1   25   32
   26    1   10    1   26   33
   27    1    2    1   27   34
   28    1    2    1   28   35
   29    1   14    1   29   36
   30    1   13    1   30   37
   31    1   12    1   31   38
   32    1   11    1   32   39
   33    1    2    1   33   40
   34    1    2    1   34   41
   35    1    2    1   35   42
   36    1    1    1   36   43
   37    1    1    1   37   44
   38    1    1    1   38   45
   39    1   15    1   39   46
```

```
    40     1     2     1    40    47
    41     1     2     1    41    48
    42     1     2     1    42    49
    43     1     1     1    43    50
    44     1     1     1    44    51
    45     1     1     1    45    52
    46     1     1     1    46    53
    47     1     1     1    47    54
    48     1    15     1    48    55
    49     1     2     1    49    56
     0
TEMP
   10.0000    40    30     1 0.300E-01        1.0 0.100E-14        0.5     1     0
0.5000E-04
...
...
0.0000E+00
    0.0000
STOP
```

3. Sample output from 2-D model

```
                              2-D RUNOFF SIMULATION MODEL

 COMMENTS
 ==========

  NONLINEAR TRANSIENT FE MODEL FOR ST. VENANT EQS.
  TRIAGULAR ELEMENT MODEL
 heterogeneous plot

 INPUT OF NODES =     0
 MAX. NUMBER OF NODES =    56
 MAX. NUMBER OF DOF PER NODES =     3
 DIMENSIONS OF PROBLEM =     2
 COORDINATE SCALE FACTORS = 0.10000E+01 0.10000E+01 0.10000E+01
 WORKSPACE IN REAL WORDS =      85000


 INPUT OF B.C. M= 0


B.C. CARDS
>>>
1110000000   0.00000   0.00000   0.00000   0.00000   0.00000   0.00000   0.00000
>>>
   56   55   54   53   52   51   50    0    0    0    0    0    0    0    0    0
>>>
0000000000   0.00000   0.00000   0.00000   0.00000   0.00000   0.00000   0.00000
TOTAL NUMBER OF NODE=    56
TOTAL NUMBER OF DOF =  168
 NUMBER OF EQUATIONS=  147
 NUMBER OF PRESCRIBED NON ZERO DOF     0
 NUMBER OF PRESCRIBED ZERO DOF    21
 TOTAL NUMBER OF PRESCRIBED DOF    21


NODAL COORDINATE      NO D.L.    X    Y    Z  NEQ
     1      3 0.00000E+00 0.00000E+00 0.00000E+00              1     2     3
     2      3 0.10000E+02 0.00000E+00 0.00000E+00              4     5     6
     3      3 0.20000E+02 0.00000E+00 0.00000E+00              7     8     9
     4      3 0.30000E+02 0.00000E+00 0.00000E+00             10    11    12
     5      3 0.40000E+02 0.00000E+00 0.00000E+00             13    14    15
     6      3 0.50000E+02 0.00000E+00 0.00000E+00             16    17    18
     7      3 0.60000E+02 0.00000E+00 0.00000E+00             19    20    21
     8      3 0.00000E+00 0.10000E+02 0.00000E+00             22    23    24
     9      3 0.10000E+02 0.10000E+02 0.00000E+00             25    26    27
    10      3 0.20000E+02 0.10000E+02 0.00000E+00             28    29    30
    11      3 0.30000E+02 0.10000E+02 0.00000E+00             31    32    33
    12      3 0.40000E+02 0.10000E+02 0.00000E+00             34    35    36
    13      3 0.50000E+02 0.10000E+02 0.00000E+00             37    38    39
    14      3 0.60000E+02 0.10000E+02 0.00000E+00             40    41    42
    15      3 0.00000E+00 0.20000E+02 0.00000E+00             43    44    45
    16      3 0.10000E+02 0.20000E+02 0.00000E+00             46    47    48
    17      3 0.20000E+02 0.20000E+02 0.00000E+00             49    50    51
    18      3 0.30000E+02 0.20000E+02 0.00000E+00             52    53    54
    19      3 0.40000E+02 0.20000E+02 0.00000E+00             55    56    57
    20      3 0.50000E+02 0.20000E+02 0.00000E+00             58    59    60
    21      3 0.60000E+02 0.20000E+02 0.00000E+00             61    62    63
    22      3 0.00000E+00 0.30000E+02 0.00000E+00             64    65    66
    23      3 0.10000E+02 0.30000E+02 0.00000E+00             67    68    69
    24      3 0.20000E+02 0.30000E+02 0.00000E+00             70    71    72
    25      3 0.30000E+02 0.30000E+02 0.00000E+00             73    74    75
    26      3 0.40000E+02 0.30000E+02 0.00000E+00             76    77    78
    27      3 0.50000E+02 0.30000E+02 0.00000E+00             79    80    81
    28      3 0.60000E+02 0.30000E+02 0.00000E+00             82    83    84
    29      3 0.00000E+00 0.40000E+02 0.00000E+00             85    86    87
    30      3 0.10000E+02 0.40000E+02 0.00000E+00             88    89    90
```

```
    31      3 0.20000E+02 0.40000E+02 0.00000E+00              91    92    93
    32      3 0.30000E+02 0.40000E+02 0.00000E+00              94    95    96
    33      3 0.40000E+02 0.40000E+02 0.00000E+00              97    98    99
    34      3 0.50000E+02 0.40000E+02 0.00000E+00             100   101   102
    35      3 0.60000E+02 0.40000E+02 0.00000E+00             103   104   105
    36      3 0.00000E+00 0.50000E+02 0.00000E+00             106   107   108
    37      3 0.10000E+02 0.50000E+02 0.00000E+00             109   110   111
    38      3 0.20000E+02 0.50000E+02 0.00000E+00             112   113   114
    39      3 0.30000E+02 0.50000E+02 0.00000E+00             115   116   117
    40      3 0.40000E+02 0.50000E+02 0.00000E+00             118   119   120
    41      3 0.50000E+02 0.50000E+02 0.00000E+00             121   122   123
    42      3 0.60000E+02 0.50000E+02 0.00000E+00             124   125   126
    43      3 0.00000E+00 0.60000E+02 0.00000E+00             127   128   129
    44      3 0.10000E+02 0.60000E+02 0.00000E+00             130   131   132
    45      3 0.20000E+02 0.60000E+02 0.00000E+00             133   134   135
    46      3 0.30000E+02 0.60000E+02 0.00000E+00             136   137   138
    47      3 0.40000E+02 0.60000E+02 0.00000E+00             139   140   141
    48      3 0.50000E+02 0.60000E+02 0.00000E+00             142   143   144
    49      3 0.60000E+02 0.60000E+02 0.00000E+00             145   146   147
    50      3 0.00000E+00 0.70000E+02 0.00000E+00             -19   -20   -21
    51      3 0.10000E+02 0.70000E+02 0.00000E+00             -16   -17   -18
    52      3 0.20000E+02 0.70000E+02 0.00000E+00             -13   -14   -15
    53      3 0.30000E+02 0.70000E+02 0.00000E+00             -10   -11   -12
    54      3 0.40000E+02 0.70000E+02 0.00000E+00              -7    -8    -9
    55      3 0.50000E+02 0.70000E+02 0.00000E+00              -4    -5    -6
    56      3 0.60000E+02 0.70000E+02 0.00000E+00              -1    -2    -3

 INPUT NODAL PROPERTIES 0 NO. OF PROPERTIES PER NODE=     1
>>>
    10.00000    10.00000    10.00000    10.00000    10.00000    10.00000    10.00000
11.00000
>>>
    11.00000    11.00000    11.00000    11.00000    11.00000    11.00000    12.00000
12.00000
>>>
    12.00000    12.00000    12.00000    12.00000    12.00000    13.00000    13.00000
13.00000
>>>
    13.00000    13.00000    13.00000    13.00000    14.00000    14.00000    14.00000
14.00000
>>>
    14.00000    14.00000    14.00000    15.00000    15.00000    15.00000    15.00000
15.00000
>>>
    15.00000    15.00000    16.00000    16.00000    16.00000    16.00000    16.00000
16.00000
>>>
    16.00000    17.00000    17.00000    17.00000    17.00000    17.00000    17.00000
17.00000
 INPUT OF ELEMENT PROPERTIES= 0
NO OF GROUPS OF PEORPERTIES=     8
NO OF PROPERTIES PER GROUP=     4


CARDS OF ELEMENT PROPERTIES
>>>     1 0.10000E+01 0.20000E+00 0.10000E+00-0.10000E+00
>>>     2 0.10000E+01 0.10000E+00 0.10000E+00-0.10000E+00
>>>     3 0.10000E+01 0.50000E-01 0.10000E+00-0.10000E+00
>>>     4 0.10000E+01 0.70000E-01 0.10000E+00-0.10000E+00
>>>     5 0.10000E+01 0.15000E+00 0.10000E+00-0.10000E+00
>>>     6 0.10000E+01 0.12500E+00 0.10000E+00-0.10000E+00
>>>     7 0.10000E+01 0.75000E-01 0.10000E+00-0.10000E+00
>>>     8 0.10000E+01 0.60000E-01 0.10000E+00-0.10000E+00
>>>     0 0.00000E+00 0.00000E+00 0.00000E+00 0.00000E+00


  INPUT OF  ELEMENTS (M= 0)
  ====================
               MAX.  NUMBER  OF ELEMENTS              (NELT)=   84
```

```
                MAX.  NUMBER  OF NODES PER ELEMENT     (NNEL)=     3
                DEFAULT  ELEMENT  TYPE                  (NTPE)=     1
                NUMBER  OF GROUPS  OF ELEMENTS          (NGRE)=     1
                INDEX  FOR NON  SYMMETRIC PROBLEM       (NSYM)=     1
                INDEX  FOR IDENTICAL  ELEMENTS        (NIDENT)=     0


                MEAN   BAND  HEIGHT=    19.9  MAXIMUM=   26
                LENGTH OF A TRIANGLE IN KG          (NKG)=      2928
                NUMBER  OF INTEGRATION POINTS        (NPG)=         0


  UNSTEADY SOLUTION  (M= 0)
 ======================

 ------------STEP   NUMBER (IPAS):    1

              INCREMENT                      (DPAS)= 0.10000E+02
              TOTAL  LEVEL                   (XPAS)= 0.10000E+02
              NUMBER  OF ITERATIONS         (NITER)=          30
              METHOD  NUMBER                (IMETH)=           1
              TOLERANCE                     (EPSDL)= 0.30000E-01
              COEFFICIENT   ALPHA           (OMEGA)= 0.10000E+01

    ITERATION  (ITER):    12  NORM (XNORM)= 0.18270E-01
```

NODES	X	Y	Z	DEGREES OF FREEDOM (* = PRESCRIBED)		
1	0.00000E+00	0.00000E+00	0.00000E+00	0.50607E-03	-0.85879E-08	-0.35456E-01
2	0.10000E+02	0.00000E+00	0.00000E+00	0.50669E-03	-0.80525E-08	-0.27830E-01
3	0.20000E+02	0.00000E+00	0.00000E+00	0.50429E-03	0.16494E-06	-0.25639E-01
4	0.30000E+02	0.00000E+00	0.00000E+00	0.49920E-03	0.11200E-06	-0.27648E-01
5	0.40000E+02	0.00000E+00	0.00000E+00	0.49695E-03	0.14581E-07	-0.30289E-01
6	0.50000E+02	0.00000E+00	0.00000E+00	0.49837E-03	-0.63033E-07	-0.28731E-01
7	0.60000E+02	0.00000E+00	0.00000E+00	0.49925E-03	0.79591E-08	-0.28558E-01
8	0.00000E+00	0.10000E+02	0.00000E+00	0.49971E-03	0.89406E-07	-0.41580E-01
9	0.10000E+02	0.10000E+02	0.00000E+00	0.50062E-03	-0.12515E-06	-0.39423E-01
10	0.20000E+02	0.10000E+02	0.00000E+00	0.50299E-03	0.17390E-07	-0.33374E-01
11	0.30000E+02	0.10000E+02	0.00000E+00	0.50096E-03	0.58550E-07	-0.25449E-01
12	0.40000E+02	0.10000E+02	0.00000E+00	0.49993E-03	-0.22236E-07	-0.27042E-01
13	0.50000E+02	0.10000E+02	0.00000E+00	0.50081E-03	0.26326E-07	-0.27723E-01
14	0.60000E+02	0.10000E+02	0.00000E+00	0.49979E-03	-0.65833E-08	-0.28652E-01
15	0.00000E+00	0.20000E+02	0.00000E+00	0.49819E-03	-0.36552E-06	-0.39251E-01
16	0.10000E+02	0.20000E+02	0.00000E+00	0.50451E-03	0.40071E-07	-0.38767E-01
17	0.20000E+02	0.20000E+02	0.00000E+00	0.50119E-03	-0.82745E-07	-0.41835E-01
18	0.30000E+02	0.20000E+02	0.00000E+00	0.50462E-03	0.28574E-07	-0.34261E-01
19	0.40000E+02	0.20000E+02	0.00000E+00	0.50330E-03	0.73970E-07	-0.29551E-01
20	0.50000E+02	0.20000E+02	0.00000E+00	0.49773E-03	0.11548E-06	-0.30428E-01
21	0.60000E+02	0.20000E+02	0.00000E+00	0.49719E-03	0.89464E-08	-0.23808E-01
22	0.00000E+00	0.30000E+02	0.00000E+00	0.49687E-03	0.19231E-06	-0.41855E-01
23	0.10000E+02	0.30000E+02	0.00000E+00	0.49240E-03	-0.16967E-06	-0.46187E-01
24	0.20000E+02	0.30000E+02	0.00000E+00	0.50193E-03	-0.24179E-06	-0.37964E-01
25	0.30000E+02	0.30000E+02	0.00000E+00	0.50065E-03	0.26838E-06	-0.41857E-01
26	0.40000E+02	0.30000E+02	0.00000E+00	0.49421E-03	0.93654E-07	-0.36979E-01
27	0.50000E+02	0.30000E+02	0.00000E+00	0.49446E-03	0.30846E-07	-0.24092E-01
28	0.60000E+02	0.30000E+02	0.00000E+00	0.49336E-03	-0.59769E-07	-0.17474E-01
29	0.00000E+00	0.40000E+02	0.00000E+00	0.48996E-03	-0.93855E-07	-0.16976E-01
30	0.10000E+02	0.40000E+02	0.00000E+00	0.49797E-03	0.27126E-07	-0.29278E-01
31	0.20000E+02	0.40000E+02	0.00000E+00	0.49642E-03	0.29056E-08	-0.51516E-01
32	0.30000E+02	0.40000E+02	0.00000E+00	0.49678E-03	-0.64792E-07	-0.28897E-01
33	0.40000E+02	0.40000E+02	0.00000E+00	0.50139E-03	-0.18235E-06	-0.17996E-01
34	0.50000E+02	0.40000E+02	0.00000E+00	0.50646E-03	-0.14477E-07	-0.18903E-01
35	0.60000E+02	0.40000E+02	0.00000E+00	0.51981E-03	-0.56358E-06	-0.19253E-01
36	0.00000E+00	0.50000E+02	0.00000E+00	0.50198E-03	0.77794E-06	-0.82637E-02
37	0.10000E+02	0.50000E+02	0.00000E+00	0.47513E-03	0.12453E-06	-0.76689E-02
38	0.20000E+02	0.50000E+02	0.00000E+00	0.44651E-03	0.28897E-06	-0.12909E-01
39	0.30000E+02	0.50000E+02	0.00000E+00	0.46231E-03	-0.64409E-06	-0.16663E-01
40	0.40000E+02	0.50000E+02	0.00000E+00	0.48434E-03	0.12450E-06	-0.22615E-01
41	0.50000E+02	0.50000E+02	0.00000E+00	0.45929E-03	0.32142E-06	-0.20891E-01

```
    42 0.60000E+02 0.50000E+02 0.00000E+00    0.45671E-03     0.74858E-06    -0.22721E-01
    43 0.00000E+00 0.60000E+02 0.00000E+00    0.53872E-03    -0.11434E-05    -0.12052E-01
    44 0.10000E+02 0.60000E+02 0.00000E+00    0.63713E-03    -0.50006E-06    -0.11793E-01
    45 0.20000E+02 0.60000E+02 0.00000E+00    0.64139E-03     0.20928E-06    -0.11809E-01
    46 0.30000E+02 0.60000E+02 0.00000E+00    0.61704E-03    -0.98305E-07    -0.11745E-01
    47 0.40000E+02 0.60000E+02 0.00000E+00    0.65018E-03    -0.66663E-07    -0.15508E-01
    48 0.50000E+02 0.60000E+02 0.00000E+00    0.62759E-03     0.52997E-06    -0.17906E-01
    49 0.60000E+02 0.60000E+02 0.00000E+00    0.55039E-03     0.14444E-05    -0.11346E-01
    50 0.00000E+00 0.70000E+02 0.00000E+00    0.00000E+00 *   0.00000E+00 *   0.00000E+00
    51 0.10000E+02 0.70000E+02 0.00000E+00    0.00000E+00 *   0.00000E+00 *   0.00000E+00
    52 0.20000E+02 0.70000E+02 0.00000E+00    0.00000E+00 *   0.00000E+00 *   0.00000E+00
    53 0.30000E+02 0.70000E+02 0.00000E+00    0.00000E+00 *   0.00000E+00 *   0.00000E+00
    54 0.40000E+02 0.70000E+02 0.00000E+00    0.00000E+00 *   0.00000E+00 *   0.00000E+00
    55 0.50000E+02 0.70000E+02 0.00000E+00    0.00000E+00 *   0.00000E+00 *   0.00000E+00
    56 0.60000E+02 0.70000E+02 0.00000E+00    0.00000E+00 *   0.00000E+00 *   0.00000E+00


 ------------STEP   NUMBER (IPAS):   40

              INCREMENT                    (DPAS)= 0.10000E+02
              TOTAL  LEVEL                 (XPAS)= 0.40000E+03
              NUMBER  OF ITERATIONS       (NITER)=          30
              METHOD  NUMBER              (IMETH)=           1
              TOLERANCE                   (EPSDL)= 0.30000E-01
              COEFFICIENT   ALPHA         (OMEGA)= 0.10000E+01

     ITERATION  (ITER):     5  NORM (XNORM)= 0.81107E-02

NODES     X           Y           Z          DEGREES OF FREEDOM (*   = PRESCRIBED)

     1 0.00000E+00 0.00000E+00 0.00000E+00    0.44205E-02    -0.10900E-03    -0.15371E+00
     2 0.10000E+02 0.00000E+00 0.00000E+00    0.54766E-02    -0.87917E-04    -0.12948E+00
     3 0.20000E+02 0.00000E+00 0.00000E+00    0.57565E-02     0.30412E-04    -0.12936E+00
     4 0.30000E+02 0.00000E+00 0.00000E+00    0.58226E-02    -0.73609E-04    -0.14044E+00
     5 0.40000E+02 0.00000E+00 0.00000E+00    0.58944E-02     0.13774E-05    -0.15974E+00
     6 0.50000E+02 0.00000E+00 0.00000E+00    0.63243E-02    -0.47884E-04    -0.15445E+00
     7 0.60000E+02 0.00000E+00 0.00000E+00    0.62877E-02     0.15336E-04    -0.15526E+00
     8 0.00000E+00 0.10000E+02 0.00000E+00    0.40942E-02     0.11934E-03    -0.16255E+00
     9 0.10000E+02 0.10000E+02 0.00000E+00    0.38725E-02    -0.31733E-04    -0.16173E+00
    10 0.20000E+02 0.10000E+02 0.00000E+00    0.40665E-02    -0.67536E-04    -0.14209E+00
    11 0.30000E+02 0.10000E+02 0.00000E+00    0.54161E-02    -0.10027E-03    -0.12155E+00
    12 0.40000E+02 0.10000E+02 0.00000E+00    0.56289E-02    -0.36426E-04    -0.13642E+00
    13 0.50000E+02 0.10000E+02 0.00000E+00    0.57132E-02     0.39803E-04    -0.14100E+00
    14 0.60000E+02 0.10000E+02 0.00000E+00    0.57251E-02    -0.77477E-04    -0.14396E+00
    15 0.00000E+00 0.20000E+02 0.00000E+00    0.38255E-02    -0.44435E-04    -0.15539E+00
    16 0.10000E+02 0.20000E+02 0.00000E+00    0.39100E-02     0.80605E-04    -0.14362E+00
    17 0.20000E+02 0.20000E+02 0.00000E+00    0.31834E-02     0.52450E-05    -0.14601E+00
    18 0.30000E+02 0.20000E+02 0.00000E+00    0.36976E-02    -0.90899E-04    -0.13670E+00
    19 0.40000E+02 0.20000E+02 0.00000E+00    0.45942E-02    -0.61111E-04    -0.12647E+00
    20 0.50000E+02 0.20000E+02 0.00000E+00    0.44505E-02    -0.25054E-04    -0.13716E+00
    21 0.60000E+02 0.20000E+02 0.00000E+00    0.55372E-02    -0.16284E-03    -0.11627E+00
    22 0.00000E+00 0.30000E+02 0.00000E+00    0.35776E-02     0.77082E-04    -0.16238E+00
    23 0.10000E+02 0.30000E+02 0.00000E+00    0.28215E-02     0.72316E-04    -0.16063E+00
    24 0.20000E+02 0.30000E+02 0.00000E+00    0.31397E-02    -0.19457E-04    -0.11958E+00
    25 0.30000E+02 0.30000E+02 0.00000E+00    0.32905E-02    -0.28019E-04    -0.13622E+00
    26 0.40000E+02 0.30000E+02 0.00000E+00    0.32169E-02    -0.70509E-04    -0.13495E+00
    27 0.50000E+02 0.30000E+02 0.00000E+00    0.42954E-02    -0.87126E-04    -0.10425E+00
    28 0.60000E+02 0.30000E+02 0.00000E+00    0.50932E-02    -0.29655E-05    -0.80096E-01
    29 0.00000E+00 0.40000E+02 0.00000E+00    0.50577E-02     0.99085E-04    -0.85696E-01
    30 0.10000E+02 0.40000E+02 0.00000E+00    0.34008E-02     0.23292E-03    -0.11698E+00
    31 0.20000E+02 0.40000E+02 0.00000E+00    0.14306E-02     0.16964E-04    -0.14390E+00
    32 0.30000E+02 0.40000E+02 0.00000E+00    0.29379E-02    -0.12144E-03    -0.10019E+00
    33 0.40000E+02 0.40000E+02 0.00000E+00    0.36544E-02    -0.10896E-04    -0.65510E-01
    34 0.50000E+02 0.40000E+02 0.00000E+00    0.38504E-02    -0.10748E-04    -0.72840E-01
    35 0.60000E+02 0.40000E+02 0.00000E+00    0.31922E-02     0.81911E-04    -0.71199E-01
    36 0.00000E+00 0.50000E+02 0.00000E+00    0.61676E-02     0.33385E-04    -0.42744E-01
    37 0.10000E+02 0.50000E+02 0.00000E+00    0.54365E-02     0.29663E-04    -0.37859E-01
    38 0.20000E+02 0.50000E+02 0.00000E+00    0.36656E-02     0.44697E-04    -0.49817E-01
    39 0.30000E+02 0.50000E+02 0.00000E+00    0.30478E-02     0.71715E-04    -0.54587E-01
    40 0.40000E+02 0.50000E+02 0.00000E+00    0.17415E-02     0.11589E-04    -0.61799E-01
```

```
   41 0.50000E+02 0.50000E+02 0.00000E+00    0.24516E-02    -0.10772E-04    -0.57079E-01
   42 0.60000E+02 0.50000E+02 0.00000E+00    0.19618E-02     0.15260E-04    -0.58612E-01
   43 0.00000E+00 0.60000E+02 0.00000E+00    0.13325E-02    -0.46476E-04    -0.31356E-01
   44 0.10000E+02 0.60000E+02 0.00000E+00    0.27175E-02    -0.12719E-05    -0.30626E-01
   45 0.20000E+02 0.60000E+02 0.00000E+00    0.22350E-02    -0.20071E-06    -0.27893E-01
   46 0.30000E+02 0.60000E+02 0.00000E+00    0.22498E-02     0.26381E-05    -0.28209E-01
   47 0.40000E+02 0.60000E+02 0.00000E+00    0.14493E-02     0.74576E-05    -0.26983E-01
   48 0.50000E+02 0.60000E+02 0.00000E+00    0.12900E-02     0.38486E-05    -0.30786E-01
   49 0.60000E+02 0.60000E+02 0.00000E+00    0.15035E-02    -0.12102E-04    -0.20604E-01
   50 0.00000E+00 0.70000E+02 0.00000E+00    0.00000E+00 *   0.00000E+00 *   0.00000E+00
   51 0.10000E+02 0.70000E+02 0.00000E+00    0.00000E+00 *   0.00000E+00 *   0.00000E+00
   52 0.20000E+02 0.70000E+02 0.00000E+00    0.00000E+00 *   0.00000E+00 *   0.00000E+00
   53 0.30000E+02 0.70000E+02 0.00000E+00    0.00000E+00 *   0.00000E+00 *   0.00000E+00
   54 0.40000E+02 0.70000E+02 0.00000E+00    0.00000E+00 *   0.00000E+00 *   0.00000E+00
   55 0.50000E+02 0.70000E+02 0.00000E+00    0.00000E+00 *   0.00000E+00 *   0.00000E+00
   56 0.60000E+02 0.70000E+02 0.00000E+00    0.00000E+00 *   0.00000E+00 *   0.00000E+00

END OF PROBLEM :      7356 UTILIZED REAL WORDS OVER     85000
```

4. Sample output from 1-D model

```
                                1-D RUNOFF SIMULATION MODEL

 COMMENTS
 ==========

  NONLINEAR TRANSIENT FE MODEL FOR ST. VENANT EQS.
  TRIAGULAR ELEMENT MODEL
 heterogeneous plot

 INPUT OF NODES =     0
 MAX. NUMBER OF NODES =    56
 MAX. NUMBER OF DOF PER NODES =     2
 DIMENSIONS OF PROBLEM =     1
 COORDINATE SCALE FACTORS = 0.10000E+01 0.10000E+01 0.10000E+01
 WORKSPACE IN REAL WORDS =      30000


 INPUT OF B.C. M= 0


B.C. CARDS
>>>
1100000000   0.00000   0.00000   0.00000   0.00000   0.00000   0.00000   0.00000
>>>
   56   55   54   53   52   51   50    0    0    0    0    0    0    0    0    0
>>>
0000000000   0.00000   0.00000   0.00000   0.00000   0.00000   0.00000   0.00000
TOTAL NUMBER OF NODE=   56
TOTAL NUMBER OF DOF =  112
 NUMBER OF EQUATIONS=   98
 NUMBER OF PRESCRIBED NON ZERO DOF    0
 NUMBER OF PRESCRIBED ZERO DOF   14
 TOTAL NUMBER OF PRESCRIBED DOF   14


NODAL COORDINATE     NO D.L.    X    Y    Z  NEQ
     1      2 0.00000E+00 0.00000E+00 0.00000E+00                1     2
     2      2 0.00000E+00 0.00000E+00 0.00000E+00                3     4
     3      2 0.00000E+00 0.00000E+00 0.00000E+00                5     6
     4      2 0.00000E+00 0.00000E+00 0.00000E+00                7     8
     5      2 0.00000E+00 0.00000E+00 0.00000E+00                9    10
     6      2 0.00000E+00 0.00000E+00 0.00000E+00               11    12
     7      2 0.00000E+00 0.00000E+00 0.00000E+00               13    14
     8      2 0.10000E+02 0.00000E+00 0.00000E+00               15    16
     9      2 0.10000E+02 0.00000E+00 0.00000E+00               17    18
    10      2 0.10000E+02 0.00000E+00 0.00000E+00               19    20
    11      2 0.10000E+02 0.00000E+00 0.00000E+00               21    22
    12      2 0.10000E+02 0.00000E+00 0.00000E+00               23    24
    13      2 0.10000E+02 0.00000E+00 0.00000E+00               25    26
    14      2 0.10000E+02 0.00000E+00 0.00000E+00               27    28
    15      2 0.20000E+02 0.00000E+00 0.00000E+00               29    30
    16      2 0.20000E+02 0.00000E+00 0.00000E+00               31    32
    17      2 0.20000E+02 0.00000E+00 0.00000E+00               33    34
    18      2 0.20000E+02 0.00000E+00 0.00000E+00               35    36
    19      2 0.20000E+02 0.00000E+00 0.00000E+00               37    38
    20      2 0.20000E+02 0.00000E+00 0.00000E+00               39    40
    21      2 0.20000E+02 0.00000E+00 0.00000E+00               41    42
    22      2 0.30000E+02 0.00000E+00 0.00000E+00               43    44
    23      2 0.30000E+02 0.00000E+00 0.00000E+00               45    46
    24      2 0.30000E+02 0.00000E+00 0.00000E+00               47    48
    25      2 0.30000E+02 0.00000E+00 0.00000E+00               49    50
    26      2 0.30000E+02 0.00000E+00 0.00000E+00               51    52
    27      2 0.30000E+02 0.00000E+00 0.00000E+00               53    54
    28      2 0.30000E+02 0.00000E+00 0.00000E+00               55    56
    29      2 0.40000E+02 0.00000E+00 0.00000E+00               57    58
    30      2 0.40000E+02 0.00000E+00 0.00000E+00               59    60
    31      2 0.40000E+02 0.00000E+00 0.00000E+00               61    62
```

```
    32     2 0.40000E+02 0.00000E+00 0.00000E+00              63    64
    33     2 0.40000E+02 0.00000E+00 0.00000E+00              65    66
    34     2 0.40000E+02 0.00000E+00 0.00000E+00              67    68
    35     2 0.40000E+02 0.00000E+00 0.00000E+00              69    70
    36     2 0.50000E+02 0.00000E+00 0.00000E+00              71    72
    37     2 0.50000E+02 0.00000E+00 0.00000E+00              73    74
    38     2 0.50000E+02 0.00000E+00 0.00000E+00              75    76
    39     2 0.50000E+02 0.00000E+00 0.00000E+00              77    78
    40     2 0.50000E+02 0.00000E+00 0.00000E+00              79    80
    41     2 0.50000E+02 0.00000E+00 0.00000E+00              81    82
    42     2 0.50000E+02 0.00000E+00 0.00000E+00              83    84
    43     2 0.60000E+02 0.00000E+00 0.00000E+00              85    86
    44     2 0.60000E+02 0.00000E+00 0.00000E+00              87    88
    45     2 0.60000E+02 0.00000E+00 0.00000E+00              89    90
    46     2 0.60000E+02 0.00000E+00 0.00000E+00              91    92
    47     2 0.60000E+02 0.00000E+00 0.00000E+00              93    94
    48     2 0.60000E+02 0.00000E+00 0.00000E+00              95    96
    49     2 0.60000E+02 0.00000E+00 0.00000E+00              97    98
    50     2 0.70000E+02 0.00000E+00 0.00000E+00             -13   -14
    51     2 0.70000E+02 0.00000E+00 0.00000E+00             -11   -12
    52     2 0.70000E+02 0.00000E+00 0.00000E+00              -9   -10
    53     2 0.70000E+02 0.00000E+00 0.00000E+00              -7    -8
    54     2 0.70000E+02 0.00000E+00 0.00000E+00              -5    -6
    55     2 0.70000E+02 0.00000E+00 0.00000E+00              -3    -4
    56     2 0.70000E+02 0.00000E+00 0.00000E+00              -1    -2

INPUT NODAL PROPERTIES 0 NO. OF PROPERTIES PER NODE=     1
>>>
    10.00000    10.00000    10.00000    10.00000    10.00000    10.00000    10.00000
11.00000
>>>
    11.00000    11.00000    11.00000    11.00000    11.00000    11.00000    12.00000
12.00000
>>>
    12.00000    12.00000    12.00000    12.00000    12.00000    13.00000    13.00000
13.00000
>>>
    13.00000    13.00000    13.00000    13.00000    14.00000    14.00000    14.00000
14.00000
>>>
    14.00000    14.00000    14.00000    15.00000    15.00000    15.00000    15.00000
15.00000
>>>
    15.00000    15.00000    16.00000    16.00000    16.00000    16.00000    16.00000
16.00000
>>>
    16.00000    17.00000    17.00000    17.00000    17.00000    17.00000    17.00000
17.00000
 INPUT OF ELEMENT PROPERTIES= 0
NO OF GROUPS OF PEORPERTIES=    15
NO OF PROPERTIES PER GROUP=     5

CARDS OF ELEMENT PROPERTIES
>>>     1 0.10000E+01 0.20000E+00 0.10000E+02 0.10000E+00-0.10000E+00
>>>     2 0.10000E+01 0.10000E+00 0.10000E+02 0.10000E+00-0.10000E+00
>>>     3 0.10000E+01 0.50000E-01 0.10000E+02 0.10000E+00-0.10000E+00
>>>     4 0.10000E+01 0.70000E-01 0.10000E+02 0.10000E+00-0.10000E+00
>>>     5 0.10000E+01 0.53300E-01 0.10000E+02 0.10000E+00-0.10000E+00
>>>     6 0.10000E+01 0.60000E-01 0.10000E+02 0.10000E+00-0.10000E+00
>>>     7 0.10000E+01 0.55000E-01 0.10000E+02 0.10000E+00-0.10000E+00
>>>     8 0.10000E+01 0.65000E-01 0.10000E+02 0.10000E+00-0.10000E+00
>>>     9 0.10000E+01 0.76000E-01 0.10000E+02 0.10000E+00-0.10000E+00
>>>    10 0.10000E+01 0.75000E-01 0.10000E+02 0.10000E+00-0.10000E+00
>>>    11 0.10000E+01 0.80000E-01 0.10000E+02 0.10000E+00-0.10000E+00
>>>    12 0.10000E+01 0.79000E-01 0.10000E+02 0.10000E+00-0.10000E+00
>>>    13 0.10000E+01 0.12500E+00 0.10000E+02 0.10000E+00-0.10000E+00
>>>    14 0.10000E+01 0.17500E+00 0.10000E+02 0.10000E+00-0.10000E+00
>>>    15 0.10000E+01 0.15000E+00 0.10000E+02 0.10000E+00-0.10000E+00
```

```
>>>     0 0.00000E+00 0.00000E+00 0.00000E+00 0.00000E+00 0.00000E+00

  INPUT OF  ELEMENTS (M= 0)
  ========================
               MAX.  NUMBER  OF ELEMENTS              (NELT)=   49
               MAX.  NUMBER  OF NODES PER ELEMENT     (NNEL)=    2
               DEFAULT  ELEMENT  TYPE                 (NTPE)=    1
               NUMBER  OF GROUPS  OF ELEMENTS         (NGRE)=    1
               INDEX  FOR NON  SYMMETRIC PROBLEM      (NSYM)=    1
               INDEX  FOR IDENTICAL  ELEMENTS       (NIDENT)=    0

               MEAN   BAND  HEIGHT=    12.5  MAXIMUM=   15
               LENGTH OF A TRIANGLE IN KG          (NKG)=      1225
               NUMBER  OF INTEGRATION POINTS        (NPG)=         0


   UNSTEADY SOLUTION  (M= 0)
 ========================

 -------------STEP   NUMBER (IPAS):    1

              INCREMENT                      (DPAS)= 0.10000E+02
              TOTAL  LEVEL                   (XPAS)= 0.10000E+02
              NUMBER  OF ITERATIONS         (NITER)=          30
              METHOD  NUMBER                (IMETH)=           1
              TOLERANCE                     (EPSDL)= 0.30000E-01
              COEFFICIENT   ALPHA           (OMEGA)= 0.10000E+01

     ITERATION  (ITER):    12  NORM (XNORM)= 0.17625E-01

NODES     X           Y           Z          DEGREES OF FREEDOM (*   = PRESCRIBED)

     1 0.00000E+00 0.00000E+00 0.00000E+00     -0.35225E-01     0.50429E-03
     2 0.00000E+00 0.00000E+00 0.00000E+00     -0.30001E-01     0.50512E-03
     3 0.00000E+00 0.00000E+00 0.00000E+00     -0.26022E-01     0.50267E-03
     4 0.00000E+00 0.00000E+00 0.00000E+00     -0.28483E-01     0.49926E-03
     5 0.00000E+00 0.00000E+00 0.00000E+00     -0.29272E-01     0.49806E-03
     6 0.00000E+00 0.00000E+00 0.00000E+00     -0.28457E-01     0.49955E-03
     7 0.00000E+00 0.00000E+00 0.00000E+00     -0.26783E-01     0.50333E-03
     8 0.10000E+02 0.00000E+00 0.00000E+00     -0.40406E-01     0.49779E-03
     9 0.10000E+02 0.00000E+00 0.00000E+00     -0.37915E-01     0.50054E-03
    10 0.10000E+02 0.00000E+00 0.00000E+00     -0.32057E-01     0.50314E-03
    11 0.10000E+02 0.00000E+00 0.00000E+00     -0.28293E-01     0.50067E-03
    12 0.10000E+02 0.00000E+00 0.00000E+00     -0.27113E-01     0.50020E-03
    13 0.10000E+02 0.00000E+00 0.00000E+00     -0.28320E-01     0.50008E-03
    14 0.10000E+02 0.00000E+00 0.00000E+00     -0.30810E-01     0.49825E-03
    15 0.20000E+02 0.00000E+00 0.00000E+00     -0.36396E-01     0.50492E-03
    16 0.20000E+02 0.00000E+00 0.00000E+00     -0.38324E-01     0.50361E-03
    17 0.20000E+02 0.00000E+00 0.00000E+00     -0.38909E-01     0.50272E-03
    18 0.20000E+02 0.00000E+00 0.00000E+00     -0.34253E-01     0.50593E-03
    19 0.20000E+02 0.00000E+00 0.00000E+00     -0.31247E-01     0.50311E-03
    20 0.20000E+02 0.00000E+00 0.00000E+00     -0.28541E-01     0.49870E-03
    21 0.20000E+02 0.00000E+00 0.00000E+00     -0.23011E-01     0.49593E-03
    22 0.30000E+02 0.00000E+00 0.00000E+00     -0.48521E-01     0.49214E-03
    23 0.30000E+02 0.00000E+00 0.00000E+00     -0.45611E-01     0.49390E-03
    24 0.30000E+02 0.00000E+00 0.00000E+00     -0.41542E-01     0.49781E-03
    25 0.30000E+02 0.00000E+00 0.00000E+00     -0.44311E-01     0.49752E-03
    26 0.30000E+02 0.00000E+00 0.00000E+00     -0.32611E-01     0.49316E-03
    27 0.30000E+02 0.00000E+00 0.00000E+00     -0.22440E-01     0.49411E-03
    28 0.30000E+02 0.00000E+00 0.00000E+00     -0.18549E-01     0.49802E-03
    29 0.40000E+02 0.00000E+00 0.00000E+00     -0.16657E-01     0.49377E-03
    30 0.40000E+02 0.00000E+00 0.00000E+00     -0.23497E-01     0.49557E-03
    31 0.40000E+02 0.00000E+00 0.00000E+00     -0.35351E-01     0.49786E-03
    32 0.40000E+02 0.00000E+00 0.00000E+00     -0.32361E-01     0.49798E-03
    33 0.40000E+02 0.00000E+00 0.00000E+00     -0.19578E-01     0.50472E-03
    34 0.40000E+02 0.00000E+00 0.00000E+00     -0.18142E-01     0.50779E-03
    35 0.40000E+02 0.00000E+00 0.00000E+00     -0.20479E-01     0.50672E-03
```

```
    36 0.50000E+02 0.00000E+00 0.00000E+00     -0.83399E-02     0.46969E-03
    37 0.50000E+02 0.00000E+00 0.00000E+00     -0.97381E-02     0.46651E-03
    38 0.50000E+02 0.00000E+00 0.00000E+00     -0.11803E-01     0.46123E-03
    39 0.50000E+02 0.00000E+00 0.00000E+00     -0.16170E-01     0.46342E-03
    40 0.50000E+02 0.00000E+00 0.00000E+00     -0.22281E-01     0.46794E-03
    41 0.50000E+02 0.00000E+00 0.00000E+00     -0.21810E-01     0.46919E-03
    42 0.50000E+02 0.00000E+00 0.00000E+00     -0.18984E-01     0.47106E-03
    43 0.60000E+02 0.00000E+00 0.00000E+00     -0.12322E-01     0.62315E-03
    44 0.60000E+02 0.00000E+00 0.00000E+00     -0.11909E-01     0.62343E-03
    45 0.60000E+02 0.00000E+00 0.00000E+00     -0.11276E-01     0.62399E-03
    46 0.60000E+02 0.00000E+00 0.00000E+00     -0.12509E-01     0.62167E-03
    47 0.60000E+02 0.00000E+00 0.00000E+00     -0.14215E-01     0.61804E-03
    48 0.60000E+02 0.00000E+00 0.00000E+00     -0.17754E-01     0.61772E-03
    49 0.60000E+02 0.00000E+00 0.00000E+00     -0.23872E-01     0.61799E-03
    50 0.70000E+02 0.00000E+00 0.00000E+00      0.00000E+00 *   0.00000E+00 *
    51 0.70000E+02 0.00000E+00 0.00000E+00      0.00000E+00 *   0.00000E+00 *
    52 0.70000E+02 0.00000E+00 0.00000E+00      0.00000E+00 *   0.00000E+00 *
    53 0.70000E+02 0.00000E+00 0.00000E+00      0.00000E+00 *   0.00000E+00 *
    54 0.70000E+02 0.00000E+00 0.00000E+00      0.00000E+00 *   0.00000E+00 *
    55 0.70000E+02 0.00000E+00 0.00000E+00      0.00000E+00 *   0.00000E+00 *
    56 0.70000E+02 0.00000E+00 0.00000E+00      0.00000E+00 *   0.00000E+00 *


 ------------STEP   NUMBER (IPAS):   40

              INCREMENT                    (DPAS)= 0.10000E+02
              TOTAL  LEVEL                 (XPAS)= 0.40000E+03
              NUMBER  OF ITERATIONS       (NITER)=          30
              METHOD  NUMBER              (IMETH)=           1
              TOLERANCE                   (EPSDL)= 0.30000E-01
              COEFFICIENT   ALPHA         (OMEGA)= 0.10000E+01

     ITERATION  (ITER):     1  NORM (XNORM)= 0.22720E-01

NODES     X           Y           Z          DEGREES OF FREEDOM (*   = PRESCRIBED)

     1 0.00000E+00 0.00000E+00 0.00000E+00     -0.15875E+00     0.52607E-02
     2 0.00000E+00 0.00000E+00 0.00000E+00     -0.15059E+00     0.60827E-02
     3 0.00000E+00 0.00000E+00 0.00000E+00     -0.14878E+00     0.69716E-02
     4 0.00000E+00 0.00000E+00 0.00000E+00     -0.16221E+00     0.66835E-02
     5 0.00000E+00 0.00000E+00 0.00000E+00     -0.16028E+00     0.62989E-02
     6 0.00000E+00 0.00000E+00 0.00000E+00     -0.15059E+00     0.60212E-02
     7 0.00000E+00 0.00000E+00 0.00000E+00     -0.13716E+00     0.61939E-02
     8 0.10000E+02 0.00000E+00 0.00000E+00     -0.16859E+00     0.36298E-02
     9 0.10000E+02 0.00000E+00 0.00000E+00     -0.16719E+00     0.40403E-02
    10 0.10000E+02 0.00000E+00 0.00000E+00     -0.15466E+00     0.50399E-02
    11 0.10000E+02 0.00000E+00 0.00000E+00     -0.14652E+00     0.58814E-02
    12 0.10000E+02 0.00000E+00 0.00000E+00     -0.14403E+00     0.60942E-02
    13 0.10000E+02 0.00000E+00 0.00000E+00     -0.14428E+00     0.57659E-02
    14 0.10000E+02 0.00000E+00 0.00000E+00     -0.15520E+00     0.52534E-02
    15 0.20000E+02 0.00000E+00 0.00000E+00     -0.12767E+00     0.37622E-02
    16 0.20000E+02 0.00000E+00 0.00000E+00     -0.14382E+00     0.38885E-02
    17 0.20000E+02 0.00000E+00 0.00000E+00     -0.15688E+00     0.37683E-02
    18 0.20000E+02 0.00000E+00 0.00000E+00     -0.14871E+00     0.42233E-02
    19 0.20000E+02 0.00000E+00 0.00000E+00     -0.14706E+00     0.50285E-02
    20 0.20000E+02 0.00000E+00 0.00000E+00     -0.14397E+00     0.54685E-02
    21 0.20000E+02 0.00000E+00 0.00000E+00     -0.12811E+00     0.64829E-02
    22 0.30000E+02 0.00000E+00 0.00000E+00     -0.16180E+00     0.24061E-02
    23 0.30000E+02 0.00000E+00 0.00000E+00     -0.15616E+00     0.28430E-02
    24 0.30000E+02 0.00000E+00 0.00000E+00     -0.14223E+00     0.34291E-02
    25 0.30000E+02 0.00000E+00 0.00000E+00     -0.16053E+00     0.34654E-02
    26 0.30000E+02 0.00000E+00 0.00000E+00     -0.14675E+00     0.44877E-02
    27 0.30000E+02 0.00000E+00 0.00000E+00     -0.11787E+00     0.59922E-02
    28 0.30000E+02 0.00000E+00 0.00000E+00     -0.10662E+00     0.70043E-02
    29 0.40000E+02 0.00000E+00 0.00000E+00     -0.83956E-01     0.44808E-02
    30 0.40000E+02 0.00000E+00 0.00000E+00     -0.10476E+00     0.39060E-02
    31 0.40000E+02 0.00000E+00 0.00000E+00     -0.13097E+00     0.27737E-02
    32 0.40000E+02 0.00000E+00 0.00000E+00     -0.12397E+00     0.33015E-02
    33 0.40000E+02 0.00000E+00 0.00000E+00     -0.92178E-01     0.50870E-02
    34 0.40000E+02 0.00000E+00 0.00000E+00     -0.91738E-01     0.55610E-02
```

```
    35 0.40000E+02 0.00000E+00 0.00000E+00     -0.10012E+00     0.50342E-02
    36 0.50000E+02 0.00000E+00 0.00000E+00     -0.47732E-01     0.72580E-02
    37 0.50000E+02 0.00000E+00 0.00000E+00     -0.49382E-01     0.59315E-02
    38 0.50000E+02 0.00000E+00 0.00000E+00     -0.53191E-01     0.48096E-02
    39 0.50000E+02 0.00000E+00 0.00000E+00     -0.64898E-01     0.41114E-02
    40 0.50000E+02 0.00000E+00 0.00000E+00     -0.79551E-01     0.31486E-02
    41 0.50000E+02 0.00000E+00 0.00000E+00     -0.76596E-01     0.30183E-02
    42 0.50000E+02 0.00000E+00 0.00000E+00     -0.74097E-01     0.38156E-02
    43 0.60000E+02 0.00000E+00 0.00000E+00     -0.39210E-01     0.29030E-02
    44 0.60000E+02 0.00000E+00 0.00000E+00     -0.40966E-01     0.34949E-02
    45 0.60000E+02 0.00000E+00 0.00000E+00     -0.41327E-01     0.40752E-02
    46 0.60000E+02 0.00000E+00 0.00000E+00     -0.39020E-01     0.32083E-02
    47 0.60000E+02 0.00000E+00 0.00000E+00     -0.32757E-01     0.21029E-02
    48 0.60000E+02 0.00000E+00 0.00000E+00     -0.39955E-01     0.20018E-02
    49 0.60000E+02 0.00000E+00 0.00000E+00     -0.43519E-01     0.12234E-02
    50 0.70000E+02 0.00000E+00 0.00000E+00      0.00000E+00 *   0.00000E+00 *
    51 0.70000E+02 0.00000E+00 0.00000E+00      0.00000E+00 *   0.00000E+00 *
    52 0.70000E+02 0.00000E+00 0.00000E+00      0.00000E+00 *   0.00000E+00 *
    53 0.70000E+02 0.00000E+00 0.00000E+00      0.00000E+00 *   0.00000E+00 *
    54 0.70000E+02 0.00000E+00 0.00000E+00      0.00000E+00 *   0.00000E+00 *
    55 0.70000E+02 0.00000E+00 0.00000E+00      0.00000E+00 *   0.00000E+00 *
    56 0.70000E+02 0.00000E+00 0.00000E+00      0.00000E+00 *   0.00000E+00 *

END OF PROBLEM :       3431 UTILIZED REAL WORDS OVER      30000
```

Vita

Name : Seonggu Hong

Date of Birth : November 17, 1964

Place of Birth : Masan, Korea

Major : Agricultural Engineering/Biological Systems Engineering

Educational Institutions Attended	Dates	Degree
Seoul National University Seoul, Korea	3/83 - 2/87	B.S.
Seoul National University Seoul, Korea	3/87 - 2/89	M.S.
Virginia Tech Blacksburg, Virginia	8/91 - 10/95	Ph.D.

Position Held :

Research Associate, Department of Agricultural Engineering, Seoul National University, 1987-1989.

Lecturer, Department of Civil Engineering, Suwon Technical Junior College, Suwon, Korea, 1990-1991.